Inverse electron demand Diels-Alder pyridazine elimination: synthetic tools for chemical immunology

Geus, M.A.R. de

Citation

Geus, M. A. R. de. (2021, October 7). *Inverse electron demand Diels-Alder pyridazine elimination: synthetic tools for chemical immunology*. Retrieved from https://hdl.handle.net/1887/3215037

Inverse electron demand Diels-Alder pyridazine elimination:

synthetic tools for chemical immunology

Proefschrift

ter verkrijging van

de graad van doctor aan de Universiteit Leiden,

op gezag van rector magnificus prof.dr.ir. H. Bijl,

volgens besluit van het college voor promoties

te verdedigen op donderdag 7 oktober 2021

klokke 13:45 uur

door

Mark Alexander Ruben de Geus

Geboren te Nootdorp in 1990

Promotiecommissie

Promotores: Dr. S.I. van Kasteren

Prof. dr. H.S. Overkleeft

Overige leden: Prof. dr. A. Kros (voorzitter)

Prof. dr. M. van der Stelt (secretaris)

Dr. D.V. Filippov

Dr. K.M. Bonger (Radboud Universiteit Nijmegen)

Prof. dr. J.M. Fox (University of Delaware, Verenigde Staten)

"All we have to do is decide what to do with the time that is given to us"

J.R.R. Tolkien

Table of contents

1

Bioorthogonal bond-forming and breaking reactions in biology

1.1 Introduction to bioorthogonal chemistry

Chemical strategies have enabled the elucidation of new elements of biology by exacting precise control over processes in cells, and even in whole organisms. The twin pillars of this control have been the bioorthogonal bond forming, and bond breaking reactions, the first of which were invented by Bertozzi at the turn of the century.[1,2] The overarching property of bioorthogonal chemistry is that its transformations readily and selectively occur under physiological conditions without interfering with native biochemical processes.[3–7] This allows, for instance, the selective modification of proteins[8,9] or the characterization of active enzymes.[10,11] Reaction components must display a balanced profile of aqueous solubility, chemical stability, cellular toxicity, reaction kinetics and selectivity,[12] where the specific application dictates which properties are most influential.[13] Bioorthogonal reactions are developed using iterative modifications of known organic transformations,[14,15] such as the adaptation
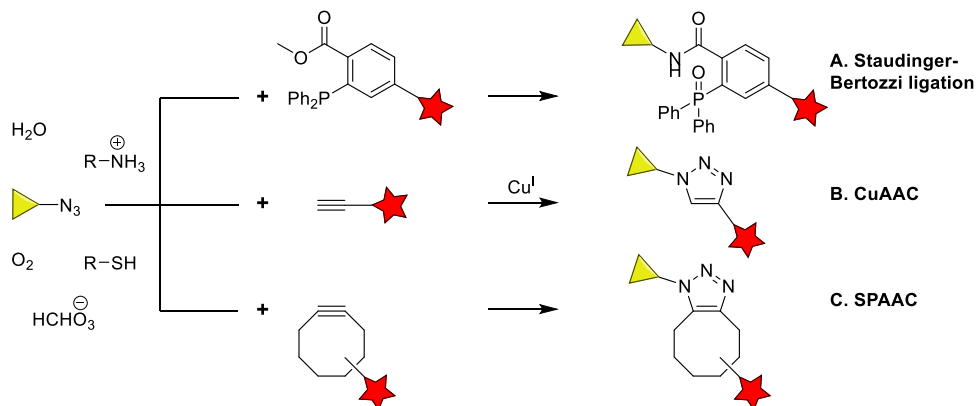
**Figure 1** Examples of bioorthogonal chemistry based on azide reactivity. A) Staudinger-Bertozzi ligation.[1-2] B) Cu(I)-catalyzed azide-alkyne cycloaddition (CuAAC).[19-22] C) Strain-promoted azide-alkyne cycloaddition (SPAAC).[24]

of the Staudinger reduction[16,17] to develop the Staudinger-Bertozzi ligation (Figure 1A).[1,2] Similarly, 1,3-dipolar cycloadditions[18] were revisited to develop the Cu(I)-catalyzed azide-alkyne cycloaddition (CuAAC),[19–22] a transformation which has become the hallmark of 'click' chemistry[23] due to its reliability and simplicity (Figure 1B). Copper induced cytotoxicity, however, limited the applicability of CuAAC in living systems and therefore prompted the development of the strain-promoted azide-alkyne cycloaddition (SPAAC; Figure 1C).[24] Other bioorthogonal ligations include strain-promoted alkyne-nitrone cycloaddition (SPANC),[25] photoinduced tetrazole ligation,[26] the formation of oximes and hydrazones from aldehydes and ketones,[27] and transition metal catalysis under aqueous conditions.[28–31]

1.2 Inverse electron demand Diels-Alder cycloaddition

A recurring theme is that most bioorthogonal reactions suffer from at least one clear disadvantage, such as slow reaction kinetics, high cytotoxicity, insufficient stability, cross reactivity with other bioorthogonal moieties, undesired physicochemical characteristics of the reactants or improper tunability of the overall method.[13–15] Amidst the current scope of bioorthogonal chemistry, the inverse electron demand Diels-Alder (IEDDA) cycloaddition between 1,2,4,5-tetrazines and strained alkenes stands out as an exceptionally versatile method (Figure 2).[32,33] Initial studies by Carboni, Linsey[34] and Sauer[35–38] were adapted for bioorthogonal utilization by Fox[39] and Hilderbrand[40] using stabilized tetrazines as dienes and *trans*-cyclooctene (TCO) and norbonene as dienophiles, respectively. These were followed by numerous other dienophiles, including bicyclooctynes (BCN),[41,42] cyclopropenes,[43–45] vinylboronic acids (VBA),[46–49] and N-acyl azetines.[50] Depending on the strained alkene and
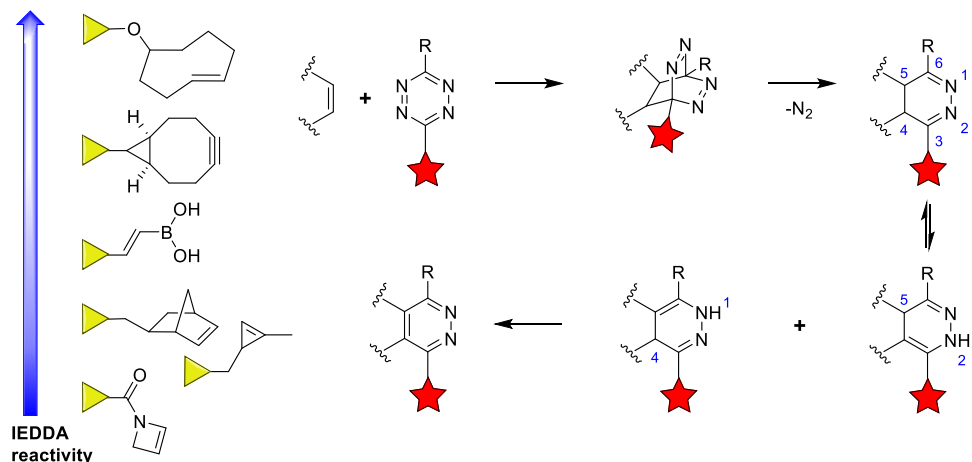
Figure 2 Mechanism and scope of the inverse electron demand Diels-Alder (IEDDA) cycloaddition between 1,2,4,5-tetrazines and strained alkenes or alkynes, including several classes of dienophiles.

tetrazine employed, second order reaction rates (k_2) range between $1 - 10^6$ $M^{-1}s^{-1}$, which is superior compared to reaction rates for the Staudinger ligation (10^{-3} $M^{-1}s^{-1}$), CuAAC ($10 - 100$ $M^{-1}s^{-1}$), SPAAC ($10^{-2} - 1$ $M^{-1}s^{-1}$) and other commonly employed bioorthogonal reactions.[32] The reaction features an initial [4+2] cycloaddition between the tetrazine and alkene components, followed by a retro Diels-Alder reaction to give a 4,5-dihydropyridazine and N_2 as the only byproduct. Tautomerization affords 1,4- and 2,5-dihydropyridazines, whilst oxidation results in a pyridazine adduct. A catalyst is not required and reaction rates are accelerated under aqueous conditions due to hydrophobic interactions.[39,51]

Advanced bioorthogonal applications, such as live cell imaging[52,53] or *in vivo* tumor pre-targeting,[54,55] enforce stringent demands on reaction kinetics to ensure fast and complete bioconjugation at low dosage and sub micromolar concentrations. These requirements stimulated the choice of TCO as a dienophile for exceptionally fast tetrazine ligation ($k_2 \geq 10^3$ $M^{-1}s^{-1}$).[39,56–59] TCO's properties as a dienophile can be rationalized by high ring strain, which elevates the highest occupied molecular orbital (HOMO) of the olefin, and a crown conformation, which minimizes geometric distortion towards an IEDDA transition state.[60] *Cis* ring fusion can enforce a half chair conformation upon TCO, which exacerbates these effects to obtain even higher reactivity (k_2 up to 10^6 $M^{-1}s^{-1}$) at the expense of stability.[61,62] Conversely, it was found that axially substituted TCOs were tenfold more reactive than equatorially substituted TCOs whilst being less susceptible towards *in vivo* isomerization to *cis*-cyclooctene (CCO) induced by copper-bound proteins.[63]

Synthetic advances towards both components of the TCO-tetrazine ligation have been of importance to enable their versatile application. For instance, the metal-catalyzed one-pot synthesis of tetrazines by Devaraj[64] expanded the precursor scope from aromatic nitriles to include alkyl nitriles and set the stage for the sustained emergence of improved methodologies towards functionalized tetrazines.[65–69] Furthermore, the direct, singlet sensitized photochemical transformation of functionalized CCOs to TCOs,[70–75] combined with selective complexation of the TCO product to Ag(I) in a flow based setup[76–78] has been a key method to simplify TCO synthesis. Modifications of this method can now synthesize TCOs in continuous flow[79] and have been applied to synthesize highly reactive *trans*-cycloheptene derivatives (k_2 = 10^7 M^{-1}s^{-1}).[80] Taken together, these developments confirm the status of the tetrazine ligation as a 'state of the art' bioorthogonal reaction, with applications branching from chemical biology towards medicine and materials science.[32]

1.3 Dissociative bioorthogonal chemistry

The selective release of a protective moiety to expose functionality within a cellular system, known as bioorthogonal bond cleavage reactions[81] or dissociative bioorthogonal chemistry,[82] constitutes the second pillar of bioorthogonal chemistry, which has been of increasing interest.[15,32,81–87] The first example of such a 'decaging' reaction was reported by Meggers[88] in 2006, where a ruthenium catalyst was employed to intracellularly cleave an allylcarbamate. Deprotection strategies via other metals, such as palladium[31] and gold,[89] through organic transformations like the Staudinger reduction,[90,91] and by means of photochemistry[92] have steadily emerged ever since.

Dissociative bioorthogonal methods based on cycloadditions have been of particular relevance towards *in vivo* applications. The IEDDA pyridazine elimination, an adaptation of the TCO-tetrazine ligation[39] reported by Robillard and co-workers in 2013,[93] was the first example of what is now regarded as 'click to release' chemistry (Figure 3A). This deprotection method can be applied to induce selective release of cytotoxic agents, such as doxorubicin and monomethyl auristatin E (MMAE), using antibody-drug conjugates (ADCs),[94,95] tetrazine-modified hydrogels,[96–98] tetrazine carbon nanotubes,[99] or enzyme-instructed supramolecular self-assembly (EISA)[100] in preclinical *in vivo* models. The method has also been increasingly applied towards chemical biology, for instance to control the activity proteins,[101–104] the recognition of antigens,[105,106] imaging and profiling of proteomes,[107] or the purification of biomolecules.[108] While the first *in* vivo application was reported in 2014 by Chen and co-workers,[101] a phase I clinical trial has already surfaced as a result of the work described by Royzen and Oneto.[98]
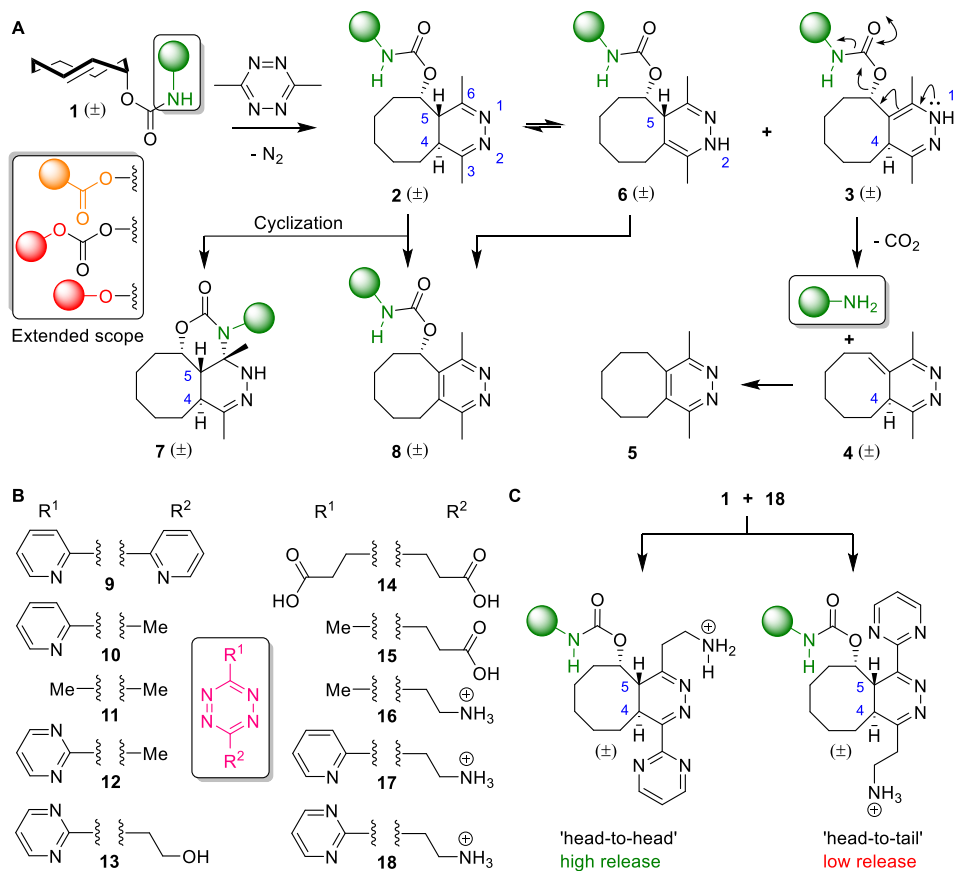
Figure 3 A) Mechanistic overview of the IEDDA pyridazine elimination, a 'click to release' bioorthogonal decaging method. B) A panel of tetrazine activators selected from literature.[93, 109, 103, 114] C) 'head-to-head' versus 'head-to-tail' click orientation affects subsequent tautomerization and elimination for asymmetric tetrazines.

Mechanistically, the IEDDA pyridazine elimination employs an axially positioned carbamate substituent, containing a 'caged' amine moiety, on the allylic position of TCO (Figure 3A, **1**). Tautomerization of the 4,5-tautomer (**2**) obtained after tetrazine ligation can therefore result in elimination from the 1,4-tautomer (**3**) to release the free amine, CO_2 and **4**, which can aromatize to form pyridazine **5**.[93] Subsequent studies by Weissleder[109] and Robillard[110] confirmed these observations and revealed the 2,5-tautomer (**6**) can contribute to additional formation of **3** by tautomerization back to **2**. Competing side reactions include 'dead end' cyclization of **2** to form **7**[109] and aromatization of **2** and **6** to form pyridazine **8**. The fast releasing **3** and the slow releasing **6** constitute a biphasic release profile which relies on formation of **3** and less

on the nature of the leaving group, thereby enabling the scope of the method to be extended to include release of esters, carbonates, and even ethers.[110–113]

Initial IEDDA ligation rate and subsequent tautomerization/elimination rate and yield are heavily affected by tetrazine substituents (Figure 3B).[93,103,109,114,115] Electron withdrawing groups (EWGs), such as 2-pyridine or pyrimidine substituents increase tetrazine ligation rates but can decrease release performance when used excessively. For instance, the poor release induced by **9** (12%) could be gradually increased to 46% (**10**) and 75% (**11**) by adding electron donating methyl substituents.[93] Chen and co-workers subsequently reported asymmetric tetrazines which combined a pyrimidine substituent for rapid tetrazine ligation with methyl (**12**) and ethanol (**13**) substituents to induce elimination.[103] Due to the profound acceleration and augmentation of release at reduced pH,[109,110] tetrazines which carry intramolecular proton sources, such as carboxylic acids (**14** and **15**)[109] and amines (**16** – **18**),[114] were developed to render the IEDDA pyridazine elimination pH independent. In this regard, the orientation of the initial IEDDA ligation for asymmetric tetrazines directs subsequent tautomerization: 'head-to-head' is desired over 'head-to-tail' (shown for **18** in Figure 3C). Notably, Mikula and co-workers[116] developed C_2-symmetric TCOs carrying double payloads to obtain fast and complete release irrespective of click orientation.

In addition to further developments concerning photodecaging[117–121] and metal induced deprotections,[122–124] various other cycloaddition-based decaging strategies have emerged in the wake of the IEDDA pyridazine elimination. For instance, Gamble and co-workers[125–127] utilized TCOs to trigger release from an azido derivatized *para*-aminobenzyloxycarbonyl (PABC) system (Figure 4A), whereas Taran and co-workers[128–134] developed a strain-promoted iminosydnone-cycloalkyne cycloaddition (SPICC) release strategy (Figure 4B). Furthermore, several additional tetrazine-induced release systems have recently surfaced. Devaraj,[135] Bernardes,[136] and Bradley[137] reported vinyl ether decaging (Figure 4C), which was extended towards vinylboronic acids by Bonger,[138] whereas Franzini reported release systems based on benzonorbornadienes[139,140] and isonitriles (Figure 4D).[141–145] Finally, reverse decaging methods, where tetrazine is the caging moiety, have been reported by Robillard[146] (Figure 4E) and Franzini[147] (Figure 4F) using highly reactive TCOs and isonitriles as triggers, respectively.
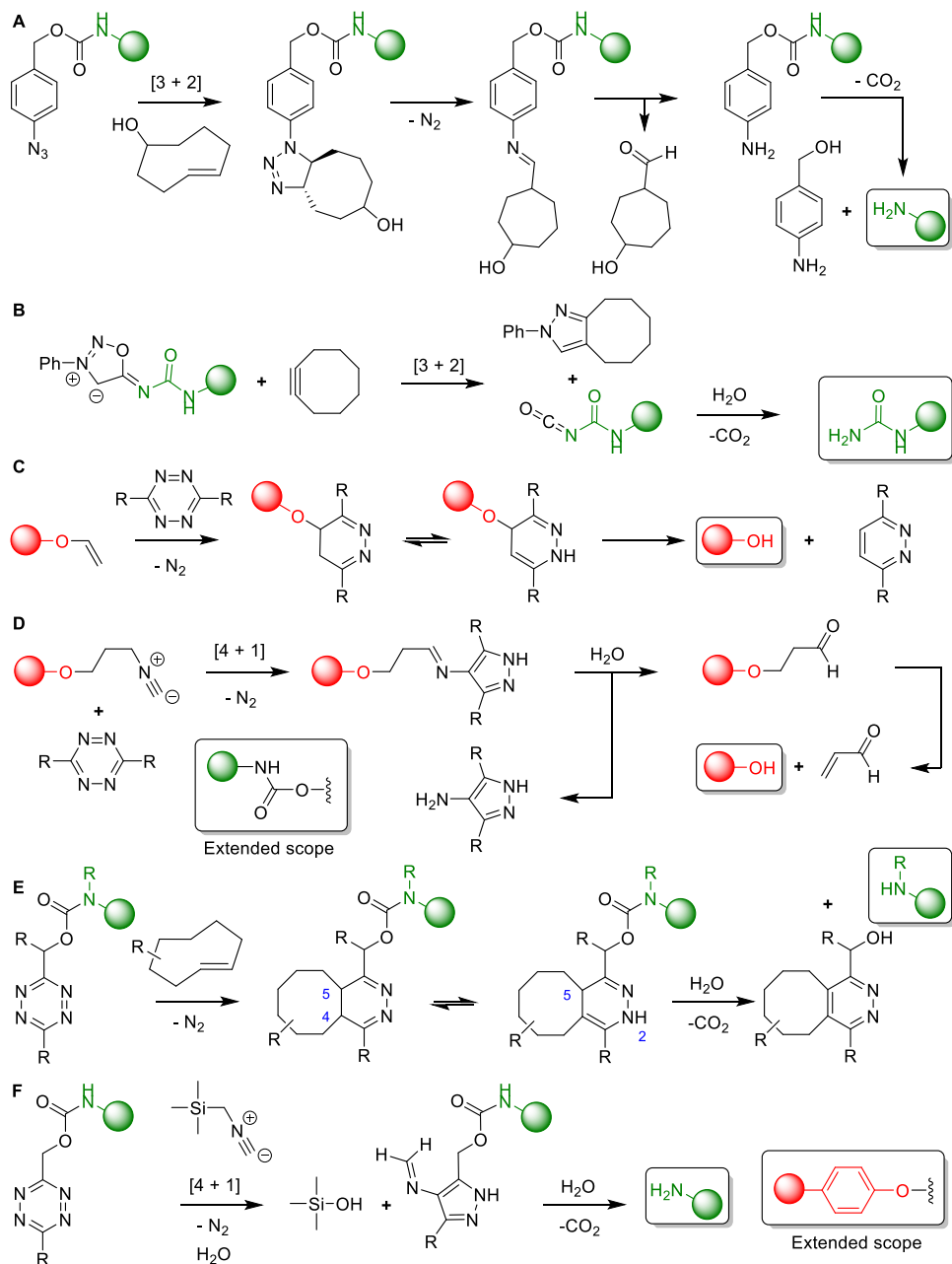
Figure 4 An overview of alternative dissociative bioorthogonal strategies based on cycloaddition chemistry A) TCO triggered release from azido derivatized *para*-aminobenzyloxycarbonyl (PABC) systems.[125-127] B) Strain-promoted iminosydnone-cycloalkyne cyloaddition (SPICC) release strategy.[128-134] C) Tetrazine-induced release from vinyl ethers.[135-137] D) Tetrazine induced release from isonitriles.[141-145] E/F) Reverse decaging methods to liberate tetrazine as the caging moiety using TCO[146] or isonitrile triggers.[147]

1.4 Outline of this Thesis

This research described in this Thesis is aimed to develop new synthetic strategies centered around the IEDDA pyridazine elimination to enable its application in chemical biology. **Chapter 2** presents an improved synthesis towards a frequently employed bifunctional TCO scaffold. **Chapter 3** describes attempts to develop an Fmoc SPPS-based strategy for TCO-modified peptide synthesis. **Chapter 4** reports an unprecedented method for *in vivo* chemical control over T-cell activation based on deprotection of TCO-modified peptide antigens. **Chapter 5** describes the design and synthesis of TCO caged glycolipid antigens to obtain chemical control over iNKT cells. **Chapter 6** reports synthetic methodology towards allylic TCO-ethers which is subsequently applied to control carbohydrate-induced protein expression in *E. coli*. **Chapter 7** summarizes this Thesis and provides future prospects based on the research conducted thus far.

1.5 References

[1]   E. Saxon, C. R. Bertozzi, *Science* **2000**, *287*, 2007–2010.

[2]   H. C. Hang, C. Yu, D. L. Kato, C. R. Bertozzi, *Proc. Natl. Acad. Sci.* **2003**, *100*, 14846–14851.

[3]   J. A. Prescher, C. R. Bertozzi, *Nat. Chem. Biol.* **2005**, *1*, 13–21.

[4]   E. M. Sletten, C. R. Bertozzi, *Angew. Chem. Int. Ed.* **2009**, *48*, 6974–6998.

[5]   E. M. Sletten, C. R. Bertozzi, *Acc. Chem. Res.* **2011**, *44*, 666–676.

[6]   C. R. Bertozzi, *Acc. Chem. Res.* **2011**, *44*, 651–653.

[7]   T. Carell, M. Vrabel, *Top. Curr. Chem.* **2016**, *374*, 1–21.

[8]   K. Lang, J. W. Chin, *Chem. Rev.* **2014**, *114*, 4764–4806.

[9]   E. A. Hoyt, P. M. S. D. Cal, B. L. Oliveira, G. J. L. Bernardes, *Nat. Rev. Chem.* **2019**, *3*, 147–171.

[10]   L. I. Willems, W. A. van der Linden, N. Li, K.-Y. Li, N. Liu, S. Hoogendoorn, G. A. van der Marel, B. I. Florea, H. S. Overkleeft, *Acc. Chem. Res.* **2011**, *44*, 718–729.

[11]   S. H. L. Verhelst, K. M. Bonger, L. I. Willems, *Molecules* **2020**, *25*, 5994.

[12]   Y. Tian, Q. Lin, *ACS Chem. Biol.* **2019**, *14*, 2489–2496.

[13]   D. M. Patterson, L. A. Nazarova, J. A. Prescher, *ACS Chem. Biol.* **2014**, *9*, 592–605.

[14]   R. D. Row, J. A. Prescher, *Acc. Chem. Res.* **2018**, *51*, 1073–1081.

[15]   S. S. Nguyen, J. A. Prescher, *Nat. Rev. Chem.* **2020**, *4*, 476–489.

[16]   H. Staudinger, J. Meyer, *Helv. Chim. Acta* **1919**, *2*, 635–646.

[17]   Y. G. Gololobov, L. F. Kasukhin, *Tetrahedron* **1992**, *48*, 1353–1406.

[18]   R. Huisgen, *Angew. Chem. Int. Ed.* **1963**, *2*, 565–598.

[19]   V. V. Rostovtsev, L. G. Green, V. V. Fokin, K. B. Sharpless, *Angew. Chem. Int. Ed.* **2002**, *41*, 2596–2599.

[20]   C. W. Tornøe, C. Christensen, M. Meldal, *J. Org. Chem.* **2002**, *67*, 3057–3064.

[21]   F. Himo, T. Lovell, R. Hilgraf, V. V. Rostovtsev, L. Noodleman, K. B. Sharpless, V. V. Fokin, *J. Am. Chem. Soc.* **2005**, *127*, 210–216.

[22]   B. T. Worrell, J. A. Malik, V. V. Fokin, *Science* **2013**, *340*, 457–460.

[23]   H. C. Kolb, M. G. Finn, K. B. Sharpless, *Angew. Chem. Int. Ed.* **2001**, *40*, 2004–2021.

[24]   J. M. Baskin, J. A. Prescher, S. T. Laughlin, N. J. Agard, P. V. Chang, I. A. Miller, A. Lo, J. A. Codelli, C. R. Bertozzi, *Proc. Natl. Acad. Sci.* **2007**, *104*, 16793–16797.

[25]   D. A. MacKenzie, A. R. Sherratt, M. Chigrinova, L. L. W. Cheung, J. P. Pezacki, *Curr. Opin. Chem. Biol.* **2014**, *21*, 81–88.

[26]   W. Song, Y. Wang, J. Qu, M. M. Madden, Q. Lin, *Angew. Chem. Int. Ed.* **2008**, *47*, 2832–2835.

[27]   J. Y. Axup, K. M. Bajjuri, M. Ritland, B. M. Hutchins, C. H. Kim, S. A. Kazane, R. Halder, J. S. Forsyth, A. F. Santidrian, K. Stafin, Y. Lu, H. Tran, A. J. Seller, S. L. Biroc, A. Szydlik, J. K. Pinkstaff, F. Tian, S. C. Sinha, B. Felding-Habermann, V. V. Smider, P. G. Schultz, *Proc. Natl. Acad. Sci.* **2012**, *109*, 16101–16106.

[28]   Y. A. Lin, J. M. Chalker, N. Floyd, G. J. L. Bernardes, B. G. Davis, *J. Am. Chem. Soc.* **2008**, *130*, 9642–9643.

[29]   J. M. Chalker, C. S. C. Wood, B. G. Davis, *J. Am. Chem. Soc.* **2009**, *131*, 16346–16347.

[30]   N. Li, R. K. V. Lim, S. Edwardraja, Q. Lin, *J. Am. Chem. Soc.* **2011**, *133*, 15316–15319.

[31]   R. M. Yusop, A. Unciti-Broceta, E. M. V. Johansson, R. M. Sánchez-Martín, M. Bradley, *Nat. Chem.* **2011**, *3*, 239–243.

[32]   B. L. Oliveira, Z. Guo, G. J. L. Bernardes, *Chem. Soc. Rev.* **2017**, *46*, 4895–4950.

[33]   S. Mayer, K. Lang, *Synthesis* **2016**, *49*, 830–848.

[34]   R. A. Carboni, R. V Lindsey Jr., *J. Am. Chem. Soc.* **1959**, *81*, 4342–4346.

[35]   J. Sauer, H. Wiest, *Angew. Chem.* **1962**, *74*, 353–353.

[36]   J. Sauer, G. Heinrichs, *Tetrahedron Lett.* **1966**, *7*, 4979–4984.

[37]   J. Balcar, G. Chrisam, F. X. Huber, J. Sauer, *Tetrahedron Lett.* **1983**, *24*, 1481–1484.

[38]   F. Thalhammer, U. Wallfahrer, J. Sauer, *Tetrahedron Lett.* **1990**, *31*, 6851–6854.

[39]   M. L. Blackman, M. Royzen, J. M. Fox, *J. Am. Chem. Soc.* **2008**, *130*, 13518–13519.

[40]   N. K. Devaraj, R. Weissleder, S. A. Hilderbrand, *Bioconjug. Chem.* **2008**, *19*, 2297–2299.

[41]   K. Lang, L. Davis, S. Wallace, M. Mahesh, D. J. Cox, M. L. Blackman, J. M. Fox, J. W. Chin, *J. Am. Chem. Soc.* **2012**, *134*, 10317–10320.

[42]   W. Chen, D. Wang, C. Dai, D. Hamelberg, B. Wang, *Chem. Commun.* **2012**, *48*, 1736–1738.

[43] J. Yang, J. Šečkutė, C. M. Cole, N. K. Devaraj, *Angew. Chem. Int. Ed.* **2012**, *51*, 7476–7479.

[44] D. M. Patterson, L. A. Nazarova, B. Xie, D. N. Kamber, J. A. Prescher, *J. Am. Chem. Soc.* **2012**, *134*, 18638–18643.

[45] J. Yang, Y. Liang, J. Šečkutė, K. N. Houk, N. K. Devaraj, *Chem. Eur. J.* **2014**, *20*, 3365–3375.

[46] S. Eising, F. Lelivelt, K. M. Bonger, *Angew. Chem. Int. Ed.* **2016**, *55*, 12243–12247.

[47] S. Eising, N. G. A. van der Linden, F. Kleinpenning, K. M. Bonger, *Bioconjug. Chem.* **2018**, *29*, 982–986.

[48] S. Eising, B.-T. Xin, F. Kleinpenning, J. J. A. Heming, B. I. Florea, H. S. Overkleeft, K. M. Bonger, *ChemBioChem* **2018**, *19*, 1648–1652.

[49] S. Eising, A. H. J. Engwerda, X. Riedijk, F. M. Bickelhaupt, K. M. Bonger, *Bioconjug. Chem.* **2018**, *29*, 3054–3059.

[50] S. B. Engelsma, L. I. Willems, C. E. van Paaschen, S. I. van Kasteren, G. A. van der Marel, H. S. Overkleeft, D. V. Filippov, *Org. Lett.* **2014**, *16*, 2744–2747.

[51] J. W. Wijnen, J. B. F. N. Engberts, *J. Org. Chem.* **1997**, *62*, 2039–2044.

[52] N. K. Devaraj, R. Upadhyay, J. B. Haun, S. A. Hilderbrand, R. Weissleder, *Angew. Chem. Int. Ed.* **2009**, *48*, 7013–7016.

[53] N. K. Devaraj, S. Hilderbrand, R. Upadhyay, R. Mazitschek, R. Weissleder, *Angew. Chem. Int. Ed.* **2010**, *49*, 2869–2872.

[54] R. Rossin, P. Renart Verkerk, S. M. van den Bosch, R. C. M. Vulders, I. Verel, J. Lub, M. S. Robillard, *Angew. Chem. Int. Ed.* **2010**, *49*, 3375–3378.

[55] R. Rossin, T. Lappchen, S. M. van den Bosch, R. Laforest, M. S. Robillard, *J. Nucl. Med.* **2013**, *54*, 1989–1995.

[56] R. Selvaraj, J. M. Fox, *Curr. Opin. Chem. Biol.* **2013**, *17*, 753–760.

[57] J. M. Fox, M. S. Robillard, *Curr. Opin. Chem. Biol.* **2014**, *21*, v–vii.

[58] R. Rossin, M. S. Robillard, *Curr. Opin. Chem. Biol.* **2014**, *21*, 161–169.

[59] J. Šečkutė, N. K. Devaraj, *Curr. Opin. Chem. Biol.* **2013**, *17*, 761–767.

[60] F. Liu, Y. Liang, K. N. Houk, *J. Am. Chem. Soc.* **2014**, *136*, 11483–11493.

[61] M. T. Taylor, M. L. Blackman, O. Dmitrenko, J. M. Fox, *J. Am. Chem. Soc.* **2011**, *133*, 9646–9649.

[62] A. Darko, S. Wallace, O. Dmitrenko, M. M. Machovina, R. A. Mehl, J. W. Chin, J. M. Fox, *Chem.*

Sci. **2014**, *5*, 3770–3776.

[63]   R. Rossin, S. M. Van Den Bosch, W. Ten Hoeve, M. Carvelli, R. M. Versteegen, J. Lub, M. S. Robillard, *Bioconjug. Chem.* **2013**, *24*, 1210–1217.

[64]   J. Yang, M. R. Karver, W. Li, S. Sahu, N. K. Devaraj, *Angew. Chem. Int. Ed.* **2012**, *51*, 5222–5225.

[65]   H. Wu, N. K. Devaraj, *Acc. Chem. Res.* **2018**, *51*, 1249–1259.

[66]   W. Mao, W. Shi, J. Li, D. Su, X. Wang, L. Zhang, L. Pan, X. Wu, H. Wu, *Angew. Chem. Int. Ed.* **2019**, *58*, 1106–1109.

[67]   W. D. Lambert, Y. Fang, S. Mahapatra, Z. Huang, C. W. am Ende, J. M. Fox, *J. Am. Chem. Soc.* **2019**, *141*, 17068–17074.

[68]   Y. Xie, Y. Fang, Z. Huang, A. M. Tallon, C. W. am Ende, J. M. Fox, *Angew. Chem. Int. Ed.* **2020**, *59*, 16967–16973.

[69]   L. Wang, J. Zhang, J. Zhao, P. Yu, S. Wang, H. Hu, R. Wang, *Catal. Rev.* **2020**, *62*, 524–565.

[70]   Y. Inoue, S. Takamuku, H. Sakurai, *Synthesis* **1977**, *1977*, 111–111.

[71]   Y. Inoue, S. Takamuku, Y. Kunitomi, H. Sakurai, *J. Chem. Soc., Perkin Trans. 2* **1980**, 1672–1677.

[72]   Y. Inoue, T. Kobata, T. Hakushi, *J. Phys. Chem.* **1985**, *89*, 1973–1976.

[73]   N. Yamasaki, Y. Inoue, T. Yokoyama, A. Tai, *J. Photochem. Photobiol. A Chem.* **1989**, *48*, 465–467.

[74]   Y. Inoue, T. Yokoyama, N. Yamasaki, A. Tai, *J. Am. Chem. Soc.* **1989**, *111*, 6480–6482.

[75]   H. Tsuneishi, T. Hakushi, Y. Inoue, *J. Chem. Soc. Perkin Trans. 2* **1996**, 1601.

[76]   M. Royzen, G. P. A. Yap, J. M. Fox, *J. Am. Chem. Soc.* **2008**, *130*, 3760–3761.

[77]   A. Darko, S. J. Boyd, J. M. Fox, *Synthesis* **2018**, *50*, 4875–4882.

[78]   J. E. Pigga, J. M. Fox, *Isr. J. Chem.* **2020**, *60*, 207–218.

[79]   D. Blanco-Ania, L. Maartense, F. P. J. T. Rutjes, *ChemPhotoChem* **2018**, *2*, 898–905.

[80]   Y. Fang, H. Zhang, Z. Huang, S. L. Scinto, J. C. Yang, C. W. am Ende, O. Dmitrenko, D. S. Johnson, J. M. Fox, *Chem. Sci.* **2018**, *9*, 1953–1963.

[81]   J. Li, P. R. Chen, *Nat. Chem. Biol.* **2016**, *12*, 129–137.

[82]   J. Tu, M. Xu, R. M. Franzini, *ChemBioChem* **2019**, *20*, 1615–1627.

[83]   N. K. Devaraj, *ACS Cent. Sci.* **2018**, *4*, 952–959.

[84]   K. Neumann, A. Gambardella, M. Bradley, *ChemBioChem* **2019**, *20*, 872–876.

[85]   A. L. Baumann, C. P. R. Hackenberger, *Curr. Opin. Chem. Biol.* **2019**, *52*, 39–46.

[86]   X. Ji, Z. Pan, B. Yu, L. K. De La Cruz, Y. Zheng, B. Ke, B. Wang, *Chem. Soc. Rev.* **2019**, *48*, 1077–1094.

[87]   T. Deb, J. Tu, R. M. Franzini, *Chem. Rev.* **2021**, *121*, 6850–6914.

[88]   C. Streu, E. Meggers, *Angew. Chem. Int. Ed.* **2006**, *45*, 5645–5648.

[89]   A. M. Pérez-López, B. Rubio-Ruiz, V. Sebastián, L. Hamilton, C. Adam, T. L. Bray, S. Irusta, P. M. Brennan, G. C. Lloyd-Jones, D. Sieger, J. Santamaría, A. Unciti-Broceta, *Angew. Chem. Int. Ed.* **2017**, *56*, 12548–12552.

[90]   J. B. Pawlak, G. P. P. Gential, T. J. Ruckwardt, J. S. Bremmers, N. J. Meeuwenoord, F. A. Ossendorp, H. S. Overkleeft, D. V. Filippov, S. I. van Kasteren, *Angew. Chem. Int. Ed.* **2015**, *54*, 5628–5631.

[91]   J. Luo, Q. Liu, K. Morihiro, A. Deiters, *Nat. Chem.* **2016**, *8*, 1027–1034.

[92]   A. Deiters, *ChemBioChem* **2009**, *11*, 47–53.

[93]   R. M. Versteegen, R. Rossin, W. ten Hoeve, H. M. Janssen, M. S. Robillard, *Angew. Chem. Int. Ed.* **2013**, *52*, 14112–14116.

[94]   R. Rossin, S. M. J. van Duijnhoven, W. ten Hoeve, H. M. Janssen, F. J. M. Hoeben, R. M. Versteegen, M. S. Robillard, *Bioconjug. Chem.* **2016**, *27*, 1697–1706.

[95]   R. Rossin, R. M. Versteegen, J. Wu, A. Khasanov, H. J. Wessels, E. J. Steenbergen, W. ten Hoeve, H. M. Janssen, A. H. A. M. van Onzen, P. J. Hudson, M. S. Robillard, *Nat. Commun.* **2018**, *9*, 1484.

[96]   J. M. Mejia Oneto, I. Khan, L. Seebald, M. Royzen, *ACS Cent. Sci.* **2016**, *2*, 476–482.

[97]   M. Czuban, S. Srinivasan, N. A. Yee, E. Agustin, A. Koliszak, E. Miller, I. Khan, I. Quinones, H. Noory, C. Motola, R. Volkmer, M. Di Luca, A. Trampuz, M. Royzen, J. M. Mejia Oneto, *ACS Cent. Sci.* **2018**, *4*, 1624–1632.

[98]   K. Wu, N. A. Yee, S. Srinivasan, A. Mahmoodi, M. Zakharian, J. M. Mejia Oneto, M. Royzen, *Chem. Sci.* **2021**, *12*, 1259–1271.

[99]   H. Li, J. Conde, A. Guerreiro, G. J. L. Bernardes, *Angew. Chem. Int. Ed.* **2020**, *59*, 16023–16032.

[100]   Q. Yao, F. Lin, X. Fan, Y. Wang, Y. Liu, Z. Liu, X. Jiang, P. R. Chen, Y. Gao, *Nat. Commun.* **2018**, *9*, 5032.

[101]   J. Li, S. Jia, P. R. Chen, *Nat. Chem. Biol.* **2014**, *10*, 1003–1005.

[102]   G. Zhang, J. Li, R. Xie, X. Fan, Y. Liu, S. Zheng, Y. Ge, P. R. Chen, *ACS Cent. Sci.* **2016**, *2*, 325–331.

[103]   X. Fan, Y. Ge, F. Lin, Y. Yang, G. Zhang, W. S. C. Ngai, Z. Lin, S. Zheng, J. Wang, J. Zhao, J. Li, P. R. Chen, *Angew. Chem. Int. Ed.* **2016**, *55*, 14046–14050.

[104]   L. Liu, Y. Liu, G. Zhang, Y. Ge, X. Fan, F. Lin, J. Wang, H. Zheng, X. Xie, X. Zeng, P. R. Chen, *Biochemistry* **2018**, *57*, 446–450.

[105]   A. M. F. van der Gracht, M. A. R. de Geus, M. G. M. Camps, T. J. Ruckwardt, A. J. C. Sarris, J. Bremmers, E. Maurits, J. B. Pawlak, M. M. Posthoorn, K. M. Bonger, D. V. Filippov, H. S. Overkleeft, M. S. Robillard, F. Ossendorp, S. I. van Kasteren, *ACS Chem. Biol.* **2018**, *13*, 1569–1576.

[106]   M. J. van de Graaff, T. Oosenbrug, M. H. S. Marqvorsen, C. R. Nascimento, M. A. R. de Geus, B. Manoury, M. E. Ressing, S. I. van Kasteren, *Bioconjug. Chem.* **2020**, *31*, 1685–1692.

[107]   S. Du, D. Wang, J.-S. Lee, B. Peng, J. Ge, S. Q. Yao, *Chem. Commun.* **2017**, *53*, 8443–8446.

[108]   E. Agustin, P. N. Asare Okai, I. Khan, M. R. Miller, R. Wang, J. Sheng, M. Royzen, *Chem. Commun.* **2016**, *52*, 1405–1408.

[109]   J. C. T. Carlson, H. Mikula, R. Weissleder, *J. Am. Chem. Soc.* **2018**, *140*, 3603–3612.

[110]   R. M. Versteegen, W. ten Hoeve, R. Rossin, M. A. R. de Geus, H. M. Janssen, M. S. Robillard, *Angew. Chem. Int. Ed.* **2018**, *57*, 10494–10499.

[111]   S. Davies, L. Qiao, B. L. Oliveira, C. D. Navo, G. Jiménez-Osés, G. J. L. Bernardes, *ChemBioChem* **2019**, *20*, 1541–1546.

[112]   S. Davies, B. L. Oliveira, G. J. L. Bernardes, *Org. Biomol. Chem.* **2019**, *17*, 5725–5730.

[113]   M. A. R. de Geus, G. J. M. Groenewold, E. Maurits, C. Araman, S. I. van Kasteren, *Chem. Sci.* **2020**, *11*, 10175–10179.

[114]   A. J. C. Sarris, T. Hansen, M. A. R. de Geus, E. Maurits, W. Doelman, H. S. Overkleeft, J. D. C. Codée, D. V. Filippov, S. I. van Kasteren, *Chem. Eur. J.* **2018**, *24*, 18075–18081.

[115]   M. A. R. Geus, E. Maurits, A. J. C. Sarris, T. Hansen, M. S. Kloet, K. Kamphorst, W. Hoeve, M. S. Robillard, A. Pannwitz, S. A. Bonnet, J. D. C. Codée, D. V. Filippov, H. S. Overkleeft, S. I. Kasteren, *Chem. Eur. J.* **2020**, *26*, 9900–9904.

[116]   M. Wilkovitsch, M. Haider, B. Sohr, B. Herrmann, J. Klubnick, R. Weissleder, J. C. T. Carlson, H. Mikula, *J. Am. Chem. Soc.* **2020**, *142*, 19132–19141.

[117]   C. W. Riggsbee, A. Deiters, *Trends Biotechnol.* **2010**, *28*, 468–475.

[118]   P. Klán, T. Šolomek, C. G. Bochet, A. Blanc, R. Givens, M. Rubina, V. Popik, A. Kostikov, J.

Wirz, *Chem. Rev.* **2013**, *113*, 119–191.

[119] S. Bonnet, *Dalt. Trans.* **2018**, *47*, 10330–10343.

[120] K. Hüll, J. Morstein, D. Trauner, *Chem. Rev.* **2018**, *118*, 10710–10747.

[121] A. Y. Vorobev, A. E. Moskalensky, *Comput. Struct. Biotechnol. J.* **2020**, *18*, 27–34.

[122] M. Yang, J. Li, P. R. Chen, *Chem. Soc. Rev.* **2014**, *43*, 6511–6526.

[123] E. Latocheski, G. M. Dal Forno, T. M. Ferreira, B. L. Oliveira, G. J. L. Bernardes, J. B. Domingos, *Chem. Soc. Rev.* **2020**, *49*, 7710–7729.

[124] P. Destito, C. Vidal, F. López, J. L. Mascareñas, *Chem. Eur. J.* **2021**, *27*, 4789–4816.

[125] S. S. Matikonda, D. L. Orsi, V. Staudacher, I. A. Jenkins, F. Fiedler, J. Chen, A. B. Gamble, *Chem. Sci.* **2015**, *6*, 1212–1218.

[126] S. S. Matikonda, J. M. Fairhall, F. Fiedler, S. Sanhajariya, R. A. J. Tucker, S. Hook, A. L. Garden, A. B. Gamble, S. S. Matikonda, *Bioconjug. Chem.* **2018**, *29*, 324–334.

[127] S. Dadhwal, J. M. Fairhall, S. K. Goswami, S. Hook, A. B. Gamble, *Chem. Asian J.* **2019**, *14*, 1143–1150.

[128] S. Bernard, D. Audisio, M. Riomet, S. Bregant, A. Sallustrau, L. Plougastel, E. Decuypere, S. Gabillet, R. A. Kumar, J. Elyian, M. N. Trinh, O. Koniev, A. Wagner, S. Kolodych, F. Taran, *Angew. Chem. Int. Ed.* **2017**, *56*, 15612–15616.

[129] M. Riomet, E. Decuypere, K. Porte, S. Bernard, L. Plougastel, S. Kolodych, D. Audisio, F. Taran, *Chem. Eur. J.* **2018**, *24*, 8535–8541.

[130] L. Plougastel, M. R. Pattanayak, M. Riomet, S. Bregant, A. Sallustrau, M. Nothisen, A. Wagner, D. Audisio, F. Taran, *Chem. Commun.* **2019**, *55*, 4582–4585.

[131] K. Porte, B. Renoux, E. Péraudeau, J. Clarhaut, B. Eddhif, P. Poinot, E. Gravel, E. Doris, A. Wijkhuisen, D. Audisio, S. Papot, F. Taran, *Angew. Chem. Int. Ed.* **2019**, *58*, 6366–6370.

[132] M. Riomet, K. Porte, L. Madegard, P. Thuéry, D. Audisio, F. Taran, *Org. Lett.* **2020**, *22*, 2403–2408.

[133] M. Riomet, K. Porte, A. Wijkhuisen, D. Audisio, F. Taran, *Chem. Commun.* **2020**, *56*, 7183–7186.

[134] K. Porte, M. Riomet, C. Figliola, D. Audisio, F. Taran, *Chem. Rev.* **2021**, *121*, 6718–6743.

[135] H. Wu, S. C. Alexander, S. Jin, N. K. Devaraj, *J. Am. Chem. Soc.* **2016**, *138*, 11429–11432.

[136] E. Jiménez-Moreno, Z. Guo, B. L. Oliveira, I. S. Albuquerque, A. Kitowski, A. Guerreiro, O. Boutureira, T. Rodrigues, G. Jiménez-Osés, G. J. L. Bernardes, *Angew. Chem. Int. Ed.* **2017**,

56, 243–247.

[137] K. Neumann, A. Gambardella, A. Lilienkampf, M. Bradley, *Chem. Sci.* **2018**, *9*, 7198–7203.

[138] L. P. W. M. Lelieveldt, S. Eising, A. Wijen, K. M. Bonger, *Org. Biomol. Chem.* **2019**, *17*, 8816–8821.

[139] M. Xu, J. Tu, R. M. Franzini, *Chem. Commun.* **2017**, *53*, 6271–6274.

[140] M. Xu, R. Galindo-Murillo, T. E. Cheatham, R. M. Franzini, *Org. Biomol. Chem.* **2017**, *15*, 9855–9865.

[141] J. Tu, M. Xu, S. Parvez, R. T. Peterson, R. M. Franzini, *J. Am. Chem. Soc.* **2018**, *140*, 8410–8414.

[142] J. Tu, D. Svatunek, S. Parvez, A. C. Liu, B. J. Levandowski, H. J. Eckvahl, R. T. Peterson, K. N. Houk, R. M. Franzini, *Angew. Chem. Int. Ed.* **2019**, *58*, 9043–9048.

[143] M. Xu, T. Deb, J. Tu, R. M. Franzini, *J. Org. Chem.* **2019**, *84*, 15520–15529.

[144] T. Deb, R. M. Franzini, *Synlett* **2020**, *31*, 938–944.

[145] J. Tu, M. Xu, R. M. Franzini, *Synlett* **2020**, *31*, 1701–1706.

[146] A. H. A. M. van Onzen, R. M. Versteegen, F. J. M. Hoeben, I. A. W. Filot, R. Rossin, T. Zhu, J. Wu, P. J. Hudson, H. M. Janssen, W. ten Hoeve, M. S. Robillard, *J. Am. Chem. Soc.* **2020**, *142*, 10955–10963.

[147] J. Tu, D. Svatunek, S. Parvez, H. J. Eckvahl, M. Xu, R. T. Peterson, K. N. Houk, R. M. Franzini, *Chem. Sci.* **2020**, *11*, 169–179.

2

# An optimized synthesis of bifunctional cyclooctenes for click to release chemistry

2.1 Introduction

Bioorthogonal chemistry is broadening in scope to include bond cleavage reactions alongside known ligation methods,[1–4] with many new reactions continuously emerging in the literature.[5–12] Amongst these, the inverse electron demand Diels-Alder (IEDDA) pyridazine elimination[13] comprises the first example of a bioorthogonal reaction that is today described as "click to release" (Figure 1 A). In the IEDDA decaging sequence, reaction of a tetrazine and a *trans*-cyclooctene (TCO) bearing a leaving group at the allylic position[14,15] results in a 4,5-dihydropyridazine intermediate. This adduct tautomerizes into 2,5- and 1,4-dihydropyridazines, the latter of which induces elimination of the allylic payload.[16,17] The biocompatibility of the tetrazine and TCO
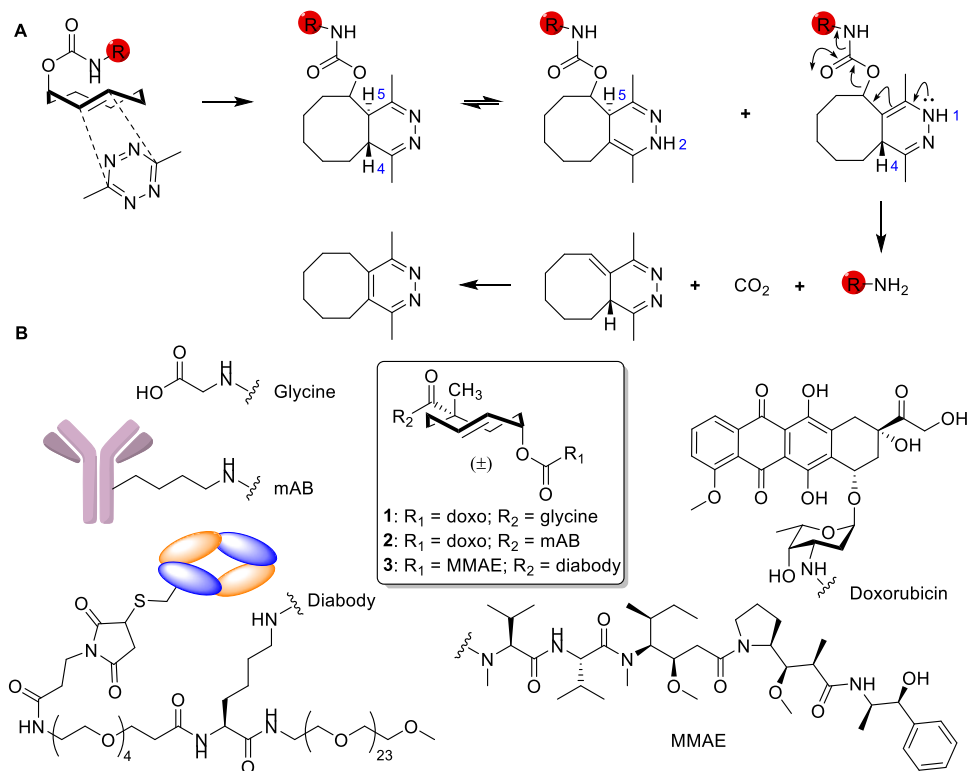
Figure 1 A) Overview of the inverse electron demand Diels-Alder (IEDDA) pyridazine elimination. B) Cytotoxic prodrugs **1-3** employed in *in vivo* experiments by Royzen and Oneto[22] and Robillard and co-workers.[18-19]

components, combined with their selectivity and overall deprotection rate have culminated in various applications, in which the area of cytotoxic (pro)drug activation[18–22] has received increasing interest.

While the tetrazine and TCO pair for this click reaction are inherently selective towards each other, the actual spatiotemporal control within biological systems is often achieved by employing another modality to direct localization of the reaction components.[18–22] Royzen and Oneto utilized tetrazine modified hydrogels in combination with TCO modified doxorubicin.[20–22] A phase 1 clinical trial towards the treatment of solid tumors is currently in progress for a tetrazine modified sodium hyaluronate and a TCO equipped with doxorubicin as payload and glycine to enhance aqueous solubility (**1**, Figure 1B).[22] This bifunctional TCO was initially reported by Robillard and co-workers to serve as cleavable linker for antibody-drug conjugates (ADCs), resulting in triggered release of doxorubicin *in vitro* and in tumor-bearing mice (**2**, Figure 1B).[18] This premise was refined with a diabody-based ADC (**3**, Figure 1B) to
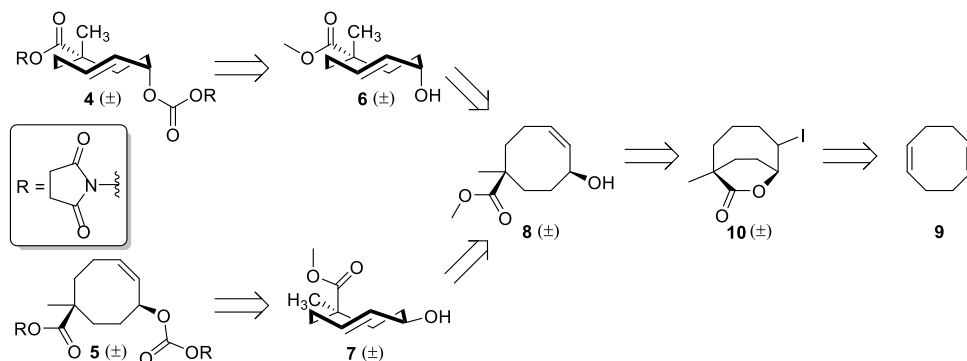
Scheme 1 Retrosynthetic route for bifunctional TCO reagent **4** and bifunctional CCO reagent **5** from a shared intermediate (**8**), which can be synthesized from **9** via **10**.

release monomethyl auristatin E (MMAE) from the same TCO motif, thereby outperforming the FDA approved, protease cleavable ADC Adcetris in two preclinical *in vivo* tumor models (LS174T and OVCAR-3, respectively).[19]

As the bifunctional TCO scaffold fulfills a central role towards *in vivo* utilization of the IEDDA pyridazine elimination, its synthetic accessibility is of importance to enable novel applications. This Chapter presents a simplified synthetic procedure towards bifunctional TCO reagent **4** based on the initially published route[18] (Scheme 1). A novel bifunctional *cis*-cyclooctene (CCO) reagent (**5**), which proved difficult to directly access from CCO intermediates, is additionally described. TCO reagent **4** and CCO reagent **5** were synthesized from TCOs **6** and **7**, respectively. Both reagents share a common intermediate (**8**), which was synthesized from 1,5-cyclooctadiene **9** via iodolactone **10**.

2.2 Results and discussion

Cyclooctadiene **9** was brominated in HBr/AcOH to obtain **11** in near-quantitative yield (Scheme 2). Nucleophilic substitution of **11** with NaCN in DMSO afforded nitrile **12** in 56% yield, which was subsequently hydrolyzed in the presence of KOH and H_2O_2 to obtain **13** in 74% yield. Reproducibility on large scale for this procedure, as described by Hartley[23] for a related system and adapted for **12** by Mitchell and co-workers,[24] was obtained by monitoring the consumption of nitrile **12** to the intermediate amide at 40°C, before refluxing overnight. Carboxylic acid **13** was α-methylated to obtain **14**, thereby preventing epimerization in subsequent steps and enabling regioselective conjugation chemistry.[18] These initial steps (bromination, cyanide substitution, oxidation, basic hydrolysis and α-methylation) were carried out using crude reaction mixtures obtained after aqueous workup. Iodolactonization of **14** afforded **10**, which was purified by crystallization from EtOH to result in a yield of 23% over five steps from
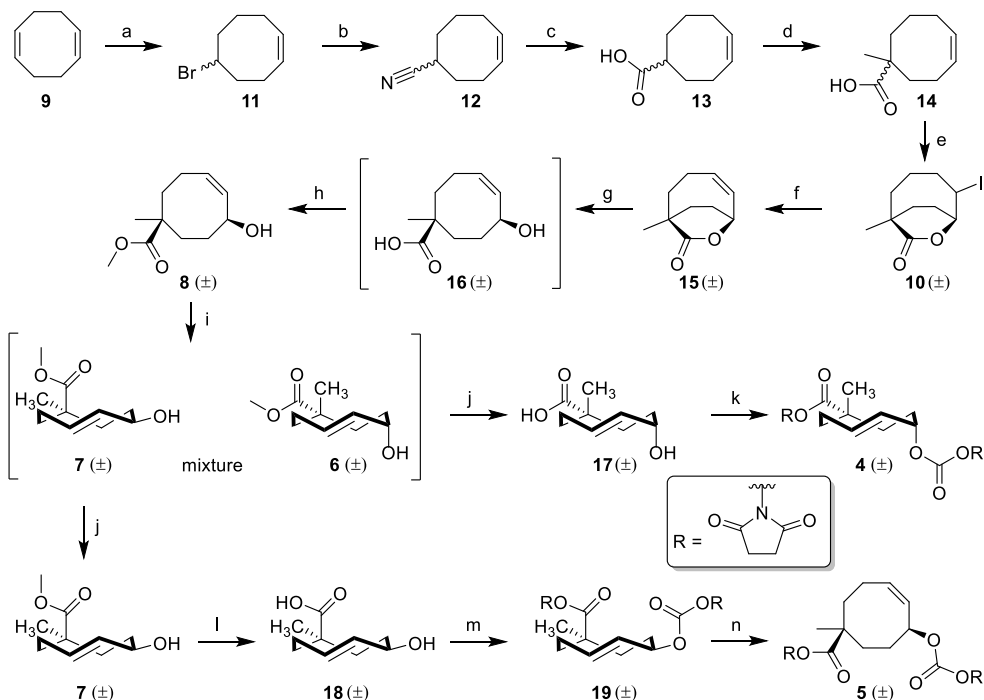
Scheme 2 Synthesis of cyclooctene reagents **4** and **5** from **9**. Reagents/conditions: (a) HBr, AcOH, 0°C to rt, 99%; (b) NaCN, DMSO, 100°C, 56%; (c) H_2O_2, KOH, H_2O, EtOH, 40 °C to reflux, 74%; (d) LDA, CH_3I, THF, -78°C to 40°C, 98%; (e) I_2, KI, $NaHCO_3$, DCM, H_2O, 0°C, 56%; (f) DBU, toluene, 70°C, 92%; (g) KOH, dioxane, H_2O, 0°C to rt; (h) CH_3I, DMF, 0°C to rt, 77% over 2 steps; (i) methyl benzoate, hν (254 nm), Et_2O/heptane, rt, 84%; (j) KOH, MeOH, H_2O, 4°C, 43% (**7**), 42% (**17**); (k) N,N'-disuccinimidyl carbonate, DIPEA, DMAP, MeCN, rt, 72%; (l) KOH, MeOH, H_2O, 50°C, 79%; (m) N,N'-disuccinimidyl carbonate, DIPEA, MeCN, rt, 66%; (n) hν (CFL), $CDCl_3$, rt, 74%.

9 at 500 mmol scale, without the need for the previously reported distillations.[18] Subsequent β-elimination in the presence of DBU afforded **15** in 92% yield.

The transesterification procedure starting from bicyclic lactone **15** (64 hours, 48% yield)[18] was replaced by a one-pot, two-step procedure to improve overall conversion and reaction time. Saponification afforded monocyclic carboxylic acid **16**, which was directly methylated to obtain methyl ester **8** in 77% yield over two steps. Photoisomerization[25] resulted in a 1 : 1.4 mixture of axial isomer **6** (axial hydroxyl, equatorial methyl ester) and equatorial isomer **7** (equatorial hydroxyl, axial methyl ester), respectively. The isomeric mixture was treated with potassium hydroxide at 4°C to selectively hydrolyze axial isomer **6**, followed by acid-base extraction to separately obtain carboxylic acid **17** and ester **7**. The bis-NHS functionalization of **17** into **4** (three days, 46% yield)[18] was accelerated using nucleophilic catalysis (DMAP). Hydrolysis of
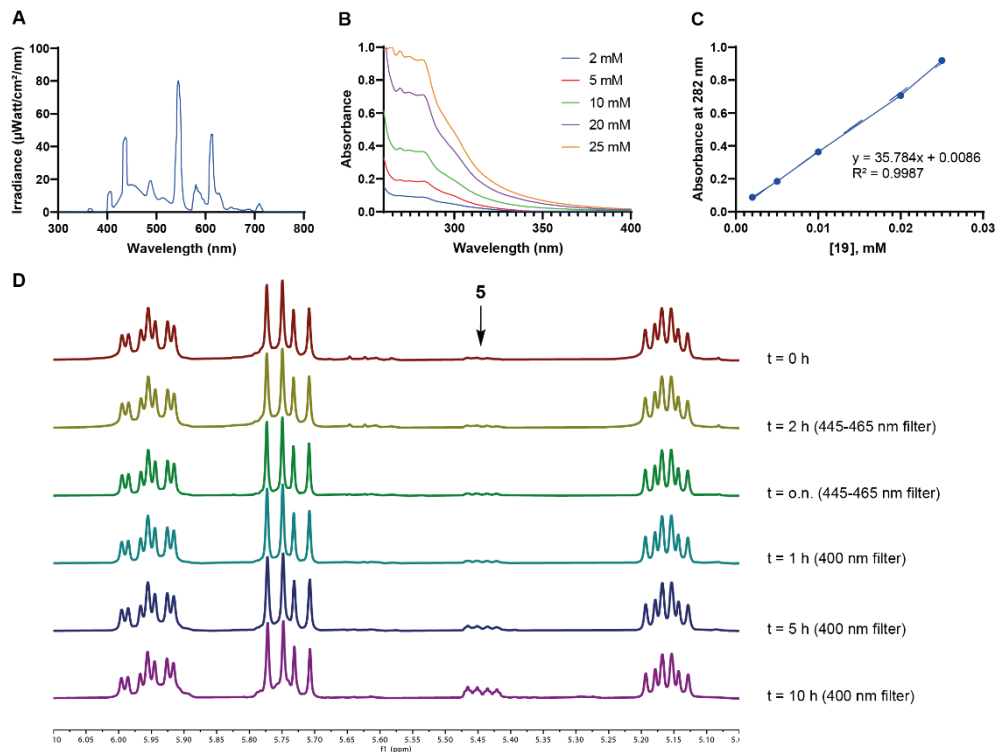
Figure 2 A) Emission spectrum of CFL lamp (Philips Tornado, 1450 lumen, 23 W, E27, ES 220-240V, 50/60 Hz, CDL 865, 170 mA, ≤ 2.5 mg Hg, 6500 K) used for photochemical conversion of **19** to **5**. B) UV-absorption of compound **19** (2, 5, 10, 20, 25 mM in CHCl$_3$). C) Linear fitting of the absorbance at 282 nm vs. the concentration of **19** yielded the extinction coefficient (ε) in L mol^{-1} cm^{-1} from the slope of the linear fit. D) ^{1}H NMR analyses of a white light irradiation experiment of **19**. Compound **19** (0.1 M in CDCl$_3$, 0.6 mL, NMR tube) was irradiated using a Xenon Arc (1000 W) at 20 cm distance. The temperature of sample was kept at 25°C using water cooling. The sample was measured before starting the experiment (top entry, red line), following irradiation with a filter which absorbs ≤ 445-465 nm ("445-465 filter"), following irradiation with a filter which absorbs ≤ 400 nm ("400 filter") at indicated times. Formation of **5** was followed by observing the characteristic signal marked at 5.45 ppm.

the product during chromatographic purification was prevented by employing neutralized silica gel, which resulted in a yield of 72%.

Synthesis of bifunctional CCO reagent **5** was envisioned from carboxylic acid **16** under similar conditions. However, attempts to directly functionalize **16** resulted in formation of bicyclic lactone **15**. Instead, equatorial isomer **7** was hydrolyzed (to afford **18**) and functionalized to obtain equatorial TCO reagent **19**, followed by *trans* to *cis* isomerization in the presence of visible light (26 W CFL bulb, Figure 2A) to obtain bifunctional CCO reagent **5**. Absorbance of **19** was characterized at 2 – 25 mM in CHCl$_3$ (Figure 2B) to reveal λ$_{max}$ = 282 nm; absorbance at this wavelength was in agreement
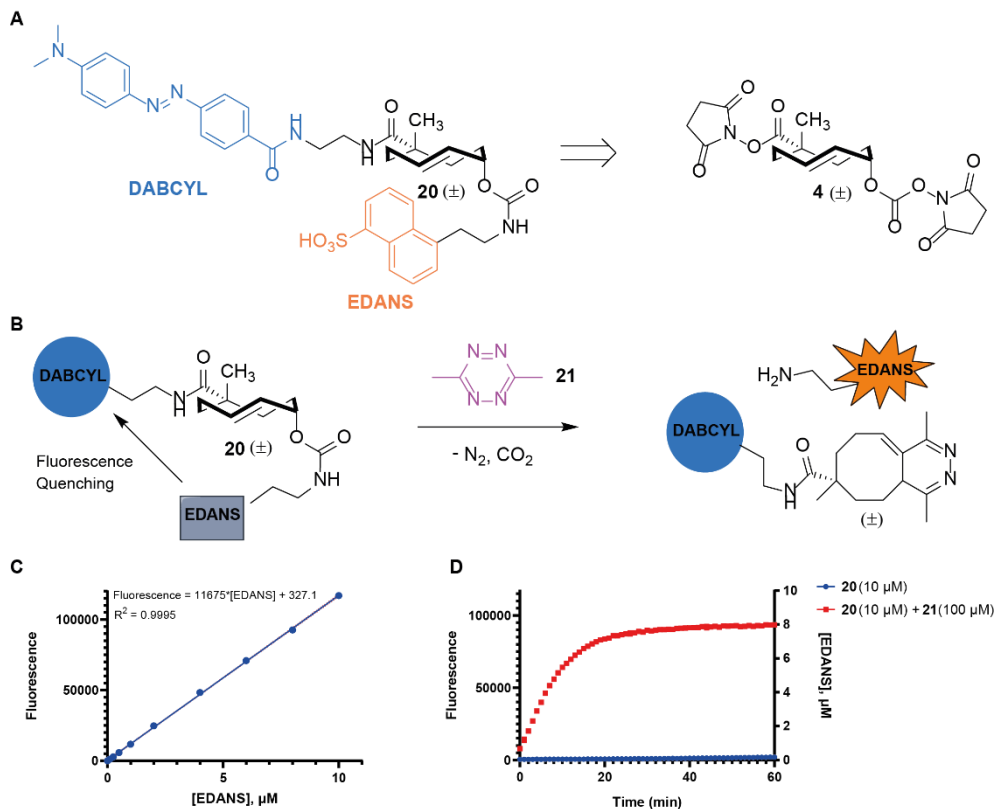
Figure 3 A) TCO **20** was projected to be synthesised from bifunctional TCO **4**. B) Schematic representation of the TCO-quenched fluorescence assay. The bifunctional TCO-reporter-quencher pair **20** does not display fluorescence in its native state due to fluorescence quenching between the EDANS fluorophore and DABCYL quencher. The EDANS fluorophore is released upon IEDDA pyridazine elimination, thereby disabling the fluorescence quenching and enabling a fluorescent readout for the elimination reaction. C/D) Quantification of fluorescence observed for TCO-reporter-quencher pair **20** (10 µM) using tetrazine **21** at 100 µM (n = 3). C) Linear regression of fluorescence observed for EDANS in µM. D) Fluororescence observed for TCO-reporter-quencher pair **20** (10 µM) upon treatment with tetrazine **21** (100 µM). The fluorescence observed was correlated to the linear regression for EDANS fluoresence, revealing an elimation efficiency of 80% after 60 minutes.

with Beer's law (Figure 2C). Xenon Arc (1000 W) irradiation of **19** with wavelength filters indicated light with a wavelength ≤ 445 nm is necessary to induce the photoisomerization of **19** to **5** (Figure 2D).

The research summarized below was conducted in collaboration with Dr. Elmer Maurits (Leiden University), Alexi J.C. Sarris (Leiden University) and Dr. Thomas Hansen (Leiden University). Full details can be found in the published article.[26]

Implementation of the IEDDA pyridazine elimination in biological systems is reliant on the identification of suitable tetrazines in terms of reaction speed with respect to both initial Diels-Alder rate, rate of the ensuing retro-Diels-Alder and final elimination step. The nature of substituents on the two tetrazine carbons can exert drastic effects on both the rate and yield of the release obtained.[13,17,27,28] Fluorogenic reporters are important tools to characterize tetrazine release behavior, and these are often supported by NMR[13,16] or LC-MS[17,27,28] analyses. The profound effect of pH and buffer concentration on IEDDA pyridazine elimination complicates such studies.[16,17] Weissleder and co-workers[17] reported a quenched fluorescence assay, in which the tetrazine was modified with a quencher moiety to suppress fluorescence until alkylamine release occurred. This method, however, does not allow the characterization of unmodified tetrazines, which lack this quencher moiety, at low concentrations.

With these considerations in mind, bifunctional TCO **4** was used to design fluorogenic TCO **20**, which combines an EDANS fluorophore and a DABCYL quencher on the bifunctional TCO scaffold (Figure 3A). Condensation of **4** with the EDANS moiety occurred with complete regioselectivity towards the carbonate due to the steric hindrance induced by the methyl group. This was followed by functionalization with the complementary DABCYL quencher to obtain TCO-reporter-quencher pair **20**. Functionalization with EDANS and DABCYL occurred with the same degree of regioselectivity for CCO reagent **5**.

TCO **20** is fluorogenic by virtue of intramolecular fluorescence quenching until the EDANS fluorophore is released from the post-ligation construct, and could thus serve to determine overall properties of the IEDDA pyridazine elimination (Figure 3B). The reaction between **20** (10 μM) and 3,6-dimethyltetrazine **21** (100 μM) was characterized by quantifying the fluorescence emitted from the liberated EDANS fluorophore (Figure 3C/D). This experiment showed an EDANS release yield of 80% after 1 h, which corresponds with other reports.[13,16,17] Furthermore, a CCO analog of **20** was unresponsive towards treatment with tetrazine **21**, as no fluorescence was detected for this reaction pair.

Fluorogenic TCO **20** was subsequently employed to evaluate a panel of tetrazines selected from literature.[17,27,28] Pseudo-first-order rate constants (k_{obs}) and elimination yields after 4 h were determined based on a 96-well plate reader setup followed by data processing according to biphasic decay trend lines. Screening different concentrations of **20** with an excess of tetrazine enabled separation of the rate constants for the initial cycloaddition step and the subsequent tautomerization/elimination process, k_{IEDDA} and $k_{release}$, respectively.

2.3 Conclusions

In conclusion, a streamlined synthetic procedure is presented for the widely used bifunctional TCO reagent **4**. Crystallization of iodolactone **10** enables the initial steps of the route to be carried out using crude reaction mixtures whilst obtaining an intermediate product of high purity. Transesterification of **15** was replaced by a two-step saponification-methylation procedure, improving yield and decreasing reaction time. Bis-NHS functionalization of axial TCO **17** was accelerated by nucleophilic catalysis and the chromatographic purification of the final product **4** was optimized. A novel CCO reagent, **5**, was synthesized by *trans* to *cis* photoisomerization of equatorial TCO **19**.

TCO reagent **4** was employed for the design and synthesis of fluorogenic TCO **4**. This fluorogenic probe (**4**) combines the EDANS-DABCYL fluorophore-quencher pair with the bifunctional TCO scaffold, thereby linking the intramolecular fluorescence quenching to **4** and intermediates which occur after tetrazine ligation, but before elimination of the allylic payload. Kinetic analysis was conducted on a panel of tetrazines, thereby demonstrating the feasibility of this 96-well plate assay.

2.4 Experimental procedures

General methods: Commercially available reagents and solvents were used as received. Moisture and oxygen sensitive reactions were performed under an argon or N_2 atmosphere (balloon). MeCN, DMSO, DMF, DCM, toluene, THF, dioxane and Et_2O were stored over (flame-dried) 4 Å molecular sieves (8-12 mesh). DIPEA was stored over KOH pellets. TLC analysis was performed using aluminum sheets, pre-coated with silica gel (Merck, TLC Silica gel 60 F_{254}). Compounds were visualized by UV absorption (λ = 254 nm), by spraying with either a solution of $KMnO_4$ (20 g/L) and K_2CO_3 (10 g/L) in H_2O, a solution of $(NH_4)_6Mo_7O_{24} \cdot 4H_2O$ (25 g/L) and $(NH_4)_4Ce(SO_4)_4 \cdot 2H_2O$ (10 g/L) in 10% H_2SO_4, 20% H_2SO_4 in EtOH, or phosphomolybdic acid in EtOH (150 g/L), where appropriate, followed by charring at ca. 150°C. Column chromatography was performed on Screening Devices b.v. Silica Gel (particle size 40-63 μM, pore diameter 60 Å). ^1H, ^{13}C APT, ^1H COSY and HSQC spectra were recorded with a Bruker AV-400 (400/100 MHz) or AV-500 (500/125 MHz) spectrometer. Chemical shifts are reported as δ values (ppm) and were referenced to tetramethylsilane (δ = 0.00 ppm) or the residual solvent peak as internal standard. *J* couplings are reported in Hz. High resolution mass spectra were recorded by direct injection (2 μL of a 1 μM solution in H_2O/MeCN 1:1 and 0.1% formic acid) on a mass spectrometer (Q Exactive HF Hybrid Quadrupole-Orbitrap) equipped with an electrospray ion source in positive mode (source voltage 3.5 kV, sheath gas flow 10, capillary temperature 275°C) with resolution R = 240,000 at m/z 400 (mass range m/z = 160-2,000) and an external lock mass. The high resolution mass spectrometer was calibrated prior to measurements with a calibration mixture (Thermo Finnigan). The synthesis of tetrazine **21** is described in Chapter 4.[29]

Preparation of neutralized silica gel: Unmodified silica gel (500 gram) was slowly dispersed into a 3 L round-bottom flask containing a stirring volume of H_2O (1.7 L). NH_4OH (28% w/w, 100 mL) was added and the alkaline suspension was stirred for 30 min. The suspension was filtered, washed with H_2O and the silica gel was dried on aluminium foil overnight at rt. The silica was transferred into a glass container and remaining traces of H_2O were removed by drying in an oven at 150°C overnight.

Photoisomerization methods: General guidelines were followed as described by Royzen *et al.*[25] Photochemical isomerization of **8** was performed using a Southern New England Ultraviolet Company Rayonet reactor (model RPR-100) equipped with 16 bulbs (part number RPR-2537A, λ = 254 nm). Photolysis was performed in a 1500 mL quartz flask (Southern New England Ultraviolet Company; part number RQV-323). A HPLC pump (Jasco; model PU-2088 Plus) was used to circulate solvent through the photolysis apparatus. An empty solid load cartridge with screw cap, frits, O-ring and end tips (40 g, iLOK, SD.0000.040, Screening Devices b.v.) was manually loaded with the specified silica gel to function as the stationary phase.

The emission spectrum of Figure 2A was recorded using an integrating sphere connected to an Avantes 2048L StarLine spectrometer detecting in the region of 300 – 1000 nm. The Avasoft 8.5 software from Avantes was used for recording the spectrum. Absorption spectra of compound **19** (Figure 2B) were recorded at room temperature with a Cary60 from Agilent and 1 cm x 1 cm quartz cuvettes from FireflySci.
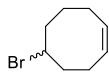
(Z)-5-Bromocyclooct-1-ene (11): A 500 mL round-bottom flask charged with HBr (33 % w/w in AcOH, 85 mL, 490 mmol, 0.98 equiv) under N_2 was cooled to 0°C before adding (1Z,5Z)-cycloocta-1,5-diene (**9**, 61.3 ml, 500 mmol, 1.0 equiv) dropwise over 30 minutes. The reaction mixture was stirred for 72 h and allowed to warm to room temperature. The reaction mixture was diluted with H_2O (500 mL) and extracted with 10% Et_2O in pentane (3 x 750 mL). The combined organic layers were washed with H_2O (250 mL) and $NaHCO_3$ (satd., 250 mL), dried over $MgSO_4$, filtered and concentrated *in vacuo*. The crude bromide **11** (93.8 g, 496 mmol, 99%) was obtained as an oil and used in the next step without further purification: R_f = 0.7 (pentane); ^1H NMR (400 MHz, $CDCl_3$) δ 5.70 – 5.54 (m, 2H), 4.40 – 4.21 (m, 1H), 2.47 – 2.37 (m, 1H), 2.34 – 2.19 (m, 3H), 2.19 – 1.99 (m, 4H), 1.79 – 1.67 (m, 1H), 1.60 – 1.48 (m, 1H); ^{13}C NMR (101 MHz, $CDCl_3$) δ 129.7, 129.3, 55.7, 39.8, 37.2, 27.1, 25.4, 25.3. Spectroscopic data was in agreement with literature.[30]
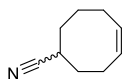
(Z)-Cyclooct-4-ene-1-carbonitrile (12): A 1 L round-bottom flask was charged with sodium cyanide (67.4 g, 1375 mmol, 2.78 equiv) and placed under N_2. Anhydrous DMSO (250 mL) was added, and the suspension was stirred at 100°C to dissolve the cyanide. The crude bromide **11** (93.7 g, 496 mmol, 1.0 equiv) was added to the reaction mixture over 30 minutes using a dropping funnel under N_2. The reaction mixture was stirred for 4 h at 100°C before cooling on ice and diluting with H_2O (2.5 L). The aqueous phase was extracted with pentane (5 x 1 L). Performing the extraction without cooling the reaction mixture often resulted in the formation of emulsions. The combined organic layers were dried over $MgSO_4$, filtered and concentrated *in vacuo*. The crude nitrile **12** (37.8 g, 280 mmol, 56%) was obtained as an orange oil and used in the next step without further purification: R_f = 0.7 (10% Et_2O in pentane); ^1H NMR (400 MHz, $CDCl_3$) δ 5.76 – 5.50 (m, 2H), 2.85 – 2.73 (m, 1H), 2.51 – 2.35 (m, 1H), 2.33 – 2.19 (m, 1H), 2.19 – 2.06 (m, 2H), 2.06 – 1.92 (m, 1H), 1.92 – 1.74 (m, 4H), 1.55 – 1.37 (m, 1H); ^{13}C NMR (101 MHz, $CDCl_3$) δ 130.8, 129.0, 123.4, 32.2, 29.5, 28.2, 27.1, 25.1, 23.4; HRMS: calculated for $C_9H_{14}N_1$ 136.11208 [M+H]$^+$; found 136.11210. Spectroscopic data was in agreement with literature.[24]
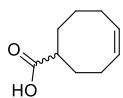
(Z)-Cyclooct-4-ene-1-carboxylic acid (13): The crude nitrile **12** (37.8 g, 280 mmol, 1.0 equiv) was dissolved in EtOH (140 mL) in a 3 L round-bottom flask. KOH (30% w/w, 420 mL) was added and the reaction mixture was stirred at 40°C. H_2O_2 (30% w/w, 250 mL, 2.45 mol, 8.75 equiv) was added to the reaction mixture over 2 h using a dropping funnel. After complete addition, the foamy reaction mixture was stirred for an additional 5 h at 40°C. TLC analysis (20% Et_2O in pentane) confirmed complete consumption of nitrile **12**. The temperature was gradually raised (increments of 20°C) to reflux. The reaction mixture was refluxed for 17 h before cooling down to room temperature. H_2O (1 L) was added and the mixture was washed with heptane (1 L). The organic layer was extracted with H_2O (2 x 750 mL). The combined aqueous layers were acidified with HCl (37% w/w) to pH 1. Then, the combined acidified aqueous layers were extracted with Et_2O (5 x 400 mL). The combined organic layers were dried over $MgSO_4$, filtered and concentrated *in vacuo*. The crude carboxylic acid **13** (31.8 g, 206 mmol, 74%) was obtained as a yellow oil and used in the next step without further purification: R_f = 0.5 (10% Et_2O, 1% AcOH in pentane); ^1H NMR (400 MHz, $CDCl_3$) δ 10.80 (br s, 1H), 6.09 – 5.26 (m, 2H), 2.56 – 2.45 (m, 1H), 2.45 – 2.32 (m, 1H), 2.21 – 2.02 (m, 4H), 1.97 – 1.84

(m, 1H), 1.79 – 1.52 (m, 3H), 1.47 – 1.33 (m, 1H); ^{13}C NMR (101 MHz, CDCl$_3$) δ 184.4, 130.7, 129.6, 43.3, 31.5, 29.3, 27.9, 26.0, 24.1; HRMS: calculated for C$_9$H$_{15}$O$_2$ 155.10666 [M+H]$^+$; found 155.10705. Spectroscopic data was in agreement with literature.[24]
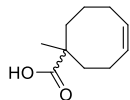
(Z)-1-Methylcyclooct-4-ene-1-carboxylic acid (14): Diisopropylamine (109 mL, 763 mmol, 3.7 equiv) was dissolved in anhydrous THF (250 mL) in a 2 L round-bottom flask under N$_2$. The solution was cooled to -50°C. *n*-Butyllithium (11 M in hexanes, 63.7 mL, 701 mmol, 3.4 eq) was added dropwise over 30 minutes whilst maintaining a temperature between -60°C and -40°C. The reaction mixture was stirred for 1 h at -50°C. Crude carboxylic acid **13** (31.8 g, 206 mmol, 1.0 equiv) was dissolved in anhydrous THF (100 mL) under N$_2$ and subsequently added to the reaction mixture using a double tipped needle under N$_2$ pressure. The reaction mixture was stirred for 1 h and allowed to warm to -20°C. Subsequently, the reaction mixture was stirred for 3 h at 50°C. Afterwards, the reaction mixture was cooled to -50°C before slowly adding CH$_3$I (51.6 mL, 825 mmol, 4.0 equiv) over 30 min. The reaction mixture was stirred for 17 h and allowed to warm to room temperature. Next, the reaction mixture was stirred for 3 h at 50°C. The reaction mixture was cooled on ice, quenched with NH$_4$Cl (satd., 50 mL) and concentrated *in vacuo*. The residue was diluted with HCl (2 M, 350 mL) and toluene (150 mL). The organic layer was washed with HCl (2 M, 100 mL). The combined aqueous layers were extracted with toluene (2 x 250 mL). The combined organic layers were dried over MgSO$_4$, filtered and concentrated *in vacuo*. The crude, methylated carboxylic acid **14** (34.15 g, 203 mmol, 98%) was obtained as a dark oil and used in the next step without further purification: R$_f$ = 0.5 (10% Et$_2$O, 1% AcOH in pentane); ^{1}H NMR (400 MHz, CDCl$_3$) δ 10.65 (br s, 1H), 5.69 (dt, *J* = 11.1, 5.5 Hz, 1H), 5.53 – 5.42 (m, 1H), 2.42 – 2.05 (m, 5H), 1.90 – 1.82 (m, 1H), 1.79 – 1.50 (m, 4H), 1.25 (s, 3H); ^{13}C NMR (101 MHz, CDCl$_3$) δ 185.0, 131.9, 126.5, 46.1, 35.2, 32.2, 27.0, 25.9, 24.7, 24.6; HRMS: calculated for C$_{10}$H$_{17}$O$_2$ 169.12231 [M+H]$^+$; found 169.12274. Spectroscopic data was in agreement with literature.[18]
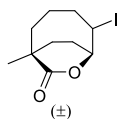
Bicyclic iodolactone 10: The crude, methylated carboxylic acid **14** (34.15 g, 203 mmol, 1.0 equiv) was dissolved in a mixture of DCM (400 mL) and H$_2$O (200 mL) in a 1 L round-bottom flask. NaHCO$_3$ (51.2 g, 609 mmol, 3.0 equiv) was added and the reaction mixture was stirred for 30 minutes before cooling to 0°C. I$_2$ (51.5 g, 203 mmol, 1.0 equiv) and KI (37.1 g, 223 mmol, 1.1 equiv) were added to a 500 mL Erlenmeyer flask and mixed with a spatula, forming a brown mixture. The iodine mixture was added portion wise to the cooled reaction mixture over 1 h. After complete addition, the reaction mixture was stirred for 4.5 h and allowed to reach room temperature. Subsequently, the reaction mixture was cooled on ice and quenched with NaHSO$_3$ (10% w/w) until discoloration was complete. Brine (200 mL) was added and the aqueous phase was extracted with DCM (2 x 250 mL). The combined organic layers were dried over MgSO$_4$, filtered and concentrated *in vacuo*. The crude product was obtained as a dark oil which was crystallized from EtOH to obtain iodolactone **10** (33.18 g, 113 mmol, 56%, 23% over 5 steps) as a solid: R$_f$ = 0.35 (10% Et$_2$O, 1% AcOH in pentane); ^{1}H NMR (400 MHz, CDCl$_3$) δ 5.04 (dt, *J* = 8.1, 2.7 Hz, 1H), 4.66 – 4.50 (m, 1H), 2.59 – 2.39 (m, 2H), 2.37 – 2.24 (m, 1H), 2.22 – 1.99 (m, 2H), 1.98 – 1.75 (m, 3H), 1.71 – 1.61 (m, 1H), 1.56 – 1.42 (m, 1H), 1.29 (s, 3H); ^{13}C NMR (101 MHz, CDCl$_3$) δ 176.5, 82.1, 43.8, 41.1, 37.0, 33.7, 32.5, 29.6, 26.8, 19.5;

HRMS: calculated for $C_{10}H_{16}IO_2$ 295.01895 [M+H]+; found 295.01856. Spectroscopic data was in agreement with literature.[18]
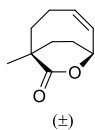
Bicyclic olefin 15: Iodolactone **10** (33.18 g, 113 mmol, 1.0 equiv) was co-evaporated with anhydrous toluene (2 x 50 mL) in a 1 L round-bottom flask, placed under N_2 and dissolved in anhydrous toluene (370 mL). DBU (22.1 mL, 147 mmol, 1.3 equiv) was added to the solution and the reaction mixture was stirred at 70°C under N_2. After 20 h, additional DBU (22.1 mL, 147 mmol, 1.3 equiv) was added and the reaction mixture was stirred for 72 h at 70°C under N_2. The reaction mixture was cooled to room temperature before washing with H_2O (2x 400 mL). The combined aqueous layers were extracted with toluene (400 mL). The combined organic layers were dried over $MgSO_4$, filtered and concentrated *in vacuo*. The crude bicyclic olefin **15** (17.24 g, 104 mmol, 92%) was obtained as an oil and used in the next step without further purification: R_f = 0.4 (20% Et_2O in pentane); 1H NMR (400 MHz, CDCl3) δ 5.95 (ddd, *J* = 11.9, 9.6, 5.4 Hz, 1H), 5.46 (ddd, *J* = 11.9, 4.8, 2.4 Hz, 1H), 5.10 (br s, 1H), 2.50 – 2.37 (m, 1H), 2.27 – 2.08 (m, 2H), 1.99 – 1.86 (m, 1H), 1.84 – 1.66 (m, 4H), 1.32 (s, 3H); 13C NMR (101 MHz, CDCl3) δ 177.2, 129.2, 127.7, 79.2, 45.2, 43.0, 31.9, 29.4, 26.6, 24.0; HRMS: calculated for $C_{10}H_{15}O_2$ 167.10666 [M+H]+; found 167.10643. Spectroscopic data was in agreement with literature.[18]
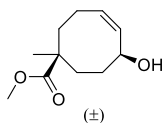
Cyclooctene methyl ester 8: The crude bicyclic olefin **15** (17.24 g, 104 mmol, 1.0 equiv) was dissolved in a mixture of dioxane (60 mL) and H_2O (60 mL) in a 1 L round-bottom flask. The mixture was cooled to 0°C before adding KOH (14.55 g, 259 mmol, 2.5 equiv) portion wise. The reaction mixture was stirred for 20 h and allowed to warm to room temperature. TLC analysis (50% EtOAc, 1% AcOH in pentane) confirmed conversion of the starting material into carboxylic acid intermediate **16**. Subsequently, the reaction mixture was concentrated *in vacuo* and co-evaporated with anhydrous toluene (3 x 60 mL) and anhydrous DMF (60 mL) to obtain the potassium salt of **16** as a crude, viscous oil: R_f = 0.5 (50% EtOAc, 1% AcOH in pentane); 1H NMR (400 MHz, CDCl3) δ 5.67 – 5.52 (m, 1H), 5.35 (ddt, *J* = 11.9, 5.6, 1.7 Hz, 1H), 5.03 – 4.88 (m, 1H), 2.36 – 2.25 (m, 1H), 2.25 – 2.13 (m, 1H), 2.13 – 2.01 (m, 3H), 1.78 – 1.65 (m, 2H), 1.65 – 1.53 (m, 1H), 1.27 (s, 3H); 13C NMR (101 MHz, CDCl3) δ 13C NMR (101 MHz, CDCl3) δ 184.2, 132.3, 129.6, 68.5, 45.9, 35.7, 33.7, 30.1, 26.8, 24.8. Compound **16** was placed under N_2, suspended in anhydrous DMF (175 mL) and cooled to 0°C. CH_3I (19.46 mL, 311 mmol, 3.0 equiv) was slowly added to the reaction mixture before stirring for 17 h and allowing the reaction mixture to warm to room temperature. H_2O (2 L) was added and the reaction mixture was extracted with Et_2O (3 x 1 L). The combined organic layers were washed with H_2O (500 mL), dried over $MgSO_4$, filtered and concentrated *in vacuo*. The crude product was purified by silica gel chromatography (10 → 20% EtOAc in pentane). Methyl ester **8** (15.78 g, 80 mmol, 77% over 2 steps) was obtained as a yellow oil: R_f = 0.4 (30% EtOAc in pentane); 1H NMR (400 MHz, CDCl3) δ 5.58 (dtd, *J* = 11.6, 5.6, 2.0 Hz, 1H), 5.41 – 5.28 (m, 1H), 5.00 – 4.86 (m, 1H), 3.66 (s, 3H), 2.36 – 2.22 (m, 1H), 2.19 – 2.00 (m, 4H), 1.77 (d, *J* = 4.7 Hz, OH), 1.74 – 1.63 (m, 2H), 1.60 – 1.52 (m, 1H), 1.22 (s, 3H); 13C NMR (101 MHz, CDCl3) δ 178.8, 132.4, 129.3, 68.4, 51.9, 46.0, 35.9, 33.7, 30.4, 26.7, 24.9; HRMS: calculated for $C_{10}H_{15}O_2$ 167.10666 [M-MeOH+H]+; found 167.10677. Spectroscopic data was in agreement with literature.[18]
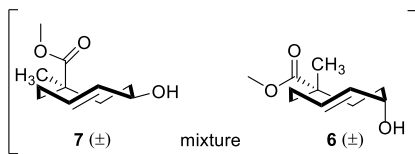
Mixture of axial TCO methyl ester 6 and equatorial TCO methyl ester 7: Methyl ester **8** (1.73 g, 8.73 mmol, 1.0 equiv) was irradiated (λ = 254 nm) for 24 h in the presence of methyl benzoate (3.30 mL, 26.2 mmol, 3.0 equiv) in a quartz flask containing a solution of Et$_2$O in heptane (1:3, 600 mL). During irradiation, the reaction mixture was continuously circulated over a silica column (40 g size, containing dry silica and 22 g of AgNO$_3$ impregnated silica[25] (10% wt, containing ca. 13 mmol AgNO$_3$, 1.5 equiv)) at a flowrate of 40 mL/min. The column was placed in the dark and shielded with aluminum foil during the irradiation. Absence of **8** from the reaction mixture was shown with ^{1}H NMR and the column was flushed with Et$_2$O/heptane (1:3, 500 mL) before drying over a stream of air. Next, the contents of the column were emptied into an Erlenmeyer flask containing NH$_4$OH (28% w/w, 200 mL) and DCM (200 mL). The biphasic mixture was stirred for ~ 1 h before filtration of the silica gel. The organic layer was separated and the aqueous layer was extracted with DCM (200 mL). The combined organic layers were washed with H$_2$O (100 mL), dried over MgSO$_4$, filtered and concentrated *in vacuo*. The crude product was purified by silica gel chromatography (33% EtOAc in pentane, isocratic) to obtain the isomeric mixture of axial isomer **6** and equatorial isomer **7** (1.46 g, 7.36 mmol, 84%, **6** : **7** in an approximate ratio of 1 : 1.4) as an oil: R$_f$ = 0.7 (axial isomer **6**, 50% EtOAc in pentane), 0.6 (equatorial isomer **7**, 50% EtOAc in pentane); ^{1}H NMR (400 MHz, CDCl$_3$) δ 6.18 – 5.96 (m, 1H, **6**), 5.80 (ddd, *J* = 15.8, 11.6, 3.9 Hz, 1H, **7**), 5.63 (dd, *J* = 16.6, 2.4 Hz, 1H, **6**), 5.37 (dd, *J* = 16.2, 9.4 Hz, 1H, **7**), 4.48 (br s, 1H, **6**), 4.21 (td, *J* = 9.8, 5.7 Hz, 1H, **7**), 3.73 (s, 3H, **7**), 3.64 (s, 3H, **6**), 2.72 (qd, *J* = 11.9, 4.6 Hz, 1H, **7**), 2.38 – 2.03 (m, 3H, **6**, 3H, **7**), 2.01 – 1.60 (m, 5H, **6**, 2H, **7**, 2OH), 1.60 – 1.46 (m, 1H, **6**, 1H, **7**), 1.38 – 1.24 (m, 1H, **7**), 1.20 (s, 3H, **7**), 1.11 (s, 3H, **6**); ^{13}C NMR (101 MHz, CDCl$_3$) δ 180.5, 177.4, 135.9, 135.1, 132.7, 130.5, 75.1, 69.8, 52.1, 51.4, 47.6, 46.0, 44.9, 44.7, 40.0, 38.9, 38.3, 34.8, 31.0, 30.9, 29.7, 18.2; HRMS: calculated for C$_{11}$H$_{18}$O$_3$Na 221.11482 [M+Na]$^+$; found 221.11471. Spectroscopic data was in agreement with literature.[18]
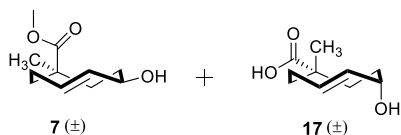
Equatorial TCO methyl ester 7, axial TCO carboxylic acid 17: The isomeric mixture of **6** and **7** (1.46 g, 7.36 mmol, 1.0 equiv) was placed under N$_2$, dissolved in MeOH (28 mL) and cooled on ice whilst stirring. A solution of KOH (4.54 g,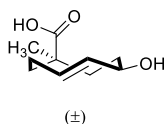 81 mmol, 11 equiv) in H$_2$O (14 mL) under N$_2$ was cooled on ice and subsequently added to the isomeric mixture. The reaction mixture was placed in the dark, shielded with aluminum foil and stirred for 68 h at 4°C. TLC (50% EtOAc in pentane) indicated complete hydrolysis of axial isomer **6**, whereas equatorial isomer **7** remained unaffected. The reaction mixture was diluted with H$_2$O (125 mL) and extracted with Et$_2$O (3 x 125 mL). The combined organic layers were washed with H$_2$O (25 mL), dried over MgSO$_4$, filtered and concentrated *in vacuo* to obtain equatorial TCO methyl ester **7** (663 mg, 3.19 mmol, 43%) as a transparent oil: R$_f$ = 0.6 (50% EtOAc in pentane); ^{1}H NMR (400 MHz, CDCl$_3$) δ 5.80 (ddd, *J* = 15.8, 11.6, 3.9 Hz, 1H), 5.37 (dd, *J* = 16.2, 9.4 Hz, 1H), 4.21 (td, *J* = 9.8, 5.7 Hz, 1H), 3.73 (s, 3H), 2.73 (qd, *J* = 11.9, 4.6 Hz, 1H), 2.30 – 2.20 (m, 1H), 2.17 – 2.05 (m, 2H), 1.93 (dddd, *J* = 14.0, 11.8, 10.2, 1.4 Hz, 1H), 1.83 – 1.71 (m, 1H + OH), 1.53 (ddd, *J* = 14.2, 12.6, 4.8 Hz, 1H), 1.31 (ddd, *J* = 15.4, 12.2, 1.4 Hz, 1H), 1.20 (s, 3H); ^{13}C NMR (101 MHz, CDCl$_3$) δ 177.4, 135.9, 132.8, 75.1, 51.5, 47.6, 46.0, 40.0, 38.9, 34.8, 31.1; HRMS: calculated for C$_{11}$H$_{19}$O$_3$ 199.13287 [M+H]$^+$;

found 199.13290. The combined aqueous layers were acidified to pH 3 with AcOH (30 mL total), followed by extraction with Et_2O (3 x 125 mL). The combined organic layers were washed with H_2O (65 mL), dried over $MgSO_4$, filtered, partially concentrated *in vacuo* and co-evaporated with distilled toluene (3 x) to obtain axial TCO carboxylic acid **17** (569 mg, 3.09 mmol, 42%) as a yellow oil which was used in the next step without further purification: R_f = 0.3 (50% EtOAc in pentane); ^{1}H NMR (400 MHz, $CDCl_3$) δ 6.07 (ddd, *J* = 16.4, 10.8, 3.4 Hz, 1H), 5.64 (dd, *J* = 16.6, 2.5 Hz, 1H), 4.49 (br s, 1H), 2.39 – 2.08 (m, 3H), 2.06 – 1.77 (m, 4H), 1.65 (dd, *J* = 15.9, 6.1 Hz, 1H), 1.11 (s, 3H); ^{13}C NMR (101 MHz, $CDCl_3$) δ 185.6, 135.1, 130.6, 69.8, 44.8, 44.5, 38.3, 30.9, 29.6, 18.0; HRMS: calculated for $C_{10}H_{17}O_3$ 185.11722 [M+H]+; found 185.11728. Spectroscopic data was in agreement with literature.[18]
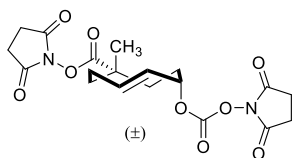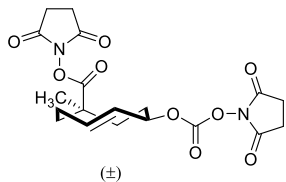
Axial TCO reagent 4: Axial TCO carboxylic acid **17** (515 mg, 2.80 mmol, 1.0 equiv) and *N,N′*-Disuccinimidyl carbonate (2.15 g, 8.39 mmol, 3.0 equiv) were combined in a 100 mL round-bottom flask. The mixture was co-evaporated with distilled toluene (3 x 5 mL), placed under N_2 and suspended in anhydrous MeCN (18 mL). DIPEA (1.95 mL, 11.2 mmol, 4.0 equiv) and DMAP (34 mg, 0.28 mmol, 0.1 equiv) were added and the resulting clear reaction mixture was placed in the dark, shielded with aluminum foil and stirred at room temperature for 17 h. The reaction mixture was concentrated *in vacuo*, co-evaporated with distilled toluene (3 x 5 mL) and subsequently purified by silica gel chromatography (neutralized silica, DCM → 2% acetone in DCM) to obtain the axial bifunctionalized product **4** (853 mg, 2.02 mmol, 72%) as a white, foamy solid: R_f = 0.3 (2% acetone in DCM); ^{1}H NMR (400 MHz, $CDCl_3$) δ 6.19 – 5.95 (m, 1H), 5.62 (dd, *J* = 16.7, 2.1 Hz, 1H), 5.28 (br s, 1H), 2.84 (2 s, 8H), 2.53 – 2.19 (m, 4H), 2.19 – 1.91 (m, 4H), 1.28 (s, 3H); ^{13}C NMR (101 MHz, $CDCl_3$) δ174.2, 169.4, 168.7, 150.7, 133.1, 128.9, 78.9, 44.4, 44.4, 35.8, 30.9, 30.2, 25.8, 25.6, 18.1; HRMS: calculated for $C_{19}H_{22}N_2O_9Na$ 445.12175 [M+Na]+; found 445.12150. Spectroscopic data was in agreement with literature.[18]

Equatorial TCO carboxylic acid 18: Equatorial TCO methyl ester **7** (350 mg, 1.77 mmol, 1.0 equiv) was placed under N_2 and dissolved in MeOH (10 mL). A solution of KOH (1.09 g, 19.4 mmol, 11 equiv) in H_2O (5 mL) under N_2 was cooled on ice and subsequently added to the methyl ester solution. The resulting reaction mixture was stirred for 6 d at 50°C, during which the reaction was kept in the dark and shielded with aluminium foil. The reaction mixture was diluted with H_2O (50 mL) and washed with Et_2O (2 x 100 mL). The combined organic layers were extracted with H_2O (50 mL). The combined aqueous layers were acidified to pH 3 with citric acid, followed by extraction with Et_2O (3 x 100 mL). The combined organic layers were dried over $MgSO_4$, filtered and concentrated *in vacuo* to obtain equatorial TCO carboxylic acid **18** (256 mg, 1.39 mmol, 79%) as a white solid: R_f = 0.3 (50% EtOAc in pentane); ^{1}H NMR (400 MHz, $CDCl_3$) δ 5.82 (ddd, *J* = 15.8, 11.6, 3.9 Hz, 1H), 5.51 (dd, *J* = 16.2, 9.4 Hz, 1H), 4.25 (td, *J* = 9.6, 6.3 Hz, 1H), 2.77 (qd, *J* = 12.0, 4.6 Hz, 1H), 2.31 – 2.21 (m, 1H), 2.20 – 2.05 (m, 3H), 1.86 – 1.76 (m, 1H), 1.55 (ddd, *J* = 14.2, 12.6, 4.9 Hz, 1H), 1.35 (ddd, *J* = 15.2, 11.0, 2.6 Hz, 1H), 1.28 (s, 3H); ^{13}C NMR (101 MHz, $CDCl_3$) δ 182.1, 135.8, 132.9, 75.2, 47.3, 45.8, 39.9, 38.9, 34.9, 30.9; HRMS: calculated for $C_{10}H_{16}O_3Na$ 207.09917 [M+Na]+; found 207.09914.

(±)

Equatorial TCO reagent 19: Equatorial TCO carboxylic acid **18** (250 mg, 1.36 mmol, 1.0 equiv) and *N,N'*-Disuccinimidyl carbonate (1.39 g, 5.43 mmol, 4.0 equiv) were combined in a 50 mL round-bottom flask. The mixture was co-evaporated with distilled toluene (2 x 5 mL), placed under N_2 and suspended in anhydrous MeCN (7 mL). DIPEA (1.78 mL, 10.2 mmol, 7.5 equiv) was added and the resulting clear reaction mixture was placed in the dark, shielded with aluminum foil and stirred at room temperature for 36 h. The reaction mixture was impregnated with Celite, concentrated *in vacuo* and purified by silica gel chromatography (50% EtOAc in pentane, isocratic) to obtain the equatorial bifunctionalized product **19** (378 mg, 0.89 mmol, 66%) as a foamy white solid: R_f = 0.3 (50% EtOAc in pentane); ¹H NMR (400 MHz, CDCl₃) δ 5.95 (ddd, *J* = 15.9, 11.6, 4.0 Hz, 1H), 5.75 (dd, *J* = 16.4, 9.6 Hz, 1H), 5.16 (td, *J* = 10.1, 5.8 Hz, 1H), 2.92 – 2.77 (m, 8H), 2.73 – 2.59 (m, 1H), 2.42 (d, *J* = 14.2 Hz, 1H), 2.33 – 2.18 (m, 2H), 1.97 (dd, *J* = 15.6, 5.7 Hz, 1H), 1.70 (ddd, *J* = 14.3, 12.9, 4.7 Hz, 1H), 1.46 (s, 3H); ¹³C NMR (101 MHz, CDCl₃) δ 171.5, 169.4, 168.9, 151.1, 135.0, 130.7, 83.5, 47.5, 45.2, 38.7, 35.1, 35.0, 30.9, 25.8, 25.6; HRMS: calculated for $C_{19}H_{22}N_2O_9Na$ 445.12175 [M+Na]⁺; found 445.12164.

(±)
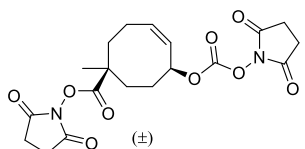
CCO reagent 5: Equatorial bifunctionalized TCO **19** (464 mg, 1.10 mmol, 1.0 equiv) was dissolved in CDCl₃ (22 mL) in a 100 mL round-bottom flask. The solution was purged with N_2, sealed and stirred whilst irradiating with a CFL (23 W, 1 cm distance to flask, see Figure 2) for 48 h. ¹H NMR analysis confirmed full conversion and the reaction mixture was concentrated *in vacuo*. The crude product was purified by silica gel chromatography (15% Et₂O in DCM, isocratic) to obtain the bifunctionalized *cis* product **5** (343 mg, 0.812 mmol, 74%) as an foamy white solid: R_f = 0.6 (30% Et₂O in DCM); ¹H NMR (400 MHz, CDCl₃) δ 6.01 – 5.86 (m, 1H), 5.82 – 5.69 (m, 1H), 5.44 (ddt, *J* = 12.0, 5.8, 1.6 Hz, 1H), 2.92 – 2.76 (m, 8H), 2.47 – 2.15 (m, 5H), 2.00 – 1.79 (m, 3H), 1.46 (s, 3H); ¹³C NMR (101 MHz, CDCl₃) δ 172.7, 169.2, 168.8, 151.3, 131.5, 125.7, 79.6, 45.8, 35.8, 29.6, 29.4, 26.5, 25.8, 25.6, 24.5; HRMS: calculated for $C_{19}H_{22}N_2O_9Na$ 445.12175 [M+Na]⁺; found 445.12154.

2.5 References

[1]   J. Li, P. R. Chen, *Nat. Chem. Biol.* **2016**, *12*, 129–137.

[2]   K. Neumann, A. Gambardella, M. Bradley, *ChemBioChem* **2019**, *20*, 872–876.

[3]   J. Tu, M. Xu, R. M. Franzini, *ChemBioChem* **2019**, *20*, 1615–1627.

[4]   N. K. Devaraj, *ACS Cent. Sci.* **2018**, *4*, 952–959.

[5]   J. Li, J. Yu, J. Zhao, J. Wang, S. Zheng, S. Lin, L. Chen, M. Yang, S. Jia, X. Zhang, P. R. Chen, *Nat. Chem.* **2014**, *6*, 352–361.

[6]   E. Jiménez-Moreno, Z. Guo, B. L. Oliveira, I. S. Albuquerque, A. Kitowski, A. Guerreiro, O. Boutureira, T. Rodrigues, G. Jiménez-Osés, G. J. L. Bernardes, *Angew. Chem. Int. Ed.* **2017**, *56*, 243–247.

[7]   A. M. Pérez-López, B. Rubio-Ruiz, V. Sebastián, L. Hamilton, C. Adam, T. L. Bray, S. Irusta, P. M. Brennan, G. C. Lloyd-Jones, D. Sieger, J. Santamaría, A. Unciti-Broceta, *Angew. Chem. Int. Ed.* **2017**, *56*, 12548–12552.

[8]   S. Bernard, D. Audisio, M. Riomet, S. Bregant, A. Sallustrau, L. Plougastel, E. Decuypere, S. Gabillet, R. A. Kumar, J. Elyian, M. N. Trinh, O. Koniev, A. Wagner, S. Kolodych, F. Taran, *Angew. Chem. Int. Ed.* **2017**, *56*, 15612–15616.

[9]   J. Tu, M. Xu, S. Parvez, R. T. Peterson, R. M. Franzini, *J. Am. Chem. Soc.* **2018**, *140*, 8410–8414.

[10]   S. S. Matikonda, D. L. Orsi, V. Staudacher, I. A. Jenkins, F. Fiedler, J. Chen, A. B. Gamble, *Chem. Sci.* **2015**, *6*, 1212–1218.

[11]   L. P. W. M. Lelieveldt, S. Eising, A. Wijen, K. M. Bonger, *Org. Biomol. Chem.* **2019**, *17*, 8816–8821.

[12]   H. Wu, S. C. Alexander, S. Jin, N. K. Devaraj, *J. Am. Chem. Soc.* **2016**, *138*, 11429–11432.

[13]   R. M. Versteegen, R. Rossin, W. ten Hoeve, H. M. Janssen, M. S. Robillard, *Angew. Chem. Int. Ed.* **2013**, *52*, 14112–14116.

[14]   J. Sauer, H. Wiest, *Angew. Chem.* **1962**, *74*, 353–353.

[15]   M. L. Blackman, M. Royzen, J. M. Fox, *J. Am. Chem. Soc.* **2008**, *130*, 13518–13519.

[16]   R. M. Versteegen, W. ten Hoeve, R. Rossin, M. A. R. de Geus, H. M. Janssen, M. S. Robillard, *Angew. Chem. Int. Ed.* **2018**, *57*, 10494–10499.

[17]   J. C. T. Carlson, H. Mikula, R. Weissleder, *J. Am. Chem. Soc.* **2018**, *140*, 3603–3612.

[18]   R. Rossin, S. M. J. van Duijnhoven, W. ten Hoeve, H. M. Janssen, F. J. M. Hoeben, R. M.

Versteegen, M. S. Robillard, *Bioconjug. Chem.* **2016**, *27*, 1697–1706.

[19]   R. Rossin, R. M. Versteegen, J. Wu, A. Khasanov, H. J. Wessels, E. J. Steenbergen, W. ten Hoeve, H. M. Janssen, A. H. A. M. van Onzen, P. J. Hudson, M. S. Robillard, *Nat. Commun.* **2018**, *9*, 1484.

[20]   J. M. Mejia Oneto, I. Khan, L. Seebald, M. Royzen, *ACS Cent. Sci.* **2016**, *2*, 476–482.

[21]   M. Czuban, S. Srinivasan, N. A. Yee, E. Agustin, A. Koliszak, E. Miller, I. Khan, I. Quinones, H. Noory, C. Motola, R. Volkmer, M. Di Luca, A. Trampuz, M. Royzen, J. M. Mejia Oneto, *ACS Cent. Sci.* **2018**, *4*, 1624–1632.

[22]   K. Wu, N. A. Yee, S. Srinivasan, A. Mahmoodi, M. Zakharian, J. M. Mejia Oneto, M. Royzen, *Chem. Sci.* **2021**, *12*, 1259–1271.

[23]   D. Hartley, *J. Chem. Soc.* **1962**, 4722.

[24]   A. J. Bloodworth, T. Melvin, J. C. Mitchell, *J. Org. Chem.* **1988**, *53*, 1078–1082.

[25]   M. Royzen, G. P. A. Yap, J. M. Fox, *J. Am. Chem. Soc.* **2008**, *130*, 3760–3761.

[26]   M. A. R. Geus, E. Maurits, A. J. C. Sarris, T. Hansen, M. S. Kloet, K. Kamphorst, W. Hoeve, M. S. Robillard, A. Pannwitz, S. A. Bonnet, J. D. C. Codée, D. V. Filippov, H. S. Overkleeft, S. I. Kasteren, *Chem. Eur. J.* **2020**, *26*, 9900–9904.

[27]   X. Fan, Y. Ge, F. Lin, Y. Yang, G. Zhang, W. S. C. Ngai, Z. Lin, S. Zheng, J. Wang, J. Zhao, J. Li, P. R. Chen, *Angew. Chem. Int. Ed.* **2016**, *55*, 14046–14050.

[28]   A. J. C. Sarris, T. Hansen, M. A. R. de Geus, E. Maurits, W. Doelman, H. S. Overkleeft, J. D. C. Codée, D. V. Filippov, S. I. van Kasteren, *Chem. Eur. J.* **2018**, *24*, 18075–18081.

[29]   A. M. F. van der Gracht, M. A. R. de Geus, M. G. M. Camps, T. J. Ruckwardt, A. J. C. Sarris, J. Bremmers, E. Maurits, J. B. Pawlak, M. M. Posthoorn, K. M. Bonger, D. V. Filippov, H. S. Overkleeft, M. S. Robillard, F. Ossendorp, S. I. van Kasteren, *ACS Chem. Biol.* **2018**, *13*, 1569–1576.

[30]   M. F. Schneider, C. Gantner, W. Obrecht, O. Nuyken, *J. Polym. Sci. Part A Polym. Chem.* **2011**, *49*, 879–885.

Towards incorporation of *trans*-cyclooctene-modified amino acids in Fmoc solid phase peptide synthesis

T. Hansen and M. S. Kloet contributed to the work described in this Chapter.

3.1 Introduction

The inverse electron demand Diels-Alder (IEDDA) cycloaddition[1] has become an intrinsic component of bioorthogonal chemistry.[2–6] Tetrazine ligation, defined as IEDDA cycloaddition between tetrazines and strained alkenes, is of particular importance when *trans*-cyclooctenes (TCOs)[7,8] acts as dienophiles, as reaction rates within $10^3 – 10^6$ $M^{-1}s^{-1}$ are encountered for this reaction pair.[7,9,10] Incorporation of TCO modified lysines via genetic code expansion has proven valuable to enable site-specific protein labeling with fluorogenic tetrazines (Figure 1A).[11–14] The utility of the TCO functionality in this regard is determined by its reaction kinetics, but also by its stability
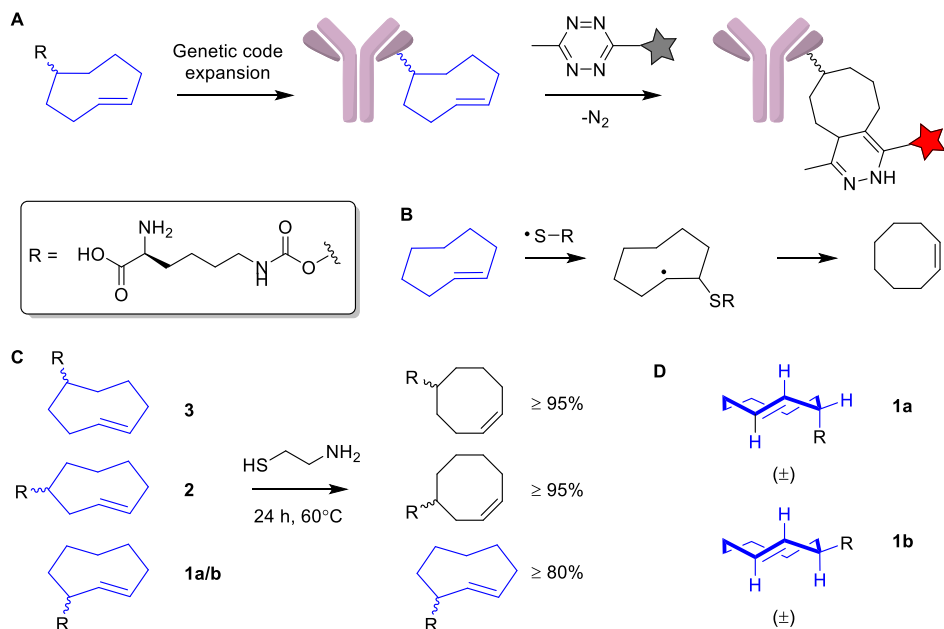
Figure 1 A) Site-specific protein labeling with fluorogenic tetrazines and TCO modified lysines.[2-6] B) Proposed mechanism for thiol-induced TCO isomerization by Fox and co-workers.[17] C) Stability studies on TCO carbamate protected lysines (**1**-**3**) in the presence of cysteamine revealed superior stability for the allylic substituted TCO **1a/b**.[18,19] D) Axial (**1a**) and equatorial (**1b**) isomers of the allylic substituted TCO derivative mentioned in C.

and solubility in biological systems. *In vivo*, high concentrations of thiols[9,10,15] and copper-containing proteins[16] are the primary causes for TCOs to isomerize to their *cis*-cyclooctene counterparts. Fox and co-workers recently demonstrated thiol-induced TCO isomerization to proceed through radical intermediates (Figure 1B).[17] Nikíc *et al.*[18] studied the stability of TCO modified lysines in the presence of cysteamine hydrochloride using ^{1}H-NMR, revealing the allylic TCO carbamate (2-ene, **1a/b**) to possess superior stability compared to 3-ene (**2**) and 4-ene (**3**) isomers (Figure 1C).[18] Within these allylic substituted TCOs, the more reactive axial isomer (**1a**) is also more resistant towards isomerization by cysteamine compared to the equatorial isomer (**1b**, Figure 1D).[19] This finding contradicts general stability trends for TCOs in which increased reactivity towards tetrazines is paired with reduced stability.[9,10]

A recently discovered elimination extension of the tetrazine ligation with TCOs, IEDDA pyridazine elimination,[20] employs allylic substituted TCOs as temporary "cages" to mask the amine functionality of antibody drug conjugates (ADCs),[21,22] protein active sites[23] and immunogenic peptides[24] as TCO carbamates (Figure 2A). Tetrazine ligation is followed by a tautomerization step, leading to liberation of the amine and
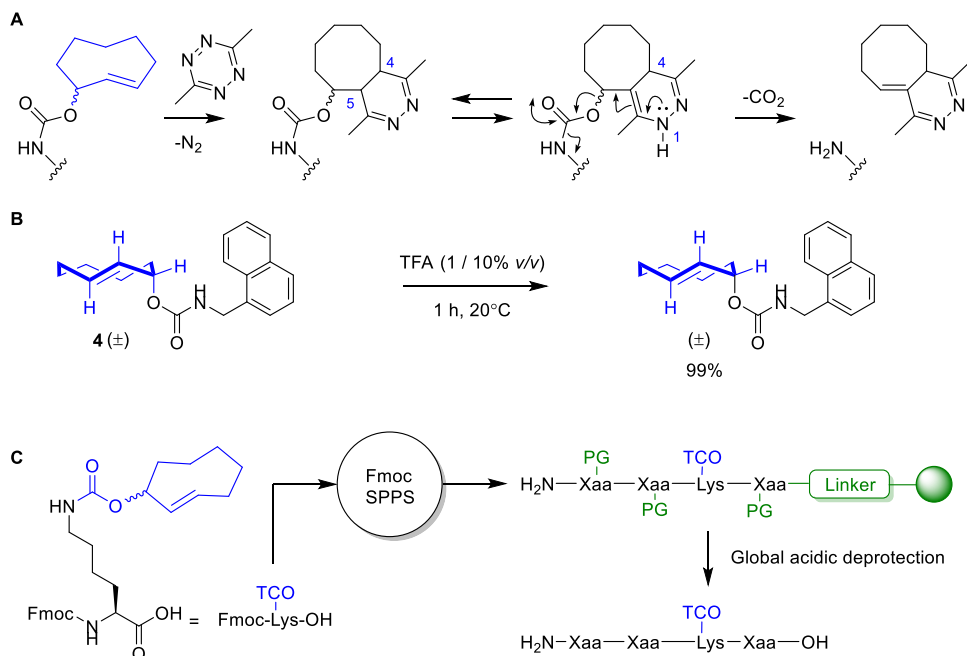
Figure 2 A) Overview of the IEDDA pyridazine elimination reaction.[20] B) Stability data of an allylic substituted TCO carbamate **4** (axial isomer) in the presence of TFA by Robillard and co-workers.[18] C) Synthetic strategy proposed in this Chapter. PG = protecting group; Xaa = unspecified amino acid.

elimination of the pyridazine and CO_2 from a 1,4-dihydropyridazine. Synthesis of these caged biomolecules often hinges on chemoselectivity of amines to obtain the TCO modified carbamate constructs. Solid phase synthetic strategies would omit this necessity and therefore increase the scope of biomolecules available to this decaging method. However, acidic (deprotection) conditions are common to these strategies, and cyclooctenes are reported to react with (strong) acids.[25–27] In this respect, Robillard and co-workers reported full stability for a model axial TCO with allylic carbamate substitution (**4**) in 1% and 10% TFA (*v/v* in CHCl$_3$, 1 hour; Figure 2B).[28] It was hypothesized that the stability of such TCO's[18,19,28] would allow its incorporation in a growing peptide chain during Fmoc solid phase peptide synthesis (SPPS), followed by acidic cleavage of the peptide from the solid support (Figure 2C). This Chapter describes the attempted development of an SPPS-based strategy for TCO-modified peptide synthesis.
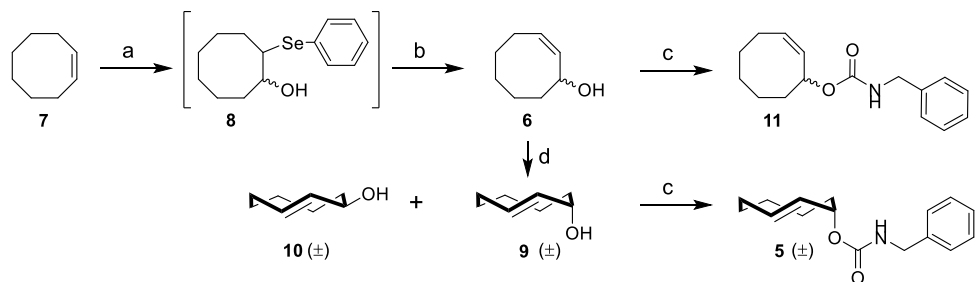
Scheme 1 Synthesis of allylic TCO carbamate **12** and allylic CCO carbamate **11**. Reagents/conditions: (a) *i*. Diphenyl diselenide, H_2O_2, DCM, 0°C; *ii*. MgSO4; *iii*. **7**, 0°C to rt; (b) tBu-OOH, 0°C to rt, 86% over 2 steps; (c) benzyl isocyanate, Et₃N, DCM, rt, 83% (**11**), 77% (**5**); (d) methyl benzoate, hv (254 nm), Et₂O / heptane, rt, 33% (**9**), 22% (**10**).

3.2 Results and discussion

Global acidic deprotection to liberate peptide sequences of their temporary protective groups and resin modalities constitutes a key step in Fmoc SPPS. Depending on the nature of these protective functionalities, varying concentrations of TFA and scavengers are employed for this reaction. In order to achieve the goal of incorporating TCO-modified amino acids into an SPPS-sequence, it was envisioned that the extent and mechanism of TFA-induced isomerization of allylic substituted TCOs would have to be characterized in detail.

Model allylic TCO carbamate **5**[20,29] was synthesized to measure the rate of TFA-induced isomerization with ¹H NMR (Scheme 1). Cyclooctenol **6** was obtained from *cis*-cyclooctene (**7**) in a one-pot, two-step procedure involving formation and subsequent oxidation of a hydroxy selenide adduct (**8**).[30,31] Photochemical isomerization of **6** gave a mixture of axial (**9**) and equatorial (**10**) TCO diastereoisomers which were separated using silica gel column chromatography.[20,32] Treatment of **6** and **9** with benzyl isocyanate gave carbamates **11** and **5**, respectively. Exposure of **5** to TFA-H (5% *v/v* in CDCl₃) for 30 – 150 minutes, followed by dilution with toluene and concentration *in vacuo* resulted in a progressively isomerized mixture on ¹H NMR (Figure 3). While **5** is still the major species after 30 and 60 minutes of incubation (64% and 48% estimated **5** intact, respectively), the spectra of the concentrated mixtures upon prolonged incubation primarily possess *cis*-cyclooctene characteristics, without directly matching reference compound **11**. The latter observation is in agreement with the reactivity of CCOs towards TFA, as described by Nordlander *et al*.[27]

Based on this initial experiment, it was decided that directly monitoring the interaction of **5** and TFA was required to obtain meaningful data. Furthermore, it was reasoned that neutralizing the acidic reaction mixture (e.g. with pyridine)[33] during such an NMR
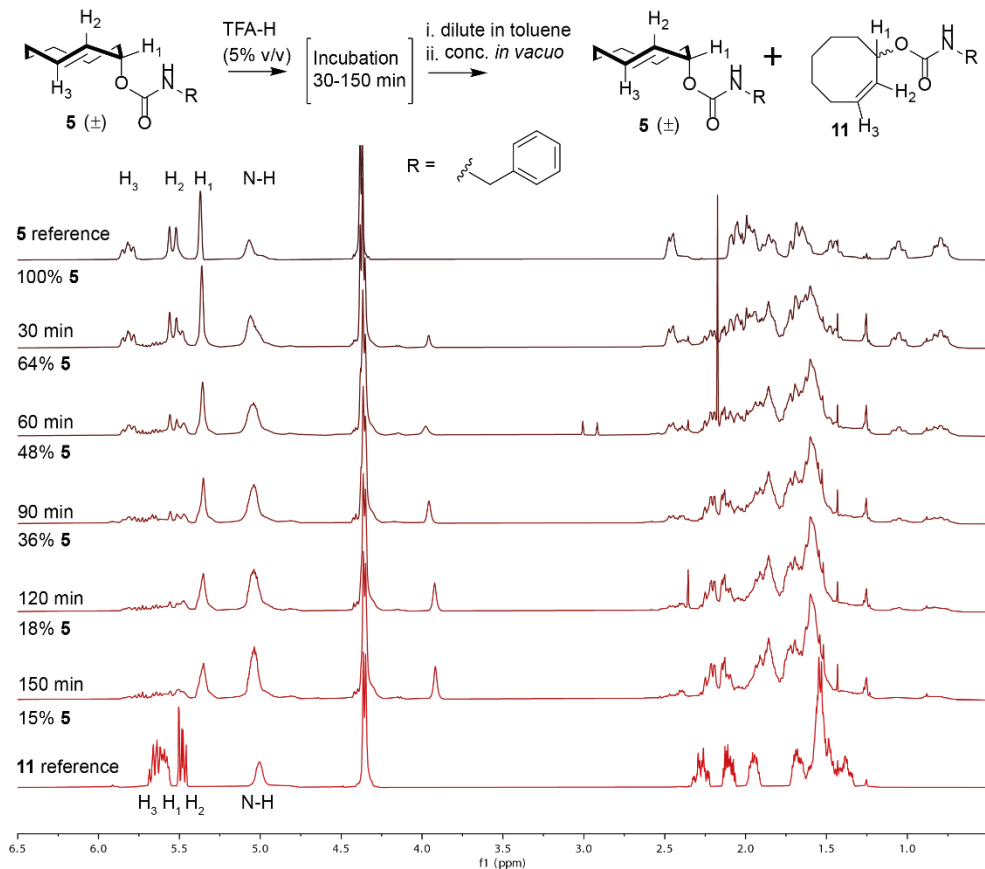
Figure 3 Isomerization/degradation of model compound **5** after incubation (30 – 150 min) with TFA-H (5% *v/v* in CDCl₃; 600 μL total volume). After the indicated incubation period, the sample was diluted with toluene (5 mL), concentrated *in vacuo* (40°C) and analyzed with ¹H NMR. The stability of **5** was estimated by comparing the H₃ signal (5.90-5.75 ppm) with the methylene signal (4.45-4.30 ppm).

experiment would negate effects of direct concentration and could be translated to Fmoc SPPS procedures.[33]

Addition of TFA-D (5% *v/v* in CDCl₃) to **5** led to a clear perturbation of the H₃-signal (δ = 5.8 ppm) towards an overlapping H₂₋₃-signal (δ = 5.7 – 5.4 ppm; Figure 4A). In a similar fashion, peak perturbation and/or broadening was visible for C₁ (δ = 74 ppm), C₂₋₃ (δ = 132 ppm) and C=O (δ = 156 ppm) on ¹³C-APT NMR (Figure 4B). Other signals in the ¹H and ¹³C NMR spectra for this cationic species showed minor shifts compared to **5**. The overall spectral appearance did not change over the course of the experiment. Administration of pyridine-D₅ (2 equivalents) after 90 minutes directly recovered the spectral appearance of the TCO model compound (**5**), without a significant degree of isomerization (94% stability based on ¹H NMR estimations).
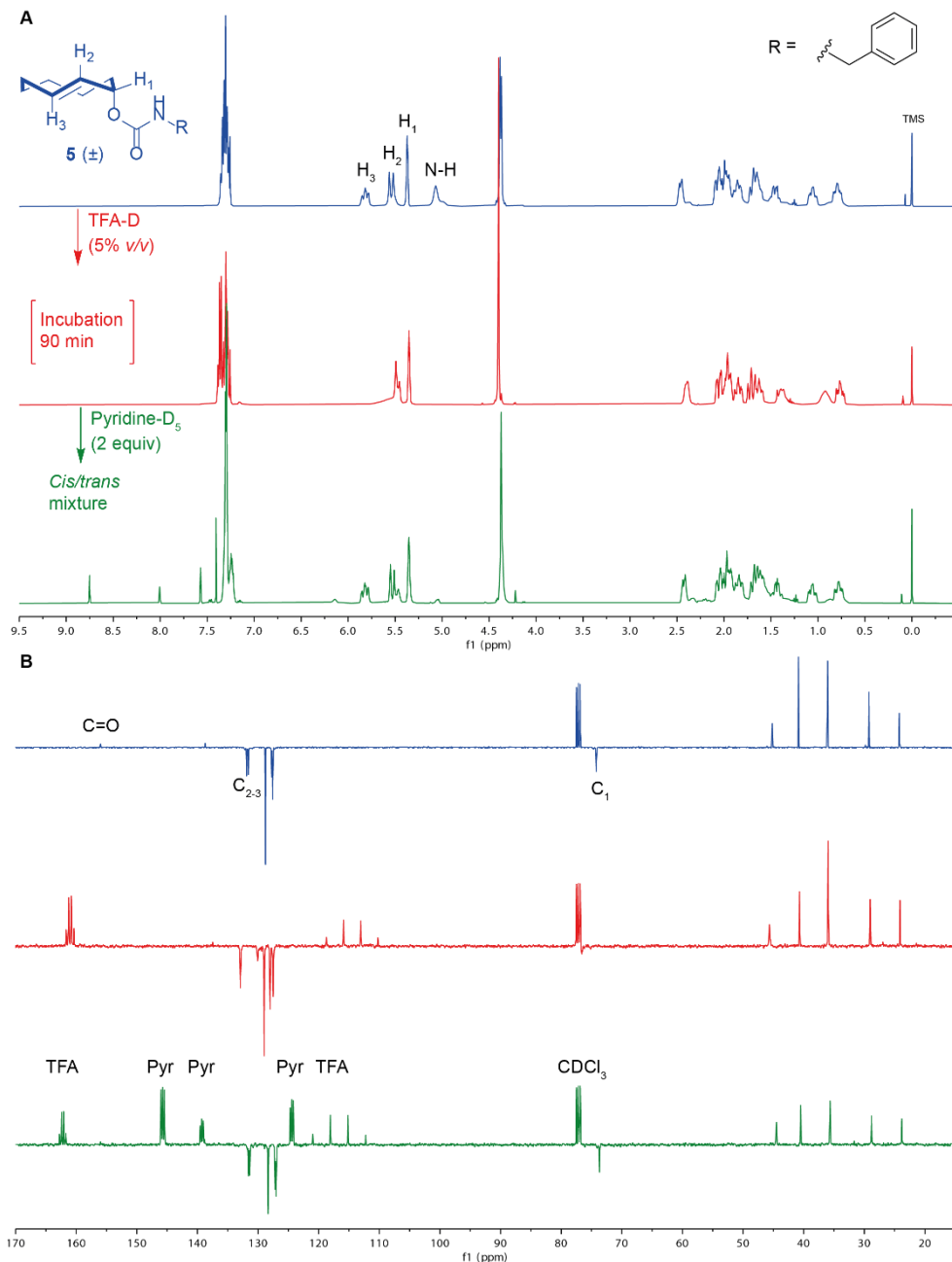
Figure 4 Stacked 1H (A; δ 9.5/-0.5 ppm) and 13C-APT (B; 170/15 ppm) NMR spectra of model TCO carbamate **5** before and upon treatment with TFA-D (5% v/v in CDCl3). Chemical shift perturbation and/or peak broadening is visible in both spectra for characteristic 1H and 13C signals (H/C_{1-3}, C=O). After 90 minutes, the mixture was quenched by adding pyridine-D_5 (2 equiv), recovering the signals for carbamate **5**. The stability of **5** was estimated to be 94% by comparing the H_3 signal (5.90-5.75 ppm) with the methylene signal (4.45-4.30 ppm).
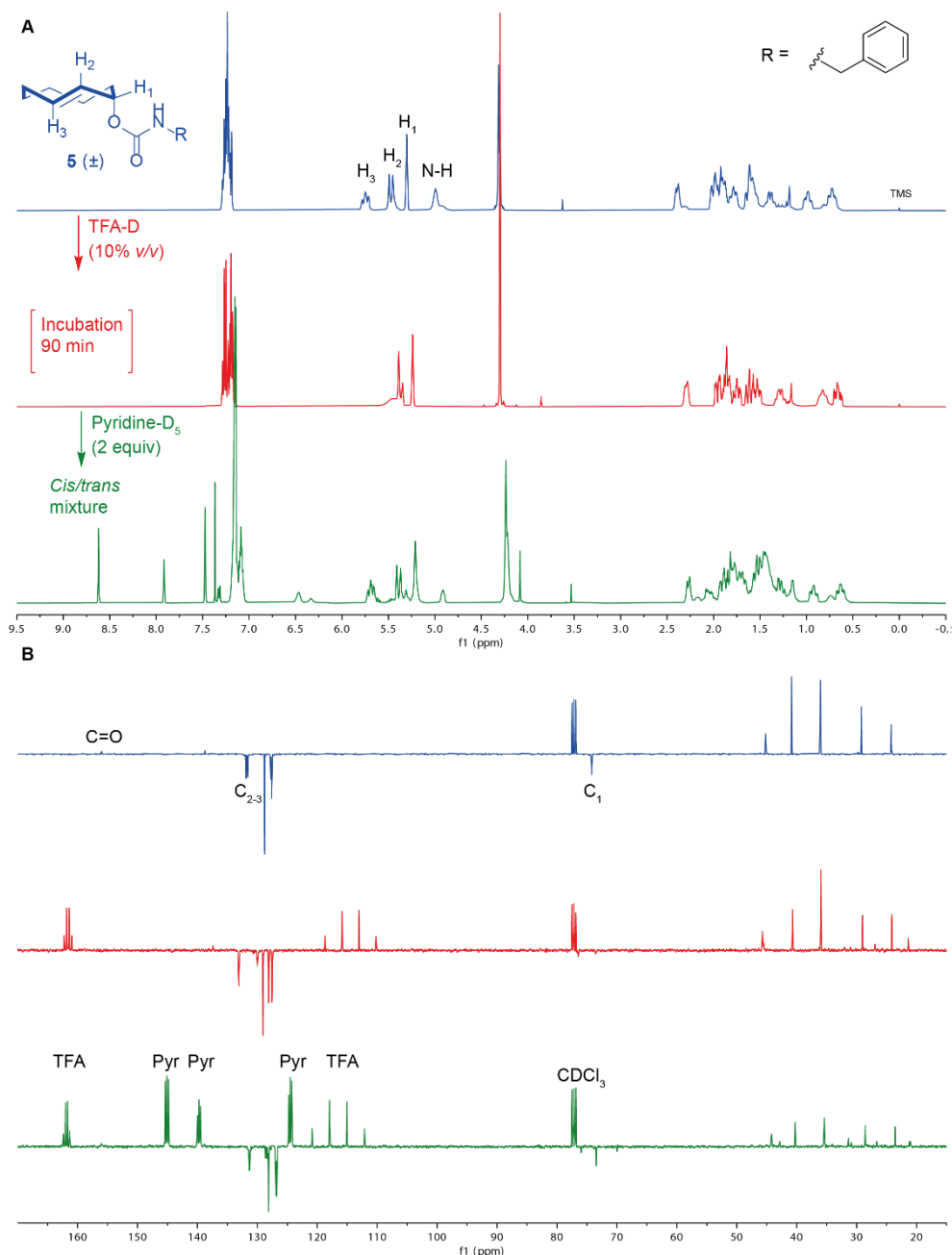
Figure 5 Stacked ^1H (A; δ 9.5/-0.5 ppm) and ^{13}C-APT (B; 170/15 ppm) NMR spectra of model TCO carbamate **5** before and upon treatment with TFA-D (10% *v/v* in CDCl$_3$). Chemical shift perturbation and/or peak broadening is visible in both spectra for characteristic ^1H and ^{13}C signals (H/C$_{1-3}$, C=O). After 90 minutes, the mixture was quenched by adding pyridine-D$_5$ (2 equiv), partially recovering the signals for carbamate **5**. The stability of **5** was estimated to be 75% by comparing the H$_3$ signal (5.90-5.75 ppm) with the methylene signal (4.45-4.30 ppm).
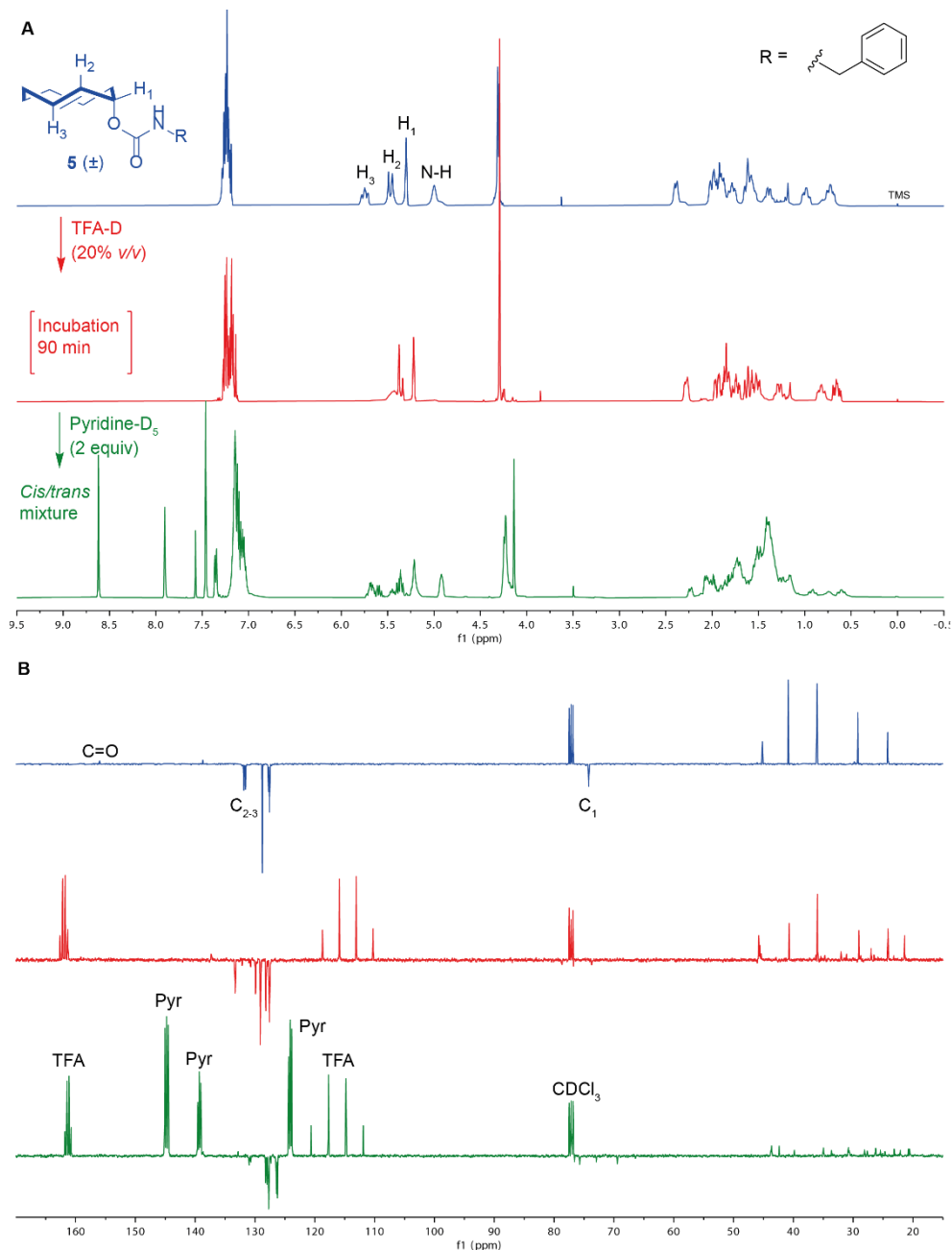
Figure 6 Stacked ^{1}H (A; δ 9.5/-0.5 ppm) and ^{13}C-APT (B; 170/15 ppm) NMR spectra of model TCO carbamate **5** before and upon treatment with TFA-D (20% *v/v* in CDCl$_3$). Chemical shift perturbation and/or peak broadening is visible in both spectra for characteristic ^{1}H and ^{13}C signals (H/C$_{1-3}$, C=O). After 90 minutes, the mixture was quenched by adding pyridine-D$_5$ (2 equiv) to obtain a complex, isomerized mixture. The stability of **5** could not be estimated for this time point due to spectral heterogenicity.

This initial experiment was repeated using 10% TFA-D (*v/v* in CDCl3; Figure 5) and 20% TFA-D (*v/v* in CDCl3; Figure 6). In both follow-up experiments, exposure to TFA-D led to the same species, with increasing prevalence of byproducts on ^{13}C-APT (δ = 135-125, 80-70, 45-20 ppm). However, upon quenching with pyridine-D5, the extent of observed isomerization was more pronounced. While incubation with 10% TFA-D led to an estimated stability of 75% **5**, 20% TFA-D led to a heterogenous spectrum in which the stability for **5** was so low that the data was deemed non extractable.

Based on these data, the existence of a stabilized cationic species was hypothesized to enable (partial) retention of the *trans* olefin configuration during acidic exposure. In an extreme scenario, direct deuteration of **5** with TFA-D likely occurs on C_2 and/or C_3, after which the positive charge can be stabilized by anchimeric assistance of the carbamate moiety. These options were evaluated by computing the (anchimerically) stabilized structures arising from both pathways (protonation on C_2 or C_3) for a model axial TCO carbamate with N-methylation (**12**, Figure 7A). DFT computations reveal that protonation on C_3, with anchimeric assistance as a five-membered ring system, is the most likely stabilized cationic species with a strong preference of 3 kcal mol^{-1}. This is also in agreement with the NMR results presented herein (Figures 4 – 6), where a direct shift of the H_3 signal was observed upon treatment with TFA-D and only a single product was initially observed. Furthermore, it is generally accepted that the formation of a five membered ring would occur faster than the formation of a six-membered ring. It is noteworthy that the computed structure for the cationic species has four carbon atoms in plane and four carbon atoms above that plain. This matches the most stable conformation of *cis*-cyclooctene, as reported by previous DFT studies,[34] but does not explain how the *trans*-configuration is retained or restored upon neutralization. Therefore, the proposed mechanism entails protonation/deuteration of **5** on C_3 and formation of a stabilized cationic species (**13**) by anchimeric assistance of the carbamate moiety towards C_2. This species retains the *trans* configuration and can rearrange into the more stable *cis* configuration (**14**) upon prolonged acidic exposure (Figure 7B).

In order to translate the NMR studies presented herein towards the envisioned Fmoc SPPS strategy, deprotection of the peptide sequence should occur under dilute TFA concentrations (<10% *v/v*). It was reasoned that introduction of the TCO-moiety via selective Lys sidechain deprotections would therefore be limited to allyloxycarbonyl (Alloc) manipulation, as 4-methyltrityl (Mtt) groups are also cleaved under dilute acid.[35] Furthermore, the utilization of a TCO-modified Lys building block could simplify future methodology for TCO-modification of other types of amino acids (Tyr, Ser, Thr) as TCO-ethers.[29,36]
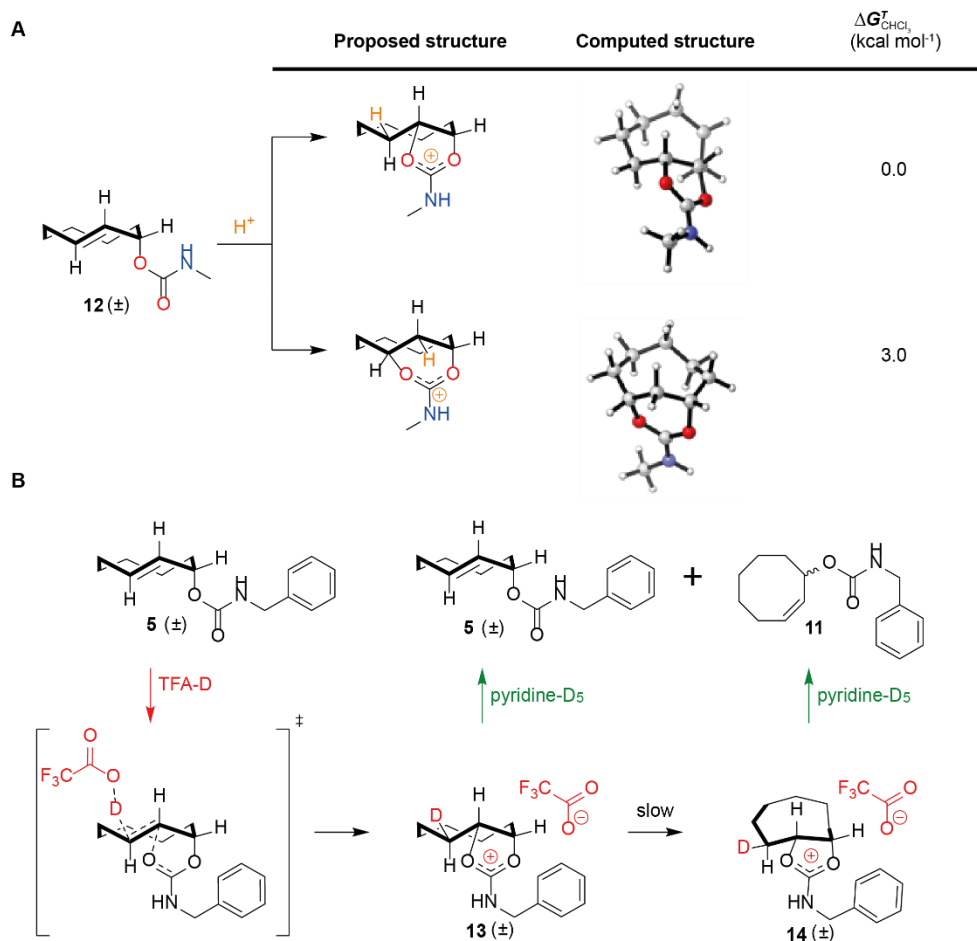
Figure 7 A) Proposed formation of stabilized cationic species upon exposure of TCO-carbamate **12** to TFA. The positive charge created by protonation of C_2 or C_3 can be stabilized by anchimeric assistance of the carbamate moiety, thereby forming either a five- or six-membered ring system. Both structures were computed with DFT, revealing that protonation on C_3 results in the most stable structure by a margin of 3.0 kcal mol^{-1}. Energies are computed at PCM(CHCl$_3$)-M06-2X/6-311++G(d,p). B) Mechanistic rationale for the NMR studies presented in this Chapter. Deuteration of **5** on C_3 and anchimeric stabilization on C_2 leads to the formation of a stabilized species cationic species (**13**). From this species, slow isomerization to the *cis*-cyclooctene conformation (**14**) or reformation of **5** (upon neutralization of the acid) can both occur. Calculations were performed by T. Hansen (Leiden University).

Axial TCO carbonates **15** and **16** were obtained by reacting axial TCO **9** with N,N'-disuccinimidyl carbonate and 4-nitrophenyl chloroformate, respectively. Fmoc-Lys(TCO)-OH (**17**)[18,23] was synthesized from Fmoc-Lys-OH (**18**) and carbonates **15** and **16** for incorporation in Fmoc SPPS (Table 1). Conditions derived from procedures

Table 1 Synthesis of Fmoc-Lys(TCO)-OH (**17**) from Fmoc-Lys-OH · HCl (**18**) and axial TCO carbonates **15** and **16**.
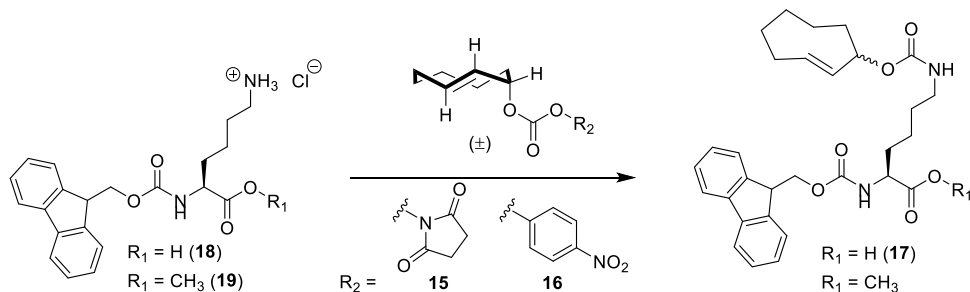
Entry	Lys (eq)	TCO (1 eq)	Scale (mmol)	Base (eq)	Solvent (M)	Time (h)	Yield (%)[a]
1	**18** (1.5)	**15**	0.26	DIPEA (2)	DMF (0.3)	19	36
2	**18** (1.5)	**15**	0.46	DIPEA (2)	DMF (0.3)	48	20
3[b]	**18** (2.0)	**15**	0.50	DIPEA (3)	DMSO (0.1)	19	40
4[c]	**19** (1.5)	**16**	0.29	DIPEA (1.5)	DMSO (0.1)	1	0
5	**19** (1.2)	**16**	0.20	DIPEA (1.2)	DCM (0.2)	4.5	0
6	**18** (1.5)	**16**	0.20	NaHCO$_3$ (3) Na$_2$CO$_3$ (1.5)	Dioxane/H$_2$O 1:1; (0.05)	22	47
7	**18** (2.0)	**16**	0.20	NaHCO$_3$ (4) Na$_2$CO$_3$ (2)	Dioxane/H$_2$O 1:1; (0.1)	19	90
8	**18** (2.0)	**16**	2.0	NaHCO$_3$ (4) Na$_2$CO$_3$ (2)	Dioxane/H$_2$O 1:1; (0.1)	4	90

[a]Isolated yield. [b]Dropwise addition of TCO carbonate **15** over 2 hours. [c]Dropwise addition of DIPEA over 4.5 hours.

by Li *et al*.[23] (entries 1-2) and Nikíc *et al*.[18] (entry 3) were initially investigated using the previously described axial TCO succinimidyl carbonate **15**. The mediocre yield obtained in these entries (20 – 40%) was reduced down to 0% when attempting similar conditions with Fmoc-Lys-OMe (**19**; entries 4-5). Although N$_\alpha$-Fmoc cleavage is very slow in the presence of tertiary amines such as DIPEA,[37,38] is has been reported that this reaction readily occurs via the ε-amino group of Lysine.[35] Finally, it is conceivable that the absence of a carboxylic acid functionality (entries 4-5) further enhanced this deprotection. The isolated yield of Fmoc-Lys(TCO)-OH (**17**) was increased up to 90% by switching to a dioxane/H$_2$O (1:1 *v/v*) solvent system in which a mixture of sodium bicarbonate and sodium carbonate was employed as base (entry 7). This optimized procedure was also executed on mmol scale in which the reaction reached completion within 4 hours (entry 8).

Fmoc-Lys(TCO)-OH (**17**) was evaluated as a building block for Fmoc SPPS in the direct synthesis of TCO-modified SIINFEKL (Figure 8A). The design and application in chemical immunology for TCO modification of this peptide sequence is described in Chapter 4. C-terminal loading was accomplished using a Tentagel resin with a TFA labile (≥ 5% *v/v* in DCM) AC linker (3-methoxy-4(hydroxymethyl)phenoxyacetic acid; Rapp polymere). Ser and Glu were incorporated with trityl (Trt; 1 - 5% TFA in DCM, *v/v*)[39] and 2-phenylisopropyl ester (2-PhiPr; 2 – 4% TFA in DCM, *v/v*)[40] protective groups, respectively. The recently introduced 4-monomethoxytrityl (MMt) protection of Asn was chosen over conventional trityl (Trt; 95% TFA in DCM, *v/v*) protection.[41]

After verifying successful assembly of the peptide sequence using an analytical deprotection with TFA/H$_2$O/TIS (95/2.5/2.5, *v/v*), the resin bound peptide (**20**) was subjected to various deprotection conditions (5/10/20% TFA in DCM, 2% TIS, *v/v*) for 60 minutes. Deprotection mixtures were neutralized in MeOH/pyridine (2 equivalents), concentrated *in vacuo* and treated with tetrazine **21** to enable estimation of the *cis/trans* ratio by LC/MS analysis. The results revealed that, in contrast to the complete deprotection of the Ser and Glu residues, the Asn residue only approached full deprotection at 20% TFA (*v/v*). Furthermore, an increasing degree of cyclooctene carbamate hydrolysis was observed for higher TFA concentrations. The peptides detected with the cyclooctene modality retained 45% (5% TFA, 2% TIS, *v/v*) to 9% (20% TFA, 2% TIS, *v/v*) of their *trans* olefin bond.

Taken together, these results indicate the deprotection of (Lys)-TCO-modified peptides from solid support should preferably constitute short exposure times with low TFA concentrations, thereby minimizing the hydrolysis and isomerization of the TCO-carbamate moiety. The feasibility of this approach was recently demonstrated by synthesizing a TLR-2 agonist with N-terminal TCO carbamate modification using Fmoc SPPS.[42] In this case, exposing the construct for 15 min to 5% TFA, 2.5% TIS, 2.5% H$_2$O in DCM (*v/v*), followed by HPLC purification, led to sufficient quantity of the desired *trans*-product.[42]

Side chain protecting groups employed for Fmoc building blocks are to be carefully selected for this strategy. In case of the SIINFEKL sequence, and C/N-terminally extended derivatives thereof, the abovementioned deprotection conditions could be feasible by incorporating the Asn residue without a sidechain protecting group. β-Cyano-aniline formation, by dehydration of Fmoc-Asn-OH during carboxylic acid activation,[43] can be minimized by employing 1-hydroxy-1H-benzotriazole (HOBt) as an additive for carbodiimide procedures or by use of activated ester derivatives of Fmoc-Asn-OH.[44,45] For long sequences, where the reduced solubility of exposed Asn sidechains is more relevant, the development of a highly acid labile (≤ 5% TFA in DCM,

A

B

Deprotection conditions →		5% TFA, 2% TIS	10% TFA, 2% TIS	20% TFA, 2% TIS
Fragment groups		Relative signal	Relative signal	Relative signal
$R^1 =$	$R^2 = H$ $R^2 = MMt$	1.0	1.0	1.0
		% *trans*: 45	% *trans*: 34	% *trans*: 9
$R^1 =$	$R^2 = H$ $R^2 = MMt$	1.23	1.94	10.71
$R^1 = H$	$R^2 = H$ $R^2 = MMt$	0.56	0.61	2.80
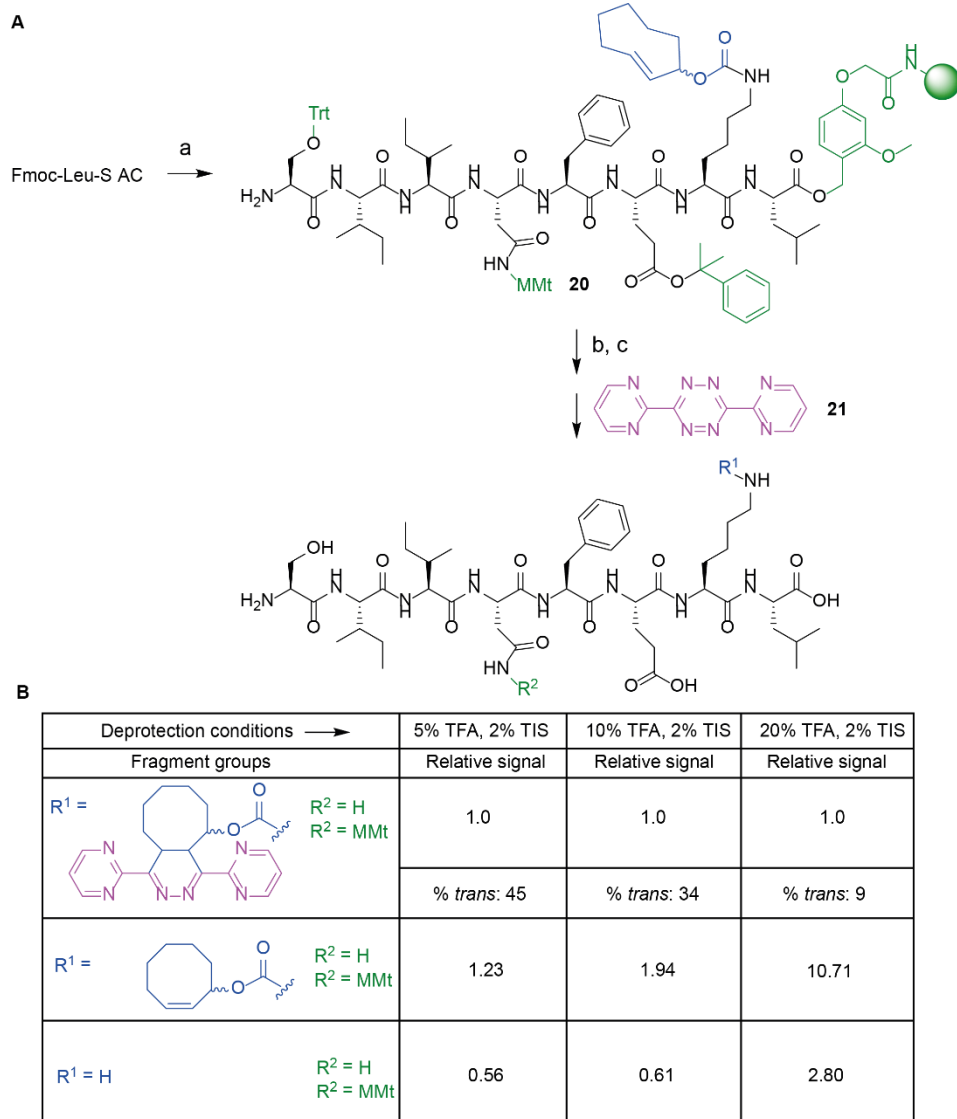
Figure 8 A) Incorporation of Fmoc-Lys(TCO)-OH (**17**) in Fmoc SPPS. Reagents/conditions: (a) Fmoc SPPS from Fmoc-Leu-S AC (tentagel resin) employing building blocks: **17**, Fmoc-Glu(2-PhiPr)-OH, Fmoc-Phe-OH, Fmoc-Asn(MMt)-OH, Fmoc-Ile-OH (x2) and Fmoc-Ser(Trt)-OH; (b) 5-20% TFA, 2% TIS in DCM (*v/v*), 1 h; (c) pyridine (2 equiv) in MeOH. B) Summary of LC/MS analyses of the deprotection mixtures. Analytical samples were treated with tetrazine **21** prior to LC/MS analysis to allow discrepancy between *cis* and *trans*-cyclooctene moieties. Relative signals of the total ion count (TIC) were calculated for the fragment groups displayed.

v/v) protective group for Asn, such as 4,4'-dimethoxytrityl (DMT), could be of importance.

3.3 Conclusions

In conclusion, approaches towards an Fmoc SPPS-based strategy for TCO-modified peptide synthesis is described. TFA induced isomerization of a model axial allylic substituted TCO carbamate was studied using ^{1}H and ^{13}C NMR. The results confirmed that global deprotection of a peptide sequence should occur under dilute TFA concentrations (< 10% *v/v*). Preferential protonation on C_3 and anchimeric assistance of the carbamate moiety towards C_2 was hypothesized to account for the stability of the cationic species formed under these acidic conditions. Optimized synthesis of an Fmoc-Lys(TCO)-OH building block was followed by its incorporation in the SIINFEKL peptide sequence on solid support. Global deprotection of this sequence under dilute TFA concentrations (5% *v/v*, 60 minutes) led to substantial TCO isomerization and carbamate hydrolysis, indicating that further optimization of this deprotection step is required. An alternative synthetic strategy, featuring solution phase coupling of the TCO moiety to peptide sequences after Fmoc SPPS, was explored in Chapter 4 as a consequence of the results described in this Chapter.

3.4 Experimental procedures

General methods: Commercially available reagents and solvents were used as received. Moisture and oxygen sensitive reactions were performed under N_2 atmosphere (balloon). DCM, toluene, dioxane and Et_2O were stored over (flame-dried) 4 Å molecular sieves (8-12 mesh). MeOH was stored over (flame-dried) 3 Å molecular sieves. DIPEA and Et_3N were stored over KOH pellets. TLC analysis was performed using aluminum sheets, pre-coated with silica gel (Merck, TLC Silica gel 60 F_{254}). Compounds were visualized by UV absorption (λ = 254 nm), by spraying with either a solution of $KMnO_4$ (20 g/L) and K_2CO_3 (10 g/L) in H_2O, a solution of $(NH_4)_6Mo_7O_{24} \cdot 4H_2O$ (25 g/L) and $(NH_4)_4Ce(SO_4)_4 \cdot 2H_2O$ (10 g/L) in 10% H_2SO_4, 20% H_2SO_4 in EtOH, or phosphomolybdic acid in EtOH (150 g/L), where appropriate, followed by charring at ca. 150°C. Column chromatography was performed on Screening Devices b.v. Silica Gel (particle size 40-63 µm, pore diameter 60 Å). Celite Hyflo Supercel (Merck) was used to impregnate the reaction mixture prior to silica gel chromatography when indicated. ^{1}H, ^{13}C APT, ^{1}H COSY, HSQC and HMBC spectra were recorded with a Bruker AV-400 (400/100 MHz) or AV-500 (500/125 MHz) spectrometer. Chemical shifts are reported as δ values (ppm) and were referenced to tetramethylsilane (δ = 0.00 ppm) or the residual solvent peak as internal standard. J couplings are reported in Hz. LC-MS analysis was performed on a Finnigan Surveyor HPLC system (detection at 200-600 nm) with an analytical C_{18} column (Gemini, 50 x 4.6 mm, 3 µm particle size, Phenomenex) coupled to a Finnigan LCQ Advantage MAX ion-trap mass spectrometer (ESI$^+$). The applied buffers were H_2O, MeCN and 1.0% TFA in H_2O (0.1% TFA end concentration). The method used was: 10% → 90% MeCN, 13.5 min (0→0.5 min: 10% MeCN; 0.5→8.5 min: gradient time; 8.5→10.5 min: 90% MeCN; 10.5→13.5 min: 90% → 10% MeCN). The synthesis of tetrazine **21** is described in Chapter 4 and a recent publication.[24]

Photoisomerization methods: General guidelines were followed as described by Royzen *et al.*[32] Photochemical isomerization was performed using a Southern New England Ultraviolet Company Rayonet reactor (model RPR-100) equipped with 16 bulbs (part number RPR-2537A, λ = 254 nm). Photolysis was performed in a 1500 mL quartz flask (Southern New England Ultraviolet Company; part number RQV-323). A HPLC pump (Jasco; model PU-2088 Plus) was used to circulate solvent through the photolysis apparatus at the indicated flow rate. An empty solid load cartridge with screw cap, frits, O-ring and end tips (40 g; SD.0000.040; iLOK™, Screening Devices b.v.) was manually loaded with the specified silica gel to function as the stationary phase.
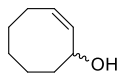
Computational methods: The density functional theory (DFT) computations were performed using Gaussian 09 rev D.01. For all computation the hybrid functional B3LYP–D3(BJ) and M06–2X were used for geometry optimization and energy calculation respectively. In terms of the basis set, 6–31+G(d) was used for geometry optimization and 6–311++G(d,p) was used for energy calculation. The internally defined super-fine grid size was used (SCF=tight, Int=veryfinegrid), which is a pruned 175,974 grid for first-row atoms and a 250,974 grid for all other atoms. Geometries were optimized without symmetry constraints. All calculated stationary points have been verified by performing a vibrational analysis, to be energy minima (no imaginary frequencies). Solvation in chloroform was taken into account in the computations using the PCM implicit solvation model. Solvent effects were explicitly used in the solving of the SCF equations

and during the optimization of the geometry and the vibrational analysis. The ring dihedral angles were constrained for all conformations. The optimized structures were illustrated using CYLview.

The denoted free Gibbs energy was calculated using Equation S1, in which ΔE_{gas} is the gas-phase energy (electronic energy), $\Delta G^T_{\text{gas,QH}}$ (T = 293.15 K, p = 1 atm., C = 1 M) is the sum of corrections from the electronic energy to the free Gibbs energy in the quasi-harmonic oscillator approximation, including zero-point-vibrational energy, and ΔG_{solv} is their corresponding free solvation Gibbs energy. The $\Delta G^T_{\text{gas,QH}}$ was computed using the quasi-harmonic approximation in the gas phase according to the work of Truhlar.[46] The quasi-harmonic approximation is the same as the harmonic oscillator approximation except that vibrational frequencies lower than 100 cm^{-1} were raised to 100 cm^{-1} as a way to correct for the breakdown of the harmonic oscillator model for the free energies of low-frequency vibrational modes.[46]

$$\Delta G^T_{\text{H2O}} = \Delta E_{\text{gas}} + \Delta G^T_{\text{gas,QH}} + \Delta G_{\text{solv}} \qquad \text{(Eq. S1)}$$

$$= \Delta G^T_{\text{gas}} + \Delta G_{\text{solv}}$$

**Cyclooctenol 6:** Synthesis was performed according to literature references.[30,31] A solution of diphenyl diselenide (10.0 g, 32.0 mmol, 1.5 equiv) in DCM (100 mL) was cooled to 0°C (ice bath) under an argon atmosphere before adding hydrogen peroxide solution (35% *w/w*, 2.85 mL, 32.6 mmol, 1.5 equiv) dropwise. The reaction mixture was stirred for 75 min before adding magnesium sulfate hydrate (11 g). The resulting suspension was stirred for 60 min before removing the ice bath and adding (Z)-cyclooctene (**7**, 2.80 mL, 21.46 mmol, 1.0 equiv). The reaction mixture was stirred for 22 h at room temperature, after which conversion to the intermediate hydroxyl selenide adduct (**8**) was shown using TLC (R_f = 0.4 (pentane)). The reaction mixture was cooled to 0°C (ice bath) before adding *tert*-butyl hydroperoxide (~5.5 M in decane, 20.73 mL, 114 mmol, 5.3 equiv) dropwise. The ice bath was removed and the reaction mixture was stirred for > 20 h at room temperature under an argon atmosphere, resulting in an orange solution with a colorless precipitate. The reaction mixture was filtered, the residue was washed with Et_2O and the orange filtrate was concentrated *in vacuo*. The crude oil was redissolved in Et_2O (~150 mL) and washed with Na_2CO_3 (5% *w/w*, 2 x 100 mL), H_2O (100 mL), Fe_2SO_4 (10% *w/w*, 2 x 100 mL), H_2O (100 mL), $NaHCO_3$ (sat., 100 mL), H_2O (100 mL) and brine (100 mL). The organic layer was then dried over $MgSO_4$, filtered and concentrated *in vacuo*. The crude product was purified by silica gel chromatography (15% → 20% Et_2O in pentane). Cyclooctenol **6** (2.34 g, 18.54 mmol, 86%) was collected as a yellow oil: R_f = 0.3 (20% Et_2O in pentane); ^{1}H NMR (400 MHz, $CDCl_3$) δ 5.60 (dddd, *J* = 10.3, 8.5, 7.0, 1.4 Hz, 1H), 5.52 (ddd, *J* = 10.8, 6.6, 1.0 Hz, 1H), 4.69 – 4.61 (m, 1H), 2.22 – 2.02 (m, 2H), 1.95 – 1.86 (m, 1H), 1.81 (s, 1H), 1.69 – 1.32 (m, 7H); ^{13}C NMR (101 MHz, $CDCl_3$) δ 135.1, 128.7, 69.6, 38.7, 29.2, 26.4, 26.0, 23.8. Spectroscopic data was in agreement with literature.[31]
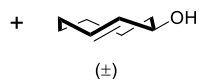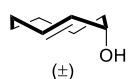
Trans-**cyclooctenol; axial diastereoisomer (9) and equatorial diastereoisomer (10):** Synthesis was performed according to literature references.[20,32] Cyclooctenol **6** (1.00 g, 7.92 mmol, 1.0 equiv) was irradiated (λ = 254 nm) for 20 h in the presence of methyl benzoate (2.60 ml, 20.60 mmol, 2.6 equiv) in a quartz flask containing a solution of Et_2O in heptane (10% *v/v*, 500 mL). During irradiation, the reaction mixture was continuously circulated over a column (40 g size, containing dry silica and 17 g of $AgNO_3$ impregnated silica[32] (10% w/w, containing ca. 10 mmol $AgNO_3$, 1.26 equiv)) at a flowrate of 40 mL/min. The column was placed in the dark and shielded with aluminum foil during the irradiation. Absence of **6** from the reaction mixture was shown with ^{1}H NMR and the column was flushed with Et_2O in heptane (10% *v/v*, 600 mL) before drying over a stream of air. Next, the contents of the column were emptied into an Erlenmeyer flask containing NH_4OH (sat., 200 mL) and DCM (200 mL). The biphasic mixture was stirred for ~ 1 h before filtration of the silica gel. The organic layer was separated and the aqueous layer was extracted with DCM (200 mL). The combined organic layers were washed with H_2O (100 mL), dried over $MgSO_4$, filtered and concentrated *in vacuo*. The crude isomeric mixture was separated and purified by silica gel chromatography (15% Et_2O in pentane; isocratic). The axial product (**9**, 328 mg, 2.60 mmol, 33%) was obtained as an oil: R_f = 0.4 (20% Et_2O in pentane); ^{1}H NMR (400 MHz, $CDCl_3$) δ 5.96 (ddd, *J* = 15.5, 11.0, 3.5 Hz, 1H), 5.58 (dd, *J* = 16.5, 2.2 Hz, 1H), 4.61 (br s, 1H), 2.52 – 2.45 (m, 1H), 2.08 – 2.00 (m, 1H), 1.99 – 1.92 (m, 2H), 1.90 – 1.80 (m, 1H), 1.72 – 1.46 (m, 4H), 1.17 – 1.06 (m, 1H), 0.82 – 0.71 (m, 1H); ^{13}C NMR (101 MHz, $CDCl_3$) δ 135.3, 130.7, 71.4, 43.3, 36.2, 36.0, 29.3, 23.3. The equatorial product (**10**, 217 mg, 1.72

mmol, 22%) was obtained as an oil: R$_f$ = 0.2 (20% Et$_2$O in pentane); ^{1}H NMR (400 MHz, CDCl$_3$) δ 5.71 – 5.61 (m, 1H), 5.54 (dd, *J* = 16.2, 9.1 Hz, 1H), 4.26 (td, *J* = 9.5, 5.6 Hz, 1H), 2.43 – 2.36 (m, 1H), 2.19 – 2.11 (m, 1H), 2.02 – 1.72 (m, 5H), 1.54 – 1.34 (m, 2H), 0.94 – 0.84 (m, 1H), 0.81 – 0.70 (m, 1H). ^{13}C NMR (101 MHz, CDCl$_3$) δ 135.8, 131.8, 76.8, 44.3, 35.9, 35.4, 29.1, 27.7. Spectroscopic data was in agreement with literature.[20]
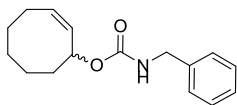
CCO carbamate 11: Cyclooctenol **6** (379 mg, 3.0 mmol, 1.0 equiv) was dissolved in anhydrous DCM (20 mL) under N$_2$. Benzyl isocyanate (1.16 ml, 9.36 mmol, 3.12 equiv) and Et$_3$N (150 µl, 1.07 mmol, 0.36 equiv) were subsequently added. The reaction mixture was stirred at room temperature for 72 h, impregnated with Celite and concentrated *in vacuo*. The impregnated crude product was purified by silica gel chromatography (10% Et$_2$O in pentane) to obtain CCO carbamate **11** (643 mg, 2.48 mmol, 83 %) as white solid: ^{1}H NMR (400 MHz, CDCl$_3$) δ 7.39 – 7.24 (m, 5H), 5.70 – 5.62 (m, 1H), 5.63 – 5.56 (m, 1H), 5.48 (ddd, *J* = 10.8, 7.0, 1.3 Hz, 1H), 4.96 (br s, 1NH), 4.36 (d, *J* = 5.9 Hz, 2H), 2.35 – 2.22 (m, 1H), 2.16 – 2.05 (m, 1H), 2.00 – 1.90 (m, 1H), 1.73 – 1.63 (m, 1H), 1.62 – 1.45 (m, 5H), 1.44 – 1.32 (m, 1H); ^{13}C NMR (101 MHz, CDCl$_3$) δ 156.3, 138.8, 131.2, 129.6, 128.7 (x2), 127.7, 127.5 (x2), 73.1, 45.1, 35.5, 28.9, 26.4, 26.0, 23.5.
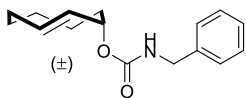
**Axial TCO carbamate 5**: Procedure was modified from existing literature.[20] Axial TCO-OH **9** (252 mg, 2.0 mmol, 1.0 equiv) was dissolved in anhydrous DCM (14 mL) under N$_2$. Benzyl isocyanate (771 µl, 6.24 mmol, 3.12 equiv) and Et$_3$N (100 µl, 0.72 mmol, 0.36 equiv) were added before shielding the reaction mixture with aluminum foil. The reaction mixture was stirred at room temperature for 72 h, impregnated with Celite and concentrated *in vacuo*. The impregnated crude product was purified by silica gel chromatography (5% Et$_2$O in pentane → 20% Et$_2$O in pentane) to obtain axial TCO carbamate **5** (401 mg, 1.55 mmol, 77 %) as white solid: ^{1}H NMR (400 MHz, CDCl$_3$) δ 7.43 – 7.19 (m, 5H), 5.92 – 5.73 (m, 1H), 5.54 (d, *J* = 16.5 Hz, 1H), 5.37 (s, 1H), 5.06 (br s, 1NH), 4.38 (d, *J* = 6.0 Hz, 2H), 2.55 – 2.29 (m, 1H), 2.13 – 1.91 (m, 3H), 1.91 – 1.77 (m, 1H), 1.75 – 1.56 (m, 2H), 1.54 – 1.39 (m, 1H), 1.13 – 0.98 (m, 1H), 0.92 – 0.70 (m, 1H); ^{13}C NMR (101 MHz, CDCl$_3$) δ 156.0, 138.7, 131.9, 131.6, 128.8 (x2), 127.8, 127.6 (x2), 74.2, 45.2, 40.9, 36.1, 36.0, 29.2, 24.2. Spectroscopic data was in agreement with literature.[20]
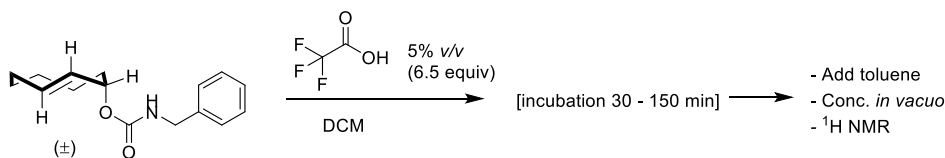
5% *v/v* TFA in DCM, incubation experiment (30 – 150 min) with axial TCO carbamate (5): Axial TCO carbamate **5** (105 mg, 0.40 mmol, 1.0 equiv) was dissolved in anhydrous DCM (3.8 mL) under N$_2$. The flask was tightly wrapped with parafilm, shielded with aluminum foil and placed in the dark. Subsequently, TFA-H (200 µL, 2.60 mmol, 6.5 equiv) was added, obtaining a 0.1 M solution of **5** in 5% TFA-H (*v/v* in DCM). The solution was stirred at room temperature for 2.5 h during which a sample (600 µL) was taken every 30 min. Samples were diluted with toluene (5 ml), concentrated *in vacuo* (40°C) and analyzed by ^{1}H NMR.
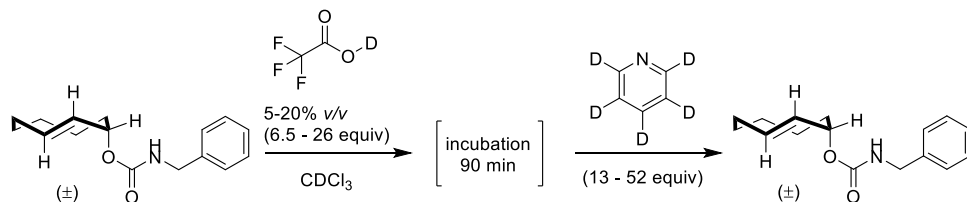
Stability NMR experiment with axial TCO carbamate 5 - 5-20% *v/v* TFA-D in DCM - incubation 90 min - quenching with pyridine D$_5$: Axial TCO-carbamate **5** (15.5 mg, 60 µmol, 1.0 equiv) was dissolved in CDCl$_3$ (570/540/480 µL) in an NMR tube. After measuring a reference spectrum (^{1}H NMR), TFA-D (30µL, 0.39 mmol, 6.5 equiv; 60µL, 0.78 mmol, 13 equiv; 120µL, 1.56 mmol, 26 equiv) was added to obtain a 0.1 M solution of **5** in 5/10/20% TFA-D (*v/v* in CDCl$_3$). The mixture was vortexed for 1 min, and subsequently characterized with NMR (^{1}H, ^{13}C, COSY, HSQC). After 90 min, the mixture was neutralized by adding pyridine-D$_5$ (63 µL, 0.78 mmol, 13 equiv; 126µL, 1.56 mmol, 26 equiv; 252µL, 3.12 mmol, 52 equiv), vortexed for 1 min and characterized with NMR (^{1}H, ^{13}C, COSY, HSQC).
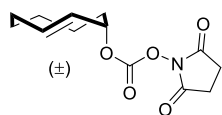
Axial TCO carbonate 15: Axial TCO-OH **9** (380 mg, 2.98 mmol, 1.0 equiv) was dissolved in anhydrous MeCN (15 mL) under N$_2$. N,N'-disuccinimidyl carbonate (1.53 g, 5.96 mmol, 2.0 equiv) and DIPEA (1.04 mL, 5.96 mmol, 2.0 equiv) were added and the reaction mixture, the reaction mixture was shielded with aluminium foil and stirred at room temperature for 120 h. The reaction mixture was concentrated *in vacuo* and the crude product was purified by silica gel chromatography (20% EtOAc in pentane; isocratic) to obtain axial TCO carbonate **15** (710 mg, 2.66 mg, 89%) as a crystalline solid: R$_f$ = 0.2 (20% EtOAc in pentane); ^{1}H NMR (400 MHz, CDCl$_3$) δ 5.97 (ddd, J = 15.6, 11.0, 3.6 Hz, 1H), 5.50 (dd, J = 16.5, 2.1 Hz, 1H), 5.40 (br s, 1H), 2.84 (s, 4H), 2.57 – 2.48 (m, 1H), 2.27 – 2.17 (m, 2H), 2.10 – 1.95 (m, 2H), 1.95 – 1.84 (m, 1H), 1.82 – 1.65 (m, 2H), 1.61 – 1.47 (m, 1H), 1.20 – 1.08 (m, 1H), 0.88 – 0.75 (m, 1H); ^{13}C NMR (101 MHz, CDCl3) δ 168.8 (x2), 150.8, 133.6, 128.4, 81.2, 40.5, 36.2, 35.9, 29.0, 25.6 (x2), 23.9.
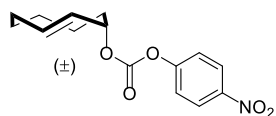
Axial TCO carbonate 16: Axial TCO-OH **9** (330 mg, 2.63 mmol, 1.0 equiv) was dissolved in anhydrous DCM (12 mL) under N$_2$. Anhydrous pyridine (0.64 mL, 7.89 mmol, 3.0 equiv) was added before cooling the reaction mixture to 0°C (ice-bath). 4-Nitrophenyl chloroformate (1.27 g, 6.32 mmol, 2.4 equiv) was added, the reaction mixture was shielded with aluminium foil, stirred for 60 h and allowed to warm to room temperature. The reaction mixture was diluted with H$_2$O (15 mL) and the aqueous layer was extracted with Et$_2$O (3 x 30 mL). The combined organic layers were washed with HCl (1 M, 2 x 20 mL), NaHCO$_3$ (satd., 2 x 30 mL) and brine (60 mL), dried over MgSO$_4$, filtered and concentrated *in vacuo*. The crude product was purified by silica gel chromatography (5% Et$_2$O in pentane, isocratic) to obtain axial TCO carbonate **16** (710 mg, 2.44 mmol, 93%) as a crystalline solid: R$_f$ = 0.2 (5% Et$_2$O in pentane); ^{1}H NMR (400 MHz, CDCl$_3$) δ 8.30 – 8.24 (m, 2H), 7.43 – 7.36 (m, 2H), 5.97 (ddd, *J* = 15.7, 11.2, 3.6 Hz, 1H), 5.57 (dd, *J* = 16.5, 2.2 Hz, 1H), 5.43 (s, 1H), 2.56 – 2.48 (m, 1H), 2.26 – 2.18 (m, 1H), 2.12 – 1.97 (m, 2H), 1.97 – 1.86 (m, 1H), 1.85 – 1.67 (m, 2H), 1.59 – 1.48 (m, 1H), 1.22 – 1.11 (m, 1H), 0.88 – 0.78 (m, 1H); ^{13}C NMR (101 MHz, CDCl$_3$) δ 155.7, 151.8, 145.4, 133.2, 129.5, 125.4 (x2),

121.9 (x2), 78.9, 40.6, 36.1, 36.0, 29.0, 24.1. Spectroscopic data was in agreement with literature.[20]
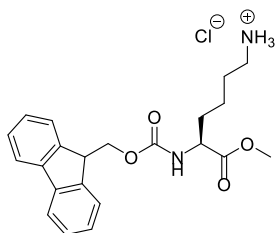
Fmoc-Lys-OMe · HCl (19): Fmoc-Lys-OH • HCl (**18**, 2.02 g, 5.0 mmol, 1.0 equiv) was dissolved in anhydrous MeOH (15 mL) under N_2. The solution was cooled to 0°C (ice-bath) before dropwise addition of $SOCl_2$ (766 µL, 10.5 mmol, 2.1 equiv) over 15 min. The reaction mixture was stirred for 20 min at 0°C and was subsequently stirred for 2 h at 50°C (oil-bath). The reaction mixture was concentrated *in vacuo* and co-evaporated with MeOH (3 x 10 mL) to obtain methyl ester **19** (1.83 g, 4.37 mmol, 87%) as an orange, foamy solid: R_f = 0.4 (20% MeOH in DCM); ^{1}H NMR (400 MHz, DMSO-d_6) δ 7.93 (br s, 3NH), 7.90 (d, *J* = 7.5 Hz, 2H), 7.80 (d, *J* = 7.7 Hz, 1NH), 7.72 (dd, *J* = 7.5, 4.5 Hz, 2H), 7.42 (t, *J* = 7.4 Hz, 2H), 7.33 (t, *J* = 7.3 Hz, 2H), 4.37 – 4.26 (m, 2H), 4.26 – 4.18 (m, 1H), 4.06 – 3.95 (m, 1H), 3.63 (s, 3H), 2.82 – 2.62 (m, 2H), 1.75 – 1.58 (m, 2H), 1.59 – 1.45 (m, 2H), 1.43 – 1.26 (m, 2H); ^{13}C NMR (101 MHz, DMSO-d_6) δ 172.9, 156.2, 143.7 (x2), 140.7 (x2), 127.7 (x2), 127.1 (x2), 125.2, 125.2, 120.2 (x2), 65.6, 53.7, 52.0, 46.6, 38.4, 30.0, 26.4, 22.4. Spectroscopic data was in agreement with literature.[47]
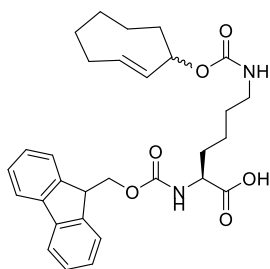
Fmoc-Lys(TCO)-OH (17): Fmoc-Lys-OH • HCl (**18**, 162 mg, 0.40 mmol, 2.0 equiv) was dissolved in H_2O (0.5 mL) before adding a solution of $NaHCO_3$ (67 mg, 0.80 mmol, 4.0 equiv) and Na_2CO_3 (42 mg, 0.40 mmol, 2.0 equiv) in H_2O (0.5 mL). The mixture was briefly cooled towards 0°C (ice-bath) before addin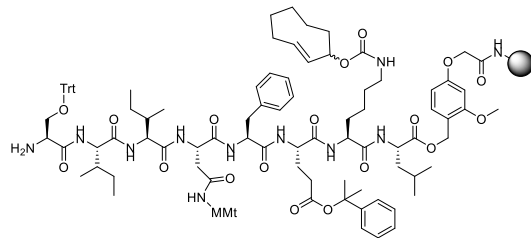g a solution of axial TCO carbonate **16** (58 mg, 0.2 mmol, 1.0 equiv) in dioxane (1 mL). The yellow reaction mixture was shielded with aluminium foil, stirred for 19 h and allowed to warm to room temperature. The reaction mixture was cooled (ice-bath), quenched with HCl (2% *w/w*, 4 mL) and partially concentrated *in vacuo* (40°C, 100 mbar). The aqueous layer was extracted with EtOAc (3 x 5 mL); the combined organic layers were dried over $MgSO_4$, filtered, impregnated with Celite and concentrated *in vacuo*. The crude, impregnated product was purified by silica gel chromatography (20% Et_2O in pentane → DCM → 0.5% MeOH, 1% AcOH in DCM) to obtain the diastereomeric mixture Fmoc-Lys(TCO)-OH (**17A + 17B**, 94 mg, 0.18 mmol, 90%) as a solid: R_f = 0.15 (2% MeOH, 1% AcOH in DCM); ^{1}H NMR (400 MHz, MeOD/CDCl$_3$; 9:1) δ 7.74 (d, *J* = 7.5 Hz, 2H), 7.63 (t, *J* = 7.1 Hz, 2H), 7.36 (t, *J* = 7.4 Hz, 2H), 7.28 (td, *J* = 7.4, 1.0 Hz, 2H), 5.81 (ddd, *J* = 15.7, 11.0, 3.6 Hz, 1H), 5.49 (d, *J* = 16.5 Hz, 1H), 5.22 (br s, 1H), 4.42 – 4.28 (m, 2H), 4.23 – 4.12 (m, 2H), 3.10 (t, *J* = 6.8 Hz, 2H), 2.48 – 2.35 (m, 1H), 2.08 – 1.76 (m, 5H), 1.76 – 1.39 (m, 8H), 1.16 – 1.03 (m, 1H), 0.87 – 0.72 (m, 1H); ^{13}C NMR (101 MHz, MeOD/CDCl$_3$; 9:1) δ 175.7, 158.2, 158.1, 144.9, 144.7, 142.2 (x2), 132.5, 132.3, 128.5 (x2), 127.9 (x2), 126.0, 126.0, 120.7 (x2), 74.7, 67.7, 54.9, 48.1, 41.4, 41.1, 36.7, 36.6, 32.1, 30.1, 29.8, 24.9, 23.8; LC-MS (linear gradient 10 → 90% MeCN, 0.1% TFA, 11 min): R_t (min): 8.70 (ESI-MS (m/z): 521.13 (M+H^{+})). Spectroscopic data was in agreement with literature.[18,23] The procedure was repeated on 2.0 mmol scale to obtain Fmoc-Lys(TCO)-OH (**17**, 942 mg, 1.81 mmol, 90%). The product was redissolved in dioxane and lyophilized to obtain a white powder for Fmoc SPPS.

*Note: no chemical shift differences were encountered on ^1H and ^{13}C NMR for the two diastereoisomers of compound **17**. The signals were therefore reported as a single compound.*

Ser(Trt)-Ile-Ile-Asn(MMt)-Phe-Glu(2-PhiPr)-Lys(TCO)-Leu-Tentagel S AC (20): Fmoc-Leu-Tentagel S AC resin (218 mg, 50 µmol, Rapp polymere) was swelled in DMF (2 mL; 30 min) and manually elongated using a repetitive cycle of: *i.* 20% piperidine in DMF (2 mL, 3 x 3 min; Fmoc deprotection); *ii.* DMF wash (4 x 2 mL); *iii.* Coupling (30 min; 60 min for **17**) with Fmoc-protected amino acid (250 µL, 1 M in DMF, 5 equiv), HCTU (250 µL, 1 M in DMF, 5 equiv) and DIPEA (500 µL, 1 M in DMF, 10 equiv); *iv.* DMF wash (4 x 2 mL); *v.* Ac₂O capping (5% *v/v* in DMF with 0.1 M DIPEA; 2 mL, 10 min); *vi.* DMF wash (4 x 2 mL). After Fmoc deprotection of the N-terminus, the resin was washed with DCM (3 x 2 mL) and Et₂O (3 x 2 mL) and subsequently dried over air to obtain **20** (254 mg) which was divided in portions for deprotection experiments.
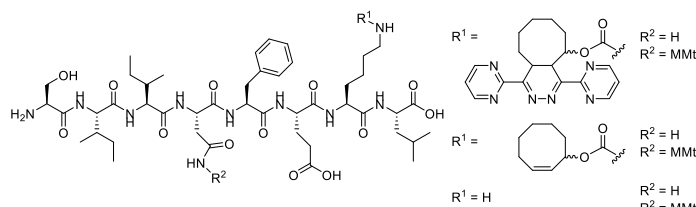
Deprotection of 20 to obtain peptide fragments: Procedures were based on existing literature.[33] Ser(Trt)-Ile-Ile-Asn(MMt)-Phe-Glu(2-PhiPr)-Lys(TCO)-Leu-Tentagel S AC (**20**, 40 mg crude resin) was shaken in DCM (1 mL, 7 x 2 min). The resin was treated with a solution of TFA (5 / 10 / 20% *v/v*; 0.66 equiv) and TIS (2% *v/v*) in DCM (410 µL) for 1 hour before draining the reaction mixture in a 10 mL round-bottom flask containing MeOH (41 µL) and pyridine (64 / 128 / 258 µL; 2 equiv). The resin was washed with a solution of TFA (5 / 10 / 20% *v/v*; 0.33 equiv) and TIS (2% *v/v*) in DCM (200 µL). The neutralized mixture was stirred for 10 min, concentrated *in vacuo* and redissolved in MeCN/H₂O/*t*-BuOH (1:1:1, 100 µL). The resulting solution was sonicated (10 min), 10 x diluted with MeCN/H₂O/*t*-BuOH (1:1:1) and analyzed by LC-MS (20 µL injection). After the first measurement, tetrazine **21** (10 mM in DMSO, 10 µL) was added and the sample was analyzed once more by LC-MS (20 µL injection).

3.5 References

[1]   J. Sauer, H. Wiest, *Angew. Chem.* **1962**, *74*, 353–353.

[2]   E. M. Sletten, C. R. Bertozzi, *Angew. Chem. Int. Ed.* **2009**, *48*, 6974–6998.

[3]   E. M. Sletten, C. R. Bertozzi, *Acc. Chem. Res.* **2011**, *44*, 666–676.

[4]   J. A. Prescher, C. R. Bertozzi, *Nat. Chem. Biol.* **2005**, *1*, 13–21.

[5]   B. L. Oliveira, Z. Guo, G. J. L. Bernardes, *Chem. Soc. Rev.* **2017**, *46*, 4895–4950.

[6]   N. K. Devaraj, *ACS Cent. Sci.* **2018**, *4*, 952–959.

[7]   M. L. Blackman, M. Royzen, J. M. Fox, *J. Am. Chem. Soc.* **2008**, *130*, 13518–13519.

[8]   R. Selvaraj, J. M. Fox, *Curr. Opin. Chem. Biol.* **2013**, *17*, 753–760.

[9]   M. T. Taylor, M. L. Blackman, O. Dmitrenko, J. M. Fox, *J. Am. Chem. Soc.* **2011**, *133*, 9646–9649.

[10]   A. Darko, S. Wallace, O. Dmitrenko, M. M. Machovina, R. A. Mehl, J. W. Chin, J. M. Fox, *Chem. Sci.* **2014**, *5*, 3770–3776.

[11]   N. K. Devaraj, R. Upadhyay, J. B. Haun, S. A. Hilderbrand, R. Weissleder, *Angew. Chem. Int. Ed.* **2009**, *48*, 7013–7016.

[12]   N. K. Devaraj, S. Hilderbrand, R. Upadhyay, R. Mazitschek, R. Weissleder, *Angew. Chem. Int. Ed.* **2010**, *49*, 2869–2872.

[13]   K. Lang, L. Davis, S. Wallace, M. Mahesh, D. J. Cox, M. L. Blackman, J. M. Fox, J. W. Chin, *J. Am. Chem. Soc.* **2012**, *134*, 10317–10320.

[14]   T. Plass, S. Milles, C. Koehler, J. Szymański, R. Mueller, M. Wießler, C. Schultz, E. A. Lemke, *Angew. Chem. Int. Ed.* **2012**, *51*, 4166–4170.

[15]   W. D. Lambert, S. L. Scinto, O. Dmitrenko, S. J. Boyd, R. Magboo, R. A. Mehl, J. W. Chin, J. M. Fox, S. Wallace, *Org. Biomol. Chem.* **2017**, *15*, 6640–6644.

[16]   R. Rossin, S. M. Van Den Bosch, W. Ten Hoeve, M. Carvelli, R. M. Versteegen, J. Lub, M. S. Robillard, *Bioconjug. Chem.* **2013**, *24*, 1210–1217.

[17]   Y. Fang, J. C. Judkins, S. J. Boyd, C. W. am Ende, K. Rohlfing, Z. Huang, Y. Xie, D. S. Johnson, J. M. Fox, *Tetrahedron* **2019**, *75*, 4307–4317.

[18]   I. Nikić, T. Plass, O. Schraidt, J. Szymański, J. A. G. Briggs, C. Schultz, E. A. Lemke, *Angew. Chem. Int. Ed.* **2014**, *53*, 2245–2249.

[19]   J.-E. Hoffmann, T. Plass, I. Nikić, I. V. Aramburu, C. Koehler, H. Gillandt, E. A. Lemke, C.

Schultz, *Chem. Eur. J.* **2015**, *21*, 12266–12270.

[20] R. M. Versteegen, R. Rossin, W. ten Hoeve, H. M. Janssen, M. S. Robillard, *Angew. Chem. Int. Ed.* **2013**, *52*, 14112–14116.

[21] R. Rossin, S. M. J. van Duijnhoven, W. ten Hoeve, H. M. Janssen, F. J. M. Hoeben, R. M. Versteegen, M. S. Robillard, *Bioconjug. Chem.* **2016**, *27*, 1697–1706.

[22] R. Rossin, R. M. Versteegen, J. Wu, A. Khasanov, H. J. Wessels, E. J. Steenbergen, W. ten Hoeve, H. M. Janssen, A. H. A. M. van Onzen, P. J. Hudson, M. S. Robillard, *Nat. Commun.* **2018**, *9*, 1484.

[23] J. Li, S. Jia, P. R. Chen, *Nat. Chem. Biol.* **2014**, *10*, 1003–1005.

[24] A. M. F. van der Gracht, M. A. R. de Geus, M. G. M. Camps, T. J. Ruckwardt, A. J. C. Sarris, J. Bremmers, E. Maurits, J. B. Pawlak, M. M. Posthoorn, K. M. Bonger, D. V. Filippov, H. S. Overkleeft, M. S. Robillard, F. Ossendorp, S. I. van Kasteren, *ACS Chem. Biol.* **2018**, *13*, 1569–1576.

[25] Y. Chiang, A. J. Kresge, *J. Am. Chem. Soc.* **1985**, *107*, 6363–6367.

[26] R. P. Kirchen, T. S. Sorensen, *J. Am. Chem. Soc.* **1979**, *101*, 3240–3243.

[27] J. E. Nordlander, K. D. Kotian, D. E. Raff, G. F. Njoroge, J. J. Winemiller, *J. Am. Chem. Soc.* **1984**, *106*, 1427–1432.

[28] M. S. Robillard, R. M. Versteegen, W. ten Hoeve, R. Rossin, *Chemically Cleavable Group*, **2014**, WO 2014/081303 A1.

[29] R. M. Versteegen, W. ten Hoeve, R. Rossin, M. A. R. de Geus, H. M. Janssen, M. S. Robillard, *Angew. Chem. Int. Ed.* **2018**, *57*, 10494–10499.

[30] T. Hori, K. B. Sharpless, *J. Org. Chem.* **1978**, *43*, 1689–1697.

[31] N. Becker, E. M. Carreira, *Org. Lett.* **2007**, *9*, 3857–3858.

[32] M. Royzen, G. P. A. Yap, J. M. Fox, *J. Am. Chem. Soc.* **2008**, *130*, 3760–3761.

[33] M. Mergler, *Synthesis of Fully Protected Peptide Fragments. In: Pennington M.W., Dunn B.M. (Eds) Peptide Synthesis Protocols. Methods in Molecular Biology, Vol 35*, Humana Press, **1994**.

[34] U. Neuenschwander, I. Hermans, *J. Org. Chem.* **2011**, *76*, 10236–10240.

[35] J. Farrera-Sinfreu, M. Royo, F. Albericio, *Tetrahedron Lett.* **2002**, *43*, 7813–7815.

[36] M. A. R. de Geus, G. J. M. Groenewold, E. Maurits, C. Araman, S. I. van Kasteren, *Chem. Sci.* **2020**, *11*, 10175–10179.

[37]   E. Atherton, C. J. Logan, R. C. Sheppard, *J. Chem. Soc., Perkin Trans. 1* **1981**, 538–546.

[38]   C.-D. Chang, M. Waki, M. Ahmad, J. Meienhofer, E. O. Lundell, J. D. Haug, *Int. J. Pept. Protein Res.* **2009**, *15*, 59–66.

[39]   K. Barlos, D. Gatos, S. Koutsogianni, W. Schäfer, G. Stavropoulos, Y. Wenging, *Tetrahedron Lett.* **1991**, *32*, 471–474.

[40]   C. Yue, J. Thierry, P. Potier, *Tetrahedron Lett.* **1993**, *34*, 323–326.

[41]   P. Sieber, B. Riniker, *Tetrahedron Lett.* **1991**, *32*, 739–742.

[42]   M. J. van de Graaff, T. Oosenbrug, M. H. S. Marqvorsen, C. R. Nascimento, M. A. R. de Geus, B. Manoury, M. E. Ressing, S. I. van Kasteren, *Bioconjug. Chem.* **2020**, *31*, 1685–1692.

[43]   D. V. Kashelikar, C. Ressler, *J. Am. Chem. Soc.* **1964**, *86*, 2467–2473.

[44]   S. Mojsov, A. R. Mitchell, R. B. Merrifield, *J. Org. Chem.* **1980**, *45*, 555–560.

[45]   H. Gausepohl, M. Kraft, R. W. Frank, *Int. J. Pept. Protein Res.* **1989**, *34*, 287–294.

[46]   R. F. Ribeiro, A. V. Marenich, C. J. Cramer, D. G. Truhlar, *J. Phys. Chem. B* **2011**, *115*, 14556–14562.

[47]   T. Huhtiniemi, T. Suuronen, M. Lahtela-Kakkonen, T. Bruijn, S. Jääskeläinen, A. Poso, A. Salminen, J. Leppänen, E. Jarho, *Bioorg. Med. Chem.* **2010**, *18*, 5616–5625.

4

Chemical control over T-cell activation *in vivo*: design and synthesis of *trans*-cyclooctene-modified MHC-I epitopes

4.1 Introduction

Cell-to-cell contact is one of the essential means of information transfer in metazoans. Few examples of such cell-cell contacts result in more drastic phenotypic changes than those between cytotoxic T-lymphocytes (CTLs) and antigen presenting cells (APCs).[1] Naïve T-cells leave the thymus as small, featureless cells with minimal metabolism, but with a strong lymph node homing capacity, reliant on L-selectin (CD62L) and various integrins.[2] Each cell has a specific T-cell receptor (TCR) capable of recognizing a

peptide presented by an APC on a major histocompatibility type-1 complex (MHC-I).[1] Upon recognition of its cognate peptide-MHC-I (pMHC), in combination with co-stimulatory signals co-presented by the APC, massive and rapid phenotypic changes will transform the naïve CTL into a cell capable of killing any non-APCs displaying this cognate peptide on their MHC-I.[3] This is one of the major mechanisms by which tumors and virus-infected cells are routinely cleared from the body and harnessing these traits underpins many of the cancer immunotherapies targeted to tumor neo-epitopes.[4]

Antigen presentation is an important prerequisite for T-cell activation. Nucleated cells proteolytically degrade endogenous proteins into small peptides, which can enter the endoplasmic reticulum (ER) via the transporter associated with antigen processing (TAP), followed by loading on MHC-I, passage to the cell surface via the Golgi system and presentation to CD8+ T-cells (CTLs).[3,5] Exogenously derived polypeptides are normally presented on MHC-II complexes to CD4+ T-cells (helper T-cells) via a different pathway by professional APCs (dendritic cells (DCs), macrophages and B-cells). Here, the MHC class II compartment (MIIC) facilitates deconstruction of the invariant chain (Ii) of MHC-II and ultimately allows binding of a peptide degraded in endosomes.[5] However, antigen cross-presentation[6] allows DCs to process exogenous polypeptides towards MHC-I presentation. It is not clear for this process whether and to which extent antigen processing occurs in the cytosol via proteasomes (cytosolic pathway) or in endocytic compartments via cathepsins (vacuolar pathway).[6]

The binding of the TCR is sensitive. As few as one copy of a cognate peptide can instigate the signaling cascade *in vitro*.[7,8] It is also selective, as this recognition takes place in the context of 10,000s of copies of non-cognate peptides on the same APC.[9,10] Even single amino acid substitutions are capable of curtailing,[11] or even abolishing T-cell activation.[12–14] A factor that complicates T-cell activation studies further is that there is no correlation between the binding strength *in vitro* and the strength of TCR-signaling that follows activation.[15] Less is known about the *in vivo* activation of T-cells.[16] The contacts between T-cells and APCs are, for example, more transient and dynamic in nature compared to those found *in vitro*.[17–20] The lack of a defined starting point to these contacts complicates the study of T-cell activation kinetics, and methods allowing the study of early T-cell activation events with real-time control over activation *in vivo* are needed to study these processes.[16]
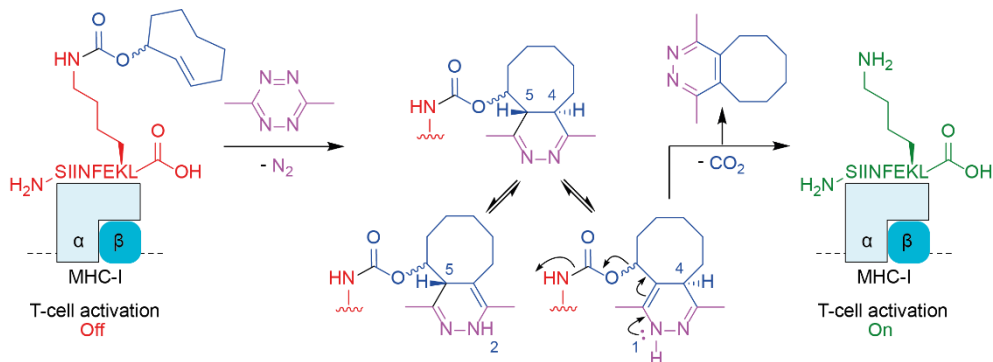
Control over T-cell activation using protecting group strategies to achieve temporal control *in vitro* is an emerging field. Two approaches have been reported in which the ε-amines of lysine residues within either a helper T-cell epitope[21,22] or a cytotoxic T-cell epitope[14] are blocked with a protecting group (Figure 1). These caged epitopes are
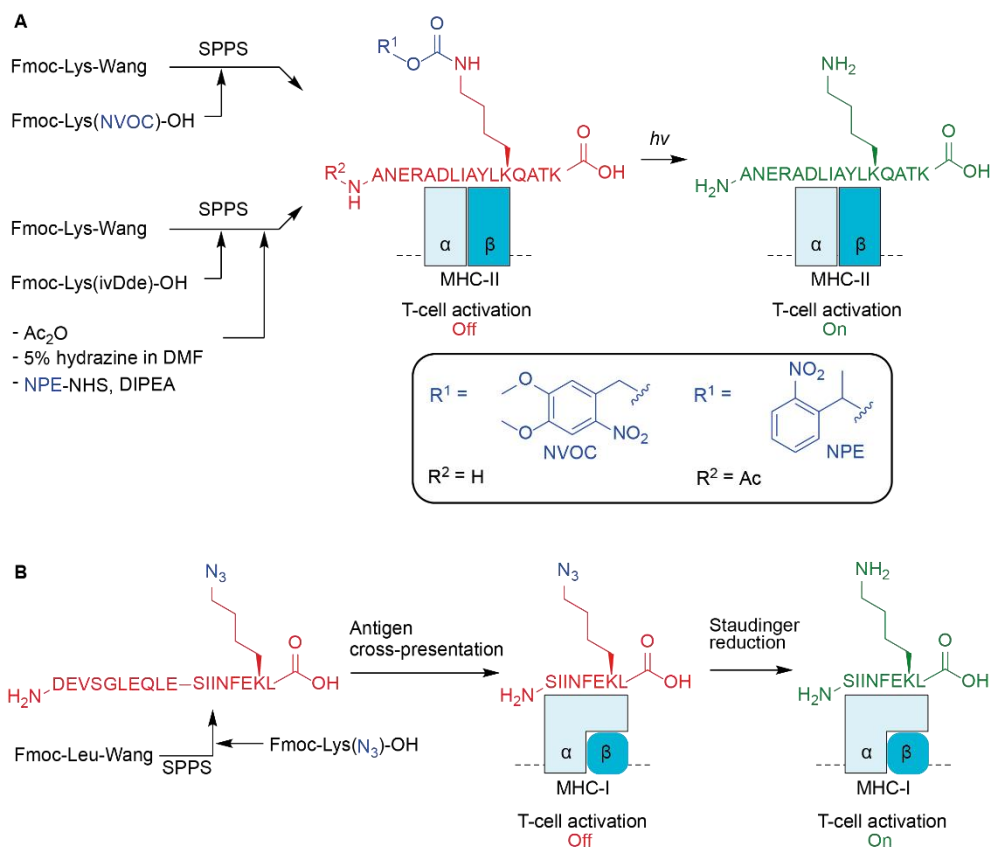
Figure 1 Previously reported *in vitro* approaches to achieve temporal control over T-cell activation, including SPPS strategies to obtain the caged antigens. A) Photodecaging strategy to gain control over helper T-cell (CD4+) activation. MHC II epitope MCC88-103 (moth cytochrome c) was protected on Lys99 using NVOC (6-nitroveratryloxycarbonyl) or NPE (1-ortho-nitrophenyl-ethyl urethane) photocages by DeMond *et al.*[21] and Huse *et al.*,[22] respectively. B) Chemodecaging strategy to study antigen cross-presentation and subsequent cytotoxic T-cell (CD8+) activation reported by Pawlak *et al.*[14] MHC I epitope OVA257-264 (ovalbumin) was protected on Lys263 using an azide which could be deprotected *in vitro* by Staudinger reduction.

accessible either by directly incorporating modified Fmoc-lysine building blocks[14,21] or by utilizing selective sidechain modifications[22] during solid phase peptide synthesis (SPPS). Addition of a deprotection reagent, such as UV-light to remove NVOC (6-nitroveratryloxycarbonyl) or NPE (1-ortho-nitrophenyl-ethyl urethane) groups,[21,22] or water-soluble phosphines to reduce azides to amines,[14,23] provided this temporal control in the petri dish.

Arguably, the use of (UV) light as a trigger to activate T-cell epitopes has intrinsic limitations: poor tissue penetration even at higher wavelengths essentially prohibits systemic application of photocaged T-cell epitopes. On paper, bioorthogonal chemistry

Figure 2 Design of caged peptides for *in vivo* control over T-cell activation. Inverse electron-demand Diels Alder (IEDDA) pyridazine elimination between a silent *trans*-cyclooctene-modified epitope and a tetrazine liberates antigenicity of the peptide. Initial [4+2] cycloaddition, tautomerization and elimination results in the free lysine ε-amine upon which a T-cell can recognize the epitope again and become activated.

has no such tissue-penetrating limits, however the chemistry needs to be effective (more so than the previously reported Staudinger reduction)[14] and all reagents able to penetrate all tissues. In this respect, the most versatile bioorthogonal chemistry developed to date for *in vivo* applications in terms of yield, speed and side reactions comprises the inverse electron demand Diels-Alder reaction (IEDDA).[24] This [4+2] cycloaddition reaction occurs between an electron-poor diene (normally an *s*-tetrazine) and an electron-rich dienophile (most often a strained alkene). The tetrazine ligation between a tetrazine and a *trans*-cyclooctene, was initially reported as an ultra-fast bioorthogonal ligation reaction by the Fox group.[25]

Recently, the IEDDA reaction was redesigned to serve as a bioorthogonal deprotection reaction.[26] In this variant of the IEDDA, the 4,5-dihydropyridazine, resulting from [4+2] cycloaddition of a tetrazine and a *trans*-cyclooctene (TCO) bearing a carbamate at the allylic position, tautomerizes to 1,4- and 2,5-dihydropyridazines. The 1,4-tautomer can then undergo elimination of a carbamate-linked biomolecule at the allylic position, resulting in the liberated biomolecule and CO_2 (Figure 2). Mechanistic investigations concerning this IEDDA pyridazine elimination reaction are currently a field of interest,[27–29] and *in vivo* applications have frequently been reported.[30–36]

This Chapter presents the design and synthesis of TCO modified MHC-I epitopes, resulting in a new method based on the IEDDA pyridazine elimination to provide chemical control over the activation of T-cells (Figure 2). The TCO protecting group was optimized for solubility and on-cell deprotection yield. This novel approach is generic based on the effectiveness for two separate epitopes and works with different T-cells *in vitro*, as well as *in vivo*.
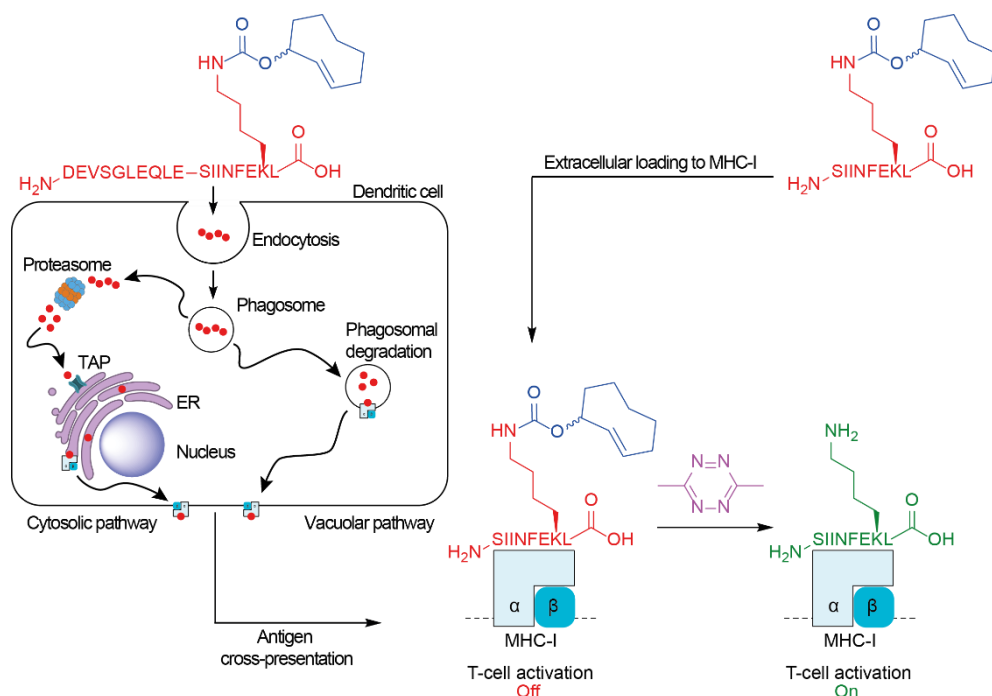
Figure 3 Rationale for TCO carbamate modification of minimal epitopes and extended peptide sequences. Minimal epitopes enable direct, extracellular loading on MHC-I, whereas an extended peptide sequence containing the epitope is initially endocytosed by DCs, followed by antigen cross-presentation via the cytosolic and/or vacuolar pathway.

4.2 Results and discussion

To determine whether IEDDA pyridazine elimination was amenable for *in vivo* T-cell activation and to compare its efficacy with that of the previously reported strategy based on Staudinger reduction,[14] OVA$_{257-264}$ (OT-I, SIINFEKL) was selected as model epitope. The crucial lysine ε-amino group within this epitope is amenable for chemical modification, thereby disabling T-cell activation without disrupting MHC-I binding affinity.[14,37] It was therefore envisioned that TCO carbamate modification of this position would result in silenced MHC-I epitopes. Modification of the minimal epitope results in a probe for direct, extracellular loading on MHC-I complexes, whereas modification of an extended peptide sequence results in a silenced epitope which is initially subjected to antigen cross-presentation (Figure 3).

A direct Fmoc SPPS based synthetic strategy, featuring a lysine building block with TCO carbamate modification, was explored in Chapter 3 without adequate results. Therefore, a synthetic strategy was devised where the TCO carbamate moiety could be installed under solution phase conditions. Cyclooctene N-hydroxysuccinimide (NHS)
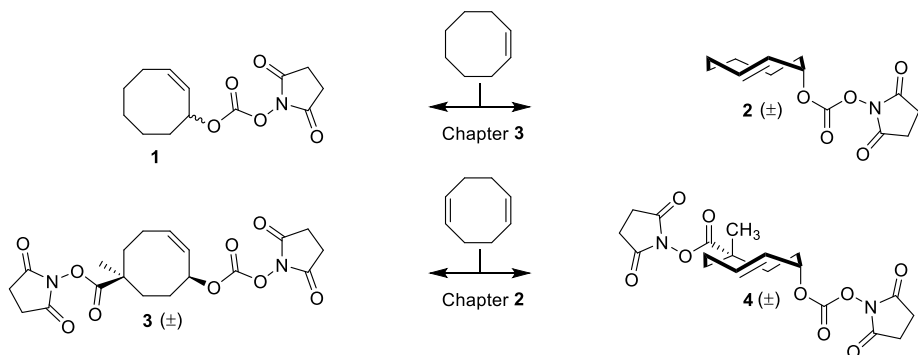
Scheme 1 CCO and TCO NHS-carbonates **1 – 4** employed in this Chapter for regioselective installation of cyclooctene carbamate moieties on lysine ε-amino groups.

carbonates **1 – 2** (Chapter 3) and bifunctional cyclooctene NHS carbonates **3 – 4** (Chapter 2) were selected as appropriate reagents for chemoselective introduction of cyclooctenes on peptide scaffolds containing a lysine ε-amino group (Scheme 1). An important requisite for these reagents was the absence of other reactive amine groups during the conjugation reaction.

The peptide sequence OVA$_{257-264}$ (SIINFEKL) was synthesized using standard Fmoc SPPS conditions followed by N-terminal protection with the methylsulfonylethyloxycarbonyl (MSc) group[38] to improve the solubility of the liberated peptide after acidic cleavage (TFA/H$_2$O/TIPS; 95:2.5:2.5 *v/v*) from the resin and to enable selective modification of the lysine ε-amine in the subsequent step (Scheme 2). From the HPLC-purified intermediate (MSc-SIINFEKL, **5**) CCO- and (axial) TCO carbamate derivatives of SIINFEKL were synthesized by reaction with NHS carbonates **1** and **2** followed by deprotection under basic conditions of the MSc group to provide the *cis*- and *trans*-cyclooctene protected SIINFEKL-derivatives **6** and **7**. Peptide **5** was also reacted with the NHS-carbonates of reagents **3** and **4** in the presence of their sterically hindered NHS-esters. Next, the latter were reacted with ethanolamine to install an extra polar moiety on the ring systems. This resulted in the more water-soluble caged SIINFEKL derivatives **8** and **9** after MSc deprotection. The first two steps of this sequence, selective NHS carbonate coupling followed by NHS ester reaction, were compatible in a one-pot procedure guided by LC-MS monitoring. Caged peptides **6 – 9** were obtained in 10 – 20% yield over 3 steps after HPLC purification.

An N-terminally extended peptide sequence, OVA$_{247-264}$ (DEVSGLEQLESIINFEKL), was synthesized with bifunctional TCO modification (Scheme 3A). This extended peptide sequence still contains only one lysine residue and no other competing sidechains (e.g. cysteine). Therefore, the MSc-protected peptide **10** could be selectively modified with
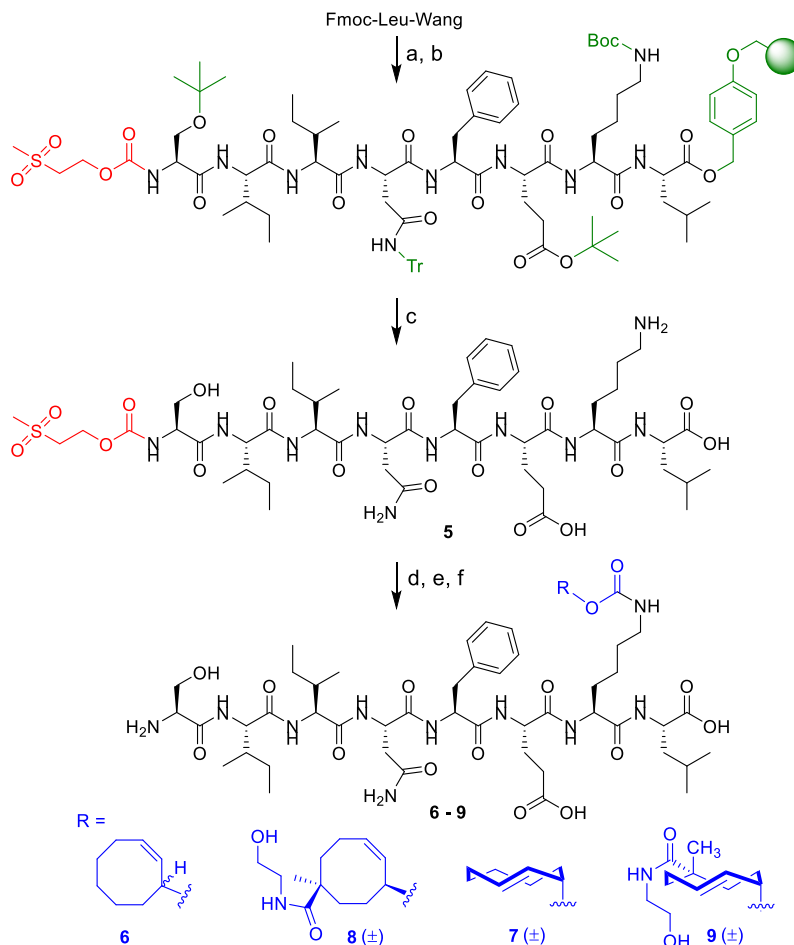
Scheme 2 Synthesis of caged peptides **6 – 9**. Reagents/conditions: (a) Fmoc SPPS from Fmoc-Leu-Wang; (b) MSc-OSu (**23**), DIPEA, NMP, rt; (c) TFA / H_2O / TIPS (95:2.5:2.5), rt, 23%; (d) NHS-CCO (**1**), NHS-TCO (**2**), NHS-bCCO (**3**) or NHS-bTCO (**4**), DIPEA, DMF, rt; (e) ethanolamine, DMF, rt; (f) dioxane/MeOH/4 M NaOH (7.5:2.25:0.25), rt, 16% (**6**), 20% (**7**), 19% (**8**), 14% (**9**) over three steps.

the TCO moiety using the established methodology after switching from DMF to DMSO as solvent for the NHS-coupling reactions. Peptide **11** was obtained in 41% yield over 3 steps after HPLC purification.

To assess whether the uncaging approach could be used for other key lysine residues as well as other MHC-I haplotype ligands, a second epitope in which T-cell recognition is dependent on a critical lysine was selected, namely the $D^bM_{187-195}$ peptide (NAITNAKII) from respiratory syncytial virus (RSV).[39–41] This nonamer sequence binds MHC-I haplotype D^b and the recognition by T-cells is critically dependent on Lys-
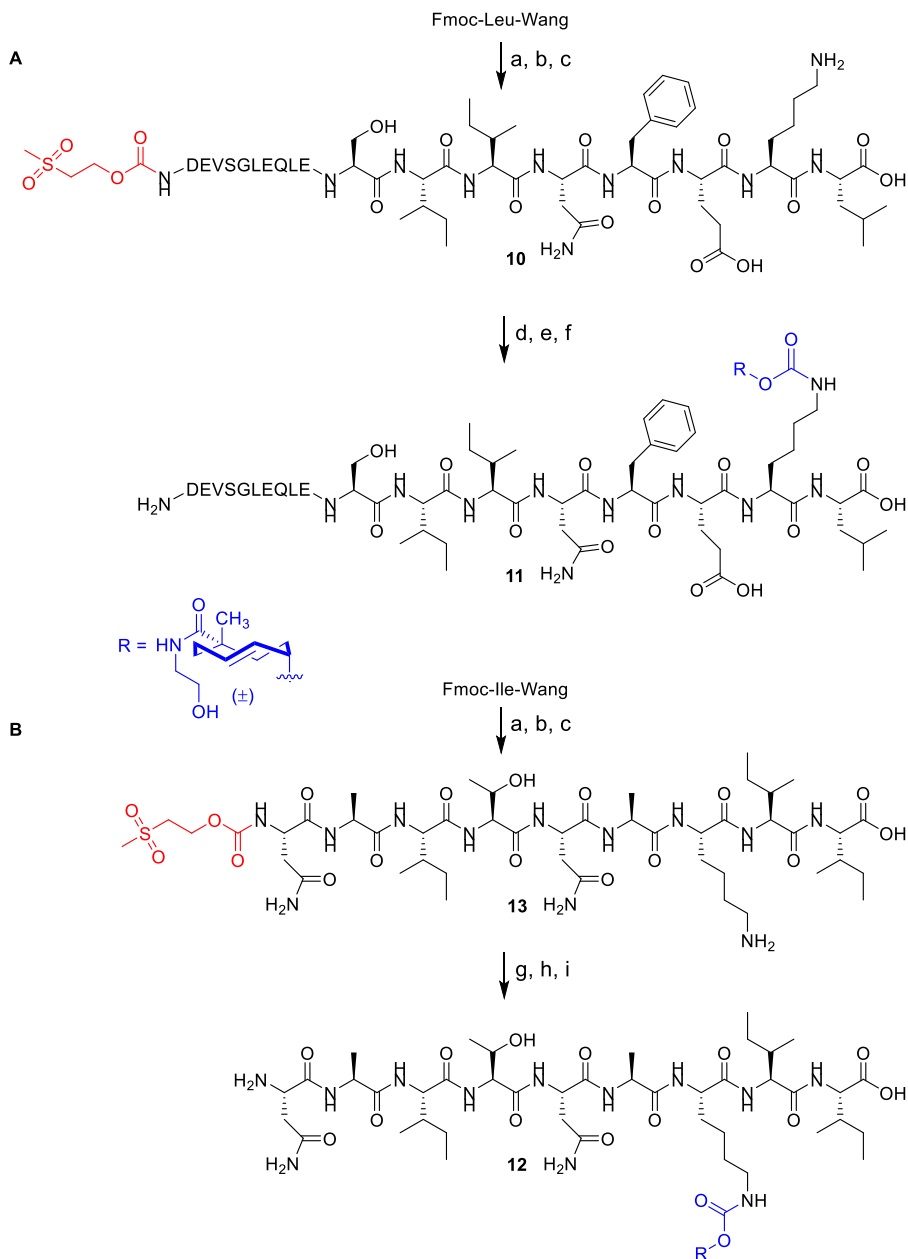
Scheme 3 Synthesis of caged peptides **11** and **12**. Reagents/conditions: (a) Fmoc SPPS from Fmoc-Leu-Wang (A) and Fmoc-Ile-Wang (B); (b) MSc-OSu (**23**), DIPEA, NMP, rt; (c) TFA / H$_2$O / TIPS (95:2.5:2.5), rt, 14% (**10**), 16% (**13**); (d) NHS-bTCO (**4**), DIPEA, DMSO, rt; (e) ethanolamine, DMSO, rt; (f) dioxane/MeOH/4 M NaOH (7.5:2.25:0.25), rt, 41% over three steps; (g) NHS-bTCO (**4**), DIPEA, DMF, rt; (h) ethanolamine, DMF, rt; (i) dioxane/MeOH/4 M NaOH (7.5:2.25:0.25), rt, 13% over three steps.
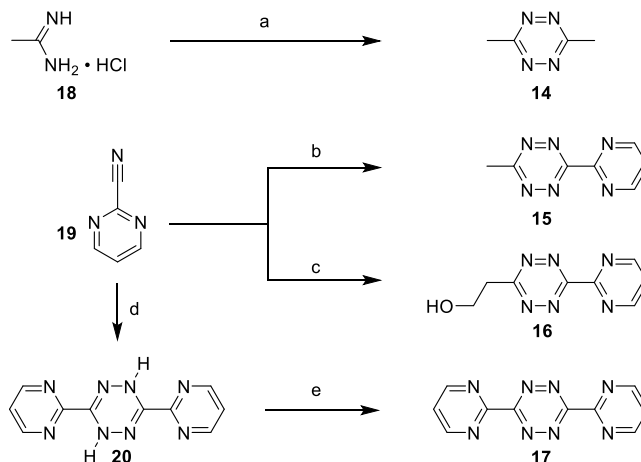
Scheme 4 Synthesis of tetrazines **14** - **17**. Reagents/conditions: (a) i. hydrazine hydrate, H_2O, rt; ii. HNO_3/H_2O, Cu, 0°C, 18% over two steps; (b) i. MeCN, Zn(OTf)$_2$, hydrazine hydrate, 60°C; ii. HNO_3/H_2O, Cu, 0°C, 31% over two steps; (c) i. 3-hydroxypropanenitrile, Zn(OTf)$_2$, hydrazine hydrate, 60°C; ii. $NaNO_2$, HCl, rt, 3% over two steps; (d) THF, HCl, hydrazine hydrate, reflux; (e) DMF, HNO_3/H_2O, Cu, rt, 14% over two steps.

193 recognition,[42] which has previously been subjected to caging.[14] The synthesis of a bifunctional TCO caged variant of this peptide (**12**) was accomplished from the MSc-protected intermediate (**13**) using the previously described method (Scheme 3B).

A panel of tetrazines (**14 – 17**) was synthesized to serve as deprotection agents for the caged peptides (Scheme 4). Cyclization of acetamidine hydrochloride (**18**) and hydrazine monohydrate under aqueous conditions was followed by direct oxidation with NO_2 (g), which was generated externally by adding HNO_3 to Cu, to afford 3,6-dimethyltetrazine (**14**)[26] in 18% yield. Condensation of **19**, MeCN and hydrazine hydrate in the presence of Zn(OTf)$_2$ afforded **15**[27] after oxidation with NO_2 (g) in 31% yield. While the initial cyclization step worked similarly for the synthesis of **16**[27], the oxidation step with NO_2 (g) primarily led to decomposition of the product. Instead, oxidation was achieved by slowly acidifying the crude reaction mixture with HCl after adding $NaNO_2$. Chromatographic purification was followed by recrystallization in EtOAc to obtain **16**.[27] Dihydrotetrazine **20** was isolated by extraction after cyclization of **19** and hydrazine hydrate under reflux conditions. Oxidation of **20** with NO_2 (g) in DMF led to the formation of a purple precipitate, which was filtered and recrystallized in CHCl$_3$ to obtain **17**.[43]

Immunological experiments summarized in this Chapter were performed by A.M.F. van der Gracht (Leiden University), N.A.M. Ligthart (Leiden University), M.G.M. Camps (Leiden University Medical Center) and T.J. Ruckwardt (NIH, USA). Full details can be found in the recently published article[44] *and PhD thesis (A.M.F. van der Gracht).*

The binding of peptides **6 – 9** to MHC-I (H2-K^b) was examined using TAP deficient RMA-S cells.[45,46] TCO modification of the SIINFEKL epitope on the Lys ε-amine did not impair MHC-I binding. The T-cell hybridoma B3Z,[47] which is specific for OVA$_{257\text{-}264}$ (SIINFEKL), was also not activated by **6 - 9** when presented on dendritic cells.

Caged epitopes **6 - 9** were loaded on dendritic cells (DC2.4 cells)[48] and incubated with 50 µM of 3,6-dimethyl-tetrazine (**14**) for 30 minutes. T-cell proliferation was measured after 17 hours as beta-galactosidase-directed CPRG (chlorophenol red-β-D-galactopyranoside) hydrolysis, which is in direct correlation with IL-2 promotor activity, due to its inclusion under the NFAT-promotor in the B3Z T-cell line.[47] No T-cell response was observed for the tetrazine-unreactive peptides **6** and **8**. However, tetrazine-reactive peptides **7** and **9** gave 42% ± 4.2% and 82% ± 4.4% of the response observed for the wild type epitope, respectively. The stability of the TCO-moiety for peptides **7** and **9** was determined in full medium and FCS (fetal calf serum), revealing poor solubility for **7** and stability up to 4 hours in FCS for **9** (Figure S1). Caged epitope **9** was selected for further experiments due to superior uncaging yield, ease of purification and enhanced solubility.

The speed of uncaging of peptide **9** was investigated using the recently reported asymmetric tetrazines by Fan *et al.*,[27] which were shown to have improved kinetics due to the combination of an electron withdrawing group (EWG) and a small, electron donating group (EDG) as substituents on the tetrazine ring (Figure 4A). 3-Methyl-6-pyrimidinyl-tetrazine (**15**) and 3-hydroxyethyl-6-pyrimidinyl-tetrazine (**16**) indeed showed improved uncaging rates and efficacy (Figure 4B-C) compared to **14** (two EDGs), with maximal T-cell activation already observed at the first (1 min) time point, while for **14** the maximal T-cell activation is reached at 30 min incubation. Conversely, 3,6-dipyrimidinyl-tetrazine (**17**) (two EWGs) showed no detectable elimination. Qualitative LC-MS confirmed these findings, including the formation of a stable IEDDA ligation product for **17**. These results are also in agreement with the hypothesis that EWGs accelerate the [4+2] cycloaddition step and suppress subsequent elimination, whereas small, EDGs are essential for the elimination reaction.[27] Tetrazine **17** therefore broadens the scope of the method presented in this Chapter: the substituents of the tetrazine employed dictate whether T-cell activation is switched on (Figure 2) or remains off (Figure 4D). The previously reported dextran-functionalized tetrazine (**21**), which has reduced yield and uncaging speed compared to **14** *in vitro*, but performs
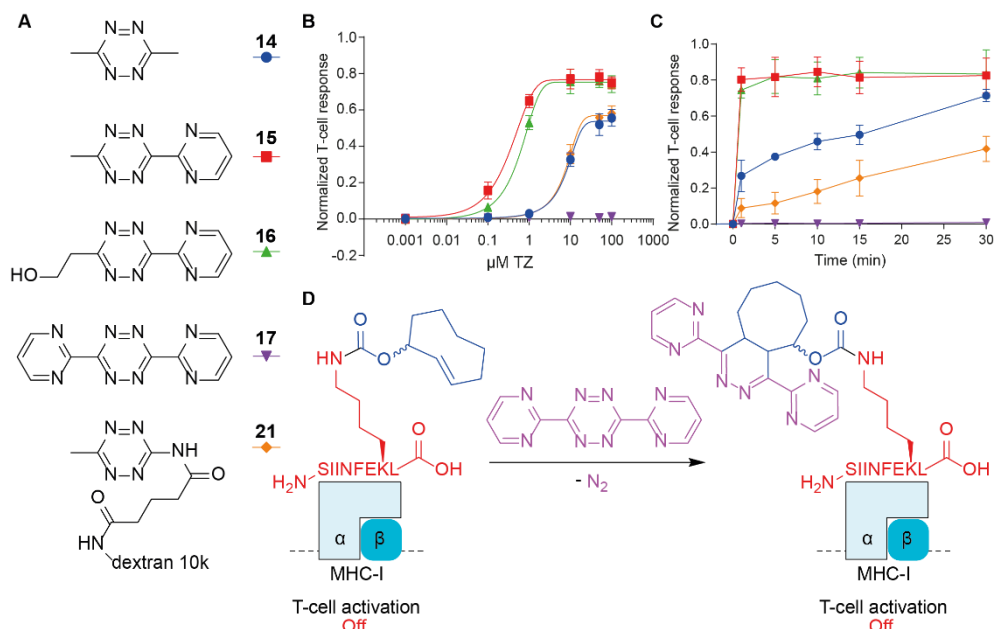
Figure 4 *In-vitro* kinetics of uncaging of peptide **9** using different tetrazines. A) Structures of tetrazines **14 – 17** and **21**. B/C) Deprotection of 100 nM **9** using DC2.4 cells as APCs and B3Z cells as T-cells. T-cell activation was compared to wild-type response (SIINFEKL; set at 1.0 normalized T-cell response) by measuring absorption (AU) of beta-galactosidase-directed CPRG hydrolysis after 17 hours. All experiments have been done twice in triplicate, error bars represent the standard deviation. Experiments were performed by A.M.F. van der Gracht (Leiden University). Tetrazine **21** was provided by Tagworks Pharmaceuticals. B) Uncaging of **9** with tetrazines **14 – 17** and **21** for 30 minutes at the indicated concentrations. C) Deprotection reaction of **9** with tetrazines **14 – 17** and **21** at 10 μM of tetrazine at increasing incubation times. Tetrazine **17** blocks T-cell activation and tetrazine **15** and **16** show improved uncaging speed compared to tetrazine **14**. Tetrazine **21** shows reduced uncaging speed and increases linear. Relative T-cell response is normalized between SIINFEKL 100 nM response as 1.0 and no peptide background signal 0.0. D) Tetrazine **17** broadens the scope of the method presented in this Chapter: the substituents of the tetrazine employed dictate whether T-cell activation is switched on (Figure 2) or remains off.

better *in vivo* due to reduced clearance,[30,49] was also evaluated in the *in vitro* assay (Figure 4A-C). Tetrazine **21** showed similar concentration dependent behavior as **14**, but slower uncaging speed although linear in time.

Stability, clearance and toxicity are other important criteria for the selection of tetrazines towards *in vivo* experiments. Stability in FCS was determined for tetrazines **14 – 17**; **17** is very unstable in serum while **14** showed no degradation. After 24 hours, 25% of **15** and 40% of **16** were still intact (Figure S2). Tetrazine **14** has been reported to be nontoxic *in vivo* up to 140 mg/kg (1.25 mmol/kg) in mice.[32] Tetrazines **14**, **16**

and **21** were selected for further experiments, which also showed negligible toxicity on APCs.

OT-I-mice, which have a homogeneous T-cell population selective for the SIINFEKL-epitope,[50] were used for *in vivo* experiments. Carboxyfluorescein succinimidyl ester (CFSE)-labeled OT-I T-cells[50] were adoptively transferred in recipient C57BL/6 mice on day -1. On day 0 the mice were either injected with peptide **9** or SIINFEKL in the tail base. After 3 days, the amount of T-cell proliferation was assessed by flow cytometry through CFSE-dilution.[51] Under these conditions, compound **9** induced very low levels of proliferation of OT-I CTLs and upon injection with tetrazine **14**, CTL proliferation was induced similarly compared to SIINFEKL (3.1% ± 0.11% vs 4.4 % ± 0.05 % divided OT-I of total lymphocytes).

Decaging of **12** with **14** (50 μM) in a mixed splenocyte assay, using (CFSE)-labeled T-cells with a specific TCR for NAITNAKII, showed the same level of control over T-cell activation as seen for SIINFEKL/OT-I, suggesting application to lysine-cognate TCRs in general.

Antigen cross-presentation of peptide **11** was studied using D1 dendritic cells and B3Z T-cells. Current results indicate **11** is cross-presented at a lower rate compared to the native peptide sequence. Furthermore, TCO-modification may alter cross presentation pathways, as the effects of inhibitors for the cytosolic and vacuolar pathways were also different. One difficulty with these studies is the persistence of presentation by D1 cells after tetrazine treatment. Additionally, if the tetrazine has adequate membrane permeability to enter D1 cells, intracellular decaging would lead to an overestimation of cross-presentation. Fixation of APCs improved reliability of current results and the development of tetrazines with intra- or extracellular targeting moieties are of importance for further experiments.

4.3 Conclusions

A new method, based on the IEDDA pyridazine elimination,[26] that allows chemical control over T-cell activation *in vitro* and *in vivo* is reported. MHC-I epitopes were synthesized using Fmoc SPPS, followed by N-terminal protection with the base-labile MSc-protecting group[38] and acidic cleavage from the resin. The desired lysine ε-amino group could then be regioselectively protected as a TCO carbamate in solution, followed by MSc deprotection under basic conditions and HPLC purification of the TCO-modified peptide. In the absence of a tetrazine, the lysine-caged epitopes show no T-cell receptor activation while MHC-I binding was not affected. Upon deprotection, T-cell receptor activation was restored. The lysine cage was implemented in two different epitopes, suggesting a generic application to lysine-sensitive TCRs.

In vivo results showed very similar T-cell proliferation potency upon decaging epitope **9** compared to the natural epitope, whereas the caged epitope showed no proliferation by itself. By combining this uncaging technique with injectable tetrazine-hydrogels[33] or antibody-epitope conjugates,[30] the activation of T-cells could even be controlled more precisely in future experiments. This can provide new angles to the study of CTL-activation *in vivo,* analogous to that which has been achieved *in vitro* using photo-[21,22,52] and chemo[14]-deprotection.

The caged epitope approach was also applied to study antigen cross-presentation. Preliminary experiments suggest that TCO-modification may alter cross-presentation pathways. One major difficulty in these experiments is to separate intra- and extracellular decaging. Current efforts are aimed towards this challenge.

4.4 Supporting figures
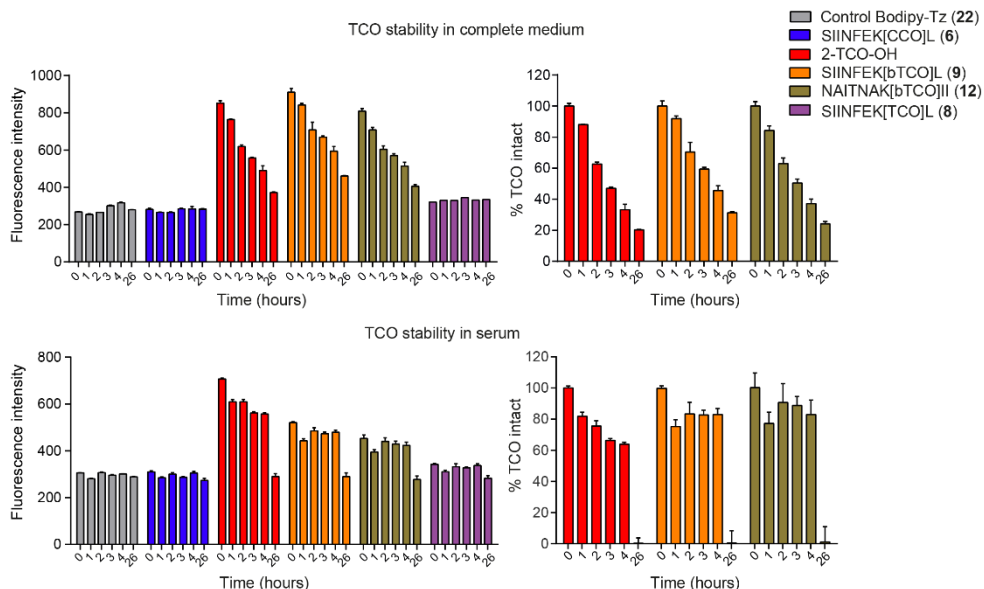
Figure S1 TCO stability in complete medium and serum. Stability of TCO constructs were determined by incubation in the desired solvent (PBS, Full Medium or Fetal Calf Serum) at 37°C over a time period of 24 h. After incubation the compounds were co-incubated with Bodipy-Tz (**22**) and fluorescence intensity was measured directly. The bar charts represent the fluorescent intensity of the samples after 50 min incubation with **22**, from which the % intact TCO was determined compared to 0 h incubation in solvent. Formula after baseline correction: time point x (t = 50 fluorescence) / time point 0 (t = 50 fluorescence) * 100% = % TCO intact. Peptide **8** was insoluble in these reactions and gave therefore no fluorescent intensity above background signal. Peptide **9** and **12** were both stable in serum up to 4 h and in complete medium gave ±25% response after 26 hours.
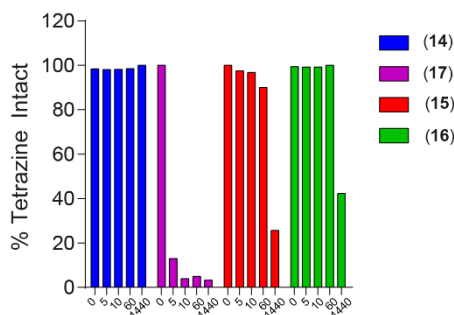
Figure S2 Tetrazine stability in serum. Stability of tetrazines were determined by incubation in Fetal Calf Serum (FCS) at room temperature, after which the characteristic absorption of tetrazines at 515 nm was quantified. At indicated times the absorption was measured and the tetrazine stability was determined with the following formula: time point x (absorption) / time point 0 (absorption) * 100% = % tetrazine intact. Tetrazine **17** is very unstable in serum while tetrazine **14** is very stable. After 24 hours 25% of **15** and 40% of **16** were still intact.

4.5 Experimental procedures

General methods: The synthesis of TCO carbonate **2** and bifunctional CCO/TCO carbonates **3** and **4** are described in Chapter 3 and 2, respectively. Dextran-modified tetrazine **21** was provided by Tagworks Pharmaceuticals.[30] Bodipy-tetrazine (**22**) was purchased from lumiprobe.com. Commercially available reagents and solvents were used as received. Moisture and oxygen sensitive reactions were performed under N_2 atmosphere (balloon). DCM, toluene, THF, dioxane and Et_2O were stored over (flame-dried) 4 Å molecular sieves (8-12 mesh). DIPEA and Et_3N were stored over KOH pellets. TLC analysis was performed using aluminum sheets, pre-coated with silica gel (Merck, TLC Silica gel 60 F$_{254}$). Compounds were visualized by UV absorption (λ = 254 nm), by spraying with either a solution of $KMnO_4$ (20 g/L) and K_2CO_3 (10 g/L) in H_2O, a solution of $(NH_4)_6Mo_7O_{24} \cdot 4H_2O$ (25 g/L) and $(NH_4)_4Ce(SO_4)_4 \cdot 2H_2O$ (10 g/L) in 10% H_2SO_4, 20% H_2SO_4 in EtOH, or phosphomolybdic acid in EtOH (150 g/L), where appropriate, followed by charring at ca. 150°C. Column chromatography was performed on Screening Devices b.v. Silica Gel (particle size 40-63 μm, pore diameter 60 Å). ^1H, ^{13}C APT, ^1H COSY, and HSQC spectra were recorded with a Bruker AV-400 (400/100 MHz) or AV-500 (500/125 MHz) spectrometer. Chemical shifts are reported as δ values (ppm) and were referenced to tetramethylsilane (δ = 0.00 ppm) or the residual solvent peak as internal standard. J couplings are reported in Hz.

LC-MS analysis was performed on a Finnigan Surveyor HPLC system (detection at 200-600 nm) with an analytical C_{18} column (Gemini, 50 x 4.6 mm, 3 μm particle size, Phenomenex) coupled to a Finnigan LCQ Advantage MAX ion-trap mass spectrometer (ESI$^+$). This system will be denoted "Setup A". Alternatively, LC-MS analysis was performed on an Agilent 1260 Infinity HPLC system (detection at 214 and 254 nm) with an analytical C_{18} column (Gemini, 50 x 4.6 mm, 3 μm particle size, Phenomenex) coupled to an Agilent 6120 quadrupole mass spectrometer (ESI$^+$). This system will be denoted "Setup B". In rare cases, this system was used with an analytical C_4 column (Gemini, 50 x 4.6 mm, 3 μm particle size, Phenomenex). For both LC-MS systems, the applied buffers were H_2O, MeCN and either 100 mM NH_4OAc in H_2O (10 mM NH_4OAc end concentration) or 1.0% TFA in H_2O (0.1% TFA end concentration). Methods used are: 10% → 90% MeCN, 13.5 min (0→0.5 min: 10% MeCN; 0.5→8.5 min: gradient time; 8.5→10.5 min: 90% MeCN; 10.5→13.5 min: 90% → 10% MeCN); 10% → 50% MeCN, 13.5 min (0→0.5 min: 10% MeCN; 0.5→8.5 min: gradient time; 8.5→10.5 min: 90% MeCN; 10.5→13.5 min: 90% → 10% MeCN); 0% → 50% MeCN, 13.5 min (0→0.5 min: 0% MeCN; 0.5→8.5 min: gradient time; 8.5→10.5 min: 50% MeCN; 10.5→13.5 min: 50% → 0% MeCN). HPLC purification was performed on a Gilson HPLC system (detection at 214 nm) coupled to a semi-preparative C_{18} column (Gemini, 250 x 10 mm, 5 μm particle size, Phenomenex). The applied buffers were H_2O, MeCN and either 100 mM NH_4OAc in H_2O (10 mM NH_4OAc end concentration) or 1.0% TFA in H_2O (0.1% TFA end concentration). High resolution mass spectra were recorded by direct injection (2 μL of a 2 μM solution in H_2O/MeCN 1:1 and 0.1% formic acid) on a mass spectrometer (Thermo Finnigan LTQ Orbitrap) equipped with an electrospray ion source in positive mode (source voltage 3.5 kV, sheath gas flow 10, capillary temperature 250°C) with resolution R = 60,000 at m/z 400 (mass range m/z = 150-2,000) and dioctylphthalate (m/z = 391.28428) as a "lock mass". The high resolution mass spectrometer was calibrated prior to measurements with a calibration mixture (Thermo Finnigan).

Photoisomerization methods: General guidelines were followed as described by Royzen *et al.*[53] Photochemical isomerization was performed using a Southern New England Ultraviolet Company Rayonet reactor (model RPR-100) equipped with 16 bulbs (part number RPR-2537A, λ = 254 nm). Photolysis was performed in a 1500 mL quartz flask (Southern New England Ultraviolet Company; part number RQV-323). A HPLC pump (Jasco; model PU-2088 Plus) was used to circulate solvent through the photolysis apparatus at the indicated flow rate. An empty solid load cartridge with screw cap, frits, O-ring and end tips (40 g; SD.0000.040; iLOK™, Screening Devices b.v.) was manually loaded with the specified silica gel to function as the stationary phase.

Peptide Synthesis. Peptide sequences were synthesized using Fmoc Solid Support Chemistry. The C-terminal amino acid was supported using a Wang resin. Elongation of the peptide sequence was accomplished using an automated and repetitive cycle of: *i.* 20% piperidine in NMP (Fmoc deprotection); *ii.* NMP wash; *iii.* Fmoc-protected amino acid (4 equiv), HCTU (4 equiv), DIPEA (8 equiv), NMP; *iv.* NMP wash; *v.* Ac$_2$O, DIPEA, NMP (capping); *vi.* NMP wash; *vii.* DCM wash. After completing the sequence, the N-terminal amino acid was also deprotected using 20% piperidine in NMP. An analytical amount of crude product was cleaved from the solid support (95% TFA, 2.5% H$_2$O, 2.5% TIS, > 1.5 h) and precipitated in cold, anhydrous Et$_2$O (TFA/Et$_2$O ≈ 1:10 *v/v*, wash resin once with TFA). The Et$_2$O solution was centrifuged, Et$_2$O was decanted and the pellet was dissolved in DMSO/MeCN/H$_2$O/*t*-BuOH (3:1:1:1 *v/v*) for LC-MS analysis.
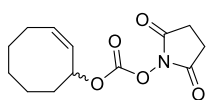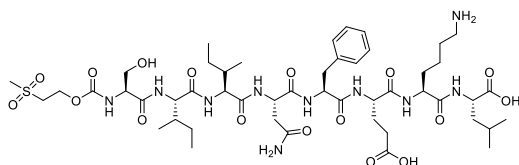

CCO carbonate 1: (Z)-Cyclooct-2-en-1-ol (Chapter 2 and 6; 276 mg, 2.19 mmol, 1.0 equiv) was placed under an argon atmosphere before dissolving in anhydrous MeCN (10 mL). N,N'-disuccinimidyl carbonate (672 mg, 2.62 mmol, 1.2 equiv) and DIPEA (0.46 ml, 2.62 mmol, 1.2 equiv) were added and the reaction mixture was stirred overnight at room temperature. TLC analysis indicated that the reaction was not complete; additional N,N'-disuccinimidyl carbonate (112 mg, 0.44 mmol, 0.2 equiv) and DIPEA (76 μL, 0.44 mmol, 0.2 equiv) were added and the reaction mixture was stirred overnight at room temperature. The reaction mixture was concentrated *in vacuo* and the crude product was purified by silica gel chromatography (20% → 30% EtOAc in pentane). The HOSu carbonate **1** (365 mg, 1.37 mmol, 62%) was obtained as a crystalline solid: R$_f$ = 0.2 (20% EtOAc in pentane); ^{1}H NMR (400 MHz, CDCl$_3$) δ 5.81 – 5.70 (m, 1H), 5.64 – 5.54 (m, 2H), 2.82 (s, 4H), 2.22 – 2.12 (m, 2H), 2.12 – 2.01 (m, 1H), 1.73 – 1.34 (m, 7H); ^{13}C NMR (101 MHz, CDCl$_3$) δ 168.9 (x2), 151.2, 131.3, 128.6, 81.0, 34.8, 28.8, 26.5, 25.8, 25.6 (x2), 23.2.
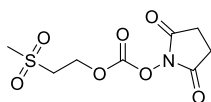
MSc-OSu (23): Synthesis was performed according to a modified procedure.[38] 2-(Methylsulfonyl)ethan-1-ol (2.03 g, 16.35 mmol, 1.0 equiv) was dissolved in anhydrous THF (40 mL) under N$_2$. The solution was cooled to 0°C (ice bath) before adding phosgene (20% *w/w* in toluene; 14 mL, 30.6 mmol, 1.9 equiv). After stirring for 30 min the reaction mixture was gradually warmed to room temperature and was stirred for an additional 4.5 h. The reaction mixture was concentrated *in vacuo* and the residual oil was cooled to -30°C under a N$_2$ atmosphere, resulting in crystallization of the acid chloride intermediate (2-(methylsulfonyl)ethyl carbonochloridate, **24**) which was used without further purification. N-

hydroxysuccinimide (1.88 g, 16.35 mmol, 1.0 equiv) was dissolved in anhydrous MeCN (16.35 mL) under a N_2 atmosphere. Et_3N (2.28 mL, 16.35 mmol, 1.0 equiv) was added and the solution was cooled to 0°C. A solution of the crude acid chloride (**24**) in MeCN (16 mL) was added dropwise to the reaction mixture. After 30 min, a precipitate ($Et_3N \cdot HCl$) was filtered off and the filtrate was concentrated *in vacuo*. A crystalline solid was precipitated from the crude product in warm isopropanol (~40°C). After filtration, the solid residue was recrystallized from MeCN to obtain MSc-OSu (**23**, 3.03 g, 11.44 mmol, 70%) as a white solid: ^{1}H NMR (400 MHz, CD_3CN) δ 4.68 (t, *J* = 5.5 Hz, 2H), 3.46 (t, *J* = 5.4 Hz, 2H), 2.94 (s, 3H), 2.75 (s, 4H); ^{13}C NMR (101 MHz, CD_3CN) δ 170.6 (x2), 152.1, 65.3, 53.5, 42.6, 26.2 (x2).

MSc-SIINFEKL (5): After SPPS, using 250 μmol Fmoc-Leu-Wang resin (1.0 equiv, based on theoretical resin loading), resin-bound SIINFEKL was washed with DCM (3 x 10 mL) and NMP (3 x 10 mL) before adding a solution of MSc-OSu (**23**, 331 mg, 1.25 mmol, 5.0 equiv) in NMP (6.0 mL). DIPEA (250 μL, 1 M in NMP, 1.0 equiv) was added and the resin suspension was shaken at room temperature for 3 h. The reaction mixture was drained and the resin-bound peptide was washed with NMP (3 x 10 mL) and DCM (3 x 10 mL). The crude product was cleaved from the solid support (95% TFA, 2.5% H_2O, 2.5% TIS, ~ 8 mL, > 1.5 h) and precipitated in cold, anhydrous Et_2O (TFA/Et_2O ≈ 1:10 *v/v*, wash resin once with TFA). The Et_2O suspension was centrifuged, Et_2O was decanted and an analytical amount of precipitated product was dissolved in DMSO/MeCN/H_2O/*t*-BuOH (3:1:1:1 *v/v*) for LC-MS analysis. The crude product was then purified with HPLC (30 → 45% MeCN in H_2O with 0.1% TFA) to obtain **5** (64.35 mg, 57.8 μmol, 23%) as a solid after lyophilization: LC-MS (setup B; linear gradient 10 → 90% MeCN, 0.1% TFA, 11 min): R_t (min): 4.74 (ESI-MS (m/z): 1113.6 (M+H^{+})); HRMS: calculated for $C_{49}H_{81}N_{10}O_{17}S$ 1113.54964 [M+H][+]; found 1113.55101.

MSc-SIINFEK(CCO)L (25): MSc-SIINFEKL (**5**, 13.23 mg, 11.9 μmol, 1.0 equiv) and NHS-CCO (**1**, 4.13 mg, 15.5 μmol, 1.3 equiv) were combined in an Eppendorf tube (15 mL) and dissolved in anhydrous DMF (1.5 mL). Anhydrous DIPEA (8.30 μL, 48 μmol, 4 equiv) was added, the tube was briefly sonicated and flushed with N_2 before shaking the reaction mixture at room temperature. After 21 h, the reaction mixture was added to cold, anhydrous Et_2O (10 mL) to precipitate the product. The Et_2O suspension was centrifuged, Et_2O was decanted and the crude product **25** was dried over a stream of N_2 before using it in the next step without further purification: LC-MS (setup B; linear gradient 10 → 90% MeCN, 0.1% TFA, 11 min): R_t (min): 6.54 (ESI-MS (m/z): 1287.6 (M+Na^{+}), 1265.6 (M+H^{+}), 1113.6 (**5**+H^{+})).
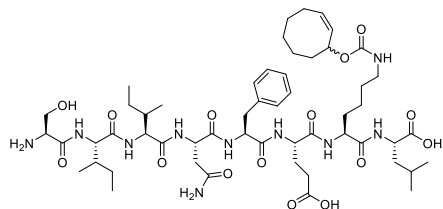
SIINFEK(CCO)L **(6):** The crude MSc-SIINFEK(CCO)L (**25**) previously described was dissolved in dioxane/MeOH/4 M NaOH (7.5:2.25:0.25 *v/v*, 12 mL). The reaction mixture was sonicated and occasionally shaken for 15 min. The reaction mixture was neutralized by adding acetic acid (68 µL, 1.2 mmol) before precipitating the product in cold, anhydrous Et$_2$O ($\sim$ 30 mL). The Et$_2$O suspension was centrifuged, Et$_2$O was decanted and the crude product **6** was dried over a stream of N$_2$. The crude product was then purified with HPLC (20 → 50% MeCN in H$_2$O with 10 mM NH$_4$OAc) to obtain **6** (2.15 mg, 1.93 µmol, 16% over two steps) as a solid after lyophilization: LC-MS (setup A; linear gradient 10 → 90% MeCN, 0.1% TFA, 12.5 min): R$_t$ (min): 6.20 (ESI-MS (m/z): 1115.73 (M+H$^+$)). LC-MS (setup B; linear gradient 10 → 90% MeCN, 0.1% TFA, 11 min): R$_t$ (min): 5.76 (diastereoisomer A, ESI-MS (m/z): 1115.6 (M+H$^+$), 963.5 (SIINFEKL+H$^+$)), 5.81 (diastereoisomer B, ESI-MS (m/z): 1115.6 (M+H$^+$), 963.5 (SIINFEKL+H$^+$)); HRMS: calculated for C$_{54}$H$_{87}$N$_{10}$O$_{15}$ 1115.63469 [M+H]$^+$; found 1115.63531.
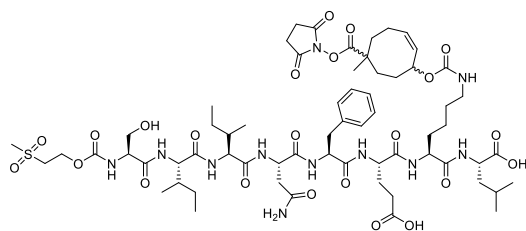
MSc-SIINFEK(NHS-bCCO)L **(26):** MSc-SIINFEKL (**5**, 40.4 mg, 36.3 µmol, 1.0 equiv) and NHS-bCCO (**3**, 21 mg, 50.0 µmol, 1.37 equiv) were combined in an Eppendorf tube (15 mL) and dissolved in anhydrous DMF (4.0 mL). Anhydrous DIPEA (25 µL, 145 µmol, 4.0 equiv) was added, the tube was briefly sonicated and flushed with N$_2$ before shaking the reaction mixture at room temperature. After 24 h, LC-MS indicated the desired product (**26**) to be the main reaction product. The reaction was continued without workup or purification: LC-MS (setup A; linear gradient 10 → 90% MeCN, 0.1% TFA, 12.5 min): R$_t$ (min): 6.42 (ESI-MS (m/z): 1420.20 (M+H$^+$)).
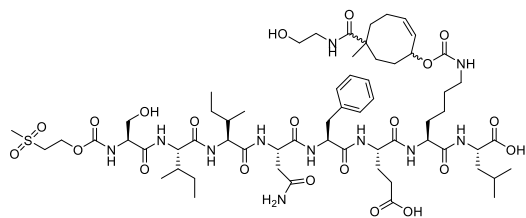
MSc-SIINFEK(mbCCO)L **(27)**: Ethanolamine (8.78 µL, 145 µmol, 4.0 equiv) was added to the reaction mixture described for **26**. The reaction was shaken at room temperature. After 22 h, LC-MS indicated the desired product (**27**) to be the main reaction product. The reaction mixture was added to cold, anhydrous Et$_2$O (45 mL) to precipitate the product. The Et$_2$O suspension was centrifuged, Et$_2$O was decanted and the crude product **27** was dried over a stream of N$_2$ before using it in the next step without further purification: LC-MS (setup A; linear gradient 10 → 90% MeCN, 0.1% TFA, 12.5 min): R$_t$ (min): 5.64 (ESI-MS (m/z): 1366.27 (M+H$^+$)).

SIINFEK(mbCCO)L (7): The crude MSc-SIINFEK(mbCCO)L (**27**) previously described was dissolved in dioxane/MeOH/4 M NaOH (7.5:2.25:0.25 *v/v*, 35 mL). The reaction mixture was sonicated and occasionally shaken for 15 min. The reaction mixture was neutralized by adding acetic acid (206 μL, 3.6 mmol) before precipitating the product in cold, anhydrous Et$_2$O ($\sim$ 40 mL). The Et$_2$O suspension was centrifuged, Et$_2$O was decanted and the crude product **7** was dried over a stream of N$_2$. The crude product was then purified with HPLC (MeCN in H$_2$O with 10 mM NH$_4$OAc) to obtain **7** (8.3 mg, 6.82 μmol, 19% over three steps) as a solid after lyophilization: LC-MS (setup A; linear gradient 10 → 90% MeCN, 0.1% TFA, 12.5 min): R$_t$ (min): 5.20 (ESI-MS (m/z): 1216.53 (M+H$^+$)); HRMS: calculated for C$_{58}$H$_{94}$N$_{11}$O$_{17}$ 1216.68237 [M+H]$^+$; found 1216.68220.

MSc-SIINFEK(TCO)L (28): MSc-SIINFEKL (**5**, 13.08 mg, 11.7 μmol, 1.0 equiv) and NHS-TCO (**2**, 4.24 mg, 15.9 μmol, 1.35 equiv) were combined in an Eppendorf tube (15 mL) and dissolved in anhydrous DMF (1.5 mL). Anhydrous DIPEA (8.21 μL, 47 μmol, 4 equiv) was added, the tube was briefly sonicated and flushed with N$_2$ before shaking the reaction mixture at room temperature. The Eppendorf tube was shielded with aluminum foil during the reaction. After 21 h, the reaction mixture was added to cold, anhydrous Et$_2$O (10 mL) to precipitate the product. The Et$_2$O suspension was centrifuged, Et$_2$O was decanted and the crude product **28** was dried over a stream of N$_2$ before using it in the next step without further purification: LC-MS (setup B; linear gradient 10 → 90% MeCN, 0.1% TFA, 11 min): R$_t$ (min): 6.41 (ESI-MS (m/z): 1287.5 (M+Na$^+$), 1113.6 (**5**+H$^+$)).

SIINFEK(TCO)L (8): The crude MSc-SIINFEK(TCO)L (**28**) previously described was dissolved in dioxane/MeOH/4 M NaOH (7.5:2.25:0.25 *v/v*, 12 mL). The reaction mixture was sonicated and occasionally shaken for 15 min. The reaction mixture was neutralized by adding acetic acid (67 μL, 1.2 mmol) before precipitating the product in cold, anhydrous Et$_2$O ($\sim$ 30 mL). The Et$_2$O suspension was centrifuged, Et$_2$O was decanted and the crude product **8** was dried over a stream of N$_2$. The crude product was then purified with HPLC (20 → 50% MeCN in H$_2$O with 10 mM NH4OAc) to obtain **8** (2.61 mg, 2.34 μmol, 20% over two steps) as a solid after lyophilization: LC-MS (setup A; linear gradient 10 → 90% MeCN, 0.1% TFA, 12.5 min): R$_t$ (min): 6.06 (ESI-MS (m/z): 1115.80 (M+H$^+$), 1137.80 (M+Na$^+$)). LC-MS (setup B; linear gradient 10 → 90% MeCN, 0.1% TFA, 11 min): R$_t$ (min): 5.66 (ESI-MS (m/z): 1115.6 (M+H$^+$), 963.6 (SIINFEKL+H$^+$)); HRMS: calculated for C$_{54}$H$_{87}$N$_{10}$O$_{15}$ 1115.63469 [M+H]$^+$; found 1115.63502.

MSc-SIINFEK(NHS-bTCO)L (29): MSc-SIINFEKL (**5**, 12.15 mg, 10.91 µmol, 1.0 equiv) and NHS-bTCO (**4**, 5.53 mg, 13.09 µmol, 1.2 equiv) were combined in an Eppendorf tube (15 mL) and dissolved in anhydrous DMF (1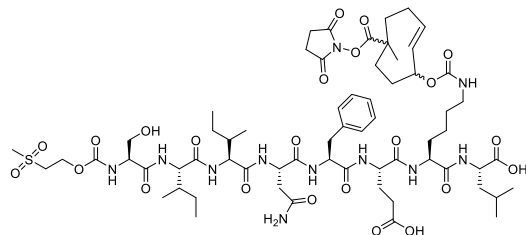.5 mL). Anhydrous DIPEA (7.62 µL, 43.64 µmol, 4.0 equiv) was added, the tube was briefly sonicated and flushed with N_2 before shaking the reaction mixture at room temperature. The Eppendorf tube was shielded with aluminum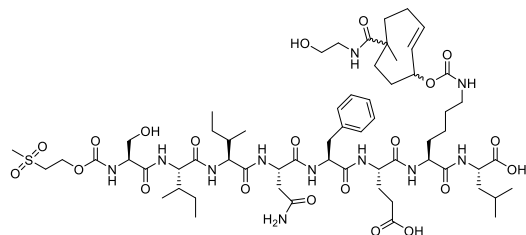 foil during the reaction. After 20 h, the reaction mixture was added to cold, anhydrous Et_2O (10 mL) to precipitate the product. The Et_2O suspension was centrifuged, Et_2O was decanted and the crude product **29** was dried over a stream of N_2 before using it in the next step without further purification: LC-MS (setup A; linear gradient 10 → 90% MeCN, 0.1% TFA, 12.5 min): R_t (min): 6.52 (ESI-MS (m/z): 1420.13 (M+H$^+$)).

MSc-SIINFEK(mbTCO)L (30): The crude MSc-SIINFEK(NHS-bTCO)L (**29**) previously described was dissolved in anhydrous DMF (1.5 mL). Ethanolamine (2.63 µL, 43.71 µmol, 4.0 equiv) was added, the tube was briefly sonicated and flushed with N_2 before shaking the reaction mixture at room temperature. The Eppendorf tube was shielded with aluminum foil during the reaction. After 22 h, the reaction mixture was added to cold, anhydrous Et_2O (10 mL) to precipitate the product. The Et_2O suspension was centrifuged, Et_2O was decanted and the crude product **30** was dried over a stream of N_2 before using it in the next step without further purification: LC-MS (setup B with C_4 column; linear gradient 10 → 90% MeCN, 0.1% TFA, 11 min): R_t (min): 4.93 (ESI-MS (m/z): 1366.6 (M+H$^+$), 1113.5 (**5**+H$^+$).

*Note: synthesis of **30** from **5** could also be performed without work-up after LC-MS analysis indicated the first step was complete.*
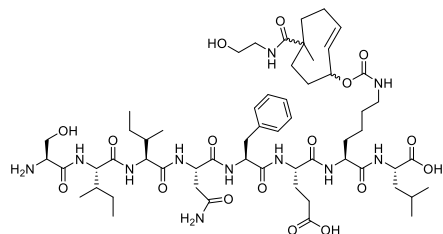
SIINFEK(mbTCO)L (9): The crude MSc-SIINFEK(mbTCO)L (**30**) previously described was dissolved in dioxane/MeOH/4 M NaOH (7.5:2.25:0.25 *v/v*, 10.9 mL). The reaction mixture was sonicated and occasionally shaken for 15 min. The reaction mixture was neutralized by adding acetic acid (62 µL, 1.09 mmol) before precipitating the product in cold, anhydrous Et_2O (~ 30 mL). The Et_2O suspension was centrifuged, Et_2O was decanted and the crude product **9** was dried over a stream of N_2. The crude product was then purified with HPLC (20 → 55% MeCN in H_2O with 10 mM NH$_4$OAc) to obtain **9** (1.81 mg, 1.49 µmol, 14% over three steps) as a solid after lyophilization: LC-MS (setup A; linear gradient 10 →

90% MeCN, 0.1% TFA, 12.5 min): R_t (min): 5.23 (ESI-MS (m/z): 1216.40 (M+H⁺)); HRMS: calculated for $C_{58}H_{94}N_{11}O_{17}$ 1216.68237 [M+H]⁺; found 1216.68391.
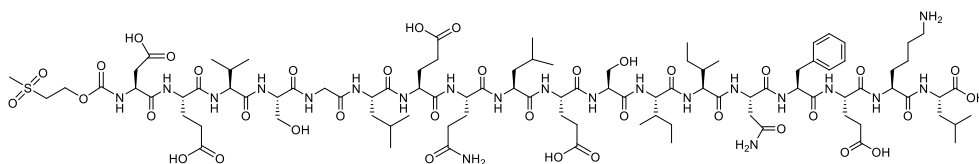
MSc- DEVSGLEQLESIINFEKL (10): After SPPS, using 250 μmol Fmoc-Leu-Wang resin (1.0 equiv, based on theoretical resin loading), resin bound DEVSGLEQLESIINFEKL was washed with DCM (3 x 10 mL) and NMP (3 x 10 mL) before adding a solution of MSc-OSu (**23**, 332 mg, 1.25 mmol, 5.0 equiv) in NMP (6 mL). DIPEA (250 μL, 1 M in NMP, 1.0 equiv) was added and the resin suspension was shaken at room temperature for 4 h. The reaction mixture was drained, MSc-OSu (**23**, 332 mg, 1.25 mmol, 5.0 equiv) in NMP (6 mL) and DIPEA (250 μL, 1 M in NMP, 1.0 equiv) were added and the resin suspension was shaken for an additional 2 h. The reaction mixture was drained and the resin-bound peptide was washed with NMP (3 x 10 ml) and DCM (3 x 10 ml). The crude product was cleaved from the solid support (95% TFA, 2.5% H_2O and 2.5% TIS, ~ 6 mL, > 1.5 h) and precipitated in cold, anhydrous Et_2O (TFA/Et_2O ≈ 1:10 *v/v*, wash resin once with TFA). The Et_2O suspension was centrifuged, Et_2O was decanted and an analytical amount of precipitated product was dissolved in DMSO/MeCN/H_2O/*t*-BuOH (3:1:1:1 *v/v*) for LC-MS analysis. The crude product was purified with HPLC (25 → 50% MeCN in H_2O with 0,1% TFA) to obtain **10** (80 mg, 36 μmol, 14%) as a solid after lyophilization: LC-MS (setup A; linear gradient 10 → 90% MeCN, 0.1% TFA, 11 min): R_t (min): 5.66 (ESI-MS (m/z): 1107.47 (M+2H⁺)).
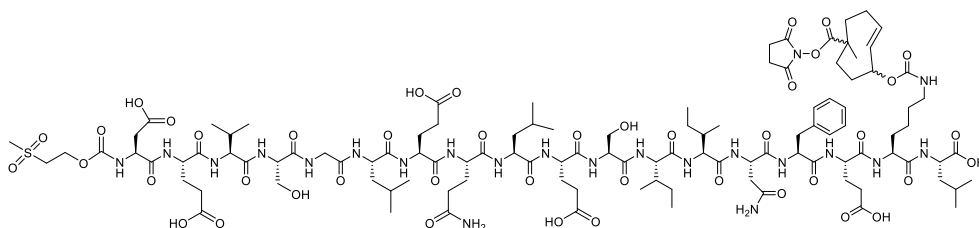
MSc-DEVSGLEQLESIINFEK(NHS-bTCO)L (31): MSc-DEVSGLEQLESIINFEKL (**10**, 20 mg, 9.04 μmol, 1.0 equiv) and NHS-bTCO(**4**, 8.7 mg, 21 μmol, 2.3 equiv) were combined in an Eppendorf tube (15 mL) and dissolved in DMSO (1.5 mL). Anhydrous DIPEA (15 μL, 86 μmol, 9.5 equiv) was added, the tube was briefly sonicated and flushed with N_2 before shaking the reaction mixture at room temperature. The Eppendorf tube was shielded with aluminum foil during the reaction. After 20 h, the reaction mixture was added to cold, anhydrous Et_2O (45 ml) to precipitate the product. The Et_2O suspension was briefly centrifuged, Et_2O was decanted and the crude product **31** was dried over a stream of N_2 before using it in the next step without further purification: LC-MS (setup A; linear gradient 10 → 90% MeCN, 0.1% TFA, 11 min): R_t (min): 6.56 (ESI-MS (m/z): 1260.67 (M+2H⁺)).
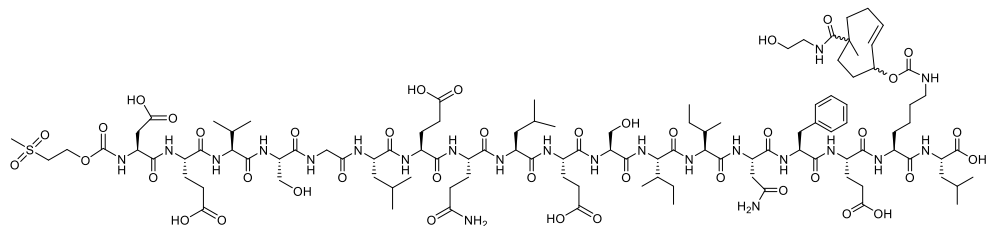
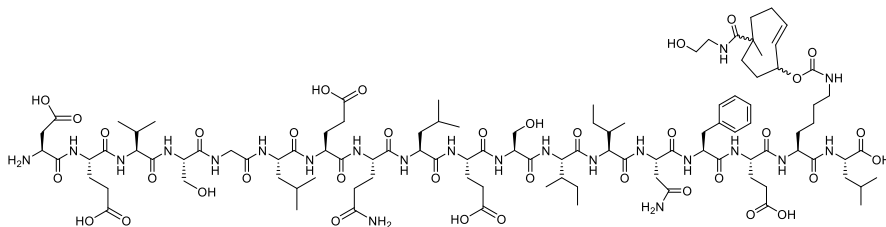**MSc-DEVSGLEQLESIINFEK(mbTCO)L   (32):** The crude MSc-DEVSGLEQLESIINFEK(NHS-bTCO)L (**31**) preciously described was dissolved in DMSO (1.5 mL). Ethanolamine (5.0 μL, 83 μmol, 9.2 equiv) was added, the tube was briefly sonicated and flushed with N$_2$ before shaking the reaction mixture at room temperature. The Eppendorf tube was shielded with aluminum foil during the reaction. After 20 h, the reaction mixture was added to cold, anhydrous Et$_2$O (45 ml) to precipitate the product. The Et$_2$O suspension was briefly centrifuged, Et$_2$O was decanted and the crude product **32** was dried over a stream of N$_2$ before using it in the next step without further purification: LC-MS (setup A; linear gradient 10 → 90% MeCN, 0.1% TFA, 11 min): R$_t$ (min): 6.07 (ESI-MS (m/z): 1233.87 (M+2H$^+$)).

*Note: synthesis of **32** from **10** could also be performed without work-up after LC-MS analysis indicated the first step was complete.*

DEVSGLEQLESIINFEK(mbTCO)L (11): The crude MSc-DEVSGLEQLESIINFEK(mbTCO)L (**32**) preciously described was dissolved in dioxane/MeOH/4 M NaOH (7.5:2.25:0.25 *v/v*, 10 mL). The reaction mixture was sonicated and occasionally shaken for 15 min. The reaction mixture was neutralized by adding acetic acid (54 μL, 0.94 mmol) before precipitating the product in cold, anhydrous Et$_2$O (~ 40 mL). The Et$_2$O suspension was centrifuged, Et$_2$O was decanted and the crude product **11** was dried over a stream of N$_2$. The crude product was then purified with HPLC (25 → 50% MeCN in H$_2$O with 10 mM NH$_4$OAc) to obtain **11** (8.6 mg, 3.71 μmol, 41% over three steps) as a solid after lyophilization: LC-MS (setup A; linear gradient 10 → 90% MeCN, 0.1% TFA, 11 min): R$_t$ (min): 5.53 (ESI-MS (m/z): 1158.73 (M+2H$^+$)); HRMS: calculated for C$_{104}$H$_{168}$N$_{22}$O$_{37}$ 1158.59649 [M+2H]$^{2+}$; found 1158.59632.
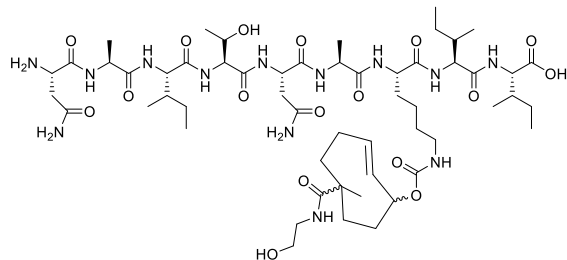
*Note: during HPLC purification of **11**, addition of NH$_4$OAc can increase the quantities of crude product injected per run.*

MSc-NAITNAKII (13): After SPPS, using 250 µmol Fmoc-Ile-Wang resin (1.0 equiv, based on theoretical resin loading), resin-bound NAITNAKII was washed with DCM (3 x 10 mL) and NMP (3 x 10 mL) before adding a solution of MSc-OSu (**23**, 331 mg, 1.25 mmol, 5.0 equiv) in NMP (6.0 mL). DIPEA (250 µL, 1 M in NMP, 1.0 equiv) was added and the reaction mixture was stirred at room temperature for 3 h. The reaction mixture was drained and the resin-bound peptide was washed with NMP (3 x 10 mL) and DCM (3 x 10 mL). The crude product was cleaved from the solid support (95% TFA, 2.5% H_2O, 2.5% TIS, ~ 8 mL, > 1.5 h) and precipitated in cold, anhydrous Et_2O (TFA/Et_2O ≈ 1:10 v/v, wash resin once with TFA). The Et_2O suspension was centrifuged, Et_2O was decanted and an analytical amount of precipitated product was dissolved in DMSO/MeCN/H_2O/t-BuOH (3:1:1:1 v/v) for LC-MS analysis. The crude product was then purified with HPLC (30 → 45% MeCN in H_2O with 0.1% TFA) to obtain **13** (43.5 mg, 39.3 µmol, 16%) as a solid after lyophilisation. The purified product still contained a capped byproduct of the SPPS. LC-MS (setup B; linear gradient 10 → 90% MeCN, 0.1% TFA, 11 min): R_t (min): 3.91 (ESI-MS (m/z): 885.5 (Acetyl-AITNAKII+H+)), 4.05 (ESI-MS (m/z): 1107.5 (M+H+)); HRMS: calculated for $C_{46}H_{83}N_{12}O_{17}S$ 1107.57144 [M+H]+; found 1107.57213.

MSc-NAITNAK(NHS-bTCO)II (33): MSc-NAITNAKII (**13**, 11.15 mg, 10.07 µmol, 1.0 equiv) and NHS-bTCO (**4**, 5.57 mg, 13.19 µmol, 1.3 equiv) were combined in an Eppendorf tube (15 mL) and dissolved in anhydrous DMF (1.5 mL). Anhydrous DIPEA (7.03 µL, 40.31 µmol, 4 equiv) was added, the tube was briefly sonicated and flushed with N_2 before shaking the reaction mixture at room temperature. The Eppendorf tube was shielded with aluminum foil during the reaction. After 23 h, the reaction mixture was added to cold, anhydrous Et_2O (12 mL) to precipitate the product. The Et_2O suspension was centrifuged, Et_2O was decanted and the crude product **33** was dried over a stream of N_2 before using it in the next step without further purification: LC-MS (setup A; linear gradient 10 → 90% MeCN, 0.1% TFA, 12.5 min): R_t (min): 6.01 (ESI-MS (m/z): 1414.60 (M+H+)).

MSc-NAITNAK(mbTCO)II (34): The crude MSc-NAITNAK(NHS-bTCO)II (**33**) previously described was dissolved in anhydrous DMF (1.4 mL). Ethanolamine (2.44 µL, 40.27 µmol, 4 equiv) was added, the tube was briefly sonicated and flushed with N_2 before shaking the reaction mixture at room temperature. The Eppendorf tube was shielded with aluminum foil during the reaction. After 24 h, the reaction mixture was added to cold, anhydrous

Et$_2$O (12 mL) to precipitate the product. The Et$_2$O suspension was centrifuged, Et$_2$O was decanted and the crude product **34** was dried over a stream of N$_2$ before using it in the next step without further purification: LC-MS (Setup A; linear gradient 10 → 90% MeCN, 0.1% TFA, 11 min): R$_t$ (min): 5.23 (ESI-MS (m/z): 1360.67 (M+H$^+$)).


NAITNAK(mbTCO)II (12): The crude MSc-NAITNAK(mbTCO)II (**34**) previously described was dissolved in dioxane/MeOH/4 M NaOH (7.5:2.25:0.25 *v/v*, 10 mL). The reaction mixture was sonicated and occasionally shaken for 15 min. The reaction mixture was neutralized by adding acetic acid (58 µL, 1.01 mmol) before precipitating the product in cold, anhydrous Et$_2$O (~ 30 mL). The Et$_2$O suspension was centrifuged, Et$_2$O was decanted and the crude product **12** was dried over a stream of N$_2$. The crude product was then purified with HPLC (10 → 30% MeCN in H$_2$O with 10 mM NH$_4$OAc) to obtain **12** (1.56 mg, 1.29 µmol, 13% over three steps) as a solid after lyophilization: LC-MS (setup A; linear gradient 10 → 50% MeCN, 0.1% TFA, 12.5 min): R$_t$ (min): 6.15 (diastereoisomer A, ESI-MS (m/z): 1210.80 (M+H$^+$), 6.60 (diastereoisomer B, ESI-MS (m/z): 1210.80 (M+H$^+$)); HRMS: calculated for C$_{55}$H$_{96}$N$_{13}$O$_{17}$ 1210.70416 [M+H]$^+$; found 1210.70437.

General procedure for oxidizing dihydrotetrazines with NO$_2$ gas: A solution of HNO$_3$ (70% *w/w*) in H$_2$O (1:1 *v/v*, 20 mL) was added dropwise to a copper coin (3.65 g, 57.4 mmol) in H$_2$O (5 mL). The NO$_2$ gas formed was led through a cannula into the tetrazine reaction mixture. After the formation of NO$_2$ was visible, the reaction mixture was cooled to 0°C (for tetrazine **14**, this also serves to reduce evaporation of product from the reaction mixture) and the flow of NO$_2$ was stimulated with an argon/N$_2$ balloon. The process was continued until the copper was completely dissolved and all nitrous gasses were led through the reaction mixture. In case the copper oxidation does not go to completion, additional HNO$_3$ (70% *w/w*) can be added dropwise to the flask containing the copper.

General procedure for HRMS analysis of tetrazines: A solution of tetrazine (10 µL, **14**, **15**, **16** or **17**, 10 mM in DMSO) was added to a solution of axial 4-TCO-OH[53,54] (1 µL, 100 mM in DMSO). The reaction mixture was diluted with MeCN/H$_2$O/*t*-BuOH (1:1:1 *v/v*; 90 µL) and subjected to HRMS analysis of the corresponding IEDDA adduct.
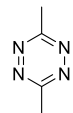

3,6-dimethyl-1,2,4,5-tetrazine (14): Acetamidine hydrochloride (**18**, 3.97 g, 42 mmol, 1.0 equiv) was dissolved in H$_2$O (20 mL). Hydrazine hydrate (4.12 mL, 84 mmol, 2.0 equiv) was added and the solution was stirred at room temperature. After stirring for 3.5 h, the reaction mixture was oxidized with NO$_2$ gas. When the formation of NO$_2$ gas stopped, the deep-red reaction mixture (pH ~ 10) was acidified with HCl (1 M, 100 mL) and extracted with DCM (3 x 75 mL). The combined organic layers were washed with HCl (1 M, 100 mL), dried over MgSO$_4$, filtered and concentrated *in vacuo* to yield 3,6-dimethyl-1,2,4,5-tetrazine (**14**, 425 mg, 3.86 mmol, 18%) as deep-purple crystals: ^{1}H NMR (400 MHz, CDCl$_3$) δ 3.04 (s, 6H);

^{13}C NMR (101 MHz, CDCl₃) δ 167.3 (x2), 21.1 (x2); HRMS (IEDDA adduct with axial 4-TCO-OH): calculated for $C_{12}H_{21}N_2O$ 209.16484 [M+H]⁺; found 209.16469. A trace of the intermediate product, 3,6-dimethyl-1,4-dihydro-1,2,4,5-tetrazine, was visible on ^{1}H and ^{13}C NMR. Spectroscopic data was in agreement with literature.[26]
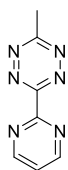
3-methyl-6-(pyrimidin-2-yl)-1,2,4,5-tetrazine (15): Synthesis was performed according to a modified procedure.[27] Pyrimidine-2-carbonitrile (**19**, 2.10 g, 20 mmol, 1.0 equiv) and zinc trifluoromethanesulfonate (1.82 g, 5.0 mmol, 0.25 equiv) were combined in a point-bottom flask before adding MeCN (5.22 mL, 100 mmol, 5.0 equiv) and hydrazine monohydrate (4.85 mL, 100 mmol, 5.0 equiv). The reaction mixture was stirred at 60°C (oil bath) under a positive N₂ gas stream. After 7 h, additional MeCN (2.5 mL, 47.9 mmol, 2.4 equiv) was added. After 24 h, the crude reaction mixture was dissolved in HCl (0.5 M, 40 mL) before oxidation with NO₂ gas. When the formation of NO₂ gas stopped, HCl (1 M, 100 mL) was added and the reaction mixture was extracted with DCM (3 x 75 mL). The combined organic layers were washed with HCl (1 M, 150 mL), dried over MgSO₄, filtered and concentrated *in vacuo*. The crude product was purified by silica gel chromatography (0% → 2% → 3% MeOH in DCM) to obtain 3-methyl-6-(pyrimidin-2-yl)-1,2,4,5-tetrazine (**15**, 1.09 g, 6.26 mmol, 31%) as deep-purple crystals: R$_f$ = 0.2 (2% MeOH in DCM); ^{1}H NMR (400 MHz, CDCl₃) δ 9.14 (d, *J* = 4.9 Hz, 2H), 7.62 (t, *J* = 4.9 Hz, 1H), 3.24 (s, 3H); ^{13}C NMR (101 MHz, CDCl₃) δ 168.8, 163.3, 159.5, 158.5, 122.6, 21.6; HRMS (IEDDA adduct with axial 4-TCO-OH): calculated for $C_{15}H_{21}N_4O$ 273.17099 [M+H]⁺; found 273.17078. Spectroscopic data was in agreement with literature.[27]
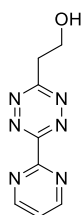
2-(6-(pyrimidin-2-yl)-1,2,4,5-tetrazin-3-yl)ethan-1-ol (16): Synthesis was performed according to literature reference.[27] Pyrimidine-2-carbonitrile (**19**, 2.10 g, 20 mmol, 1.0 equiv) and zinc trifluoromethanesulfonate (1.82 g, 5.0 mmol, 0.25 equiv) were combined in a point-bottom flask before adding 3-hydroxypropanenitrile (6.84 mL, 100 mmol, 5.0 equiv) and hydrazine monohydrate (4.85 mL, 100 mmol, 5.0 equiv). The reaction mixture was stirred at 60°C (oil bath) under a positive N₂ gas stream. After 24 h, the reaction mixture was dissolved into a solution of sodium nitrite (1 M, 200 mL). The resulting mixture was acidified to pH ∼ 3 by slowly adding HCl (1 M). The mixture was extracted with DCM (3 x 150 mL) and the combined organic layers were washed with brine (∼ 250 mL), dried over MgSO₄, filtered and concentrated *in vacuo*. The crude product was purified by silica gel chromatography (0% → 3% MeOH in DCM) and subsequent crystallization from EtOAc to obtain 2-(6-(pyrimidin-2-yl)-1,2,4,5-tetrazin-3-yl)ethan-1-ol (**16**, 142 mg, 0.70 mmol, 3%) as pink crystals: R$_f$ = 0.2 (3% MeOH in DCM); ^{1}H NMR (400 MHz, CDCl₃) δ 9.13 (d, *J* = 4.8 Hz, 2H), 7.61 (t, *J* = 4.8 Hz, 1H), 4.37 (t, *J* = 5.8 Hz, 2H), 3.76 (t, *J* = 5.8 Hz, 2H), 2.80 (s, 1H); ^{13}C NMR (101 MHz, CDCl₃) δ 169.9, 163.6, 159.4, 158.6 (x2), 122.8, 60.1, 38.0; HRMS (IEDDA adduct with axial 4-TCO-OH): calculated for $C_{16}H_{23}N_4O_2$ 303.18155 [M+H]⁺; found 303.18141. Spectroscopic data was in agreement with literature.[27]
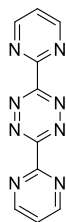
3,6-di(pyrimidin-2-yl)-1,2,4,5-tetrazine (17): Synthesis was performed according to literature reference.[43] Pyrimidine-2-carbonitrile (**19**, 3.00 g, 28.5 mmol, 1.0 equiv) and HCl (37% *w/w*, 4.5 mL, 56.3 mmol, 2.0 equiv) were dissolved in THF (40 mL). Hydrazine hydrate (8.0 mL, 165 mmol, 5.8 equiv) was added dropwise and the resulting mixture was stirred under reflux overnight. Conversion of **19** into the dihydrotetrazine intermediate (3,6-di(pyrimidin-2-yl)-1,4-dihydro-1,2,4,5-tetrazine, **20**, R_f = 0.5 (5% MeOH in DCM)) was shown using TLC. H_2O (40 mL) was added and THF was evaporated *in vacuo* (up to ~ 150 mbar, 40°C) before extracting the reaction mixture with DCM (~ 2 – 3 L total). The combined organic layers were concentrated *in vacuo* to yield the orange dihydrotetrazine intermediate (**20**) as an orange solid. The intermediate product was dissolved in DMF (100 mL) before oxidation with NO_2 gas. During oxidation, a purple precipitate was formed which was filtrated after ~ 45 min and washed twice with ice cold H_2O. The purple precipitate (2.38 g) was recrystallized from $CHCl_3$ to obtain 3,6-di(pyrimidin-2-yl)-1,2,4,5-tetrazine (**17**, 0.95 g, 3.99 mmol, 14%) as a purple solid: ^{1}H NMR (400 MHz, CDCl₃) δ 9.19 (d, *J* = 4.9 Hz, 4H), 7.64 (t, *J* = 4.9 Hz, 2H); ^{13}C NMR (126 MHz, CDCl₃) δ 163.9 (x2), 159.5 (x2), 158.7 (x4), 122.9 (x2); HRMS (IEDDA adduct with axial 4-TCO-OH): calculated for $C_{18}H_{21}N_6O$ 337.17714 $[M+H]^+$; found 337.17707. Spectroscopic data was in agreement with literature.[43]
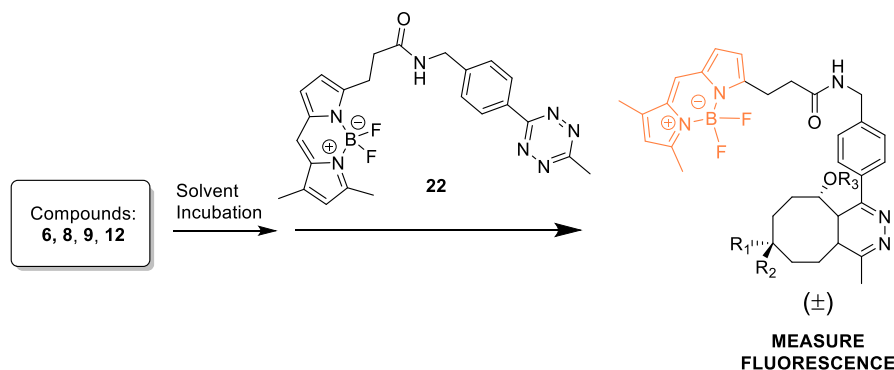
Stability of TCO constructs (Figure S1): Stability of TCO constructs were determined by incubation in the desired solvent (Full Medium or Fetal Calf Serum) at 37°C over a time period of 24 h. 30 µl of a 200 µM solution of TCO-construct (**6**, **8**, **9**, **12**) in DMSO was dissolved in 2970 µl solvent. The resulting 2 µM solution was incubated at 37°C. At time points 0, 1, 2, 3, 4 and 24 h three times 100 µl was transferred to separate wells in a Greiner flat black 96 well plate and each was diluted with 100 µl of a freshly prepared solution of Bodipy-Tz **22** (10 µM), resulting in three 200 µl solutions (1 µM TCO-construct, 5 µM Bodipy-Tz **22**). Solution fluorescence was measured using a Tecan Infinite M1000 Pro (λ_{ex} = 491 nm, λ_{em} = 525 nm) for 60 minutes at 1 min intervals and TCO stability was determined as a relative percentage to time point 0 (for each compound individually). Control samples containing 100 µl solvent (1% DMSO) were diluted with 100 µl Bodipy-Tz (**22**, 10 µM) and measured at all time points to establish a baseline. Formula after baseline correction:

Time point x (t = 50 fluorescence) / time point 0 (t = 50 fluorescence) * 100% = % TCO intact.

Stability of tetrazines (Figure S2): Stability of tetrazines were determined by incubation in Fetal Calf Serum (FCS) at room temperature. 10 µl of a 100 mM solution of tetrazine (**14 – 17**) in DMSO was dissolved in 990 µl FCS. Intact tetrazine present in the resulting 1 mM solution was quantified by the intensity of its characteristic absorption at 515 nm. After initial mixing of the sample, 500 µl was measured at time points 0, 1, 5, 10 and 60 min, and the remaining 500 µl was measured after 24 h. A control solvent sample (1% DMSO) was measured initially at 0 min and 24 h to establish a 0% value. Formula after 0% correction:

Time point x (absorption) / time point 0 (absorption) * 100% = % tetrazine intact.

4.6 References

[1]   A. Lanzavecchia, *Nature* **1998**, *393*, 413–414.

[2]   S. D. Rosen, *Annu. Rev. Immunol.* **2004**, *22*, 129–156.

[3]   J. W. Yewdell, E. Reits, J. Neefjes, *Nat. Rev. Immunol.* **2003**, *3*, 952–961.

[4]   T. N. Schumacher, R. D. Schreiber, *Science* **2015**, *348*, 69–74.

[5]   J. Neefjes, M. L. Jongsma, P. Paul, O. Bakke, *Nat Rev Immunol* **2011**, *11*, 823–36.

[6]   O. P. Joffre, E. Segura, A. Savina, S. Amigorena, *Nat. Rev. Immunol.* **2012**, *12*, 557–569.

[7]   D. J. Irvine, M. A. Purbhoo, M. Krogsgaard, M. M. Davis, *Nature* **2002**, *419*, 845–849.

[8]   R. N. Germain, *FEBS Lett.* **2010**, *584*, 4814–4822.

[9]   J. Huang, M. Brameshuber, X. Zeng, J. Xie, Q. Li, Y. Chien, S. Valitutti, M. M. Davis, *Immunity* **2013**, *39*, 846–857.

[10]   G. Altan-Bonnet, R. N. Germain, *PLoS Biol.* **2005**, *3*, e356.

[11]   D. Zehn, S. Y. Lee, M. J. Bevan, *Nature* **2009**, *458*, 211–214.

[12]   R. H. Schwartz, *Annu. Rev. Immunol.* **1985**, *3*, 237–261.

[13]   J. B. Pawlak, B. J. Hos, M. J. van de Graaff, O. A. Megantari, N. Meeuwenoord, H. S. Overkleeft, D. V. Filippov, F. Ossendorp, S. I. van Kasteren, *ACS Chem. Biol.* **2016**, *11*, 3172–3178.

[14]   J. B. Pawlak, G. P. P. Gential, T. J. Ruckwardt, J. S. Bremmers, N. J. Meeuwenoord, F. A. Ossendorp, H. S. Overkleeft, D. V. Filippov, S. I. van Kasteren, *Angew. Chem. Int. Ed.* **2015**, *54*, 5628–5631.

[15]   J. D. Stone, A. S. Chervin, D. M. Kranz, *Immunology* **2009**, *126*, 165–176.

[16]   D. Lodygin, A. Flügel, *Cell Calcium* **2017**, *64*, 118–129.

[17]   K. A. Markey, K. H. Gartlan, R. D. Kuns, K. P. A. MacDonald, G. R. Hill, *J. Immunol. Methods* **2015**, *423*, 40–44.

[18]   G. A. Azar, F. Lemaître, E. A. Robey, P. Bousso, *Proc. Natl. Acad. Sci.* **2010**, *107*, 3675–3680.

[19]   T. R. Mempel, S. E. Henrickson, U. H. von Andrian, *Nature* **2004**, *427*, 154–159.

[20]   S. Halle, K. A. Keyser, F. R. Stahl, A. Busche, A. Marquardt, X. Zheng, M. Galla, V. Heissmeyer, K. Heller, J. Boelter, K. Wagner, Y. Bischoff, R. Martens, A. Braun, K. Werth, A. Uvarovskii, H. Kempf, M. Meyer-Hermann, R. Arens, M. Kremer, G. Sutter, M. Messerle, R.

Förster, *Immunity* **2016**, *44*, 233–245.

[21]   A. L. DeMond, T. Starr, M. L. Dustin, J. T. Groves, *J. Am. Chem. Soc.* **2006**, *128*, 15354–15355.

[22]   M. Huse, L. O. Klein, A. T. Girvin, J. M. Faraj, Q.-J. Li, M. S. Kuhns, M. M. Davis, *Immunity* **2007**, *27*, 76–88.

[23]   J. Luo, Q. Liu, K. Morihiro, A. Deiters, *Nat. Chem.* **2016**, *8*, 1027–1034.

[24]   J. Sauer, H. Wiest, *Angew. Chem.* **1962**, *74*, 353–353.

[25]   M. L. Blackman, M. Royzen, J. M. Fox, *J. Am. Chem. Soc.* **2008**, *130*, 13518–13519.

[26]   R. M. Versteegen, R. Rossin, W. ten Hoeve, H. M. Janssen, M. S. Robillard, *Angew. Chem. Int. Ed.* **2013**, *52*, 14112–14116.

[27]   X. Fan, Y. Ge, F. Lin, Y. Yang, G. Zhang, W. S. C. Ngai, Z. Lin, S. Zheng, J. Wang, J. Zhao, J. Li, P. R. Chen, *Angew. Chem. Int. Ed.* **2016**, *55*, 14046–14050.

[28]   J. C. T. Carlson, H. Mikula, R. Weissleder, *J. Am. Chem. Soc.* **2018**, *140*, 3603–3612.

[29]   R. M. Versteegen, W. ten Hoeve, R. Rossin, M. A. R. de Geus, H. M. Janssen, M. S. Robillard, *Angew. Chem. Int. Ed.* **2018**, *57*, 10494–10499.

[30]   R. Rossin, S. M. J. van Duijnhoven, W. ten Hoeve, H. M. Janssen, F. J. M. Hoeben, R. M. Versteegen, M. S. Robillard, *Bioconjug. Chem.* **2016**, *27*, 1697–1706.

[31]   R. Rossin, R. M. Versteegen, J. Wu, A. Khasanov, H. J. Wessels, E. J. Steenbergen, W. ten Hoeve, H. M. Janssen, A. H. A. M. van Onzen, P. J. Hudson, M. S. Robillard, *Nat. Commun.* **2018**, *9*, 1484.

[32]   G. Zhang, J. Li, R. Xie, X. Fan, Y. Liu, S. Zheng, Y. Ge, P. R. Chen, *ACS Cent. Sci.* **2016**, *2*, 325–331.

[33]   J. M. Mejia Oneto, I. Khan, L. Seebald, M. Royzen, *ACS Cent. Sci.* **2016**, *2*, 476–482.

[34]   M. Czuban, S. Srinivasan, N. A. Yee, E. Agustin, A. Koliszak, E. Miller, I. Khan, I. Quinones, H. Noory, C. Motola, R. Volkmer, M. Di Luca, A. Trampuz, M. Royzen, J. M. Mejia Oneto, *ACS Cent. Sci.* **2018**, *4*, 1624–1632.

[35]   Q. Yao, F. Lin, X. Fan, Y. Wang, Y. Liu, Z. Liu, X. Jiang, P. R. Chen, Y. Gao, *Nat. Commun.* **2018**, *9*, 5032.

[36]   J. Zhao, Y. Liu, F. Lin, W. Wang, S. Yang, Y. Ge, P. R. Chen, *ACS Cent. Sci.* **2019**, *5*, 145–152.

[37]   D. H. Fremont, E. A. Stura, M. Matsumura, P. A. Peterson, I. A. Wilson, *Proc. Natl. Acad. Sci.* **1995**, *92*, 2479–2483.

[38]   G. I. Tesser, I. C. Balvert-Geers, *Int. J. Pept. Protein Res.* **1975**, *7*, 295–305.

[39]   J. A. Rutigliano, M. T. Rock, A. K. Johnson, J. E. Crowe, B. S. Graham, *Virology* **2005**, *337*, 335–343.

[40]   R. Lozano, M. Naghavi, K. Foreman, S. Lim, K. Shibuya, V. Aboyans, J. Abraham, T. Adair, R. Aggarwal, S. Y. Ahn, M. A. AlMazroa, M. Alvarado, H. R. Anderson, L. M. Anderson, K. G. Andrews, C. Atkinson, L. M. Baddour, S. Barker-Collo, D. H. Bartels, M. L. Bell, E. J. Benjamin, D. Bennett, K. Bhalla, B. Bikbov, A. Bin Abdulhak, G. Birbeck, F. Blyth, I. Bolliger, S. Boufous, C. Bucello, M. Burch, P. Burney, J. Carapetis, H. Chen, D. Chou, S. S. Chugh, L. E. Coffeng, S. D. Colan, S. Colquhoun, K. E. Colson, J. Condon, M. D. Connor, L. T. Cooper, M. Corriere, M. Cortinovis, K. C. de Vaccaro, W. Couser, B. C. Cowie, M. H. Criqui, M. Cross, K. C. Dabhadkar, N. Dahodwala, D. De Leo, L. Degenhardt, A. Delossantos, J. Denenberg, D. C. Des Jarlais, S. D. Dharmaratne, E. R. Dorsey, T. Driscoll, H. Duber, B. Ebel, P. J. Erwin, P. Espindola, M. Ezzati, V. Feigin, A. D. Flaxman, M. H. Forouzanfar, F. G. R. Fowkes, R. Franklin, M. Fransen, M. K. Freeman, S. E. Gabriel, E. Gakidou, F. Gaspari, R. F. Gillum, D. Gonzalez-Medina, Y. A. Halasa, D. Haring, J. E. Harrison, R. Havmoeller, R. J. Hay, B. Hoen, P. J. Hotez, D. Hoy, K. H. Jacobsen, S. L. James, R. Jasrasaria, S. Jayaraman, N. Johns, G. Karthikeyan, N. Kassebaum, A. Keren, J.-P. Khoo, L. M. Knowlton, O. Kobusingye, A. Koranteng, R. Krishnamurthi, M. Lipnick, S. E. Lipshultz, S. L. Ohno, J. Mabweijano, M. F. MacIntyre, L. Mallinger, L. March, G. B. Marks, R. Marks, A. Matsumori, R. Matzopoulos, B. M. Mayosi, J. H. McAnulty, M. M. McDermott, J. McGrath, Z. A. Memish, G. A. Mensah, T. R. Merriman, C. Michaud, M. Miller, T. R. Miller, C. Mock, A. O. Mocumbi, A. A. Mokdad, A. Moran, K. Mulholland, M. N. Nair, L. Naldi, K. M. V. Narayan, K. Nasseri, P. Norman, M. O'Donnell, S. B. Omer, K. Ortblad, R. Osborne, D. Ozgediz, B. Pahari, J. D. Pandian, A. P. Rivero, R. P. Padilla, F. Perez-Ruiz, N. Perico, D. Phillips, K. Pierce, C. A. Pope, E. Porrini, F. Pourmalek, M. Raju, D. Ranganathan, J. T. Rehm, D. B. Rein, G. Remuzzi, F. P. Rivara, T. Roberts, F. R. De León, L. C. Rosenfeld, L. Rushton, R. L. Sacco, J. A. Salomon, U. Sampson, E. Sanman, D. C. Schwebel, M. Segui-Gomez, D. S. Shepard, D. Singh, J. Singleton, K. Sliwa, E. Smith, A. Steer, J. A. Taylor, B. Thomas, I. M. Tleyjeh, J. A. Towbin, T. Truelsen, E. A. Undurraga, N. Venketasubramanian, L. Vijayakumar, T. Vos, G. R. Wagner, M. Wang, W. Wang, K. Watt, M. A. Weinstock, R. Weintraub, J. D. Wilkinson, A. D. Woolf, S. Wulf, P.-H. Yeh, P. Yip, A. Zabetian, Z.-J. Zheng, A. D. Lopez and C. J. Murray, *Lancet* **2012**, *380*, 2095–2128.

[41]   T. J. Ruckwardt, C. Luongo, A. M. W. Malloy, J. Liu, M. Chen, P. L. Collins, B. S. Graham, *J. Immunol.* **2010**, *185*, 4673–4680.

[42]   P. Billam, K. L. Bonaparte, J. Liu, T. J. Ruckwardt, M. Chen, A. B. Ryder, R. Wang, P. Dash, P. G. Thomas, B. S. Graham, *J. Biol. Chem.* **2011**, *286*, 4829–4841.

[43]   M. A. Lemes, A. Pialat, S. N. Steinmann, I. Korobkov, C. Michel, M. Murugesu, *Polyhedron* **2016**, *108*, 163–168.

[44]   A. M. F. van der Gracht, M. A. R. de Geus, M. G. M. Camps, T. J. Ruckwardt, A. J. C. Sarris, J. Bremmers, E. Maurits, J. B. Pawlak, M. M. Posthoorn, K. M. Bonger, D. V. Filippov, H. S. Overkleeft, M. S. Robillard, F. Ossendorp, S. I. van Kasteren, *ACS Chem. Biol.* **2018**, *13*, 1569–1576.

[45]   J. J. Neefjes, L. Smit, M. Gehrmann, H. L. Ploegh, *Eur. J. Immunol.* **1992**, *22*, 1609–1614.

[46]   A. Porgador, J. W. Yewdell, Y. Deng, J. R. Bennink, R. N. Germain, *Immunity* **1997**, *6*, 715–726.

[47]   J. Karttunen, N. Shastri, *Proc. Natl. Acad. Sci.* **1991**, *88*, 3972–3976.

[48]   Z. Shen, G. Reznikoff, G. Dranoff, K. L. Rock, *J. Immunol.* **1997**, *158*, 2723–30.

[49]   N. K. Devaraj, G. M. Thurber, E. J. Keliher, B. Marinelli, R. Weissleder, *Proc. Natl. Acad. Sci.* **2012**, *109*, 4762–4767.

[50]   K. A. Hogquist, S. C. Jameson, W. R. Heath, J. L. Howard, M. J. Bevan, F. R. Carbone, *Cell* **1994**, *76*, 17–27.

[51]   A. B. Lyons, C. R. Parish, *Determination of Lymphocyte Division by Flow Cytometry*, **1994**.

[52]   M. Huse, *Immunology* **2010**, *130*, 151–157.

[53]   M. Royzen, G. P. A. Yap, J. M. Fox, *J. Am. Chem. Soc.* **2008**, *130*, 3760–3761.

[54]   J. A. Neal, D. Mozhdehi, Z. Guan, *J. Am. Chem. Soc.* **2015**, *137*, 4846–4850.

5

Chemical activation of iNKT-cells: design and synthesis of caged α-galactosylceramide derivatives

M.M.E. Isendoorn contributed to the work described in this Chapter.

5.1 Introduction

Natural killer T (NKT) cells act as immunomodulators upon recognition of endogenous and foreign (glyco)lipid antigens presented by major histocompatibility complex type-1 (MHC-I)-like CD1d proteins.[1] These T-cells combine properties of natural killer (NK) cells with CD1d-restricted αβ T-cell receptors (TCRs),[2] and whilst they constitute less than 1% of total T-cells present in blood,[3,4] their activation triggers rapid release of cytokines without relying on clonal expansion, making them key mediators in many branches of the immune response.[5,6]

A

B
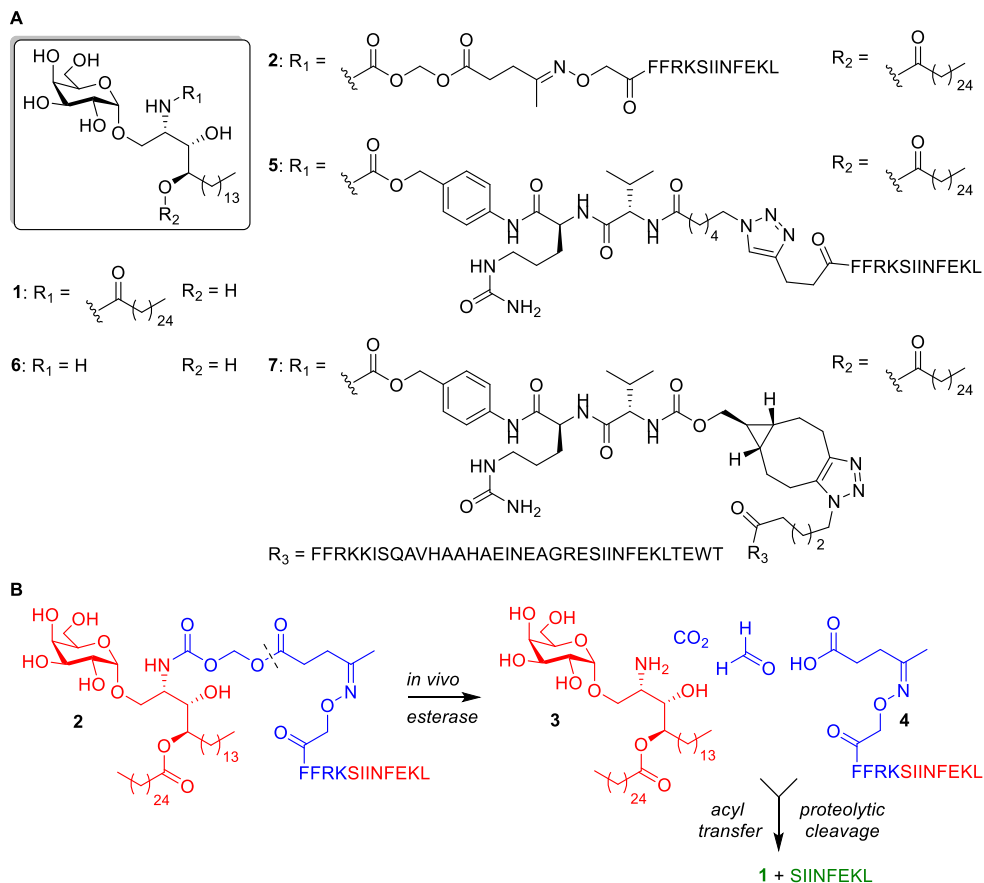
Figure 1 A) Synthetic glycolipid-peptide conjugates (**2**, **5**, **7**) developed as vaccines by Painter, Hermans and co-workers.[32, 36-40] The glycolipid portion of these vaccines are based on (a rearranged structure of) αGalCer (**1**). B) Mode of action of glycolipid vaccine **2**.[32] Upon uptake by a DC, esterases cleave the acyloxymethyl carbamate linker to give **3** and peptide fragment **4**. Intramolecular rearrangement of **3** provides **1** and proteolytic cleavage of **4**, which is accelerated by the N-terminal FFRK sequence,[34] affords the MHC-I epitope SIINFEKL. The combined MHC-I and CD1d activation triggers DC priming and results in a potent CD8+ T-cell response.

Invariant NKT (iNKT) cells, or type I NKT cells, account for 80% of NKT cells[3] and express a highly conserved TCR α-chain in conjunction with a limited scope of β-chains.[2–5] Isolation of agelasphins, α-linked galactosylceramides with antitumor properties, from the marine sponge *Agelas mauritianus*[7] and subsequent structure-activity relationship (SAR) studies[8] identified αGalCer (KRN7000, **1**, Figure 1A)[8] as a potent model antigen for iNKT cells.[2,9] Rigid binding of the acyl- and phytosphingosine lipid tails of **1** in the respective A'- and F'-pockets of CD1d enables surface exposure of the α-galactosyl moiety for recognition by type I NKT TCRs.[1,10] Presentation of **1** by dendritic cells (DCs) and subsequent activation of iNKT cells triggers secretion of both

pro-inflammatory T_H1 (for instance IFN-γ, TNF and IL-2) and immunomodulatory T_H2
(for instance IL-4, IL-10 and IL-13) cytokines,[6] thereby stimulating DC maturation.
This iNKT-DC interaction, which operates via IL-12 signaling, subsequently triggers NK
cell transactivation,[11] resulting in high levels of IFN-γ release, and stimulates both
antigen cross presentation and T-cell activation.[4,12,13] Additionally, iNKT cells promote
B-cell, macrophage and neutrophil activity.[4,12]

Following its discovery, compound **1** was initially considered as a stand-alone drug in
cancer immunotherapy.[8] However, the majority of clinical trials conducted in this
context have shown that compound **1** falls short in this;[14–16] predominantly because
the effect of IFN-γ, as induced by compound **1**, is limited due to a mixed T_H1/T_H2
response. The induction of iNKT cell anergy[17,18] and hepatotoxicity[19] further limits its
use. Ongoing studies to identify and develop novel αGalCer derivatives which elicit
skewed T_H1 or T_H2 responses[20,21] are supported by novel approaches, such as the
discovery of CD1d ligands which display covalent binding.[22]

Co-administration of **1** with peptide vaccines to enhance CD8+ and CD4+ T-cell
responses has previously been established.[23–27] It was shown that this stimulatory
effect requires presentation of both the specific peptide antigen and **1** by the same
DC,[26,28] which emphasizes the targeted delivery of both components *in vivo*. In this
regard, a particularly promising development is the employment of **1** as a covalent
adjuvant[29] to stimulate the effectiveness of synthetic carbohydrate[30,31] and peptide[32]
vaccines. Notably, Painter, Hermans and co-workers[32] reported a self-adjuvanting
strategy, where an inactive pro-adjuvant (**2**) rearranges into **1** upon esterase activity:
cleavage of the acyloxymethyl carbamate moiety[33] enables intramolecular oxygen-to-
nitrogen acyl transfer from **3** to afford **1** (Figure 1B).[32] Additionally, proteolytic
cleavage of the N-terminal FFRK sequence[34] afforded the MHC-I antigen SIINFEKL
($OVA_{257-264}$; OT-I)[35] from the aminooxy linked peptide fragment (**4**, Figure 1B).[32]
Vaccine conjugate **2** was able to elicit a potent and specific CD8+ T-cell response:
effective release of IFN-γ was observed, owing to transactivation of NK cells, whilst
reduced levels of IL-4 were detected and fewer NKT cells were activated compared to
co-administration of **1** and the peptide construct.[32]

An additional advantage to these conjugate glycolipid-peptide vaccines, which induce
iNKT-assisted priming of DCs to obtain potent CD8+ T-cell responses, is their cost-
effective synthesis: advanced intermediates can be stored and subsequently conjugated
to the desired epitope regions in a single step. Consequently, the versatility of the self-
adjuvanting approach[32] was explored for *in vivo* treatment of tumors,[36–38]
influenza,[39] and malaria.[40] These studies also introduced protease-sensitive valine-
citrulline-*para*-amino-benzyl (VC-PAB) linkers[41] for enhanced *in vivo* stability and
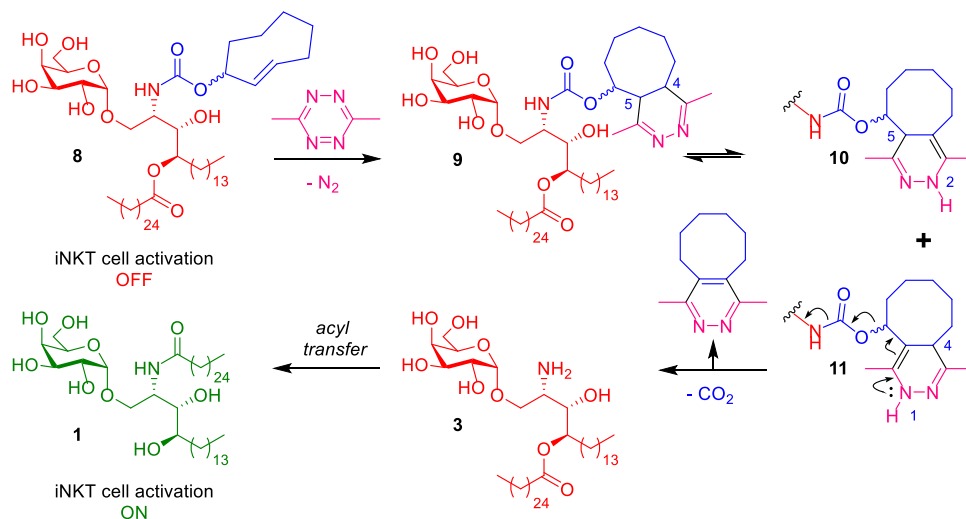
Figure 2 Design of TCO caged αGalCer **7**, which is unable to elicit iNKT activation via CD1d recognition. Upon ligation to a tetrazine, the 4,5-dihydropyridazine (**9**) can tautomerize to form the 2,5- and 1,4-tautomers (**10** and **11**, respectively). Elimination of CO_2 and the pyridazine adduct from **11** affords **3**, which can then undergo intramolecular acyl transfer to afford **1**, which induces iNKT activation.

both copper(I)-catalyzed alkyne-azide cycloaddition (CuAAC) and strain-promoted alkyne-azide cycloaddition (SPAAC) as alternative conjugation strategies (see for example Figure 1A, **5**).[36,39] The identification and application of α-galactosylphytosphingosine (αGalPhs, Figure 1A, **6**)[38] as partial agonist towards iNKTs enables further fine-tuning of the conjugate vaccines, for instance to reduce *in vivo* hepatotoxicity.[38] Another development is the use of synthetic long peptides (SLPs), containing both CD4+ and CD8+ T-cell epitopes, to encompass large immunogenic regions of target proteins (see for example, Figure 1A, **7**).[37–40]

It was hypothesized that a chemical trigger to activate covalent glycolipid-peptide vaccines would provide enhanced control over the priming of DCs, whilst retaining the favorable delivery observed for these conjugates.[32,36–38,40] In this regard, Trauner and co-workers recently demonstrated photochemical control over cytokine secretion with azobenzene-functionalized αGalCer derivatives.[42] The inverse electron demand Diels-Alder (IEDDA) pyridazine elimination,[43] a dissociative bioorthogonal reaction,[44–46] constitutes another attractive option for this approach. This "click-to-release" technique has demonstrated particular promise towards the (tetrazine mediated) activation of antibody-drug-conjugates (ADCs, Chapter 2), as shown by Robillard[47,48] as well as Royzen and Oneto,[49] MHC-I antigens (Chapter 4),[50] TLR ligands,[51] and even protein active sites.[52] It was therefore reasoned that protection of the amine
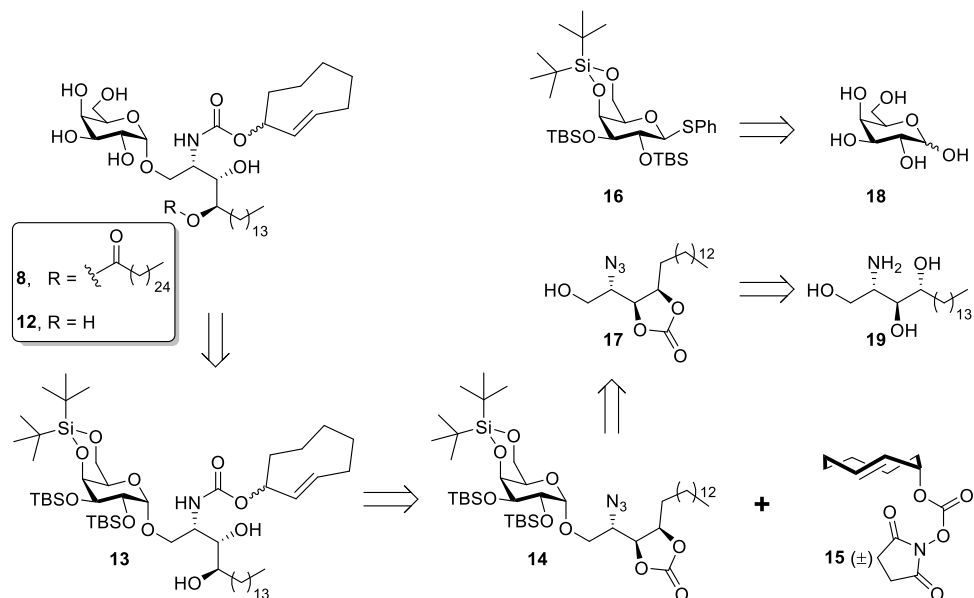
**Scheme 1** Retrosynthetic design for caged αGalCer **8** and caged αGalPhs **12** from a shared intermediate (**13**), which can be synthesized from glycosylation partners **16** and **17**.

functionality of pro-adjuvant **3** with an allylic, substituted *trans*-cyclooctene (TCO) modality would render rearrangement of the resulting caged α-GalCer (**8**) under tetrazine control (Figure 2). In this scenario, tetrazine ligation of **8** with 3,6-dimethyltetrazine results in 4,5-dihydropyridazine **9**. Compound **9** tautomerizes to form 2,5-dihydropyridazine **10** and 1,4-dihydropyridazine **11**, the latter of which is able to eliminate **3** for subsequent acyl transfer to obtain **1**.

5.2 Results and discussion

With the aim to evaluate chemical control over CD1d-mediated glycolipid recognition by means of click-to-release IEDDA chemistry, this Chapter describes the synthesis of caged lipids **8** and **12**, based on (pro)αGalCer (**3**) and αGalPhs (**6**), respectively (Scheme 1). Both compounds were synthesized from TCO-protected intermediate **13**, which in turn was obtained from the α-galactosylated intermediate **14** and axial TCO carbonate **15** (Chapter 3) in three steps. Late-stage (global) deprotection of (*para*-methoxy) benzyl protecting groups by means of hydrogenolysis or acid, as is often the case for αGalCer (**1**) syntheses reported in literature,[20] was ruled out with regard to preservation of the TCO moiety. Formation of **14** was envisaged by combining 4,6-di-*tert*-butylsilylene (DTBS)-directed α-galactosylation[53–55] with an azide protected phytosphingosine acceptor, as reported by Veerapen *et al.*[56] However, instead of protecting the remaining alcohol functionalities as benzoyl esters, 2,3-TBS-4,6-DTBS
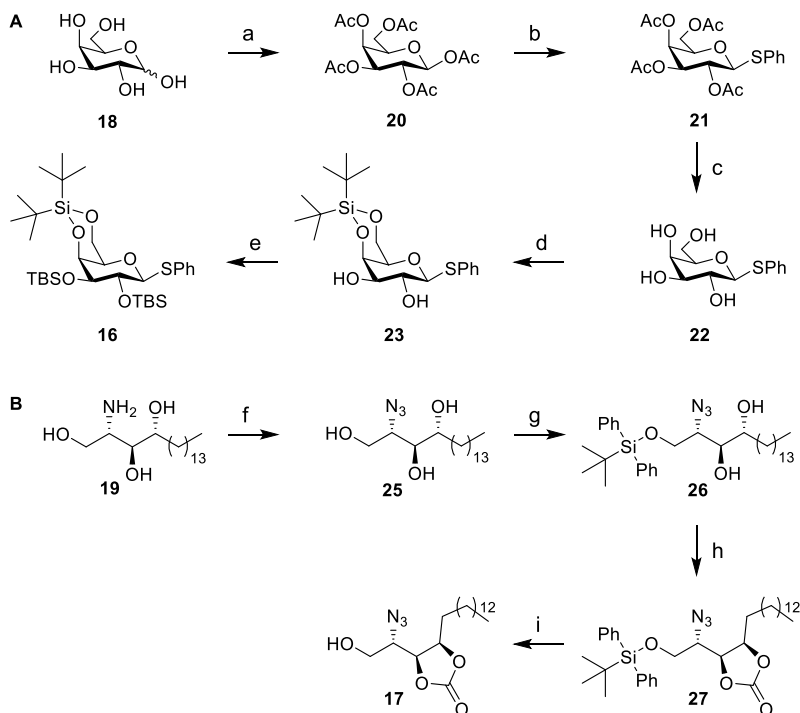
Scheme 2 Synthesis of galactose donor **16** (A) and phytosphingosine acceptor **17** (B). Reagents/conditions: (a) Ac$_2$O, NaOAc, reflux, 52%; (b) PhSH, BF$_3 \cdot$ OEt$_2$, DCM, 0°C to rt, 95%; (c) NaOMe, MeOH, rt, 95%; (d) DTBS(OTf)$_2$, pyridine, DMF, -40°C, 83%; (e) TBS-OTf, DMAP, pyridine, 0°C to rt, 95%; (f) imidazole-1-sulfonyl azide hydrogen sulfate (**24**), K$_2$CO$_3$, Cu(II) $\cdot$ 5 H$_2$O, MeOH, DCM, rt; (g) TBDPS-Cl, Et$_3$N, DMAP, DCM, rt, 83% over two steps; (h) CDI, DCM, rt, 79%; (i) HF $\cdot$ pyridine, pyridine, rt, 92%.

protected donor **16** and 2-azido-3,4-cyclic carbonate acceptor **17** were selected, as reported by Gold *et al.*[57] and Panza *et al.*[58], respectively. This approach would enable selective deprotection of the cyclic carbonate moiety after glycosylation, in addition to a mild desilylation as the final deprotection step. Additionally, if required, the reactivity of donor could be enhanced by transforming **16** into a more reactive imidate donor.[57] Therefore, donor **16** was synthesized from D-galactose (**18**) and acceptor **17** was synthesized from D-*ribo*-phytosphingosine (**19**).

Peracetylation of **18** by refluxing in a mixture Ac$_2$O and NaOAc afforded **20** after crystallization in 52% yield. Anchimerically assisted installation of the anomeric thiophenol modality was achieved in the presence of BF$_3 \cdot$ OEt$_2$ to obtain **21**, which gave **22** after Zemplén deacetylation. The 4,6-DTBS protecting group[59] was installed by treating **22** with DTBS(OTf)$_2$, and subsequent treatment with pyridine, to obtain **23** in 85% isolated yield after chromatographic purification. Finally, the 2-OH and 3-OH
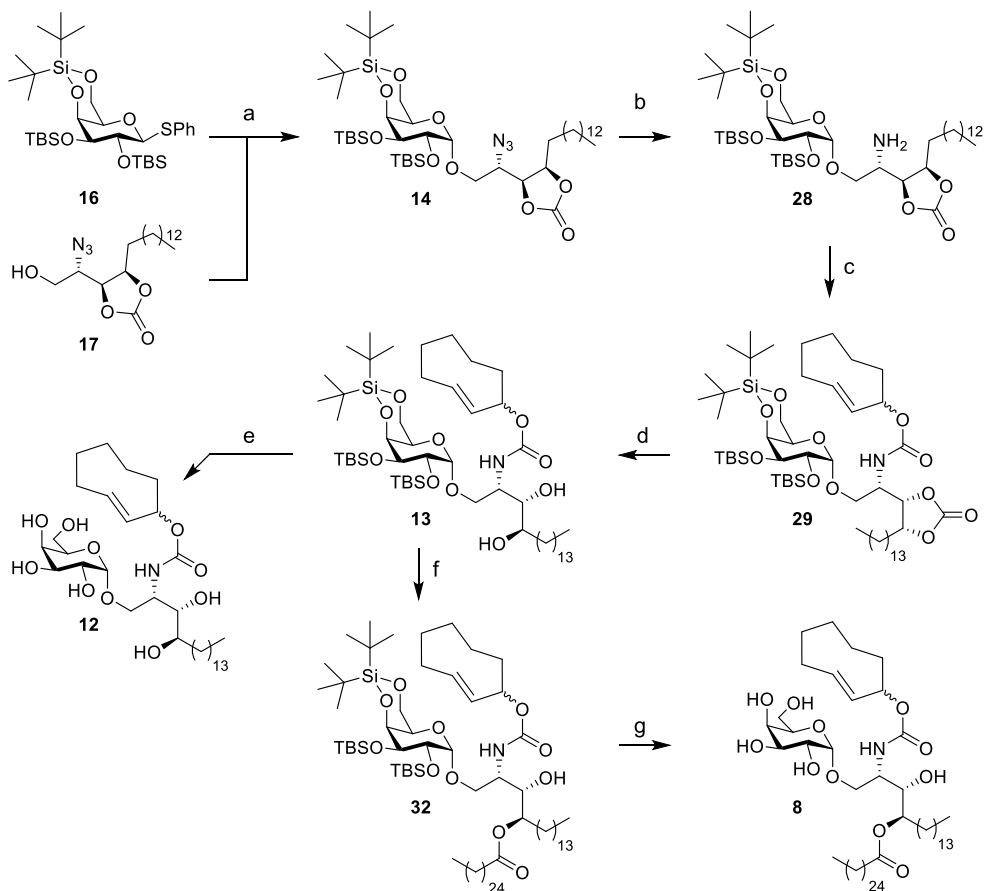
Scheme 3 Synthesis of caged glycolipids **8** and **12** from galactose donor **16** and phytosphingosine acceptor **17**. Reagents/conditions: (a) NIS, TMS-OTf, DCM, -40°C, 67%; (b) PtO₂, H₂ (g), THF, rt; (c) TCO-NHS (**15**), DIPEA, DMAP, DMF, rt, 89% over two steps; (d) LiOH, THF, H₂O, rt, quant.; (e) Et₃N · 3HF, THF, rt, 84%; (f) hexacosonoic acid (**30**), EDC · HCl, DIPEA, DMAP, DCM, rt, 31-34%; (g) Et₃N · 3HF, THF, rt, 23%.

positions of **23** were protected as TBS esters using TBS-OTf in the presence of 4-dimethylaminopyridine (DMAP) and pyridine to give donor **16** in 95% yield. D-*ribo*-phytosphingosine (**19**) was protected by diazotransfer with imidazole-1-sulfonyl azide hydrogen sulfate (**24**)[60,61] in the presence of K₂CO₃ and Cu(II) · 5 H₂O to obtain azide **25**, followed by silylation of the primary alcohol to obtain *tert*-butyldiphenylsilyl (TBDPS) ester (**26**) in 83% over two steps. The 3,4-diol functionality was protected as the cyclic carbonate using 1,1'-carbonyldiimidazole (CDI) to obtain **27** in 79% yield. Desilylation in the presence of HF · pyridine afforded acceptor **17** in 92% yield. Direct formation of **17** from **25** using diphosgene, as reported by Panza *et al*.[58], did not provide reproducible results when moving beyond small scale preparations.

Table 2 Glycosylation of galactose donor **16** and phytosphingosine acceptor **17** to form **14**.
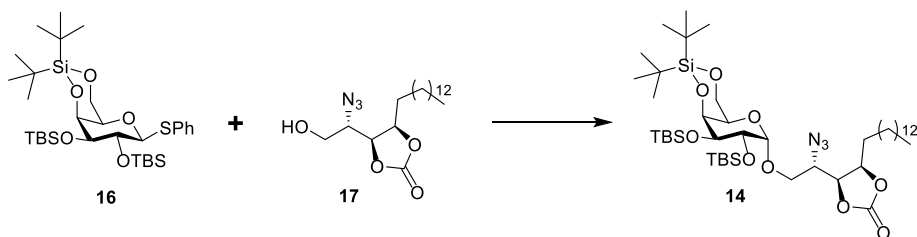
Entry	Scale (mmol)	Donor 16 (equiv)	Promotor system (equiv)	Solvent (M)	Temp. (°C)	Time (min)	Yield (%)[a]
1	0.1	1.5	IDCP (3.0)	DCM (0.2)	0 → rt	-	-
2	0.15	1.5	NIS (1.5), AgOTf (0.3)	DCM (0.2)	0 → rt	-	-
3	0.1	1.5	NIS (1.5), TfOH (0.2)	DCM (0.1)	-40	15	63
4	0.4	1.5	NIS (1.5), TfOH (0.2)	DCM (0.1)	-40	60	52
5	0.6	1.5	NIS (1.5), TfOH (0.1)	DCM (0.1)	-40	60	34
6	0.2	1.5	NIS (1.5), TMS-OTf (0.2)	DCM (0.1)	-40	15	85
7	2.4	1.2	NIS (1.5), TMS-OTf (0.2)	DCM (0.1)	-40	180	59
8	5.3	1.5	NIS (1.5), TMS-OTf (0.2)	DCM (0.1)	-40	300	67

[a]Isolated yield after aqueous workup and chromatographic purification.

Glycosylation of donor **16** and acceptor **17** was investigated next (Scheme 3; Table 1). Iodoniumdicollidine perchlorate (IDCP) proved unable to activate donor **16** (Table 1, entry 1). Instead, promotor systems based on N-iodosuccinimide (NIS) were evaluated. Activation of donor **16** with NIS/AgOTf resulted in a complex mixture of products (Table 1, entry 2). However, employing a mixture of NIS and catalytic TfOH at -40°C, as reported by Veraapen *et al*.[56] for a similar glycosylation, resulted in rapid α-selective glycosylation using donor **16** and 1.5 equivalents of acceptor **17** to obtain **14** in 63% yield (Table 1, entry 3). Additional experiments on small scale (≤ 1 mmol **16**) confirmed these findings (Table 1, entries 4 and 5) and also identified TMS-OTf as a more effective activator when used in combination with NIS (Table 1, entry 6). Glycosylation at 5 mmol scale, although requiring a prolonged reaction time, resulted in a yield of 67% (Table 1, entry 8).

Hydrogenation of the α-galactosylated product (**14**) in the presence of Adam's catalyst afforded amine **28**. Subsequently, axial TCO carbonate **15** (Chapter 3) was employed as a reagent to install the TCO carbamate moiety on **28**, in the presence of DIPEA and DMAP, to obtain **29** in 89% over two steps after chromatographic purification. Saponification of the cyclic carbonate functionality was performed with LiOH in a

Table 2 Esterification of **13** to obtain **32**.
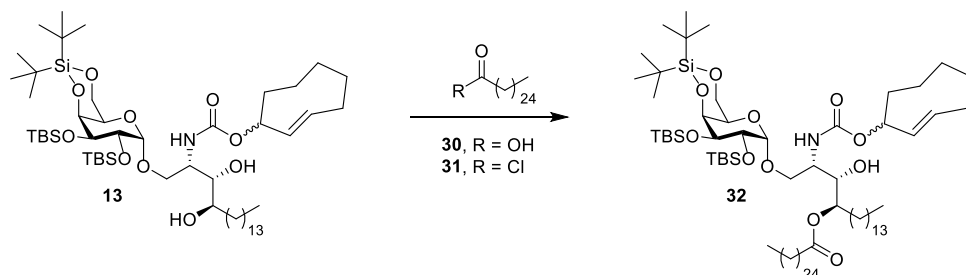
Entry	Scale (mmol)	Reagent (equiv)	Coupling conditions (equiv)	Solvent (M)	Temp. (°C)	Time (min/h/d)	Yield (%)[a]
1	0.08	**30** (1.5)	PyBOB (1.5) DIPEA (3.0)	DCM (0.04)	rt	5 d	-
2	0.09	**30** (1.3)	EEDQ (2.0)	EtOH (0.06)	0 → rt → 50	2 d	-
3	0.10	**31** (1.3)	DIPEA (4.0)	DCM (0.02)	-20 → rt	30 min	-
4	0.10	**30** (1.5)	EDC · HCl (1.5), DMAP (6.0) DIPEA (3.0)	DCM (0.03)	0 → rt	20 h	31
5	0.2	**30** (1.5)	EDC · HCl (1.5), DMAP (6.0) DIPEA (3.0)	DCM (0.05)	0 → rt	3 d	32
6	0.08	**30** (1.5)	TCBC (6.0), DMAP (6.0) Et$_3$N (6.0)	DCM (0.04)	rt	3 d	34

[a]Isolated yield after aqueous workup and chromatographic purification.

mixture of THF and H$_2$O to obtain **13** as a crude product which could be directly used for subsequent steps. An alternative three step reaction sequence for the conversion of **14** to **13** was initially investigated by subjugating **13** to saponification of the cyclic carbonate functionality, followed by Staudinger reduction in the presence of trimethylphosphine and NaOH and installation of the TCO carbamate as the final step. While this reaction sequence showed promising results on small scale, it resulted in a complicated purification procedure for **13** and generally resulted in lowered yields and increased reaction time.

Acylation with hexacosonoic acid (**30**) was investigated for **13** (Table 2). Esterification in the presence of benzotriazol-1-yl-oxytripyrrolidinophosphonium hexafluorophosphate (PyBOP) or N-ethoxycarbonyl-2-ethoxy-1,2-dihydro quinoline (EEDQ)[62] proved ineffective, despite prolonged reaction times (entries 1 and 2). Reaction of **13** with hexacosanoyl chloride (**31**) resulted in a complex reaction mixture. Instead, Steglich esterification[63] of **13** and **30** in the presence of 1-ethyl-3-(3 - dimethylaminopropyl) carbodiimide hydrochloride (EDC · HCl), DMAP and DIPEA afforded **32** in 31% yield (entry 4). Extending the reaction time for this procedure gave similar results (entry 5). Yamaguchi esterification[64–67] in the presence of 2,4,6-trichlorobenzoyl chloride (TCBC), DMAP and Et$_3$N also afforded **32** in a comparable yield.

Table 3 Silyl deprotection of **13** and **32** to obtain **12** and **8**.

13: R$_1$ = H
32: R$_1$ =

12: R$_1$ = H
8: R$_1$ =
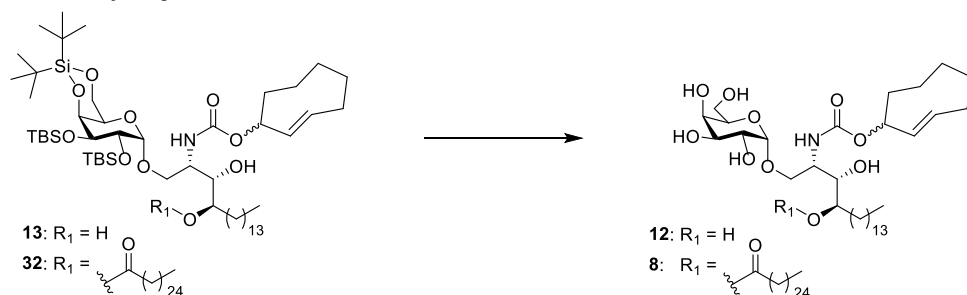
Entry	Compound (mmol)	Deprotection conditions (equiv)	Solvent (M)	Temp. (°C)	Time (h)	Yield (%)[a]
1	**13** (0.08)	HF · pyridine (excess)	-	rt	16	-
2	**13** (0.06)	HF · pyridine (10)	THF (0.03)	0	16	-
3	**13** (0.03)	HF · pyridine (10)	Pyridine (0.03)	rt	72	-
4	**13** (0.10)	TBAF (15)	THF (0.1)	rt	16	-
5	**13** (0.10)	TBAF (15), AcOH (4)	THF (0.1)	rt	16	-
6	**13** (0.10)	Et$_3$N · 3 HF (6)	THF (0.1)	0 → rt	16	**12** (28)
7	**13** (0.56)	Et$_3$N · 3 HF (6)	THF (0.1)	0 → rt	96	**12** (84)
8	**32** (0.30)	Et$_3$N · 3 HF (10)	THF (0.1)	0 → rt	27	**8** (23)

[a]Isolated yield after aqueous workup and chromatographic purification.

Simultaneous deprotection of the cyclic DTBS protecting group and two TBS groups on the galactose moiety was evaluated for both **13** and **32** to obtain **12** and **8**, respectively (Table 3). Initial attempts relied on HF · pyridine and tetra-*n*-butylammoniumfluoride (TBAF), as individual reports on αGalCer derivatives have shown both of these reagents to be effective for 4,6-DTBS deprotection.[56,68,69] Treatment of **13** with HF · pyridine (neat) resulted in a complex mixture of products (entry 1) , which could not be circumvented by performing the deprotection at low temperature in THF (entry 2). Diluting the reaction mixture with pyridine resulted in a lack of conversion, despite prolonged incubation (entry 3). Deprotection of **13** in the presence of TBAF resulted in partial deprotection of silyl esters and TCO carbamate hydrolysis (entry 4). Addition of AcOH to the deprotection with TBAF also resulted in a complex mixture of reaction products (entry 5).

As an alternative, global deprotection of **13** with Et$_3$N · 3HF was investigated in THF, resulting in an isolated yield of 28% (**12**, entry 6) after 16 hours. Prolonging the incubation time for this deprotection resulted in an increased yield of 84% (**12**, entry 7). Finally, Et$_3$N · 3HF mediated deprotection conditions also enabled conversion of **32** to **8** in 23% yield without observing hydrolysis of the ester bond (entry 8).

NMR analysis for both **32** and **8** indicated the presence of a regioisomeric byproduct, implying the ester bond was installed without complete regioselectivity. Furthermore,

migration of the ester moiety was not observed during the deprotection of **32** to **8**. Additionally, LC-MS experiments with a non-releasing tetrazine (Chapter 3 and 4) confirmed the *trans* configuration of the double bond for **12** and **8**. Taken together, while further optimization for the esterification and deprotection steps is warranted for **8** specifically, the results described confirm the compatibility of the deprotection conditions towards the envisioned synthetic strategy.

5.3 Conclusions

In conclusion, the synthesis of two TCO caged derivatives (**8** and **12**) of pro-αGalCer (**3**) and αGalPhs (**6**) is reported. α-Selective glycosylation of a 2,3-TBS-4,6-DTBS protected thiogalactoside (**16**) with a 2-azido-3,4-cyclic carbonate protected phytosphingosine (**17**) afforded key intermediate **14**, which was converted in three steps - hydrogenation, TCO carbamate formation and saponification - to obtain TCO protected intermediate **13**. Direct desilylation afforded **12**, whilst esterification and concomitant deprotection gave **8**.

Looking ahead to future research, TCO protected glycolipids **8** and **12** are to be evaluated for the envisaged *in vivo* chemical control over iNKT cell activation. Initial *in vitro* experiments should compare the cytokine release profiles of **8** with **1** and **12** with **6**, respectively. These conditions can subsequently be compared to ones where a tetrazine trigger is additionally present. The detection of IFN-γ and IL-4 secreted by an NKT cell line, such as the DN32-D3 NKT hybridoma or isolated human iNKT cells, can establish whether chemical control over iNKT cell activation is offered by **8** and/or **12**, and will aid in designing *in vivo* experiments and also more advanced constructs which also incorporate a peptide antigen.

5.4 Experimental procedures

General methods: Commercially available reagents and solvents were used as received. Moisture and oxygen sensitive reactions were performed under N_2 atmosphere (balloon). DCM, toluene, THF, dioxane and Et_2O were stored over (flame-dried) 4 Å molecular sieves (8-12 mesh). Methanol was stored over (flame-dried) 3 Å molecular sieves. Pyridine, DIPEA and Et_3N were stored over KOH pellets. TLC analysis was performed using aluminum sheets, pre-coated with silica gel (Merck, TLC Silica gel 60 F_{254}). Compounds were visualized by UV absorption (λ = 254 nm), by spraying with either a solution of $KMnO_4$ (20 g/L) and K_2CO_3 (10 g/L) in H_2O, a solution of $(NH_4)_6Mo_7O_{24} \cdot 4H_2O$ (25 g/L) and $(NH_4)_4Ce(SO_4)_4 \cdot 2H_2O$ (10 g/L) in 10% H_2SO_4, 20% H_2SO_4 in EtOH, or phosphomolybdic acid in EtOH (150 g/L), where appropriate, followed by charring at ca. 150°C. Column chromatography was performed on Screening Devices b.v. Silica Gel (particle size 40-63 μm, pore diameter 60 Å). Celite Hyflo Supercel (Merck) was used to impregnate the reaction mixture prior to silica gel chromatography when indicated. ^1H, ^{13}C APT, ^1H COSY, HSQC and HMBC spectra were recorded with a Bruker AV-400 (400/100 MHz), AV-500 (500/125 MHz) or AV-600 (600/150 MHz) spectrometer. Chemical shifts are reported as δ values (ppm) and were referenced to tetramethylsilane (δ = 0.00 ppm) or the residual solvent peak as internal standard. *J* couplings are reported in Hz. High resolution mass spectra were recorded by direct injection (2 μL of a 1 μM solution in H_2O/MeCN 1:1 and 0.1% formic acid) on a mass spectrometer (Q Exactive HF Hybrid Quadrupole-Orbitrap) equipped with an electrospray ion source in positive mode (source voltage 3.5 kV, sheath gas flow 10, capillary temperature 275°C) with resolution R = 240,000 at m/z 400 (mass range m/z = 160-2,000) and an external lock mass. The high resolution mass spectrometer was calibrated prior to measurements with a calibration mixture (Thermo Finnigan). The synthesis of TCO carbonate **15** is described in Chapter 3.
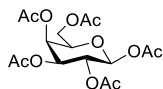
Peracetylated β-D-galactopyranoside 20: Synthesis was performed according to a modified procedure.[70] A suspension of sodium acetate (25.0 g, 305 mmol, 1.1 equiv) in acetic anhydride (350 mL, 3.71 mol, 13.4 equiv) was stirred in a three-neck, round-bottom flask and heated towards reflux in an oil bath set at 160°C. When the suspension was fully refluxing, the flask was removed from the oil bath and D-galactose (**18**, 50.0 g, 278 mmol, 1.0 equiv) was slowly added in portions to the mixture. The reaction mixture turned into a clear, yellow solution and was stirred for a further 5-10 min before pouring it into ice water (2 L). The aqueous mixture was stirred for 1 h at room temperature. DCM (600 mL) was added and the organic layer was washed with H_2O (1.5 L), $NaHCO_3$ (satd., 1.5 L), brine (1 L), dried over $MgSO_4$, filtered and concentrated *in vacuo*. The crude product was obtained as a light yellow solid and purified by recrystallization in EtOH to obtain **20** (56.4 g, 144 mmol, 52%) as white crystals: R_f = 0.4 (30% EtOAc in pentane); ^1H NMR (400 MHz, $CDCl_3$) δ ^1H NMR (400 MHz, $CDCl_3$) δ 5.71 (d, J = 8.3 Hz, 1H), 5.43 (dd, J = 3.4, 1.1 Hz, 1H), 5.34 (dd, J = 10.4, 8.3 Hz, 1H), 5.09 (dd, J = 10.4, 3.4 Hz, 1H), 4.21 – 4.03 (m, 3H), 2.17 (s, 3H), 2.13 (s, 3H), 2.05 (2 s, 6H), 2.00 (s, 3H); ^{13}C NMR (101 MHz, $CDCl_3$) δ 170.4, 170.2, 170.0, 169.5, 169.1, 92.2, 71.8, 70.9, 67.9, 66.9, 61.1, 20.9, 20.7, 20.7, 20.6; HRMS: calculated for $C_{16}H_{22}O_{11}Na$ 413.10543 [M+Na]⁺; found 413.10521. Spectroscopic data was in agreement with literature.[70]

Thiogalactoside 21: Synthesis was performed according to a modified procedure.[70] β-D-galactose pentaacetate (**20**, 32.8 g, 84.0 mmol, 1.0 equiv) was dissolved in anhydrous DCM (~600 mL) under N_2. The solution was cooled down to 0°C before slowly adding thiophenol (12.9 mL, 126 mmol, 1.5 equiv) and boron trifluoride etherate (15.5 mL, 126 mmol, 1.5 equiv). The reaction mixture was stirred for 24 h and allowed to warm to room temperature. The reaction mixture was cooled to 0°C and quenched by adding Et_3N (20 mL, 143 mmol, 1.7 equiv) and subsequently washed with $NaHCO_3$ (satd., 1 L) and back-extracted with DCM (500 mL). The combined organic layers were washed with NaOH (5 % w/w, 1 L), dried over $MgSO_4$, filtered and concentrated *in vacuo.* The crude product was purified by silica gel chromatography (20% EtOAc in pentane → 30% EtOAc in pentane) to obtain **21** (35.2 g, 79.9 mmol, 95%) as a colorless waxy solid: R_f = 0.7 (50% EtOAc in pentane); ^{1}H NMR (400 MHz, $CDCl_3$) δ 7.55 – 7.48 (m, 2H), 7.35 – 7.29 (m, 3H), 5.42 (d, *J* = 2.7 Hz, 1H), 5.24 (t, *J* = 10.0 Hz, 1H), 5.05 (dd, *J* = 9.9, 3.3 Hz, 1H), 4.72 (d, *J* = 10.0 Hz, 1H), 4.20 (dd, *J* = 11.3, 7.0 Hz, 1H), 4.12 (dd, *J* = 11.3, 6.2 Hz, 1H), 3.94 (t, *J* = 6.6 Hz, 1H), 2.13 (s, 3H), 2.10 (s, 3H), 2.05 (s, 3H), 1.98 (s, 3H); ^{13}C NMR (101 MHz, $CDCl_3$) δ 170.5, 170.3, 170.2, 169.6, 132.7 (x2), 132.6, 129.0 (x2), 128.3, 86.8, 74.6, 72.1, 67.4, 67.3, 61.8, 21.0, 20.8, 20.8, 20.7; HRMS: calculated for $C_{20}H_{24}O_9SNa$ 463.10332 [M+Na]+; found 463.10277. Spectroscopic data was in agreement with literature.[70]
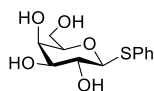

Thiogalactoside 22: Compound **21** (35.1 g, 79.8 mmol, 1.0 equiv) was dissolved in anhydrous MeOH (250 mL) under N_2. The pH of the reaction mixture was adjusted to > 10 by adding slowly adding sodium whilst stirring. The resulting reaction mixture was stirred overnight and subsequently neutralized by adding Amberlyst® (H+ form, washed 3 x with MeOH prior to usage) in small portions, gently swirling the flask and monitoring the pH until neutral. The neutralized solution was filtered and concentrated *in vacuo* to obtain **22** (20.6 g, 75.6 mmol, 95%) as a colorless oil: R_f = 0.4 (20% MeOH in DCM); ^{1}H NMR (400 MHz, MeOD) δ 7.58 – 7.52 (m, 2H), 7.32 – 7.25 (m, 2H), 7.25 – 7.19 (m, 1H), 4.60 (d, *J* = 9.7 Hz, 1H), 3.91 (d, *J* = 3.2 Hz, 1H), 3.77 (dd, *J* = 11.4, 6.9 Hz, 1H), 3.71 (dd, *J* = 11.5, 5.2 Hz, 1H), 3.62 (t, *J* = 9.4 Hz, 1H), 3.57 (t, *J* = 6.1 Hz, 1H), 3.51 (dd, *J* = 9.2, 3.3 Hz, 1H); ^{13}C NMR (101 MHz, MeOD) δ 136.0, 132.0 (x2), 129.8 (x2), 127.9, 90.2, 80.5, 76.2, 70.9, 70.3, 62.5; HRMS: calculated for $C_{12}H_{16}O_5SNa$ 295.06107 [M+Na]+; found 295.06106. Spectroscopic data was in agreement with literature.[71,72]
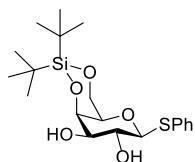

Thiogalactoside 23: compound **22** (15.8 g, 57.9 mmol, 1.0 equiv) was co-evaporated with anhydrous DMF (150 mL) in a 1 L round-bottom flask before dissolving the starting material in anhydrous DMF (240 mL) under N_2. The solution was cooled to -40°C before slowly adding di-*tert*-butylsilyl bis(trifluoromethanesulfonate) (24.2 g, 55.0 mmol, 0.95 equiv). The reaction mixture was stirred at -40°C for 30 min before adding anhydrous pyridine (14.1 mL, 174 mmol, 3.0 equiv). The reaction mixture was stirred for 45 min and was subsequently diluted with Et_2O (1 L), washed with H_2O (4 x 500 mL), brine (750 mL), dried over $MgSO_4$, filtered and concentrated *in vacuo*. The crude product was purified by silica gel chromatography (5% acetone in DCM, isocratic) to obtain the silylated product **23** (19.8 g, 48.0 mmol, 83%) as a clear viscous oil which crystallized under reduced pressure: R_f = 0.4 (5% acetone in DCM); ^{1}H NMR (500 MHz, $CDCl_3$) δ 7.58 – 7.52 (m, 2H), 7.33 – 7.25 (m, 3H), 4.56 (d, *J* = 9.8 Hz, 1H), 4.44 (d, *J* = 3.4 Hz, 1H),

4.29 – 4.22 (m, 2H), 3.75 (t, J = 9.3 Hz, 1H), 3.58 – 3.50 (m, 1H), 3.47 (s, 1H), 2.86 (br s, 2OH), 1.05 (s, 9H), 1.03 (s, 9H); ^{13}C NMR (126 MHz, CDCl$_3$) δ 133.2, 132.7 (x2), 129.0 (x2), 128.0, 89.1, 75.3, 75.2, 72.6, 70.7, 67.2, 27.6 (x3), 27.5 (x3), 23.4, 20.7; HRMS: calculated for C$_{20}$H$_{32}$O$_5$SSiNa 435.16319 [M+Na]$^+$; found 435.16279. Spectroscopic data was in agreement with literature.[57]
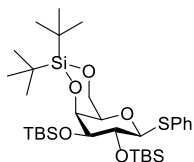
Thiogalactoside donor 16: Compound **23** (2.06 g, 5.0 mmol, 1.0 equiv) and DMAP (61 mg, 0.5 mmol, 0.1 equiv) were dissolved in anhydrous pyridine (20 mL) under N$_2$. The solution was cooled to 0°C before slowly adding TBS-OTf (4.59 mL, 20.0 mmol, 4.0 equiv). The reaction mixture was stirred for 16 h and allowed to warm to room temperature. The reaction mixture was concentrated *in vacuo*, diluted with 100 mL EtOAc, washed with HCl (1 M, 100 mL), NaHCO$_3$ (satd., 100 mL) and brine (100 mL). The aqueous layers were back-extracted with EtOAc (50 mL). The combined organic layers were dried over MgSO$_4$, filtered and concentrated *in vacuo*. The crude product was purified by silica gel chromatography (pentane → 20% DCM in pentane → 40% DCM in pentane) to obtain **23** (3.03 g, 4.73 mmol, 95%) as a clear oil: R$_f$ = 0.3 (40% DCM in pentane); ^{1}H NMR (400 MHz, CDCl$_3$) δ 7.51 – 7.45 (m, 2H), 7.29 – 7.19 (m, 4H), 4.56 (d, J = 9.4 Hz, 1H), 4.32 (dd, J = 3.0, 1.0 Hz, 1H), 4.19 (dd, J = 12.2, 1.6 Hz, 1H), 4.15 (dd, J = 12.1, 1.7 Hz, 1H), 4.01 (t, J = 9.0 Hz, 1H), 3.52 (dd, J = 8.6, 2.8 Hz, 1H), 3.36 – 3.31 (m, 1H), 1.12 (s, 9H), 1.04 (s, 9H), 0.96 (s, 9H), 0.95 (s, 9H), 0.26 (s, 3H), 0.15 (s, 3H), 0.12 (s, 3H), 0.10 (s, 3H); ^{13}C NMR (101 MHz, CDCl$_3$) δ 136.0, 131.8 (x2), 128.8 (x2), 127.1, 90.6, 78.0, 74.8, 74.7, 70.4, 67.4, 27.9 (x3), 27.5 (x3), 26.7 (x3), 26.6 (x3), 23.6, 20.9, 18.4, 18.4, -1.9, -3.2, -3.3, -3.6; HRMS: calculated for C$_{36}$H$_{64}$O$_5$SSi$_3$N 658.38075 [M+NH$_4$]$^+$; found 658.38031. Spectroscopic data was in agreement with literature.[57]

*Note:* this *procedure could also be performed at 10 gram scale (24 mmol) to obtain similar results.*
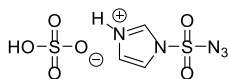
Imidazole-1-sulfonyl azide hydrogen sulfate (24): Synthesis was performed according to literature precedence.[61] Sodium azide (7.50 g, 115 mmol, 1.0 equiv) was placed in a 500 mL round-bottom flask and subsequently dissolved in anhydrous ethyl acetate (120 mL) under N$_2$. The suspension was cooled to 0°C before slowly adding sulfuryl chloride (9.38 mL, 115 mmol, 1.0 equiv) over 10 min. The yellow reaction mixture was stirred for 19 h and allowed to warm to room temperature. Subsequently, the reaction mixture was cooled to 0°C before slowly adding imidazole (14.9 g, 219 mmol, 1.9 equiv) over 5 min whilst maintaining an inert atmosphere. The reaction mixture was stirred for 3 h at 0°C before slowly adding NaHCO$_3$ (satd., 225 mL) to basify the reaction mixture. The organic layer was washed with H$_2$O (225 mL) and dried over MgSO$_4$. The dried organic phase was filtered, cooled to 0°C and placed under a continuous stream of N$_2$ before slowly adding sulfuric acid (6.15 mL, 115 mmol, 1.0 equiv) over 5 min. The acidified solution was stirred for 30 min and allowed to warm to room temperature. A colorless precipitate formed, which was collected by filtration to obtain **24** (22.5 g, 83.0 mmol, 72%) as a white solid. Spectroscopic data was in agreement with literature.[61]
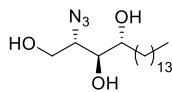
Phytosphingosine 25: D-*ribo*-phytosphingosine (**19**, 10.0 g, 31.5 mmol, 1.0 equiv) was suspended in a mixture of MeOH (300 mL) and DCM (100 mL) under N_2. K_2CO_3 (10.5 g, 76.0 mmol, 2.4 equiv) and Cu(II) · 5 H_2O (79 mg, 0.32 mmol, 1.0 mol%) were dissolved in H_2O (100 mL) and the resulting aqueous solution was added to the suspension to give a foamy reaction mixture. After 5 min, imidazole-1-sulfonyl azide hydrogen sulfate (**24**, 10.3 g, 37.8 mmol, 1.2 equiv) was added and the reaction mixture was stirred for 20 h at room temperature. The reaction mixture was partially concentrated *in vacuo* (≥ 100 mbar, 40°C) before adding HCl (1 M, 250 mL). The aqueous phase was extracted with EtOAc (3 x 350 mL, 40°C). The combined organic layers were washed with NaHCO$_3$ (satd., 250 mL), brine (250 mL), dried over MgSO$_4$, filtered and concentrated *in vacuo* to obtain **25** (10.8 g, 31.5 mmol, 100%) as a solid which was used in the next step without further purification: R_f = 0.5 (10% MeOH in DCM); ^{1}H NMR (400 MHz, CDCl$_3$) δ 4.00 (dd, *J* = 11.7, 5.5 Hz, 1H), 3.89 (dd, *J* = 11.7, 4.5 Hz, 1H), 3.84 – 3.74 (m, 2H), 3.66 (q, *J* = 4.9 Hz, 1H), 1.65 – 1.44 (m, 3H), 1.38 – 1.21 (m, 23H), 0.88 (t, *J* = 7.0 Hz, 3H); ^{13}C NMR (101 MHz, CDCl$_3$) δ 74.7, 72.7, 63.2, 61.8, 32.1, 32.0, 29.8 (x2), 29.8, 29.8 (x2), 29.7, 29.7 (x2), 29.5, 25.9, 22.8, 14.3; HRMS: calculated for $C_{18}H_{38}N_3O_3$ 344.29077 [M+H]$^+$; found 344.29020. Spectroscopic data was in agreement with literature.[73,74]
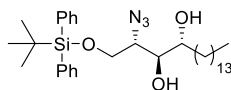
Phytosphingosine 26: Synthesis was performed according to a modified procedure.[75] Crude 2-azido-phytosphingosine (**25**, 10.8 g, 31.5 mmol, 1.0 equiv) was dissolved in anhydrous DCM (155 mL) and anhydrous DMF (35 mL) under N_2. The solution was cooled to 0°C before adding Et$_3$N (11.0 mL, 79.0 mmol, 2.5 equiv), DMAP (192 mg, 1.58 mmol, 0.1 equiv) and *tert*-butyldiphenylchlorosilane (TBDPS-Cl, 9.83 mL, 37.8 mmol, 1.2 equiv). The reaction mixture was stirred for 25 h and allowed to warm to room temperature. The reaction mixture was quenched with MeOH (1.53 mL, 37.8 mmol, 1.2 equiv) and diluted with EtOAc (1 L). The organic phase was washed with brine (2 x 600 mL) and the combined aqueous layers were back-extracted with EtOAc (500 mL). The combined organic layers were dried over MgSO$_4$, filtered and concentrated *in vacuo*. The crude product was purified by silica gel chromatography (pentane → 2.5% acetone in pentane → 10% acetone in pentane) to obtain **26** (15.1 g, 26.0 mmol, 83% over 2 steps) as an oil: R_f = 0.2 (5% acetone in pentane); ^{1}H NMR (400 MHz, CDCl$_3$) δ 7.74 – 7.64 (m, 4H), 7.51 – 7.35 (m, 6H), 4.03 (dd, J = 10.9, 4.2 Hz, 1H), 3.91 (dd, J = 11.0, 5.7 Hz, 1H), 3.72 – 3.64 (m, 2H), 3.59 – 3.53 (m, 1H), 2.52 (d, J = 4.1 Hz, 1OH), 2.00 (br s, 1OH), 1.57 – 1.37 (m, 3H), 1.37 – 1.20 (m, 23H), 1.08 (s, 9H), 0.88 (t, J = 6.8 Hz, 3H); ^{13}C NMR (101 MHz, CDCl$_3$) δ 135.8 (x2), 135.7 (x2), 132.7, 132.6, 130.2 (x2), 128.1 (x2), 128.0 (x2), 74.3, 72.5, 64.3, 63.5, 32.1, 32.0, 29.8, 29.8, 29.8, 29.8 (x2), 29.8, 29.7, 29.7, 29.5, 26.9 (x3), 25.8, 22.8, 19.2, 14.3; HRMS: calculated for $C_{34}H_{55}N_3O_3SiNa$ 604.39049 [M+Na]$^+$; found 604.39029. Spectroscopic data was in agreement with literature.[75]
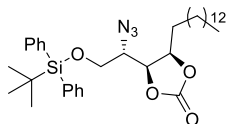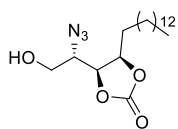
Phytosphingosine 27: Phytosphingosine **26** (8.40 g, 14.4 mmol, 1.0 equiv) was dissolved in anhydrous DCM (100 mL) under N_2. 1,1'-Carbonyldiimidazole (CDI, 7.02 g, 43.3 mmol, 3.0 equiv) was added and the reaction mixture was stirred for 72 h at room temperature. The reaction mixture was concentrated *in vacuo* and the resulting crude product was purified by silica gel chromatography (pentane → 5% Et$_2$O in pentane) to obtain **27** (6.95 g, 11.4 mmol, 79%) as a

white solid: R_f = 0.2 (5% Et$_2$O in pentane); ^{1}H NMR (400 MHz, CDCl$_3$) δ 7.71 – 7.65 (m, 4H), 7.50 – 7.39 (m, 6H), 4.69 (ddd, J = 10.4, 7.2, 2.7 Hz, 1H), 4.54 (dd, J = 10.1, 7.2 Hz, 1H), 4.03 (dd, J = 11.1, 2.7 Hz, 1H), 3.88 (dd, J = 11.1, 6.1 Hz, 1H), 3.61 (ddd, J = 9.7, 6.1, 2.7 Hz, 1H), 1.80 – 1.68 (m, 1H), 1.68 – 1.55 (m, 2H), 1.48 – 1.19 (m, 23H), 1.09 (s, 9H), 0.88 (t, J = 6.8 Hz, 3H); ^{13}C NMR (101 MHz, CDCl$_3$) δ 135.7 (x2), 135.7 (x2), 132.5, 132.3, 130.3, 130.2, 128.1 (x2), 128.1 (x2), 79.6, 75.6, 64.3, 60.0, 32.1, 29.8, 29.8, 29.8 (x2), 29.7, 29.6, 29.5, 29.5, 29.3, 29.0, 26.9 (x3), 25.6, 22.8, 19.3, 14.3.

Note: the ^{13}C signal for the carbonate protecting group (C=O) was not reported due to a lack of resolution on the spectrum of **27**.

Phytosphingosine acceptor 17: Phytosphingosine **27** (6.95 g, 11.4 mmol, 1.0 equiv) was dissolved in HF · pyridine (10.3 mL, 114 mmol, 10 equiv) in a plastic tube under N$_2$. The reaction mixture was stirred for 22 h at room temperature. The reaction mixture was slowly added to NaHCO$_3$ (satd., 50 mL) and the resulting mixture was extracted with DCM (3 x 50 mL). The combined organic layers were washed with CuSO$_4$ (1 M, 3 x 30 mL), H$_2$O (30 mL), dried over MgSO$_4$, filtered and concentrated *in vacuo*. The crude product was purified by silica gel chromatography (20% EtOAc in pentane, isocratic) to obtain acceptor **17** (3.88 g, 10.5 mmol, 92%) as a white solid: R_f = 0.3 (20% EtOAc in pentane); ^{1}H NMR (400 MHz, CDCl$_3$) δ 4.76 (ddd, J = 10.4, 7.3, 2.9 Hz, 1H), 4.62 (dd, J = 9.9, 7.3 Hz, 1H), 4.08 (dd, J = 11.9, 2.4 Hz, 1H), 3.91 (dd, J = 11.9, 5.5 Hz, 1H), 3.70 (ddd, J = 9.8, 5.4, 2.7 Hz, 1H), 3.38 (br s, 1OH), 1.84 – 1.65 (m, 2H), 1.64 – 1.53 (m, 1H), 1.49 – 1.18 (m, 23H), 0.88 (t, J = 6.8 Hz, 3H); ^{13}C NMR (101 MHz, CDCl$_3$) δ 154.2, 79.9, 75.8, 62.3, 59.8, 32.0, 29.7, 29.7, 29.7 (x2), 29.6, 29.6, 29.4, 29.4, 29.2, 28.9, 25.6, 22.7, 14.1; HRMS: calculated for C$_{19}$H$_{36}$N$_3$O$_4$ 370.27003 [M+H]$^+$; found 370.26988. Spectroscopic data was in agreement with literature.[58]
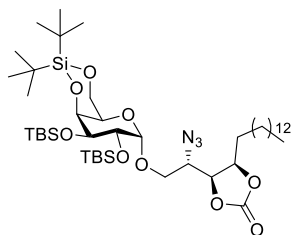
Compound 14: Galactose donor **16** (5.07 g, 7.91 mmol, 1.5 equiv) and phytosphingosine acceptor **17** (1.95 g, 5.27 mmol, 1.0 equiv) were co-evaporated with toluene (3 x 3 mL) before dissolving the reactants in anhydrous DCM (40 mL) in the presence of flame-dried molecular sieves (3Å) under N$_2$. After 15 min, the reaction mixture was cooled to -40°C before adding *N*-iodosuccinimide (NIS, 1.78 g, 7.91 mmol, 1.5 equiv) and trimethylsilyl trifluoromethanesulfonate (TMS-OTf, 191 µL, 1.05 mmol, 0.2 equiv). The reaction mixture was stirred for 5 h at -40°C and subsequently quenched by adding Et$_3$N (7.35 mL, 52.7 mmol, 10 equiv). The crude mixture was diluted with EtOAc (250 mL), washed with NaHCO$_3$ (satd.,150 mL), Na$_2$S$_2$O$_3$ (satd., 150 mL) and brine (150 mL), dried over MgSO$_4$, filtered, impregnated with Celite and concentrated *in vacuo*. The impregnated crude product was purified by silica gel chromatography (pentane → 2% EtOAc in pentane → 5% EtOAc in pentane) to obtain the glycosylated product **14** (3.19 g, 3.54 mmol, 67%) as a yellow oil: R_f = 0.3 (5% EtOAc in pentane); ^{1}H NMR (400 MHz, CDCl$_3$) δ 4.83 (d, J = 3.4 Hz, 1H), 4.77 – 4.70 (m, 2H), 4.32 (d, J = 2.2 Hz, 1H), 4.26 (dd, J = 12.5, 1.8 Hz, 1H), 4.18 – 4.12 (m, 3H), 3.87 (dd, J = 9.6, 2.9 Hz, 1H), 3.72 – 3.65 (m, 2H), 3.62 – 3.54 (m, 1H), 1.86 – 1.74 (m, 1H), 1.73 – 1.55 (m, 2H), 1.47 – 1.19 (m, 23H), 1.04 (s, 9H), 1.04 (s, 9H), 0.93 (s, 9H), 0.91 (s, 9H), 0.88 (t, J = 6.7 Hz, 3H), 0.09 (s, 3H), 0.09 (s, 3H), 0.07 (s, 6H); ^{13}C NMR (101 MHz, CDCl$_3$) δ 153.5, 101.4, 79.5, 75.3, 74.9, 70.9, 69.2, 68.4, 68.3, 67.3, 57.9,

32.1, 29.8, 29.8, 29.8 (x2), 29.7, 29.6, 29.5, 29.5, 29.3, 29.0, 27.6 (x3), 27.5 (x3), 26.2 (x3), 26.1 (x3), 25.6, 23.6, 22.8, 20.8, 18.2, 18.2, 14.3, -4.0, -4.1, -4.3, -4.5; HRMS: calculated for $C_{45}H_{93}N_4O_9Si_3$ 917.62449 [M+NH$_4$]$^+$; found 917.62451.
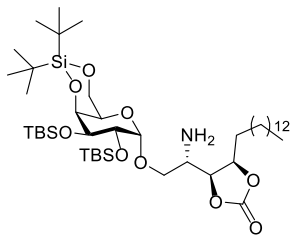
Compound 28: Azide **14** (1.34 g, 1.49 mmol, 1 equiv) was dissolved anhydrous THF (30 mL) under N_2. N_2 was purged through the stirring solution for 15 min (flow) before adding PtO$_2$ (101 mg, 0.45 mmol, 0.3 equiv) and purging N_2 through the stirred suspension for 15 min (flow). The reaction mixture was purged with H_2 (balloon) whilst stirring and was subsequently left to stir under H_2 (balloon) for 24 h. The reaction mixture was purged with N_2 (flow), filtered over a pad of 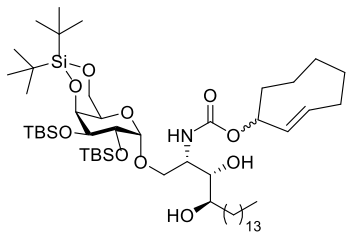Celite and concentrated *in vacuo* to obtain the crude amine **28** (1.31 g) as a yellow oil which was used in the next step without further purification: R_f = 0.2 (15% EtOAc in pentane); ^{1}H NMR (400 MHz, CDCl$_3$) δ 4.80 (d, J = 3.4 Hz, 1H), 4.75 – 4.68 (m, 1H), 4.50 (dd, J = 9.8, 7.2 Hz, 1H), 4.31 (d, J = 2.4 Hz, 1H), 4.23 (dd, J = 12.4, 1.6 Hz, 1H), 4.15 – 4.09 (m, 2H), 3.87 – 3.81 (m, 2H), 3.61 (br s, 1H), 3.38 (dd, J = 10.0, 5.8 Hz, 1H), 3.16 (ddd, J = 9.2, 5.7, 3.1 Hz, 1H), 1.91 – 1.81 (m, 1H), 1.72 – 1.54 (m, 2H), 1.41 – 1.19 (m, 23H), 1.03 (s, 9H), 1.03 (s, 9H), 0.93 (s, 9H), 0.89 (s, 9H), 0.87 (t, J = 7.0 Hz, 3H), 0.09 (s, 6H), 0.08 (s, 3H), 0.07 (s, 3H); ^{13}C NMR (101 MHz, CDCl$_3$) δ 154.4, 101.2, 80.2, 78.9, 74.9, 71.2, 70.9, 69.5, 68.0, 67.3, 49.7, 32.0, 29.8, 29.8, 29.8 (x2), 29.7, 29.6, 29.6, 29.5, 29.4, 28.8, 27.6 (x3), 27.4 (x3), 26.2 (x3), 26.1 (x3), 25.6, 23.5, 22.8, 20.8, 18.2, 18.2, 14.2, -3.9, -4.2, -4.2, -4.5; HRMS: calculated for $C_{45}H_{92}NO_9Si_3$ 874.60744 [M+H]$^+$; found 874.60676.
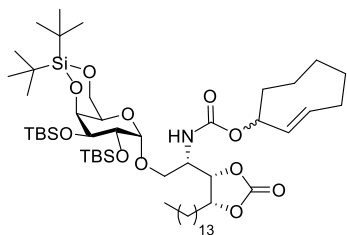
Compound 29: The crude amine **28** (1.31 g) obtained in the previous hydrogenation step and axial TCO carbonate **15** (481 mg, 1.80 mmol, 1.2 equiv) were dissolved in anhydrous DMF (15 mL) under N_2. DIPEA (0.39 mL, 2.25 mmol, 1.5 equiv) and DMAP (37 mg, 0.30 mmol, 0.2 equiv) were added and the reaction mixture was stirred for 21 h at room temperature. Subsequently, EtOAc (100 mL) was added and the orga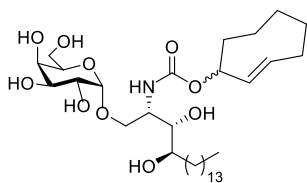nic phase was washed with HCl (1 M, 80 mL), NaHCO$_3$ (satd., 3 x 80 mL), brine (80 mL), dried over MgSO$_4$, filtered and concentrated *in vacuo*. The crude product was purified by silica gel chromatography (7% EtOAc in pentane, isocratic) to obtain the diastereomeric mixture **29** (**29$_A$** : **29$_B$**, ~ **1** : **1**, 1.36 g, 1.32 mmol, 89% over two steps) as a yellow oil: R_f = 0.3 (10% EtOAc in pentane); ^{1}H NMR (400 MHz, CDCl$_3$) δ 5.81 – 5.67 (m, 1H, **29$_A$** + **29$_B$**), 5.54 (dd, J = 16.6, 1.9 Hz, 1H, **29$_A$** + **29$_B$**), 5.41 – 5.20 (m, 1H + 1NH, **29$_A$** + **29$_B$**), 4.82 (d, J = 3.5 Hz, 1H, **29$_A$** + **29$_B$**), 4.81 – 4.76 (m, 1H, **29$_A$** + **29$_B$**), 4.75 – 4.67 (m, 1H, **29$_A$** + **29$_B$**), 4.32 (br s, 1H, **29$_A$** + **29$_B$**), 4.21 (d, J = 12.6 Hz, 1H, **29$_A$** + **29$_B$**), 4.17 – 4.04 (m, 3H, **29$_A$** + **29$_B$**), 3.85 (d, J = 9.4 Hz, 1H, **29$_A$** + **29$_B$**), 3.81 – 3.73 (m, 1H, **29$_A$** + **29$_B$**), 3.68 (dd, J = 10.4, 2.8 Hz, 1H, **29$_A$** + **29$_B$**), 3.59 (br s, 1H, **29$_A$** + **29$_B$**), 2.52 – 2.39 (m, 1H, **29$_A$** + **29$_B$**), 2.08 – 1.95 (m, 3H, **29$_A$** + **29$_B$**), 1.94 – 1.82 (m, 1H, **29$_A$** + **29$_B$**), 1.81 – 1.20 (m, 30H, **29$_A$** + **29$_B$**), 1.04 (s, 18H, **29$_A$** + **29$_B$**), 0.95 (s, 9H, **29$_A$**), 0.94 (s, 9H, **29$_B$**), 0.91 (s, 9H, **29$_A$** + **29$_B$**), 0.88 (t, J = 6.9 Hz, 3H, **29$_A$** + **29$_B$**), 0.84 – 0.73 (m, 1H, **29$_A$** + **29$_B$**), 0.13 (s, 3H, **29$_A$**), 0.12 (s, 3H, **29$_A$** + **29$_B$**), 0.11 (s, 3H, **29$_B$**), 0.10 (s, 3H, **29$_A$** + **29$_B$**), 0.09 (s, 3H, **29$_A$** + **29$_B$**); ^{13}C NMR (101 MHz, CDCl$_3$) δ 155.0, 155.0, 153.9 (x2), 131.9 (x2), 131.4, 131.2,

101.4, 101.3, 79.9, 79.8, 77.7, 77.3, 74.8, 74.8, 74.6, 74.6, 71.2, 71.1, 69.4, 69.4, 68.2, 68.1, 67.2, 67.2, 67.1, 67.1, 49.4 (x2), 40.8, 40.7, 36.0, 36.0, 36.0, 35.9, 32.0 (x2), 29.8 (x2), 29.8 (x2), 29.8 (x4), 29.7 (x2), 29.7 (x2), 29.6 (x2), 29.5 (x2), 29.5 (x2), 29.2 (x2), 29.1, 29.0, 28.6, 28.6, 27.5 (x6), 27.4 (x6), 26.2 (x6), 26.1 (x3), 26.1 (x3), 25.7, 25.6, 24.2, 23.5 (x2), 22.8 (x2), 20.8 (x2), 18.2, 18.2 (x2), 14.2 (x2), -3.8, -3.9, -4.1 (x2), -4.2 (x2), -4.6 (x2); HRMS: calculated for $C_{54}H_{104}NO_{11}Si_3$ 1026.69117 [M+H]$^+$; found 1026.69013.

Compound 13: Carbonate **29** (1.36 g, 1.32 mmol, 1.0 equiv) was dissolved in a mixture of THF (7.5 mL) and H_2O (2.5 mL) under N_2. The solution was cooled to 0°C before adding LiOH (253 mg, 10.6 mmol, 8.0 equiv). The reaction mixture was stirred for 24 h and allowed to warm to room temperature. The pH of the reaction mixture was neutralized by adding dry ice. Subsequently, the reaction mixture was concentrated *in vacuo* to obtain the crude diol **13** (**13$_A$** : **13$_B$**, ~ **1** : **1**, 1.32 g, 1.32 mmol, quant.) as an oil which was used for the next step without further purification: R$_f$= 0.4 (10% EtOAc in pentane); ^{1}H NMR (400 MHz, CDCl$_3$) δ 5.86 – 5.65 (m, 1H, **13$_A$** + **13$_B$**), 5.59 – 5.40 (m, 1H + 1NH, **13$_A$** + **13$_B$**), 5.39 – 5.26 (m, 1H, **13$_A$** + **13$_B$**), 4.89 – 4.81 (m, 1H, **13$_A$** + **13$_B$**), 4.30 (d, *J* = 2.0 Hz, 1H, **13$_A$** + **13$_B$**), 4.24 – 4.05 (m, 4H, **13$_A$** + **13$_B$**), 4.02 – 3.87 (m, 1H, **13$_A$** + **13$_B$**), 3.79 (td, *J* = 9.5, 8.5, 3.0 Hz, 1H, **13$_A$** + **13$_B$**), 3.68 (d, *J* = 10.2 Hz, 1H, **13$_A$** + **13$_B$**), 3.62 – 3.46 (m, 3H, **13$_A$** + **13$_B$**), 2.49 – 2.40 (m, 1H, **13$_A$** + **13$_B$**), 2.08 – 1.93 (m, 3H, **13$_A$** + **13$_B$**), 1.92 – 1.21 (m, 31H, **13$_A$** + **13$_B$**), 1.03 (s, 18H, **13$_A$** + **13$_B$**), 0.95 (s, 9H, **13$_A$**), 0.94 (s, 9H, **13$_B$**), 0.92 (s, 9H, **13$_A$** + **13$_B$**), 0.88 (t, *J* = 6.8 Hz, 3H, **13$_A$** + **13$_B$**), 0.85 – 0.72 (m, 1H, **13$_A$** + **13$_B$**), 0.12 (s, 9H, **13$_A$** + **13$_B$**), 0.10 (s, 3H, **13$_A$** + **13$_B$**); ^{13}C NMR (101 MHz, CDCl$_3$) δ 155.5, 155.3, 132.0, 132.0, 131.6, 131.4, 100.4, 100.1, 77.0, 76.9, 74.8, 74.8, 74.2, 73.9, 73.2 (x2), 71.6, 71.5, 69.4, 69.3, 68.3, 68.2, 67.2, 67.1, 66.7 (x2), 50.7, 50.5, 40.9, 40.9, 36.1, 36.1, 36.0 (x2), 34.3, 34.2, 32.1 (x2), 29.9 (x2), 29.8 (x10), 29.8 (x4), 29.8 (x2), 29.5 (x2), 29.2, 29.1, 27.6 (x6), 27.4 (x6), 26.3 (x6), 26.2 (x6), 24.2 (x2), 23.5, 23.5, 22.8 (x2), 20.8 (x2), 18.4, 18.2, 14.3 (x2), -3.8, -3.8, -4.1 (x2), -4.3, -4.3, -4.5 (x2); HRMS: calculated for $C_{53}H_{106}NO_{10}Si_3$ 1000.71190 [M+H]$^+$; found 1000.71102.

TCO Caged αGalPhs (12): The crude diol **13** (562 mg, 0.56 mmol, 1.0 equiv) was dissolved in anhydrous THF (5.6 mL) under N_2. The solution was cooled to 0°C before adding Et$_3$N · 3HF (0.55 mL, 3.40 mmol, 6.0 equiv). The reaction mixture was stirred for 96 h and allowed to warm to room temperature. Subsequently, the reaction mixture was concentrated *in vacuo*, redissolved in distilled EtOAc (150 mL), washed with H_2O (2 x 100 mL), brine (100 mL), dried over MgSO$_4$, filtered, impregnated with Celite and concentrated *in vacuo*. The impregnated crude product was purified by silica gel chromatography (1% MeOH in DCM → 2.5% MeOH in DCM → 5% MeOH in DCM → 10% MeOH in DCM) to obtain caged αGalPhs **12** (**12$_A$** : **12$_B$**, ~ **1** : **1**, 297 mg, 0.47 mmol, 84%) as a crystalline solid: R$_f$ = 0.25 (10% MeOH in DCM); ^{1}H NMR (600 MHz, Pyridine-*d$_5$*) δ 7.94 (d, *J* = 9.0 Hz, 1NH, **12$_A$**), 7.89 (d, *J* = 8.8 Hz, 1NH, **12$_B$**), 7.11 – 5.95 (m, 6OH, **12$_A$** + **12$_B$**), 5.88 (ddd, *J* = 15.1, 11.5, 3.2 Hz, 1H, **12$_A$**), 5.82 (ddd, *J* = 15.2, 11.5, 3.2 Hz, 1H, **12$_B$**), 5.61 (br s, 1H, **12$_A$** + **12$_B$**), 5.59 (d, *J* = 14.2 Hz, 1H, **12$_A$**), 5.53 (d, *J* = 16.2 Hz, 1H, **12$_B$**), 5.48 (d, *J* =

3.4 Hz, 1H, **12$_A$** + **12$_B$**), 4.94 – 4.85 (m, 1H, **12$_A$** + **12$_B$**), 4.66 – 4.60 (m, 1H, **12$_A$** + **12$_B$**), 4.59 – 4.55 (m, 1H, **12$_A$** + **12$_B$**), 4.54 – 4.46 (m, 1H, **12$_A$** + **12$_B$**), 4.43 – 4.18 (m, 7H, **12$_A$** + **12$_B$**), 2.37 – 2.28 (m, 1H, **12$_A$** + **12$_B$**), 2.27 – 2.18 (m, 1H, **12$_A$** + **12$_B$**), 2.16 – 2.09 (m, 1H, **12$_A$** + **12$_B$**), 1.99 – 1.79 (m, 4H, **12$_A$** + **12$_B$**), 1.77 – 1.68 (m, 1H, **12$_A$** + **12$_B$**), 1.68 – 1.58 (m, 2H, **12$_A$** + **12$_B$**), 1.56 – 1.48 (m, 1H, **12$_A$** + **12$_B$**), 1.48 – 1.15 (m, 23H, **12$_A$** + **12$_B$**), 1.13 – 1.01 (m, 1H, **12$_A$** + **12$_B$**), 0.92 (t, J = 7.1 Hz, 3H, **12$_A$** + **12$_B$**), 0.76 – 0.66 (m, 1H, **12$_A$** + **12$_B$**); ^{13}C NMR (151 MHz, Pyridine-d_5) δ 157.1, 157.1, 133.3, 133.0, 132.4, 132.0, 101.8, 101.7, 77.1, 77.1, 74.4, 74.4, 73.3, 73.3, 73.0, 72.9, 72.0 (x2), 71.5, 71.5, 70.7, 70.7, 68.8 (x2), 63.1, 63.1, 53.5 (x2), 41.6, 41.6, 36.8 (x2), 36.7, 36.6, 34.9, 34.8, 32.8 (x2), 31.0, 31.0, 30.8, 30.8, 30.7 (x2), 30.7 (x8), 30.6 (x2), 30.3 (x2), 29.8, 29.8, 27.1, 27.1, 25.0, 25.0, 23.6 (x2), 15.0 (x2); ^{1}H NMR (500 MHz, Dioxane-d_8) δ 6.16 – 5.96 (m, 1NH, **12$_A$** + **12$_B$**), 5.86 – 5.69 (m, 1H, **12$_A$** + **12$_B$**), 5.53 (d, J = 16.4 Hz, 1H, **12$_A$** + **12$_B$**), 5.27 (br s, 1H, **12$_A$** + **12$_B$**), 4.84 (d, J = 4.2 Hz, 1H, **12$_A$**), 4.83 (d, J = 3.9 Hz, 1H, **12$_B$**), 4.04 – 3.94 (m, 1H, **12$_A$** + **12$_B$**), 3.92 – 3.70 (m, 4H, **12$_A$** + **12$_B$**), 3.68 – 3.57 (m, 4H, **12$_A$** + **12$_B$**), 3.49 – 3.37 (m, 2H, **12$_A$** + **12$_B$**), 2.51 – 2.38 (m, 1H, **12$_A$** + **12$_B$**), 2.08 – 1.90 (m, 3H, **12$_A$** + **12$_B$**), 1.89 – 1.78 (m, 1H, **12$_A$** + **12$_B$**), 1.72 – 1.56 (m, 3H, **12$_A$** + **12$_B$**), 1.56 – 1.42 (m, 2H, **12$_A$** + **12$_B$**), 1.41 – 1.19 (m, 24H, **12$_A$** + **12$_B$**), 1.13 – 1.01 (m, 1H, **12$_A$** + **12$_B$**), 0.88 (t, J = 6.9 Hz, 3H, **12$_A$** + **12$_B$**), 0.86 – 0.79 (m, 1H, **12$_A$** + **12$_B$**); ^{13}C NMR (126 MHz, Dioxane-d_8) δ 156.0 (x2), 133.3, 133.1, 131.8, 131.5, 100.7 (x2), 76.7, 76.6, 74.3, 74.3, 72.5, 72.5, 72.3, 72.2, 71.5 (x2), 70.6, 70.5, 70.2 (x2), 68.2, 68.1, 62.6, 62.6, 52.5 (x2), 41.2, 41.2, 36.8 (x2), 36.4, 36.4, 34.2, 34.2, 32.7 (x2), 30.6, 30.6, 30.6, 30.5 (x5), 30.5 (x6), 30.4 (x2), 30.1 (x2), 29.8, 29.7, 26.6 (x2), 25.1, 25.0, 23.4 (x2), 14.4 (x2); HRMS: calculated for $C_{33}H_{62}NO_{10}$ 632.43682 [M+H]$^+$; found 632.43640. Compound **12** was redissolved in dioxane and lyophilized in small quantities for immunology experiments.
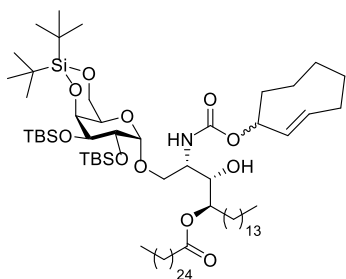

Compound 32: Hexacosanoic acid (60 mg, 0.15 mmol, 1.5 equiv), EDC · HCl (29 mg, 0.15 mmol, 1.5 equiv) and DMAP (73 mg, 0.60 mmol, 6 equiv) were dissolved in anhydrous DCM (1.0 mL) under N$_2$. The suspension was cooled to 0°C and stirred for 45 min. A solution of compound **13** (100 mg, 100 μmol, 1.0 equiv) in anhydrous DCM (2.0 mL) under N$_2$ was subsequently added to the reaction mixture. DIPEA (52 μL, 0.30 mmol, 3.0 equiv) was added and the reaction mixture was stirred for 20 h and allowed to warm to room temperature. The reaction mixture was diluted with EtOAc (30 mL), washed with HCl (1 M, 20 mL), NaHCO$_3$ (satd., 20 mL), brine (20 mL), dried over MgSO$_4$, filtered and concentrated *in vacuo*. The crude product was purified by silica gel chromatography (3% EtOAc in pentane, isocratic) to obtain compound **32** (**32$_A$** : **32$_B$**, ~ **1** : **1**, 42.3 mg, 31.0 μmol, 31%) as a yellow oil: R$_f$ = 0.7 (10% EtOAc in pentane); ^{1}H NMR (500 MHz, CDCl$_3$) δ 5.86 – 5.68 (m, 1H, **32$_A$** + **32$_B$**), 5.55 – 5.46 (m, 1H, **32$_A$** + **32$_B$**), 5.42 (d, J = 8.2 Hz, 1NH, **32$_A$**), 5.37 (d, J = 8.1 Hz, 1NH, **32$_B$**), 5.34 – 5.26 (m, 1H, **32$_A$** + **32$_B$**), 4.95 – 4.85 (m, 2H, **32$_A$** + **32$_B$**), 4.31 (d, J = 1.9 Hz, 1H, **32$_A$** + **32$_B$**), 4.28 – 4.20 (m, 2H, **32$_A$** + **32$_B$**), 4.18 – 4.12 (m, 2H, **32$_A$** + **32$_B$**), 3.80 – 3.71 (m, 2H, **32$_A$** + **32$_B$**), 3.70 – 3.61 (m, 3H, **32$_A$** + **32$_B$**), 2.51 – 2.41 (m, 1H, **32$_A$** + **32$_B$**), 2.38 (t, J = 7.4 Hz, 2H, **32$_A$** + **32$_B$**), 2.36 – 2.26 (m, 3H, **32$_A$** + **32$_B$**), 2.08 – 1.92 (m, 3H, **32$_A$** + **32$_B$**), 1.90 – 1.81 (m, 1H, **32$_A$** + **32$_B$**), 1.73 – 1.20 (m, 73H, **32$_A$** + **32$_B$**), 1.05 – 1.01 (m, 18H, **32$_A$** + **32$_B$**), 0.95 – 0.93 (m, 9H, **32$_A$** + **32$_B$**), 0.93 – 0.91 (m, 9H, **32$_A$** + **32$_B$**), 0.88 (t, J = 7.0 Hz, 6H, **32$_A$** + **32$_B$**), 0.83 – 0.73 (m, 1H, **32$_A$** + **32$_B$**), 0.14 (s, 3H, **32$_A$** + **32$_B$**), 0.12 (s,

3H, **32$_A$ + 32$_B$**), 0.11 (s, 3H, **32$_A$**), 0.11 (s, 3H, **32$_B$**), 0.10 (s, 3H, **32$_A$**), 0.10 (s, 3H, **32$_B$**); 177.4 (x2),* 174.1 (x2), 155.5 (x2), 155.2 (x2),* 132.1 (x2), 131.9 (x2),* 131.6 (x2),* 131.3 (x2), 101.3 (x2), 78.0, 78.0, 75.0 (x2),* 74.8 (x2), 74.3, 74.2, 73.9*, 74.8,* 71.5 (x2), 70.9, 70.8, 69.5 (x2), 69.2 (x2)* 68.3 (x2), 67.5, 67.2 (x3), 51.6, 51.4, 43.0 (x2), 40.8 (x2), 36.0 (x4), 34.6 (x2), 34.5, 34.3, 34.3, 33.8, 32.1 (x2), 29.9 (x 50), 29.7 (x2), 29.6 (x2), 29.5 (x2), 29.5 (x2), 29.4 (x2), 29.3 (x2), 29.2, 29.2, 27.6 (x6), 27.5 (x6), 26.3 (x6), 26.2 (x6), 25.1 (x3), 24.9, 24.2, 24.0, 23.6, 22.8 (x2), 20.8, 18.5, 18.2, 14.3 (x4), -3.9 (x2), -4.0 (x2), -4.3 (x2), -4.6 (x2).

*Note: Additional ^{13}C signals encountered which indicate the presence of an additional regioisomer are denoted.**
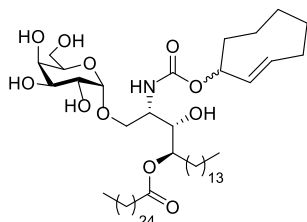
TCO caged αGalCer produg (8): Compound **32** (41.0 mg, 30.0 μmol, 1.0 equiv) was dissolved in anhydrous THF (300 μL) under N$_2$. The solution was cooled to 0°C before adding Et$_3$N · 3HF (48 μL, 297 μmol, 10.0 equiv). The reaction mixture was stirred for 27 h and allowed to warm to room temperature. The reaction mixture was concentrated *in vacuo*, redissolved in distilled EtOAc (20 mL), washed with H$_2$O (2 x 10 mL), brine (10 mL), dried over MgSO$_4$, filtered and concentrated *in vacuo*. The crude product was purified by silica gel chromatography (100% distilled EtOAc, isocratic) to obtain caged αGalCer **8** (**8$_A$** : **8$_B$**, ~ **1** : **1**, 7.0 mg, 6.93 μmol, 23%) as a crystalline solid: R$_f$ = 0.2 (100% EtOAc); ^{1}H NMR (600 MHz, Dioxane-d_8) δ 6.27 (d, *J* = 9.3 Hz, 1NH)*, 6.04 (d, *J* = 9.1 Hz, 1NH, **8$_A$**), 6.01 (d, *J* = 8.8 Hz, 1NH, **8$_B$**), 5.85 – 5.66 (m, 1H, **8$_A$ + 8$_B$**), 5.52 (d, *J* = 16.4 Hz, 1H, **8$_A$ + 8$_B$**), 5.24 (d, *J* = 13.7 Hz, 1H, **8$_A$ + 8$_B$**), 4.99 – 4.85 (m, 1H, **8$_A$ + 8$_B$**), 4.81 – 4.68 (m, 1H, **8$_A$ + 8$_B$**), 4.21 – 4.09 (m, 1H, **8$_A$ + 8$_B$**), 3.98 – 3.38 (m, 9H, **8$_A$ + 8$_B$**), 2.51 – 2.39 (m, 1H, **8$_A$ + 8$_B$**), 2.35 – 2.26 (m, 2H, **8$_A$ + 8$_B$**), 2.22 (t, *J* = 7.4 Hz, 1H)*, 2.09 – 1.90 (m, 3H, **8$_A$ + 8$_B$**), 1.88 – 1.77 (m, 1H, **8$_A$ + 8$_B$**), 1.73 – 1.13 (m, 75H, **8$_A$ + 8$_B$**), 1.12 – 0.99 (m, 1H, **8$_A$ + 8$_B$**), 0.88 (t, *J* = 6.9 Hz, 6H, **8$_A$ + 8$_B$**); ^{13}C NMR (151 MHz, Dioxane-d_8) δ 174.8 (x2),* 173.8 (x2), 156.0 (x2), 133.3,* 133.2, 133.1, 133.1,* 131.8, 131.5, 101.5,* 101.3,* 100.5, 100.4, 77.0 (x2), 74.5 (x2), 72.4 (x2), 71.5 (x2), 70.7, 70.6, 70.4 (x2), 70.3 (x2), 67.9,* 67.8,* 67.5, 67.4, 62.6, 62.5, 52.9 (x2),* 52.0 (x2), 42.9,* 41.2 (x2), 36.8 (x2), 36.4 (x2), 34.9, 34.8, 34.0,* 33.9,* 32.7 (x4), 30.4 (x 50), 30.1 (x6), 30.0 (x2), 29.7 (x2), 26.4, 26.1, 25.9, 25.7, 25.6, 25.5, 25.1, 25.1, 24.5,* 24.1,* 23.4 (x4), 14.5 (x4); HRMS: calculated for C$_{59}$H$_{111}$NO$_{11}$ 1010.82299 [M+H]$^+$; found 1010.82277. Compound **8** was redissolved in dioxane and lyophilized in small quantities for immunology experiments.

*Note: Additional ^{1}H and ^{13}C signals encountered which indicate the presence of an additional regioisomer are denoted.**

5.5 References

[1]   N. A. Borg, K. S. Wun, L. Kjer-Nielsen, M. C. J. Wilce, D. G. Pellicci, R. Koh, G. S. Besra, M. Bharadwaj, D. I. Godfrey, J. McCluskey, J. Rossjohn, *Nature* **2007**, *448*, 44–49.

[2]   D. I. Godfrey, H. R. MacDonald, M. Kronenberg, M. J. Smyth, L. Van Kaer, *Nat. Rev. Immunol.* **2004**, *4*, 231–237.

[3]   A. Bendelac, P. B. Savage, L. Teyton, *Annu. Rev. Immunol.* **2007**, *25*, 297–336.

[4]   P. J. Brennan, M. Brigl, M. B. Brenner, *Nat. Rev. Immunol.* **2013**, *13*, 101–17.

[5]   J. Rossjohn, D. G. Pellicci, O. Patel, L. Gapin, D. I. Godfrey, *Nat. Rev. Immunol.* **2012**, *12*, 845–57.

[6]   D. B. Stetson, M. Mohrs, R. L. Reinhardt, J. L. Baron, Z.-E. Wang, L. Gapin, M. Kronenberg, R. M. Locksley, *J. Exp. Med.* **2003**, *198*, 1069–1076.

[7]   T. Natori, M. Morita, K. Akimoto, Y. Koezuka, *Tetrahedron* **1994**, *50*, 2771–2784.

[8]   M. Morita, K. Motoki, K. Akimoto, T. Natori, T. Sakai, E. Sawa, K. Yamaji, Y. Koezuka, E. Kobayashi, H. Fukushima, *J. Med. Chem.* **1995**, *38*, 2176–2187.

[9]   T. Kawano, J. Cui, Y. Koezuka, I. Toura, Y. Kaneko, K. Motoki, H. Ueno, R. Nakagawa, H. Sato, E. Kondo, H. Koseki, M. Taniguchi, *Science* **1997**, *278*, 1626–1629.

[10]   M. Koch, V. S. Stronge, D. Shepherd, S. D. Gadola, B. Mathew, G. Ritter, A. R. Fersht, G. S. Besra, R. R. Schmidt, E. Y. Jones, V. Cerundolo, *Nat. Immunol.* **2005**, *6*, 819–826.

[11]   C. Carnaud, D. Lee, O. Donnars, S. H. Park, A. Beavis, Y. Koezuka, A. Bendelac, *J. Immunol.* **1999**, *163*, 4647–50.

[12]   M. M. Venkataswamy, S. a. Porcelli, *Semin. Immunol.* **2010**, *22*, 68–78.

[13]   P. B. Savage, L. Teyton, A. Bendelac, *Chem. Soc. Rev.* **2006**, *35*, 771-779.

[14]   S. Nair, M. V. Dhodapkar, *Front. Immunol.* **2017**, *8*, 1178.

[15]   Y. Zhang, R. Springfield, S. Chen, X. Li, X. Feng, R. Moshirian, R. Yang, W. Yuan, *Front. Immunol.* **2019**, *10*, DOI 10.3389/fimmu.2019.01126.

[16]   M. Waldowska, A. Bojarska-Junak, J. Roliński, *Cent. Eur. J. Immunol.* **2017**, *2*, 181–195.

[17]   V. V. Parekh, M. T. Wilson, D. Olivares-Villagómez, A. K. Singh, L. Wu, C.-R. Wang, S. Joyce, L. Van Kaer, *J. Clin. Invest.* **2005**, *115*, 2572–83.

[18]   B. A. Sullivan, M. Kronenberg, *J. Clin. Invest.* **2005**, *115*, 2328–2329.

[19]   Y. Osman, T. Kawamura, T. Naito, K. Takeda, L. Van Kaer, K. Okumura, T. Abo, *Eur. J.*

Immunol. **2000**, *30*, 1919–1928.

[20]   T. Tashiro, *Biosci. Biotechnol. Biochem.* **2012**, *76*, 1055–1067.

[21]   A. Banchet-Cadeddu, E. Hénon, M. Dauchez, J.-H. Renault, F. Monneaux, A. Haudrechy, *Org. Biomol. Chem.* **2011**, *9*, 3080-3104.

[22]   J. Kishi, S. Inuki, E. Kashiwabara, T. Suzuki, N. Dohmae, Y. Fujimoto, *ACS Chem. Biol.* **2020**, *15*, 353–359.

[23]   G. Gonzalez-Aseguinolaza, L. Van Kaer, C. C. Bergmann, J. M. Wilson, J. Schmieg, M. Kronenberg, T. Nakayama, M. Taniguchi, Y. Koezuka, M. Tsuji, *J. Exp. Med.* **2002**, *195*, 617–624.

[24]   S.-I. Fujii, K. Shimizu, C. Smith, L. Bonifaz, R. M. Steinman, *J. Exp. Med.* **2003**, *198*, 267–279.

[25]   S. Fujii, K. Liu, C. Smith, A. J. Bonito, R. M. Steinman, *J. Exp. Med.* **2004**, *199*, 1607–1618.

[26]   I. F. Hermans, J. D. Silk, U. Gileadi, M. Salio, B. Mathew, G. Ritter, R. Schmidt, A. L. Harris, L. Old, V. Cerundolo, *J. Immunol.* **2003**, *171*, 5140–5147.

[27]   D. Stober, I. Jomantaitė, R. Schirmbeck, J. Reimann, *J. Immunol.* **2003**, *170*, 2540–2548.

[28]   V. Semmling, V. Lukacs-Kornek, C. A. Thaiss, T. Quast, K. Hochheiser, U. Panzer, J. Rossjohn, P. Perlmutter, J. Cao, D. I. Godfrey, P. B. Savage, P. A. Knolle, W. Kolanus, I. Förster, C. Kurts, *Nat. Immunol.* **2010**, *11*, 313–320.

[29]   P. B. Savage, *Nat. Chem. Biol.* **2014**, *10*, 882–883.

[30]   M. Cavallari, P. Stallforth, A. Kalinichenko, D. C. K. Rathwell, T. M. A. Gronewold, A. Adibekian, L. Mori, R. Landmann, P. H. Seeberger, G. De Libero, *Nat. Chem. Biol.* **2014**, *10*, 950–956.

[31]   F. Broecker, S. Götze, J. Hudon, D. C. K. Rathwell, C. L. Pereira, P. Stallforth, C. Anish, P. H. Seeberger, *J. Med. Chem.* **2018**, *61*, 4918–4927.

[32]   R. J. Anderson, C. Tang, N. J. Daniels, B. J. Compton, C. M. Hayman, K. a Johnston, D. a Knight, O. Gasser, H. C. Poyntz, P. M. Ferguson, D. S. Larsen, F. Ronchese, G. F. Painter, I. F. Hermans, *Nat. Chem. Biol.* **2014**, *10*, 943–949.

[33]   J. Alexander, R. Cargill, S. R. Michelson, H. Schwam, *J. Med. Chem.* **1988**, *31*, 318–322.

[34]   J. B. Flechtner, K. P. Cohane, S. Mehta, P. Slusarewicz, A. K. Leonard, B. H. Barber, D. L. Levey, S. Andjelic, *J. Immunol.* **2006**, *177*, 1017–1027.

[35]   O. Rötzschke, K. Falk, S. Stevanovic, G. Jung, P. Walden, H.-G. Rammensee, *Eur. J. Immunol.* **1991**, *21*, 2891–2894.

[36]   R. J. Anderson, B. J. Compton, C. W. Tang, A. Authier-Hall, C. M. Hayman, G. W. Swinerd, R.

Kowalczyk, P. Harris, M. A. Brimble, D. S. Larsen, O. Gasser, R. Weinkove, I. F. Hermans, G. F. Painter, *Chem. Sci.* **2015**, *6*, 5120–5127.

[37]   C. Grasso, C. S. Field, C.-W. Tang, P. M. Ferguson, B. J Compton, R. J. Anderson, G. F. Painter, R. Weinkove, I. F Hermans, M. V Berridge, *Immunotherapy* **2020**, *12*, 395–406.

[38]   B. J. Compton, K. J. Farrand, C. Tang, T. L. Osmond, M. Speir, A. Authier-Hall, J. Wang, P. M. Ferguson, S. T. S. Chan, R. J. Anderson, T. R. Cooney, C. M. Hayman, G. M. Williams, M. A. Brimble, C. R. Brooks, L.-K. Yong, L. S. Metelitsa, D. M. Zajonc, D. I. Godfrey, O. Gasser, R. Weinkove, G. F. Painter, I. F. Hermans, *Org. Biomol. Chem.* **2019**, *17*, 1225–1237.

[39]   R. J. Anderson, J. Li, L. Kedzierski, B. J. Compton, C. M. Hayman, T. L. Osmond, C. Tang, K. J. Farrand, H.-F. Koay, C. F. D. S. S. E. Almeida, L. R. Holz, G. M. Williams, M. A. Brimble, Z. Wang, M. Koutsakos, K. Kedzierska, D. I. Godfrey, I. F. Hermans, S. J. Turner, G. F. Painter, *ACS Chem. Biol.* **2017**, *12*, 2898–2905.

[40]   L. E. Holz, Y. C. Chua, M. N. de Menezes, R. J. Anderson, S. L. Draper, B. J. Compton, S. T. S. Chan, J. Mathew, J. Li, L. Kedzierski, Z. Wang, L. Beattie, M. H. Enders, S. Ghilas, R. May, T. M. Steiner, J. Lange, D. Fernandez-Ruiz, A. M. Valencia-Hernandez, T. L. Osmond, K. J. Farrand, R. Seneviratna, C. F. Almeida, K. M. Tullett, P. Bertolino, D. G. Bowen, A. Cozijnsen, V. Mollard, G. I. McFadden, I. Caminschi, M. H. Lahoud, K. Kedzierska, S. J. Turner, D. I. Godfrey, I. F. Hermans, G. F. Painter, W. R. Heath, *Sci. Immunol.* **2020**, *5*, eaaz8035.

[41]   G. M. Dubowchik, R. A. Firestone, L. Padilla, D. Willner, S. J. Hofstead, K. Mosure, J. O. Knipe, S. J. Lasch, P. A. Trail, *Bioconjug. Chem.* **2002**, *13*, 855–869.

[42]   N. Hartrampf, T. Seki, A. Baumann, P. Watson, N. A. Vepřek, B. E. Hetzler, A. Hoffmann-Röder, M. Tsuji, D. Trauner, *Chem. Eur. J.* **2020**, *26*, 4476–4479.

[43]   R. M. Versteegen, R. Rossin, W. ten Hoeve, H. M. Janssen, M. S. Robillard, *Angew. Chem. Int. Ed.* **2013**, *52*, 14112–14116.

[44]   J. Li, P. R. Chen, *Nat. Chem. Biol.* **2016**, *12*, 129–137.

[45]   J. Tu, M. Xu, R. M. Franzini, *ChemBioChem* **2019**, *20*, 1615–1627.

[46]   K. Neumann, A. Gambardella, M. Bradley, *ChemBioChem* **2019**, *20*, 872–876.

[47]   R. Rossin, S. M. J. van Duijnhoven, W. ten Hoeve, H. M. Janssen, F. J. M. Hoeben, R. M. Versteegen, M. S. Robillard, *Bioconjug. Chem.* **2016**, *27*, 1697–1706.

[48]   R. Rossin, R. M. Versteegen, J. Wu, A. Khasanov, H. J. Wessels, E. J. Steenbergen, W. ten Hoeve, H. M. Janssen, A. H. A. M. van Onzen, P. J. Hudson, M. S. Robillard, *Nat. Commun.* **2018**, *9*, 1484.

[49]   K. Wu, N. A. Yee, S. Srinivasan, A. Mahmoodi, M. Zakharian, J. M. Mejia Oneto, M. Royzen, *Chem. Sci.* **2021**, *12*, 1259–1271.

[50]   A. M. F. van der Gracht, M. A. R. de Geus, M. G. M. Camps, T. J. Ruckwardt, A. J. C. Sarris, J.

Bremmers, E. Maurits, J. B. Pawlak, M. M. Posthoorn, K. M. Bonger, D. V. Filippov, H. S. Overkleeft, M. S. Robillard, F. Ossendorp, S. I. van Kasteren, *ACS Chem. Biol.* **2018**, *13*, 1569–1576.

[51]   M. J. van de Graaff, T. Oosenbrug, M. H. S. Marqvorsen, C. R. Nascimento, M. A. R. de Geus, B. Manoury, M. E. Ressing, S. I. van Kasteren, *Bioconjug. Chem.* **2020**, *31*, 1685–1692.

[52]   J. Li, S. Jia, P. R. Chen, *Nat. Chem. Biol.* **2014**, *10*, 1003–1005.

[53]   A. Imamura, H. Ando, S. Korogi, G. Tanabe, O. Muraoka, H. Ishida, M. Kiso, *Tetrahedron Lett.* **2003**, *44*, 6725–6728.

[54]   A. Kimura, A. Imamura, H. Ando, H. Ishida, K. Makoto, *Synlett* **2006**, *15*, 2379–2382.

[55]   A. Imamura, N. Matsuzawa, S. Sakai, T. Udagawa, S. Nakashima, H. Ando, H. Ishida, M. Kiso, *J. Org. Chem.* **2016**, *81*, 9086–9104.

[56]   N. Veerapen, M. Brigl, S. Garg, V. Cerundolo, L. R. Cox, M. B. Brenner, G. S. Besra, *Bioorganic Med. Chem. Lett.* **2009**, *19*, 4288–4291.

[57]   H. Gold, R. G. Boot, J. M. F. G. Aerts, H. S. Overkleeft, J. D. C. Codée, G. A. van der Marel, *Eur. J. Org. Chem.* **2011**, 1652–1663.

[58]   L. Panza, F. Compostella, D. Imperio, *Carbohydr. Res.* **2019**, *472*, 50–57.

[59]   D. Kumagai, M. Miyazaki, S.-I. I. Nishimura, *Tetrahedron Lett.* **2001**, *42*, 1953–1956.

[60]   E. D. Goddard-Borger, R. V Stick, *Org. Lett.* **2007**, *9*, 3797–3800.

[61]   G. T. Potter, G. C. Jayson, G. J. Miller, J. M. Gardiner, *J. Org. Chem.* **2016**, *81*, 3443–3446.

[62]   B. Zacharie, T. P. Connolly, C. L. Penney, *J. Org. Chem.* **1995**, *60*, 7072–7074.

[63]   B. Neises, W. Steglich, *Angew. Chem. Int. Ed.* **1978**, *17*, 522–524.

[64]   J. Inanaga, K. Hirata, H. Saeki, T. Katsuki, M. Yamaguchi, *Bull. Chem. Soc. Jpn.* **1979**, *52*, 1989–1993.

[65]   Y. Kawanami, Y. Dainobu, J. Inanaga, T. Katsuki, M. Yamaguchi, *Bull. Chem. Soc. Jpn.* **1981**, *54*, 943–944.

[66]   I. Dhimitruka, J. SantaLucia, *Org. Lett.* **2006**, *8*, 47–50.

[67]   P. L. van der Peet, C. Gunawan, M. Watanabe, S. Yamasaki, S. J. Williams, *J. Org. Chem.* **2019**, *84*, 6788–6797.

[68]   A. Lee, K. J. Farrand, N. Dickgreber, C. M. Hayman, S. Jürs, I. F. Hermans, G. F. Painter, *Carbohydr. Res.* **2006**, *341*, 2785–2798.

[69]   N. Veerapen, E. A. Leadbetter, M. B. Brenner, L. R. Cox, G. S. Besra, *Bioconjug. Chem.* **2010**, *21*, 741–747.

[70]   G. A. van der Marel, J. D. C. Codée, P. Kovác, *Carbohydrate Chemistry: Proven Synthetic Methods, Volume 2*, **2014**.

[71]   J. Ohlsson, G. Magnusson, *Carbohydr. Res.* **2000**, *329*, 49–55.

[72]   H.-M. Chen, S. G. Withers, *Carbohydr. Res.* **2010**, *345*, 2596–2604.

[73]   R. J. B. H. N. van den Berg, C. G. N. Korevaar, G. A. van der Marel, H. S. Overkleeft, J. H. van Boom, *Tetrahedron Lett.* **2002**, *43*, 8409–8412.

[74]   R. J. B. H. N. van den Berg, T. J. Boltje, C. P. Verhagen, R. E. J. N. Litjens, G. a van der Marel, H. S. Overkleeft, *J. Org. Chem.* **2006**, *71*, 836–839.

[75]   S. Kim, S. Lee, T. Lee, H. Ko, D. Kim, *J. Org. Chem.* **2006**, *71*, 8661–8664.

6

Synthetic methodology towards allylic *trans*-cyclooctene-ethers enables modification of carbohydrates: bioorthogonal manipulation of the *lac* repressor

6.1 Introduction

Bioorthogonal bond cleavage reactions have garnered significant interest in recent years.[1–4] Amongst these new "click-to-release" reactions, the inverse electron demand Diels-Alder (IEDDA) pyridazine elimination has shown particular promise for bioorthogonal utilization.[5] The method employs a *trans*-cyclooctene (TCO) carrying an allylic substituent that upon [4 + 2] cycloaddition with a 1,2,4,5-tetrazine results in the formation of a 4,5-dihydropyridazine.[6] This 4,5-tautomer can rearrange to form two
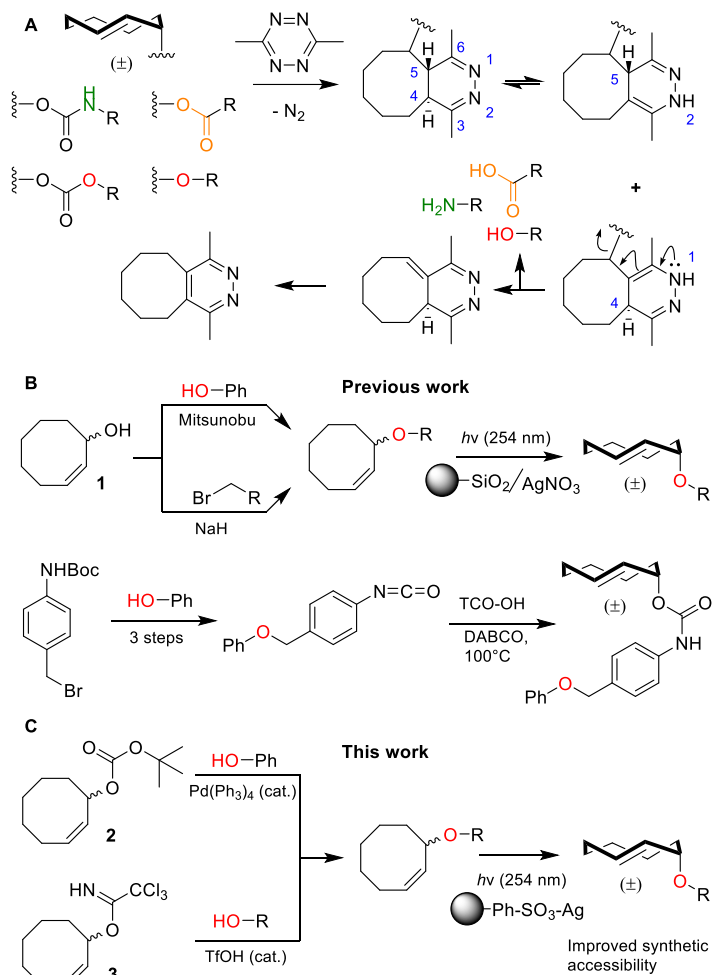
Figure 1 A) Overview of the inverse electron demand Diels-Alder (IEDDA) pyridazine elimination reaction, including the current scope of this method to decage carbamates, carbonates, ethers and esters to obtain amines (green), alcohols (red) and carboxylic acids (orange), respectively. B) Overview of the current synthetic methods to obtain allylic TCO ethers, including methods from Robillard and co-workers (top)[8] and Bernardes and co-workers (bottom).[21] C) Novel synthetic methods described in this work, including reagents **2** and **3**.

new tautomers of which the 1,4-tautomer can release the allylic payload, followed by rearomatization to the pyridazine (Figure 1A).[7,8] The excellent biocompatibility and high bimolecular reaction rate of the IEDDA pyridazine elimination[9] has given rise to a multitude of *in vitro* and *in vivo* applications such as the regulation of protein activity[10–12] and the activation of pro-drugs, in which spatiotemporal control is achieved by antibody-drug conjugates (ADCs),[13–15] nanoparticles,[16] enzymatic supramolecular self-assembly[17] or hydrogel injection.[18,19]

To date, nearly all applications for this reaction have relied on the protection of (primary) amines as TCO-carbamates (Figure 1A, green). Recently, Robillard[8] and Bernardes[20,21] showed that release of other functional groups, such as carboxylic acids (from TCO-esters) and alcohols (from TCO-carbonates or TCO-ethers), is indeed possible (Figure 1A, orange and red). Whilst TCO-esters and carbonates suffer from reduced hydrolytic stability in biological systems,[8,20,21] TCO-ethers are particularly appealing due to their high stability and surprisingly fast decaging kinetics when compared to vinyl ether analogues.[8,22–24] Unfortunately, widespread use of TCO-ethers is constricted by their challenging synthesis. Formation of the crucial *cis*-cyclooctene (CCO) ether bond, employing either Mitsunobu chemistry or nucleophilic substitution of a primary alkyl bromide with **1**, is followed by photochemical isomerization[25] to the TCO-ether and isolation of the desired axial isomer (Figure 1B, top).[8] One exception is the direct alkylation of axial TCO-OH to form a benzylic TCO-ether.[8] Additionally, Bernardes and co-workers developed a self-immolative linker in which a TCO-carbamate is connected to a benzyl ether (Figure 1B, bottom).[21] Although **1** was used as a Mitsunobu substrate with moderate success,[8] this method essentially limits the scope to phenolic nucleophiles and excludes the formation of ethers from aliphatic alcohols.[26] Furthermore, direct nucleophilic substitution with **1** is limited to primary positions,[8] in which the desired aliphatic alcohol requires an additional transformation into a leaving group. The self-immolative linker[21] requires at least four synthetic steps from the substrate, which to date has also been limited to phenols. Taken together, synthesis and utilization of TCO-ethers derived from functionalized aliphatic alcohols encountered in biological systems is currently unfeasible. To overcome this limitation, the development was undertaken of novel synthetic methods for the (regioselective) installation of TCO-ethers in biomolecules as caging moieties, based on reagents **2** and **3**, and the results these studies are presented here (Figure 1C). The methodology was applied to enable the synthesis and bioorthogonal decaging of a TCO-ether modified carbohydrate, as no TCO-protected variants of these biomolecules currently exist.

6.2 Results and discussion

A two-step procedure was envisioned in which the use of electrophilic cyclooctene reagents secured formation of a CCO-ether bond under mild conditions, followed by photochemical isomerization[25] to the desired TCO-ether. Palladium catalysis enables mild, decarboxylative conversion of allyl carbonates to allyl ethers via a reactive π-allyl cation species.[27,28] For phenols, a ring strained variant of this reaction was found feasible by transforming *para*-nitrophenyl carbonate **4** into cyclooctene ether **5** under Pd(PPh$_3$)$_4$ catalysis (50°C) in 92% yield (Scheme 1). Based on these initial observations, the palladium-catalyzed method for direct allylation by Grover and co-workers[29]
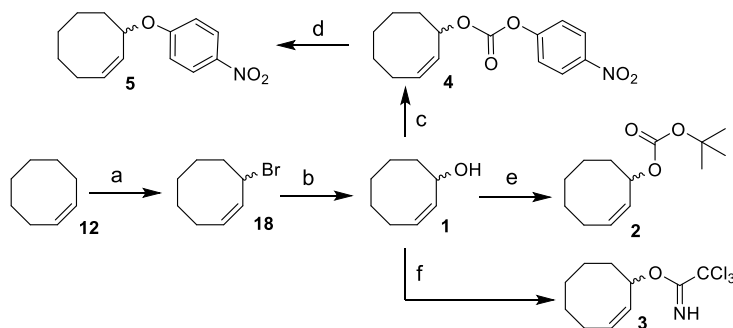
Scheme 1 Synthesis of **1**, **2**, **3**, **4** and **5** from *cis*-cyclooctene (**12**). Reagents/conditions: (a) NBS, AIBN, cyclohexane, reflux, 71%; (b) acetone, H_2O, $NaHCO_3$, reflux, 83%; (c) 4-nitrophenyl chloroformate, pyridine, DCM, 0°C to rt, 83%; (d) $Pd(PPh_3)_4$, toluene, 50°C, 92%; (e) NaHMDS, Boc-ON, THF, 0°C to rt, 81%; (f) trichloroacetonitrile, DBU, $NaHCO_3$, DCM, 0°C to rt, ~ 80% (Table S1).

would enable cyclooctene ether formation in a single step. Therefore, cyclooctene *tert*-butyl carbonate reagent **2** was designed, which decarboxylates upon coordination with a palladium catalyst (Scheme 2A). The spectator *tert*-butoxide formed in this step[29] ensures rapid deprotonation of the phenol nucleophile, which can subsequently attack the π-allyl electrophile to form the ether bond. Cyclooctene ether formation with N-trifluoroacetyl-protected L-tyrosine methyl ester **6** using reagent **2** (1.2 equivalents) under $Pd(PPh_3)_4$ catalysis (80°C) was examined instead of the previously reported Mitsunobu procedure (12% yield),[8] obtaining cyclooctene ether **7** in 80% yield (Scheme 2A).

In parallel, a second reagent (**3**) was designed for the synthesis of cyclooctene ethers from aliphatic alcohols (Scheme 2B). Lewis acid triggered activation of cyclooctene trichloroimidate **3** can result in elimination and rearrangement pathways, including the formation of ionic intermediates.[30,31] Cyclooctene trichloroamide **8**, trichloroacetamide (**9**) and the desired cyclooctene ether can be formed from these reactive intermediates. N-trifluoroacetyl-protected L-serine methyl ester **10** was alkylated using 2 equivalents of **3** under triflic acid catalysis (-35°C to 0°C) to obtain **11** in 46% yield (Scheme 2B, Table S2). Furthermore, reagents **2** and **3** were both synthesized from *cis*-cyclooctene (**12**) in 3 steps (~48% yield) with a common intermediate (**1**) and a single chromatographic purification (Scheme 1, Table S1).

Carbohydrates orchestrate a diverse array of biological processes and as such, spatiotemporal control over these biological activities would be a powerful addition to the "click-to-release" toolkit. A classic example of a biological process directed by glycans is the switching of the *lac* operon.[32,33] It is a regulatory element that is used to control nutrient-dependent transcription in *E.coli*. When lactose concentration is low,
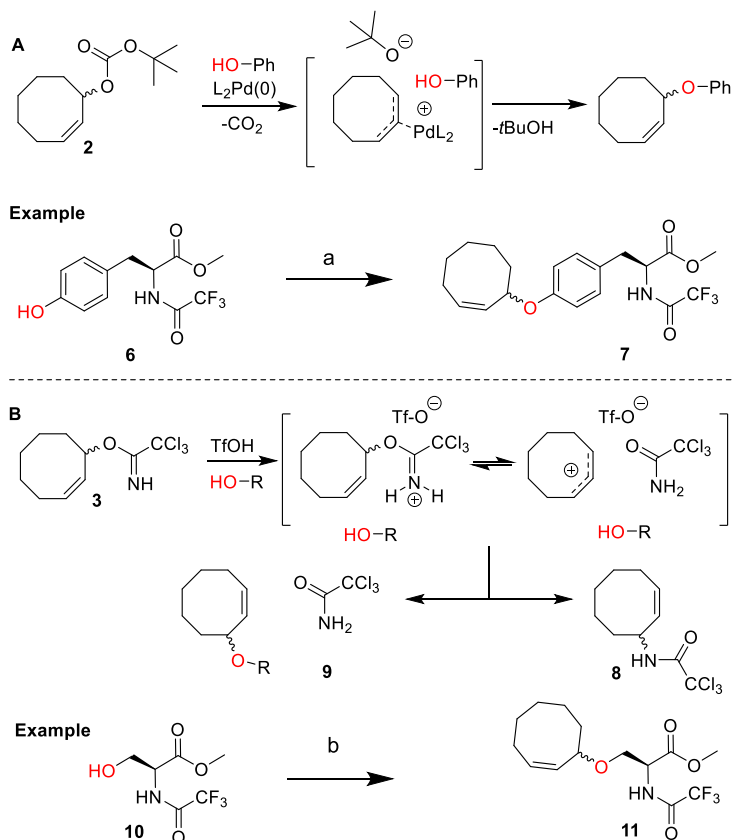
Scheme 2 A) Design of cyclooctene *tert*-butyl carbonate reagent **2** for the palladium catalyzed installation of cyclooctene ethers on phenols, including the proposed mechanism based on the work of Grover and co-workers.[29] Reagents/conditions: (a) **2**, Pd(PPh₃)₄, dioxane, 80°C, 80%; B) Design of cyclooctene trichloroimidate reagent **3** for the Lewis acid triggered formation of cyclooctene ethers from aliphatic alcohols. Proposed mechanism and products observed upon treating **3** with catalytic triflic acid are shown. Reagents/conditions: (b) **3**, TfOH, DCM, -35°C to 0°C, 46% (Table S2).

the activity of the operon is inhibited by a repressor element.[34] When the concentration of lactose increases, it will bind to the repressor, leading to a decreased affinity of the lactose-repressor complex for the operon.[35] This results in enhanced gene transcription for proteins under control of this promotor. This system has been extensively used for the expression of recombinant proteins in *E. coli* and the synthetic *lac* operon inducer isopropyl β-D-1-thiogalactopyranoside (IPTG, **13**) is a key reagent here. Control over its activity has previously been attempted using both photochemical[36] and hypoxia-triggered[37] induction strategies. IPTG (**13**) was therefore deemed an excellent model to test IEDDA pyridazine elimination on carbohydrates. Initial experiments with peracetylated IPTG (**14**) under conditions
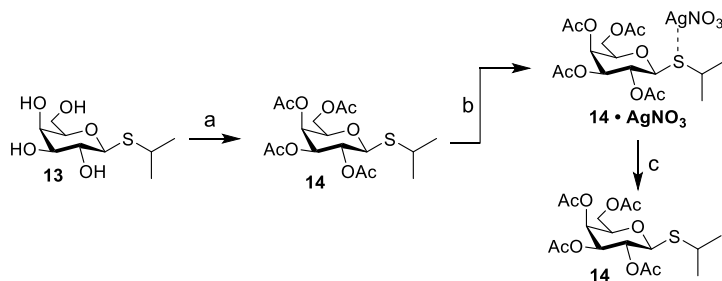
Scheme 3 Evaluation of the fate of peracetylated IPTG (**14**) during photoisomerization conditions. Reagents/conditions: (a) Ac$_2$O, pyridine, rt, 100%; (b) methyl benzoate, hν (254 nm), Et$_2$O, heptane, rt; (c) NH$_4$OAc (aq), DCM, rt, 61%.

typically used for photochemical isomerization of cyclooctenes confirmed the high affinity of the thioacetal functionality towards the silver nitrate used for enrichment of the TCO-isomers upon photoisomerization (Scheme 3). Therefore, a novel inducer for the *lac* operon was designed, substituting the sulfur with oxygen to obtain an O-glycoside, isopropyl β-D-1-galactopyranoside (IPG, **15**, Scheme 4).

Starting from peracetylated β-D-galactopyranoside **16**, installation of the beta isopropyl group on the anomeric center was achieved in a one-pot, two-step procedure in 70% yield. The 'disarmed' pentaacetate was first transformed into an anomeric bromide, which was subsequently activated with stoichiometric I$_2$ in the presence of isopropanol to obtain **17**, according to a method reported by Field and colleagues.[38] Deacetylation gave IPG (**15**) in 90% yield. Stannylene acetal-mediated alkylation of IPG (**15**) with (Z)-3-bromocyclooct-1-ene (**18**) in the presence of CsF or TBAI as an additive at 105°C was initially investigated (Table S3). A mixture of 3-CCO-IPG (**19**, ~ 20% yield) and 6-CCO-IPG (**20**, ~ 20% yield) was obtained and purified via chromatographic separation. Decomposition of **18** at high temperature into 1,3-cyclooctadiene and hydrogen bromide[39] limited its use. Attempts to alkylate 6-TBS and 4,6-DTBS functionalized derivatives of **15** in a regioselective manner with **18** were unsuccessful (Table S4).
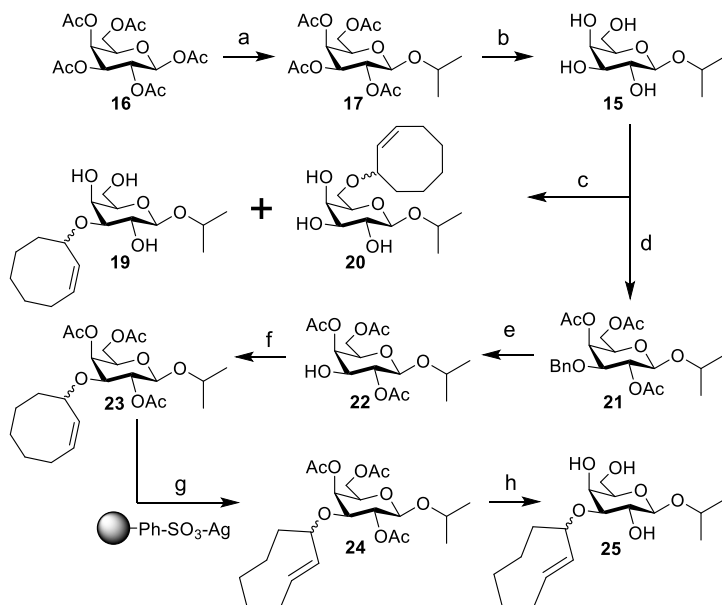
Scheme 4 Synthesis of IPG (**15**), 3-CCO-IPG (**19**), 6-CCO-IPG (**20**), and 3-TCO-IPG (**25**) from peracetylated β-D-galactopyranoside (**16**). Reagents/conditions: (a) i. HBr, AcOH, DCM, 0°C to rt; ii. 2-propanol, I_2, DCM, 0°C to 4°C, 70% over 2 steps; (b) NaOMe, MeOH, DCM, rt, 90%; (c) i. Bu_2SnO, toluene, 105°C; ii.**18**, CsF, toluene, 105°C, ~20% (**19**), ~ 20% (**20**) (Table S3); (d) i. Bu_2SnO, toluene, 105°C; ii. benzyl bromide, TBABr, toluene, 70°C; iii. Ac_2O, pyridine, rt, 91% over 2 steps; (e) Pd(OH)$_2$/C, H_2, EtOAc, rt, 86%; (f) **3**, TfOH, DCM, -40°C to rt, ~ 30% (Table S5); (g) methyl benzoate, hν (254 nm), Et_2O/isopropanol, rt; (h) NaOMe, MeOH, rt, ~ 30% over 2 steps (Table S6).

Instead, IPG (**15**) was regioselectively benzylated using organotin chemistry followed by acetylation to obtain 2,4,6-OAc-3-OBn-IPG (**21**) in 91% yield over two steps. Hydrogenation of **21** in the presence of Pearlman's catalyst afforded 2,4,6-OAc-IPG (**22**) in 86% yield. Alkylation of **22** could be achieved in the timespan of hours at low temperature (≤ 0°C), typically employing 4 equivalents of trichloroimidate **3** and 10 mol% of triflic acid (Table S5). The crude reaction mixture was washed with aqueous NaOH (to remove **9**)[40] before purification by silica gel chromatography to obtain **23** in ≥ 30% yield. Singlet sensitized photoisomerization of **23** to **24** (Table S6) was executed with the general flow setup described by Fox and co-workers[25] using silver (I) exchanged tosic acid silica gel (TAg silica) as the stationary phase.[41] Irradiation (λ = 254 nm) of mixture of **23** and methyl benzoate in Et_2O for ± 24 h, whilst continuously circulating the reaction mixture over the stationary phase, was followed by treatment of the stationary phase with NH_3 in MeOH to obtain (partially deacetylated) **24**. Zemplén deacetylation of **24** afforded **25** after extractive desalting in ≥ 30% yield over 2 steps. This final product, 3-TCO-IPG (**25**), was exclusively obtained as the desired
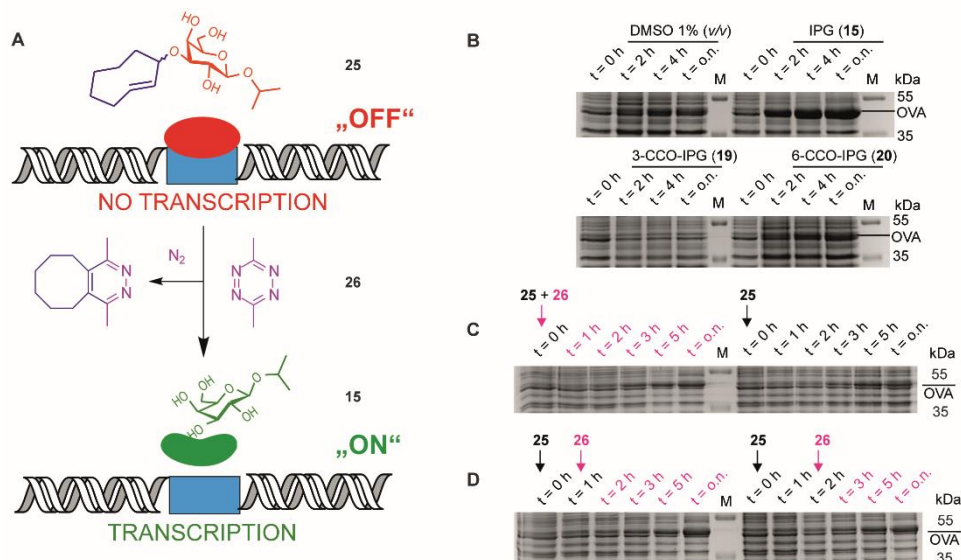
Figure 2 Recombinant expression of proteins with caged IPG variants. A) Schematic representation of the chemical control over *lac* operon activity, mediated by 3-TCO-IPG (**25**), which does not induce expression. IEDDA pyridazine elimination with 3,6-dimethyl-tetrazine (**26**) liberates IPG (**15**), which induces overexpression of the protein of interest. B) Recombinant OVA expression, comparing the effects of DMSO (negative control, 1% *v/v*), IPG (**15**, positive control, 1 mM), 3-CCO-IPG (**19**, 1 mM) and 6-CCO-IPG (**20**, 1 mM). The respective compounds were added at t = 0 h after which protein expression was followed over time. C-D) Temporal control of OVA expression via addition of tetrazine **26** (2.5 mM) in the presence of 3-TCO-IPG (**25**, 1 mM). C) Direct addition of **25** and **26** at t = 0 h (left) or addition of **25** at t = 0 h (right). D) Addition of **26** 1 h (left) or 2 h (right) after adding **25** at t = 0 h.

axial TCO isomer and its purity was optimized by carefully increasing the polarity of the photoisomerization reaction mixture with isopropanol (2 – 5%; Figure S1).

Subsequent experiments were performed to evaluate whether the TCO-modified IPG **25** could be used to control transcription (Figure 2A). For this *E. coli* was transformed to express the model protein ovalbumin (OVA) under control of the *lac* operon. Overnight cultures were inoculated in LB medium supplemented with 1% glucose to inhibit leaky expression. Next, cultures were grown in fresh LB medium (no glucose) before adding (caged) inducers (1 mM) and tetrazine (2.5 mM) in DMSO. It was first tested whether IPG (**15**) could induce expression, which it did in a comparable level to IPTG (**13**; Figure 2B and S2). Furthermore, up to 10% DMSO was tolerated for IPG (**15**) induced OVA expression (Figure S3).
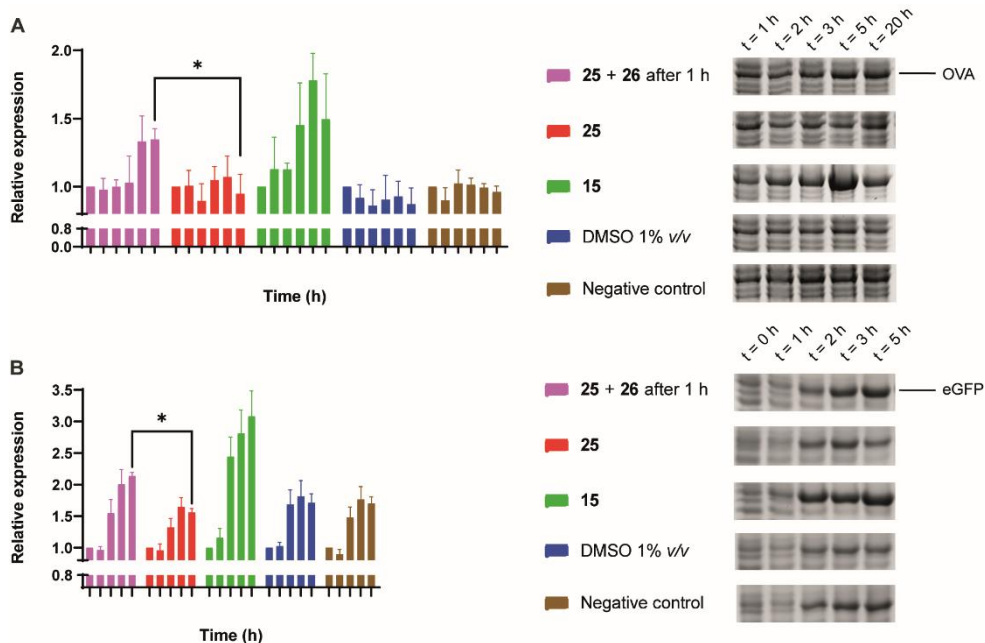
Figure 3 Replicate expression experiments for OVA (3A; N = 3) and eGFP_A206K (3B; N = 4) comparing decaging conditions (1 mM **25** at t = 0 and 2.5 mM **26** at 1 = 1 h) with addition of **25** (1 mM), **15** (1 mM), DMSO (1% *v/v*) and a negative control. Mean quantification values (Coomassie) were plotted with SD as error bars. Representative gel sections are shown to serve as an example. Relative band intensity was measured via densitometry for all experiments. For eGFP (2F), quantification was based on the Coomassie signal of the monomeric protein. *Significant difference based on an unpaired, two-tailed t-test (P < 0.05).

To assess the functionality of the TCO-protecting group, 3-TCO-IPG (**25**) was shown to not affect expression levels in the absence of a deprotection agent (Figure S4). Subsequently, it was analyzed whether deprotection with the prokaryote-compatible 3,6-dimethyl-tetrazine (**26**) could be used to switch on recombinant protein expression.[12,42] The presence of **26** was found to cause a minor delay on IPG (**15**) induced OVA expression without reducing overall expression levels (Figure S5).

Deprotection of 3-TCO-IPG (**25**) with **26** was studied in a time course experiment (Figure 2C-D). Simultaneous addition of both **25** and **26** at the same time did not result in an overexpression. However, a preincubation of 1 or 2 hours with **25** before addition of **26** did result in overexpression of OVA. This was particularly striking at late time points (Figure 2D). Replicate experiments (N = 3) confirmed these findings (Figure 3A). Control compounds 3-CCO-IPG (**19**) and 6-CCO-IPG (**20**) failed to induce overexpression (Figure 2B). A reduction in expression compared to the DMSO background was even observed for **19** (Figure 2B and S4).

The method was next applied to the expression of two other proteins, eGFP (Figure 3B; N = 4) and DsRed2 (Figure S6). Again, overexpression after addition of **26** was observed for both proteins based on Coomassie quantification. For eGFP, a significant overexpression was found after 5 hours (Figure 3B). Taken together, it appears this chemical method can be utilized as a general tool for temporally controlled gene expression in *E.coli*.

6.3 Conclusions

In conclusion, the synthesis of TCO-ethers using two unprecedented reagents (**2-3**) is reported, providing facile access to TCO-protected phenols and aliphatic alcohols, respectively. This methodology enables access to the modification of complex biomolecules as TCO-ethers. A carbohydrate probe, 3-TCO-IPG (**25**), made in this manner was successfully used to chemically modulate *lac* operon activity, thereby providing a first example of control over glycan activity by IEDDA pyridazine elimination. The spatiotemporal control available to this method also bodes well for other applications in which carbohydrate/receptor interactions direct biological processes.

6.4 Supporting figures
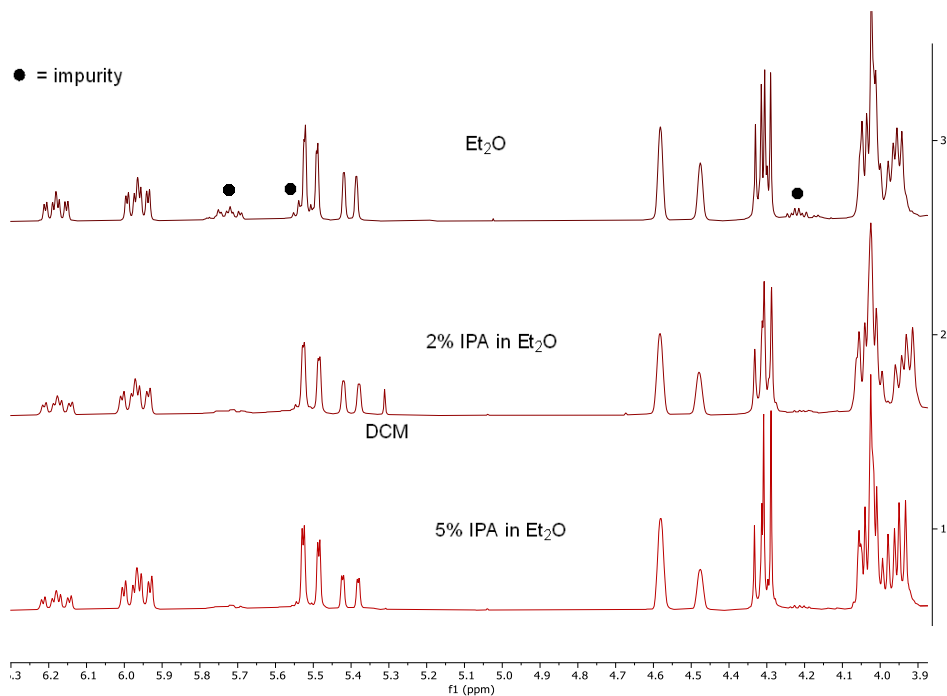
Figure S1 Partial ^{1}H NMR stack (in CDCl$_3$; 6.3 to 3.9 ppm) of 3-TCO-IPG (**25**) which was obtained as the final product after photoisomerization of **23** to **24** in the presence of different reaction solvents (Et$_2$O, 2% IPA in Et$_2$O and 5% IPA in Et$_2$O), followed by deacetylation of **24** to **25** in NaOMe in MeOH (0.5 M) and subsequent extractive workup. An impurity (marked with •) was encountered in **25**, which could be significantly reduced by carefully increasing the polarity of the photoisomerization reaction mixture with IPA.
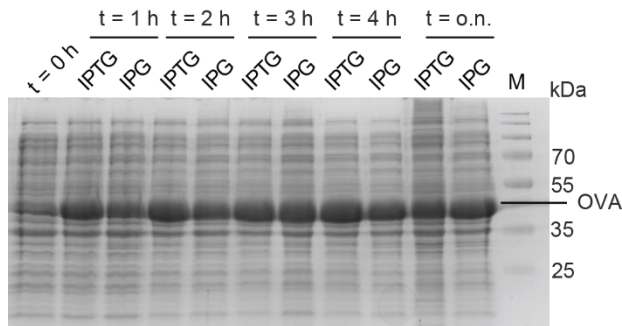
Figure S2 Overexpression of OVA with IPTG (**13**, 1 mM) and IPG (**15**, 1 mM). Samples were collected 1, 2, 3 and 4 h as well as overnight after addition of the inducer.
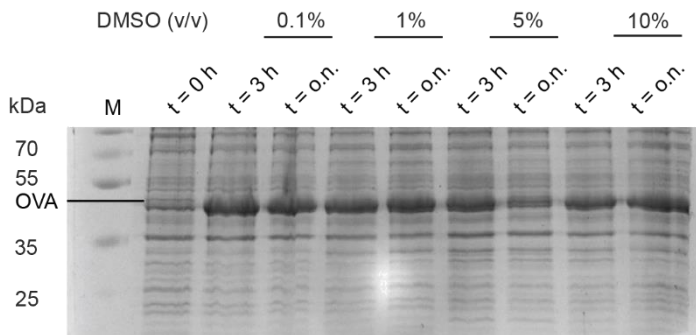
Figure S3 Effect of DMSO on IPG (**15**, 1 mM) induced ovalbumin expression levels. DMSO was used in varying volume percentages (0.1, 1, 5 and 10 % v/v) and samples were taken after 3 h and overnight.
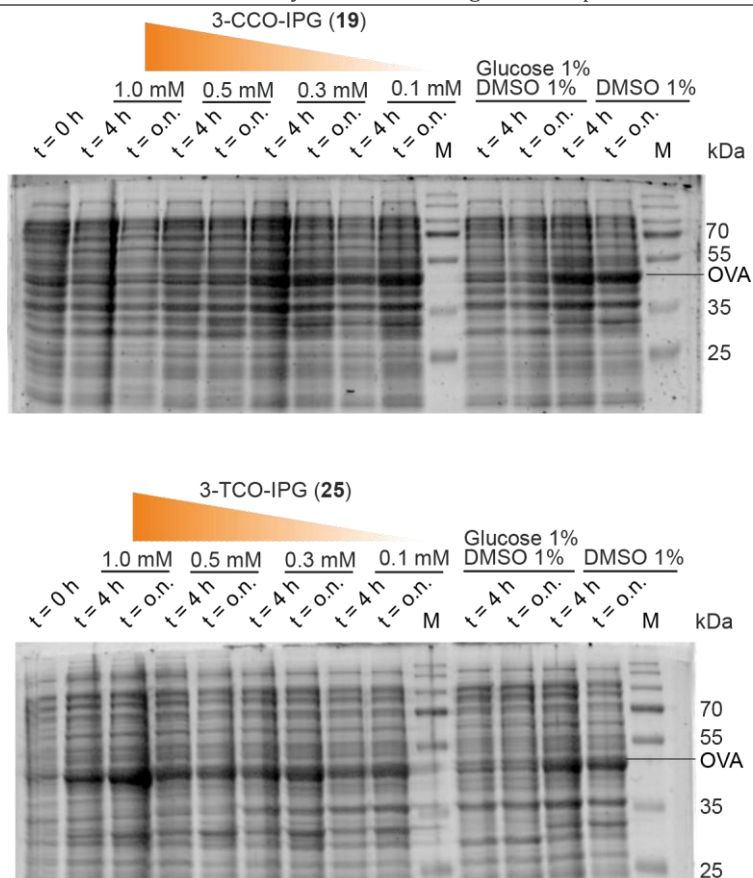
Figure S4 Inhibition of OVA expression with 3-CCO-IPG (**19**, left) at distinct concentrations (1 mM, 0.5 mM, 0.3 mM, 0.1 mM). Right: impact of 3-TCO-IPG (**25**) on OVA expression at different concentrations (1 mM, 0.5 mM, 0.3 mM, 0.1 mM). Positive control: glucose 1% (v/v) + DMSO 1% (v/v), negative control: DMSO 1% (v/v). Orange triangle indicates the decrease in concentration.
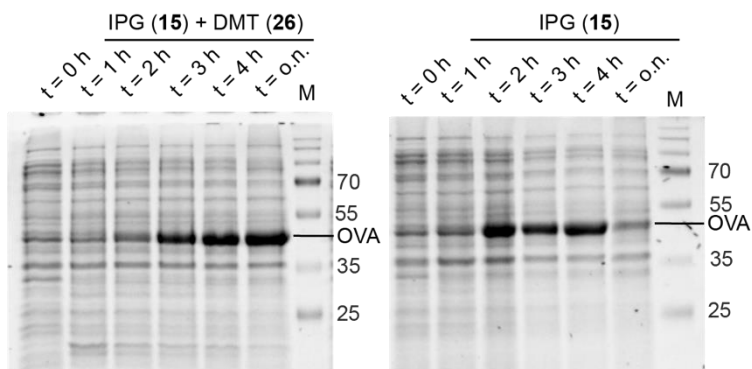
Figure S5 Left: effect of 3,6-dimethyl-tetrazine (**26**, 2.5 mM) on IPG (**15**, 1 mM) induced expression levels. Right: IPG (**15**, 1 mM) induced expression. Samples were taken at 1 - 4 h and overnight.
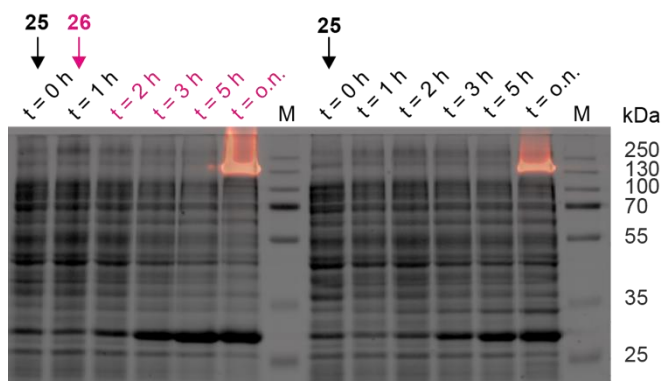
Figure S6 Temporal control of dsRed2_S4T expression via addition of tetrazine **26** (2.5 mM) after 1 h of expression in the presence of 3-TCO-IPG (**25**, 1 mM). Overlayed images of Coomassie staining and in-gel fluorescence of dsRed2 is shown. The right side represent a control (**25**) without the addition of tetrazine **26**.

6.5 Supporting Tables

Table S1 Synthesis of Reagent **3** from cyclooctenol **1.**
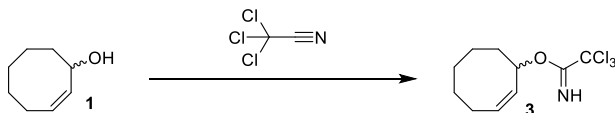
Entry	Scale (mmol)	CCl₃CN (equiv)	Base (equiv)	Solvent (M)	Temperature (°C)	Time (h)	Purification Method[a]	Yield (%)[b]
				Reaction Conditions[a]				
1	5.23	2.5	DBU (2.5)	DCM (0.2)	0	1.5	Celite, Conc., Silica Gel	7
2	5.17	5.0	K₂CO₃ (5)	DCM (0.5)	0 to rt	24	-	-
2 (cont.)	-	-	DBU (0.05)	DCM (0.5)	0	2	Filter, Conc., Neutralized Silica Gel	85
3	10.08	5.0	DBU (0.05)	DCM (0.5)	0	2	Conc., Silica Gel	64
4	8.25	5.0	K₂CO₃ (5) DBU (0.05)	DCM (0.5)	0	3	Filter, Conc., Silica Gel	75
5	100	5.0	K₂CO₃ (5) DBU (0.05)	DCM (0.5)	0	4	Filter, Conc., Silica Gel	81
6	100	5.0	K₂CO₃ (5) DBU (0.05)	DCM (0.5)	0	4.5	Filter, Conc., Silica Gel	86

[a]Purification method, indicating the steps performed with the crude reaction mixture to obtain the purified reagent **3**. [b]Isolated yield. The following abbreviations were used: **Celite**: Celite was added to the reaction mixture; **Filter**: the reaction mixture was filtered (to remove K₂CO₃); **Conc.**: the reaction mixture was concentrated *in vacuo*; **Silica Gel**: the crude product was purified by silica gel chromatography; **Neutralized Silica Gel**: the crude product was purified by silica gel chromatography using neutralized silica gel (described in the experimental section).

Table S2 Synthesis of cyclooctene ethers **7** and **11** using cyclooctene reagent **2** and **3**.
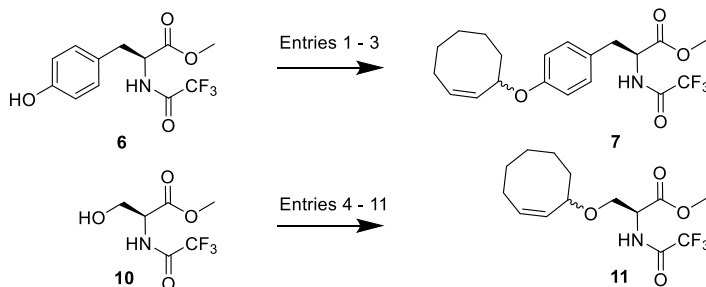
| Reaction Conditions[a]						
Entry	Starting material (mmol)	CCO-reagent (equiv)	Additive (equiv)	Solvent (M)	Temperature (°C)	Time (h)	Product (Yield)[b]
1	**6** (0.1)	**2** (1.2)	Pd(PPh₃)₄ (0.05)	THF (0.1)	50	overnight	-
2	**6** (0.1)	**2** (1.2)	Pd(PPh₃)₄ (0.12)	Dioxane (0.1)	80	20	**7** (81%)
3	**6** (8.47)	**2** (1.2)	Pd(PPh₃)₄ (0.06)	Dioxane (0.1)	80	41	**7** (80%)
4	**10** (0.14)	**2** (1.4)	Pd(PPh₃)₄ (0.14)	Dioxane (0.1)	80	72	-
5	**10** (0.14)	**2** (1.5)	Pd(PPh₃)₄ (0.10)	Toluene (0.1)	105	20	-
5 (cont.)	-	-	-	Dioxane (0.1)	100	120	-
6	**10** (0.27)	**2** (1.4)	TfOH (0.1)[c] MS (4 Å)	DCM (0.1)	0	2	**11** (15%)
7	**10** (0.37)	**2** (2.0)	TfOH (0.1)[c]	DCM (0.1)	0 to rt	63	**11** (24%)
8	**10** (0.31)	**2** (2.1)	TfOH (0.1)[c]	DCM (0.1)	-50 to -30	2	**11** (45%)
9	**10** (0.34)	**2** (2.1)	TfOH (0.1)[d] MS (4Å)	DCM (0.1)	-60 to -30	overnight	**11** (26%)
10	**10** (0.31)	**2** (1.9)	TMS-OTf (0.1)[e]	DCM (0.1)	-35 to 0	4	**11** (38%)
11	**10** (0.32)	**2** (2.1)	TfOH (0.1)[e]	DCM (0.1)	-35 to 0	4	**11** (46%)

[a]**Entry 1:** Reactants (**6** + **2**) were combined in a 10 mL round-bottom flask, dissolved in THF under N₂ and degassed for 10 min by sonication. Pd(PPh₃)₄ was added, the container was purged with N₂ before sealing the flask and starting the reaction. **Entries 2 – 4:** Reactants (**6** or **10** + **2** + Pd(PPh₃)₄) were co-evaporated with anhydrous dioxane in a round-bottom flask, placed under N₂ and dissolved in anhydrous solvent. The reaction mixture was frozen at -78°C (ethanol bath) and subsequently purged with N₂ for 45 min to achieve degassing. Afterwards, the flask was sealed and the reaction was launched. **Entries 5 – 10:** Reactants (**10** + **3**) were co-evaporated with anhydrous toluene (3 x 2 mL) in a 25 mL round-bottom flask, placed under N₂ (balloon) and dissolved in anhydrous solvent. Lewis acid was added after cooling the reaction mixture in an ethanol bath. Reactions were quenched with Et₃N (2 equivalents compared to Lewis acid), impregnated with Celite Hyflo Supercel (Merck), concentrated *in vacuo* and purified by silica gel chromatography. [b]Yields denote isolated yields (%) after column chromatography. When no yield was reported (-; entries 1,4 and 5), no detectable degree of reaction took take place and the starting material (**6** or **10**) could be recovered. [c]Direct addition. [d]Addition from a freshly prepared stock solution (0.1 M in DCM) on activated molecular sieves (4Å). [e]Addition from a freshly prepared stock solution (0.1 M in DCM).

Table S3 Investigation of stannylene acetal mediated alkylation of **15** with **18**.
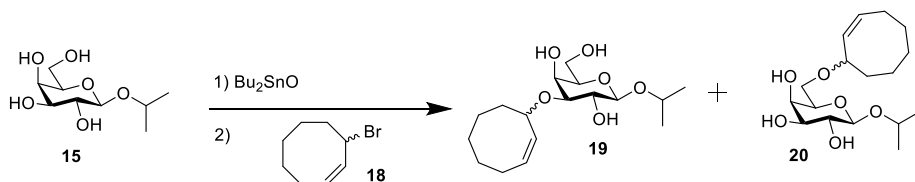
| Entry	Stage 1: Acetal formation[a]					Stage 2: Alkylation[b]					Yield[c]	
	Scale (mmol)	Bu2SnO (equiv)	Solvent (M)	Temp (°C)[d]	Time	**18** (equiv)	Additive (equiv)	Solvent (M)	Temp (°C)[d]	Time	**19** (%)	**20** (%)
1	0.5	1.15 eq	Toluene (0.1)	105	o.n.	1.05	-	Toluene (0.1)	105/90	o.n.	-	-
1 cont.	-	-	-	-	-	-	TBABr (1.05)	Toluene (0.1)	90	48 h	-	-
2	1.5	1.05 eq	Toluene (0.1)	Reflux	o.n.	2.0	CsF (2.5)	DMF (0.13)	65	48 h	-	-
3	1.0	1.2 eq	Toluene (0.1)	Reflux	o.n.	3 x 1.2	CsF (1.2)	Toluene (0.1)	reflux	48 h	23	21
4	1.15	1.2	Toluene (0.1)	105	o.n.	1.2	CsF (1.2)	Toluene (1.0)	105	o.n.	17	13
5	1.12	1.2	Toluene (0.1)	105	o.n.	2.5	CsF (2.5)	Toluene (1.0)	105	o.n.	22	18
6	1.0	1.2	Toluene (0.1)	105	o.n.	1.2	CsF (1.2) TBAI (1.2)	Toluene (1.0)	105	o.n.	16	7
7	1.0	1.2	Toluene (0.1)	105	o.n.	1.2	TBAI (1.2)	Toluene (1.0)	105	o.n.	15	7
8	1.09	1.2	Toluene (0.1)	105	o.n.	Excess	CsF (1.2)	CCO-Br (1.0)	105	o.n.	-	-
9	0.48	1.2	Toluene (0.1)	105	o.n.	Excess	CsF (1.2)	Toluene /CCO-Br, 1:1 (1.0)	105	o.n.	-	-
10	4.77	1.2	Toluene (0.1)	105	o.n.	3	CsF (1.2) DIPEA (3)	Toluene (1.0)	105	o.n.	~20	~20
11	13.53	1.2	Toluene (0.4)	105	o.n.	3	CsF(1.2) MS (3Å)	Toluene (1.0)	105	o.n.	~22	~19

[a]After dialkylstannylene acetal formation, the reaction mixture was concentrated *in vacuo* and co-evaporated 3x with anhydrous toluene. [a,b] Reactions were typically carried out in a sealed round-bottom flask (10, 25 or 50-mL) under N_2 (balloon). [c]Yields denote isolated yields after column chromatography. [d]Oil bath. **Notes for specific entries: entries 8 – 9:** Complete pyrolysis of the reaction mixture was observed; **entries 10 – 11**: Extra byproducts encountered (presumably 2-CCO-IPG), which made purification of **19** and **20** significantly more laborious compared to previous entries.

Table S4 Investigation of stannylene acetal mediated alkylation of **27** and **28** with **18**.
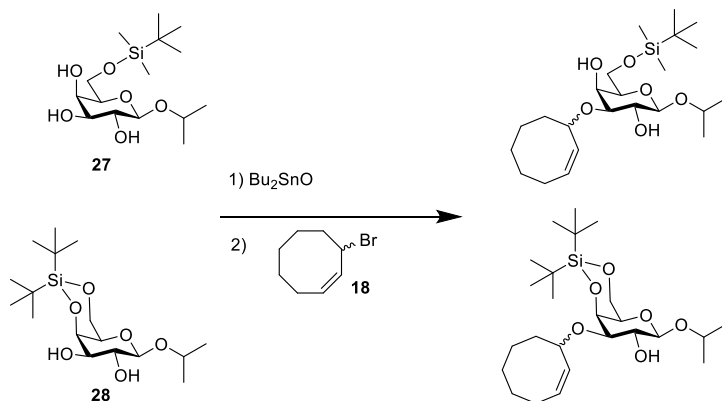
Entry	Stage 1: Acetal formation[a]					Stage 2: Alkylation[b]					Yield[c]
	6-TBS/ 4,6-DTBS (mmol)	Bu$_2$SnO (equiv)	Solvent (M)	Temp (°C)[d]	Time	**18** (equiv)	Additive (equiv)	Solvent (M)	Temp (°C)[d]	Time	3-alkyl (%)
1	**27** (0.5)	1.15 eq	Toluene (0.1)	105	o.n.	1.05	-	Toluene (0.1)	105/ 90	o.n.	-
1 cont.	-	-	-	-	-	-	TBABr (1.05)	Toluene (0.1)	90	48 h	-
2	**28** (0.5)	1.15 eq	Toluene (0.1)	105	o.n.	1.05	-	Toluene (0.1)	105/ 90	o.n.	-
2 cont	-	-	-	-	-	-	TBABr (1.05)	Toluene (0.1)	90	48 h	-
3	**27** (1.0)	1.2	Toluene (0.1)	105	o.n.	1.2	TBAI (1.2)	Toluene (1.0)	105	o.n.	-
4	**28** (1.0)	1.2	Toluene (0.1)	105	o.n.	1.2	TBAI (1.2)	Toluene (1.0)	105	o.n.	-

[a]After dialkylstannylene acetal formation, the reaction mixture was concentrated *in vacuo* and co-evaporated 3x with anhydrous toluene. [a,b] Reactions were typically carried out in a sealed round-bottom flask (10, 25 or 50-mL) under N$_2$ (balloon). [c]Yields denote isolated yields after column chromatography. [d]Oil bath.

Table S5 Investigation of Lewis acid catalyzed alkylation of **22** with reagent **3**.
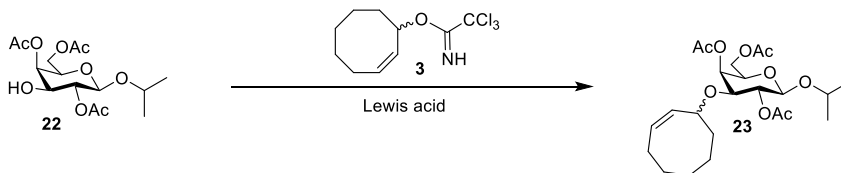
Reaction conditions[a]							
Entry	Scale (mmol)	reagent **2** (equiv)	Activator[b] (equiv)	Solvent (M)	Temperature (°C)	Time (h)	Yield[c] (%)
1	0.1	2.0	TfOH (0.1)	DCM (0.1)	-50 to -30	4	27
2	0.1	4.5	TfOH (0.1)	DCM (0.1)	-40 to -5	4	45
3	0.1	9.4	TfOH (0.1)	DCM (0.05)	-45 to 0	5	47
4	0.1	4.4	BF$_3$ · OEt$_2$ (0.5)	DCM (0.1)	-30 to 0	4	42
5	1.0	4.0	TfOH (0.1)	DCM (0.1)	-50 to -5	4	40
6	1.0	4.0	TfOH (0.05)	DCM (0.05)	-30	6	20
7	1.0	4.0	TfOH (0.01)	DCM (0.1)	-40 to 0	5.5	-
Cont.	-	-	TfOH (0.02)	DCM (0.1)	0	1.5	24
8	1.0	0 -> 4.1	TfOH (0.1)	DCM (1.0 -> 0.1)	-45 to -30	22	47
9	10.1	4.0	TfOH (0.1)	DCM (0.1)	-40 to 0	6.5	29
10	21.8	3.95	TfOH (0.1)	DCM (0.1)	-30	4	34

[a]Reactants (**22** + **3**) were co-evaporated with anhydrous toluene (3x) in a round-bottom flask, placed under N$_2$ (balloon) and dissolved in anhydrous solvent. Lewis acid activator was added after cooling the reaction mixture in an ethanol bath. Reactions were quenched with Et$_3$N (2 equivalents compared to Lewis acid), diluted with Et$_2$O, washed with NaOH (1 M, 3x) and brine. The organic layer was dried over MgSO$_4$, filtered and concentrated *in vacuo*. Crude products were purified by silica gel chromatography. **Notes for specific entries: entry 3**: precipitation of reactants was observed, which resolved back into a clear solution after warming to -10°C; **entry 8**: slow addition over 3 h of **3** in 9 mL of DCM to the reaction mixture containing **22** in 1 mL DCM and TfOH. [b]Triflic acid was added from a freshly prepared stock solution (0.1 M in DCM, entries 1-3, 5-8). At large scale, triflic acid was added directly (entries 9-10). BF$_3$ · OEt$_2$ was added as a 0.1 M solution (commercially available, entry 4). [c]Yields denote isolated yields after column chromatography.

Table S6 Photoisomerization of **23** to **24** and subsequent deacetylation to afford **25**.
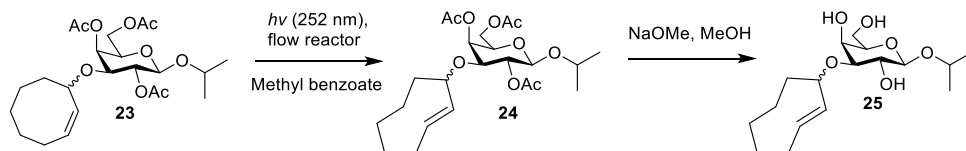
Entry	Scale (mmol)	Methyl benzoate (equiv)	Stationary phase (equiv)	Column fill material[b]	Solvent (M)	Flow (mL/min)	Time (h)	Yield **24**	Yield **25**
			Reaction Conditions[a]						
1	0.44	3	AgNO$_3$ · SiO$_2$ (3.4)	SiO$_2$	50% EtOAc in heptane (4 mM)	25	47	-	-
1 cont.	0.44	3	AgNO$_3$ · SiO$_2$ (1.3)	SiO$_2$	25% EtOAc in heptane (4 mM)	25	43	-	-
2	0.66	3	TAg (1.5)	Cotton	50% EtOAc in heptane (5 mM)	12.5	48	-	-
3	1.58	3 + 9	TAg (1.8)	-	25% EtOAc in heptane (13 mM)	10	48	21%	N.D.
4	0.52	3	TAg (3.0)	Cotton	Et$_2$O (3 mM)	10	17	30%	67%
5	2.90	3	TAg (3.0)	Cotton	Et$_2$O (5 mM)	30	20	Crude	40% over 2 steps
6	0.50	3	TAg (3.0)	Cotton	2% IPA in Et$_2$O (3 mM)	15	24	Crude	47% over 2 steps
7	0.50	10	TAg (3.0)	Cotton	10% IPA in Et$_2$O (3 mM)	15	90	Crude	7% over 2 steps
8	0.50	5.7	TAg (3.0)	Cotton	5% IPA in Et$_2$O (3 mM)	20	24	Crude	35% over 2 steps
9	0.51	10	TAg (3.0)	Cotton	5% IPA in Et$_2$O (3 mM)	20	48	Crude	27% over 2 steps

[a]AgNO$_3$ · SiO$_2$ (10% wt) was prepared according to the procedure by Royzen *et al*.[25] Tosic Acid Silica (ion exchange capacity 0.60 meg/g) was subjected to ion exchange with AgNO$_3$ according to the procedure by Darko *et al*.[41] Other general considerations about the photoisomerization method can be found in the Experimental Section. When deemed necessary, a sample (~ 30 mL) of the reaction mixture was concentrated *in vacuo* and measured with ^{1}H NMR to evaluate the progress of the photoisomerization reaction. Afterwards, the column containing the trapped product (**24**) was washed with additional solvent (2 x reaction volume), dried over N$_2$ and fractionally eluted with NH$_3$ in MeOH (7 M). Fractions containing the partially deacetylated product (**24**) were combined and concentrated *in vacuo*. This crude product (**24**) was treated with NaOMe in MeOH (0.5 M) overnight, concentrated *in vacuo* and extractively purified to obtain **25**. [b]Material used to completely pack the column after loading of the stationary phase was complete. **Notes for specific entries:** **entry 1**: Leaching of Ag was observed (50% EtOAc in pentane). The crude, unreacted reaction mixture was re-used for the second part of the experiment (25% EtOAc in pentane); **entry 3**: additional methyl benzoate (9 equiv) was added after 26 h, **24** was purified with silica gel chromatography and was not reacted further**; entry 4**: **24** was purified by silica gel chromatography, **25** was purified by silica gel chromatography. Reduced yield for **entries 3 and 4** may partially be explained by loss of partially deacylated product during silica gel chromatography.

6.6 Experimental procedures - chemistry

General methods: Commercially available reagents and solvents were used as received. Moisture and oxygen sensitive reactions were performed under N_2 atmosphere (balloon). DCM, toluene, THF, dioxane and Et_2O were stored over (flame-dried) 4 Å molecular sieves (8-12 mesh). Methanol and isopropanol were stored over (flame-dried) 3 Å molecular sieves. Pyridine, DIPEA and Et_3N were stored over KOH pellets. TLC analysis was performed using aluminum sheets, pre-coated with silica gel (Merck, TLC Silica gel 60 F_{254}). Compounds were visualized by UV absorption (λ = 254 nm), by spraying with either a solution of $KMnO_4$ (20 g/L) and K_2CO_3 (10 g/L) in H_2O, a solution of $(NH_4)_6Mo_7O_{24} \cdot 4H_2O$ (25 g/L) and $(NH_4)_4Ce(SO_4)_4 \cdot 2H_2O$ (10 g/L) in 10% H_2SO_4, 20% H_2SO_4 in EtOH, or phosphomolybdic acid in EtOH (150 g/L), where appropriate, followed by charring at ca. 150°C. Column chromatography was performed on Screening Devices b.v. Silica Gel (particle size 40-63 μm, pore diameter 60 Å). Celite Hyflo Supercel (Merck) was used to impregnate the reaction mixture prior to silica gel chromatography when indicated. ^{1}H, ^{13}C APT, ^{19}F, ^{1}H COSY, HSQC and HMBC spectra were recorded with a Bruker AV-400 (400/100 MHz) or AV-500 (500/125 MHz) spectrometer. Chemical shifts are reported as δ values (ppm) and were referenced to tetramethylsilane (δ = 0.00 ppm) or the residual solvent peak as internal standard. *J* couplings are reported in Hz. High resolution mass spectra were recorded by direct injection (2 μL of a 1 μM solution in H_2O/MeCN 1:1 and 0.1% formic acid) on a mass spectrometer (Q Exactive HF Hybrid Quadrupole-Orbitrap) equipped with an electrospray ion source in positive mode (source voltage 3.5 kV, sheath gas flow 10, capillary temperature 275°C) with resolution R = 240,000 at m/z 400 (mass range m/z = 160-2,000) and an external lock mass. The high resolution mass spectrometer was calibrated prior to measurements with a calibration mixture (Thermo Finnigan). The synthesis of tetrazine **26** is described in Chapter 4 and a recent publication.[43]

Preparation of neutralized silica gel: Unmodified silica gel (500 gram) was slowly dispersed into a 3 L round-bottom flask containing a stirring volume of H_2O (1.7 L). NH_4OH (28% w/w, 100 mL) was added and the alkaline suspension was stirred for 30 min. The suspension was filtered, washed with H_2O and the silica gel was dried on aluminium foil overnight at rt. The silica was transferred into a glass container and remaining traces of H_2O were removed by drying in an oven at 150°C overnight.

Photoisomerization methods: General guidelines were followed as described by Royzen *et al.*[25] Photochemical isomerization was performed using a Southern New England Ultraviolet Company Rayonet reactor (model RPR-100) equipped with 16 bulbs (part number RPR-2537A, λ = 254 nm). Photolysis was performed in a 187 mL or 1500 mL quartz flask (Southern New England Ultraviolet Company; part number RQV-118 or RQV-323, respectively). A HPLC pump (Jasco; model PU-2088 Plus) was used to circulate solvent through the photolysis apparatus at the indicated flow rate. An empty solid load cartridge with screw cap, frits, O-ring and end tips (4 g / 40 g; SD.0000.004 / SD.0000.040; iLOK™, Screening Devices b.v.) was manually loaded with the specified silica gel to function as the stationary phase.

Preparation of TAg silica gel: Preparation was based on the procedure described by Darko *et al.*[41] Siliabond Tosic Acid Functionalized Silica (Silicycle, product number R60530B, lot number

156773, particle size 40-63 μm, pore diameter 60 Å, endcapped, functional loading 0.6 mmol/g, 100 gram) was transferred to a glass silica column wrapped in aluminium foil. A solution of AgNO₃ (0.5 M in MeCN/H₂O, 9:1, 1 L) was passed over the column whilst monitoring the pH shift from acidic to neutral. The column was washed with MeOH (2 x 400 mL), acetone (2 x 400 mL) and pentane (2 x 400 mL). The TAg silica gel was dried over a dream of air and transferred to a bottle wrapped in aluminium foil for storage.
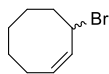
(Z)-3-bromocyclooct-1-ene (18): Synthesis was performed according to a modified procedure.[44] N-bromosuccinimide (100 g, 562 mmol, 1.0 equiv) was placed under N₂ in a 1 L round-bottom flask. Cyclohexane (400 mL), (Z)-cyclooctene (**12**, 100 mL, 770 mmol, 1.37 equiv) and AIBN (0.2 M in toluene, 2.0 mL, 0.4 mmol, 0.07 mol%) were added before connecting the flask to a reflux condenser which was subsequently purged with N₂. The mixture was refluxed (oil bath at 100°C) under N₂ for 4 h, after which the reaction mixture was allowed to cool to room temperature. The white precipitates were removed by filtration after cooling the mixture to 0°C (ice bath). The crude reaction mixture was concentrated *in vacuo* (60°C, ≤ 20 mbar) before purifying the crude product by fractional vacuum distillation to obtain **18** (75.2 g, 398 mmol, 71%, bp = 85°C at 1.3 mbar) as a colorless liquid: R_f = 0.8 (pentane); ¹H NMR (400 MHz, CDCl₃) δ 5.82 – 5.73 (m, 1H), 5.65 – 5.54 (m, 1H), 5.00 – 4.89 (m, 1H), 2.30 – 2.05 (m, 3H), 2.05 – 1.92 (m, 1H), 1.76 – 1.63 (m, 2H), 1.63 – 1.47 (m, 2H), 1.45 – 1.24 (m, 2H); ¹³C NMR (101 MHz, CDCl₃) δ 133.3, 129.9, 49.0, 40.9, 29.1, 26.6, 26.2, 25.7. Spectroscopic data was in agreement with literature.[44]
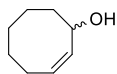
(Z)-cyclooct-2-en-1-ol (1): Synthesis was performed according to a modified procedure.[10] Cyclooctene bromide **18** (75.1 g, 397 mmol, 1.0 equiv) was dissolved in a mixture of acetone (600 mL) and H₂O (300 mL) in a 3 L round-bottom flask. NaHCO₃ (66.7 g, 795 mmol, 2.0 equiv) was added and the reaction mixture was stirred under reflux (oil bath at 75°C) for 4.5 h. The reaction mixture was allowed to cool to room temperature and filtered to remove excess NaHCO₃. The filtrate was extracted with Et₂O (3 x 500 mL). The combined organic layers were dried over MgSO₄, filtered and concentrated *in vacuo* to obtain **1** (41.4 g, 328 mmol, 83%) as an oil which was used in subsequent reactions without further purification: R_f = 0.3 (20% Et₂O in pentane); ¹H NMR (400 MHz, CDCl₃) δ 5.61 (dddd, *J* = 10.3, 8.5, 7.0, 1.4 Hz, 1H), 5.52 (ddd, *J* = 10.8, 6.5, 0.8 Hz, 1H), 4.73 – 4.56 (m, 1H), 2.24 – 2.01 (m, 2H), 1.96 – 1.85 (m, 1H), 1.73 (s, 1OH), 1.69 – 1.32 (m, 7H); ¹³C NMR (101 MHz, CDCl₃) δ 135.1, 128.6, 69.4, 38.7, 29.2, 26.4, 26.0, 23.8. Spectroscopic data was in agreement with literature.[10,43,45]
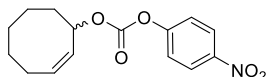
Cyclooctene carbonate 4: Cyclooctenol **1** (1.19 g, 9.45 mmol, 1.0 equiv) was dissolved in anhydrous DCM (30 mL) in a 100 mL round-bottom flask under N₂. Anhydrous pyridine (1.15 mL, 14.2 mmol, 1.5 equiv) was added and the reaction mixture was cooled to 0°C (ice bath) before adding 4-nitrophenyl chloroformate (2.29 g, 11.3 mmol, 1.2 equiv). The reaction was stirred for 48 h and allowed to warm to room temperature. The reaction mixture was diluted with H₂O (30 mL) and the aqueous layer was extracted with Et₂O (3 x 75 mL). The combined organic layers were washed with HCl (0.5 M, 2 x 100 mL), NaHCO₃ (satd., 2 x 100 mL) and brine (200 mL), dried over MgSO₄, filtered, impregnated with Celite and concentrated *in vacuo*. The impregnated crude

product was purified by silica gel chromatography (pentane → 3% Et$_2$O in pentane) to obtain **4** (2.29 g, 7.86 mmol, 83%) as a pale yellow oil: R$_f$ = 0.6 (5% Et$_2$O in pentane); ^{1}H NMR (400 MHz, CDCl$_3$) δ 8.33 – 8.22 (m, 2H), 7.44 – 7.34 (m, 2H), 5.78 (td, J = 9.3, 7.5 Hz, 1H), 5.70 – 5.53 (m, 2H), 2.31 – 2.03 (m, 3H), 1.78 – 1.47 (m, 6H), 1.47 – 1.36 (m, 1H); ^{13}C NMR (101 MHz, CDCl$_3$) δ 155.7, 152.0, 145.4, 131.1, 129.2, 125.3 (x2), 121.9 (x2), 78.4, 34.9, 28.8, 26.5, 25.8, 23.3.
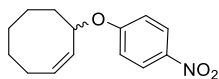
Cyclooctene ether 5: The experiment was based on a procedure for the synthesis of 1-(allyloxy)-4-nitrobenzene with palladium catalysis.[46] Cyclooctene carbonate **4** (171 mg, 0.59 mmol, 1.0 equiv) was dissolved in anhydrous toluene (2.5 mL) under N$_2$ in a 10 mL round-bottom flask. The reaction mixture was degassed under sonication for 10 min before adding Pd(PPh$_3$)$_4$ (16 mg, 14 μmol, 2.4 mol%). The reaction mixture was stirred for 90 min at 50°C (oil bath) under N$_2$. The reaction mixture was directly applied on a silica gel column and purified (pentane → 2% Et$_2$O in pentane) to obtain **5** (133 mg, 0.54 mmol, 92%) as a pale yellow oil: R$_f$ = 0.9 (5% Et$_2$O in pentane); ^{1}H NMR (400 MHz, CDCl$_3$) δ 8.23 – 8.03 (m, 2H), 6.98 – 6.80 (m, 2H), 5.91 – 5.72 (m, 1H), 5.45 (dd, J = 10.8, 7.2 Hz, 1H), 5.24 – 5.06 (m, 1H), 2.37 – 2.18 (m, 2H), 2.10 (ddt, J = 12.8, 8.6, 4.5 Hz, 1H), 1.85 – 1.36 (m, 8H);^{13}C NMR (101 MHz, CDCl$_3$) δ 163.5, 141.2, 131.6, 131.3, 125.8 (x2), 115.4 (x2), 76.4, 35.7, 29.0, 26.8, 26.1, 23.3.
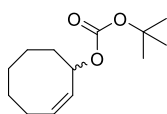
Cyclooctene reagent 2: Cyclooctenol **1** (2.28 g, 18.1 mmol, 1.0 equiv) was dissolved in anhydrous THF (40 mL) in a 250 mL round-bottom flask under N$_2$. The reaction mixture was cooled to 0°C (ice bath) before adding NaHMDS (40% w/w in THF, 26.9 mL, 52.4 mmol, 2.9 equiv) dropwise. The reaction mixture was stirred for 30 min at 0°C. 2-(*tert*-Butoxycarbonyloxyimino)-2-phenylacetonitrile (Boc-ON; 12.9 g, 52.2 mmol, 2.9 equiv) was dissolved in anhydrous THF (40 mL) in a 100 mL pear-shaped flask under N$_2$ and added to the reaction mixture dropwise using a double tipped needle under positive N$_2$ pressure. The reaction mixture was stirred overnight and allowed to warm to room temperature. The reaction was quenched by adding NH$_4$Cl (satd., 300 mL) and subsequently diluted with Et$_2$O (300 mL). The aqueous layer was extracted with Et$_2$O (300 mL). The combined organic layers were washed with HCl (1 M, 250 mL), NaHCO$_3$ (satd., 250 mL) and brine (250 mL), dried over MgSO$_4$, filtered, impregnated with Celite and concentrated *in vacuo*. The impregnated crude product was purified by silica gel chromatography (pentane → 0.5% Et$_2$O in pentane) to obtain **2** (3.30 g, 14.6 mmol, 81%) as a pale yellow oil: R$_f$ = 0.5 (2% Et$_2$O in pentane); ^{1}H NMR (400 MHz, CDCl$_3$) δ 5.74 – 5.62 (m, 1H), 5.53 (ddd, J = 10.6, 7.0, 1.2 Hz, 1H), 5.49 – 5.40 (m, 1H), 2.33 – 2.19 (m, 1H), 2.18 – 2.06 (m, 1H), 2.03 – 1.90 (m, 1H), 1.74 – 1.51 (m, 6H), 1.49 (s, 9H), 1.44 – 1.32 (m, 1H) ; ^{13}C NMR (101 MHz, CDCl$_3$) δ 153.2, 130.7, 129.9, 82.0, 75.3, 35.1, 28.9, 27.9 (x3), 26.5, 25.9, 23.4.
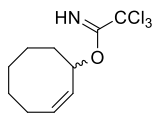
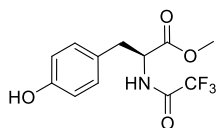**Cyclooctene reagent 3:** Cyclooctenol **1** (12.64 g, 100 mmol, 1.0 equiv) was dissolved in anhydrous DCM (200 mL) in a 500 mL round-bottom flask under N$_2$. The reaction mixture was cooled to 0°C (ice bath) before adding K$_2$CO$_3$ (69.2 g, 501 mmol, 5.0 equiv), trichloroacetonitrile (50.2 mL, 501 mmol, 5.0 equiv) and DBU (0.755 mL, 5.01 mmol, 5.0 mol%). The suspension was stirred on ice for 4 h, filtered and concentrated *in vacuo*. The brown crude product was suspended in a small volume of toluene and

purified by silica gel chromatography (pentane → 1% Et₂O in pentane → 2% Et₂O in pentane) to obtain cyclooctene imidate **3** (21.88 g, 81 mmol, 81%) as an oil: R_f = 0.4 (2% Et₂O in pentane); ¹H NMR (400 MHz, CDCl₃) δ 8.26 (s, 1NH), 5.82 – 5.66 (m, 2H), 5.66 – 5.52 (m, 1H), 2.36 – 2.22 (m, 1H), 2.21 – 2.04 (m, 2H), 1.77 – 1.50 (m, 7H), 1.50 – 1.37 (m, 1H); ¹³C NMR (101 MHz, CDCl₃) δ 162.2, 130.5, 130.2, 92.0, 77.6, 34.5, 28.8, 26.5, 25.9, 23.3. Reagent **3** was stored at -30°C under N₂ as a solid.

*Note: Full conditions investigated for the synthesis of **3** are reported in Table S1.*
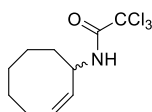
Cyclooctene amide 8: This compound was often encountered as a crude byproduct during column chromatography purifications of compounds **11** and **23**, resulting from the various reactive intermediates formed upon activation of reagent **3** with a potent Lewis acid (TfOH): ¹H NMR (400 MHz, CDCl₃) δ 5.83 – 5.73 (m, 2H), 5.62 – 5.53 (m, 1H), 2.33 – 2.12 (m, 2H), 2.12 – 1.98 (m, 1H), 1.77 – 1.29 (m, 7H); ¹³C NMR (101 MHz, CDCl₃) δ 161.4, 131.4, 128.6, 90.3, 78.4, 34.5, 28.7, 26.5, 25.8, 23.2.
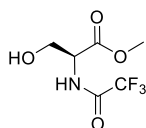
N-trifluoroacetyl-protected L-tyrosine methyl ester 6: L-tyrosine methyl ester hydrochloride (10.05 g, 43,4 mmol, 1.0 equiv) was dissolved in anhydrous DCM (80 mL) in a 250 mL round-bottom flask under N₂. The reaction mixture was cooled to 0°C (ice bath) before adding anhydrous Et₃N (6.05 mL, 43.4 mmol, 1.0 equiv). The reaction mixture was stirred for 30 min at 0°C. Subsequently, trifluoroacetic anhydride (7.35 mL, 52.1 mmol, 1.2 equiv) was added slowly to the neutralized, milky reaction mixture over 10 min. The reaction mixture was stirred and allowed to warm to room temperature. After 2 h, additional Et₃N (6.05 mL, 43.4 mmol, 1.0 equiv) was added. After 24 h reaction time, the reaction mixture was pouring in ice-cooled H₂O (100 mL). HCl (1 M, 100 mL) was added and the aqueous layer was extracted with DCM (100 mL). The combined organic layers were washed with brine (150 mL), dried over MgSO₄, filtered and partially concentrated *in vacuo*. The crude product was purified by crystallization in DCM to obtain **6** (5.44 g, 18.7 mmol, 43%) as white crystals: R_f = 0.3 (20% EtOAc in pentane); ¹H NMR (500 MHz, MeOD) δ 7.07 – 6.96 (m, 2H), 6.77 – 6.63 (m, 2H), 4.65 (dd, *J* = 9.9, 5.3 Hz, 1H), 3.72 (s, 3H), 3.17 (dd, *J* = 14.0, 5.3 Hz, 1H), 2.91 (dd, *J* = 14.0, 9.9 Hz, 1H); ¹³C NMR (126 MHz, MeOD) δ 172.2, 158.7 (q, *J* = 37.7 Hz), 157.5, 131.2 (x2), 128.4, 117.3 (q, *J* = 286.7 Hz), 116.3 (x2), 55.8, 53.0, 36.9; ¹⁹F NMR (471 MHz, MeOD) δ -76.8; HRMS: calculated for C₁₂H₁₃F₃NO₄ 292.07912 [M+H]⁺; found 292.07899. Spectroscopic data was in agreement with literature.[8]
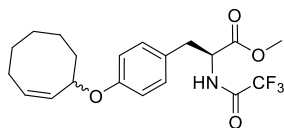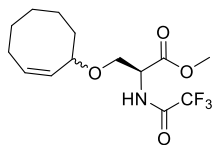
Cyclooctene ether 7: L-tyrosine methyl ester **6** (2.466 g, 8.47 mmol, 1.0 equiv) and cyclooctene *tert*-butyl carbonate reagent **2** (2.30 g, 10.2 mmol, 1.2 equiv) were combined in a 250 mL round-bottom flask, co-evaporated using anhydrous dioxane, placed under N₂ and dissolved in anhydrous dioxane (85 mL). Pd(PPh₃)₄ (567 mg, 0.49 mmol, 5.8 mol%) was added before freezing the reaction mixture at -78°C (ethanol bath) and subsequently purging N₂ over the frozen reaction mixture for 45 min to achieve degassing. The flask was sealed with parafilm before stirring the reaction mixture at 80°C (oil bath) for 41 h. The reaction mixture was allowed to cool to room temperature, impregnated by adding Celite and concentrated *in vacuo*. The impregnated crude product was purified by silica gel chromatography (1% EtOAc in pentane

→ 5% EtOAc in pentane) to obtain the diastereomeric mixture of cyclooctene ethers **7** (**7$_A$** : **7$_B$**, ~ **1 : 1**, 2.69 g, 6.73 mmol, 80%) as a thick oil: R_f = 0.15 (5% EtOAc in pentane); ^{1}H NMR (400 MHz, CDCl$_3$) δ 6.99 – 6.88 (m, 2H), 6.83 – 6.70 (m, 2H + 1NH), 5.82 – 5.65 (m, 1H), 5.55 – 5.42 (m, 1H), 5.11 – 4.96 (m, 1H), 4.90 – 4.74 (m, 1H), 3.78 (s, 3H), 3.20 – 3.03 (m, 2H), 2.37 – 2.15 (m, 2H), 2.07 (ddt, J = 12.9, 8.9, 4.7 Hz, 1H), 1.79 – 1.38 (m, 7H); ^{13}C NMR (101 MHz, CDCl$_3$) δ 170.6, 170.6, 157.9 (x2), 156.6 (q, J = 36.2 Hz), 156.6 (q, J = 36.2 Hz), 133.0 (x2), 130.2 (x6), 126.1 (x2), 115.9 (x4), 115.7 (q, J = 287.8 Hz, x2), 75.3 (x2), 53.7, 53.7, 53.0, 52.9, 36.5 (x2), 35.9, 35.9, 29.2 (x2), 26.9 (x2), 26.3 (x2), 23.5 (x2); HRMS: calculated for C$_{20}$H$_{24}$F$_3$NO$_4$Na 422.15496 [M+Na]$^+$; found 422.15463. Spectroscopic data was in agreement with literature.[8]

*Note: No chemical shift differences were encountered on ^{1}H NMR for the two diastereoisomers of compound **7**. The ^{1}H NMR signals were therefore reported as a single compound. The ^{13}C NMR reports distinct signals of the two diastereoisomers. Full conditions investigated for the synthesis of **7** are reported in Table S2.*

N-trifluoroacetyl-protected L-serine methyl ester 10: L-serine methyl ester hydrochloride (7.20 g, 46.3 mmol, 1.0 equiv) was dissolved in anhydrous MeOH (100 mL) in a 250 mL round-bottom flask under N$_2$. The reaction mixture was cooled to 0°C (ice bath) before adding anhydrous Et$_3$N (7.10 mL, 50.9 mmol, 1.1 equiv) dropwise. The reaction mixture was stirred for 15 min at 0°C. Ethyl trifluoroacetate (11.1 mL, 93.0 mmol, 2 equiv) was added dropwise and the reaction mixture was stirred and allowed to warm to room temperature. After 2 h, additional Et$_3$N (7.10 mL, 50.9 mmol, 1.1 equiv) was added. After 48 h the reaction mixture was concentrated *in vacuo*, redissolved in EtOAc (250 mL), washed with NaHCO$_3$ (satd., 200 mL), HCl (1 M, 200 mL) and brine (200 mL), dried over MgSO$_4$, filtered and concentrated *in vacuo*. The crude product was purified by silica gel chromatography (30% EtOAc in pentane → 40% EtOAc in pentane) to obtain **10** (4.74 g, 22.0 mmol, 48%) as an oil: R_f = 0.3 (30% EtOAc in pentane); ^{1}H NMR (500 MHz, CDCl$_3$) δ 7.55 (d, J = 6.0 Hz, 1NH), 4.72 – 4.65 (m, 1H), 4.10 (dd, J = 11.5, 3.4 Hz, 1H), 3.96 (dd, J = 11.5, 3.3 Hz, 1H), 3.83 (s, 3H); ^{13}C NMR (126 MHz, CDCl$_3$) δ 169.7, 157.5 (q, J = 37.7 Hz), 115.7 (q, J = 288 Hz), 62.1, 54.8, 53.3; ^{19}F NMR (471 MHz, CDCl$_3$) δ -75.9. Spectroscopic data was in agreement with literature.[47]

Cyclooctene ether 11: L-serine methyl ester **10** (68.0 mg, 0.32 mmol, 1.0 equiv) and cyclooctene imidate **3** (181 mg, 0.67 mmol, 2.1 equiv) were co-evaporated with anhydrous toluene (3 x 2 mL) in a 25 mL round-bottom flask and dissolved in anhydrous DCM (3.0 mL) under N$_2$. The reaction mixture was cooled to -35°C (ethanol bath) before adding triflic acid (0.1 M in DCM, 0.32 mL, 32 µmol, 0.1 equiv). The reaction mixture was stirred for 4 h and gradually allowed to warm to 0°C. The reaction was quenched by adding Et$_3$N (8.8 µL, 63 µmol, 0.2 equiv) before adding Celite and concentrating *in vacuo*. The impregnated crude product was purified by silica gel chromatography (5% EtOAc in pentane, isocratic) to obtain the diastereomeric mixture of cyclooctene ethers **11** (**11$_A$** : **11$_B$**, ~ **1 : 1**, 47.0 mg, 0.145 mmol, 46%) as an oil: R_f = 0.2 (5% EtOAc in pentane); ^{1}H NMR (400 MHz, CDCl$_3$) δ 7.14 (d, J = 6.7 Hz, 1NH, **11$_A$** + **11$_B$**), 5.78 – 5.65 (m, 1H, **11$_A$** + **11$_B$**), 5.43 – 5.27 (m, 1H, **11$_A$** + **11$_B$**), 4.76 – 4.65 (m, 1H, **11$_A$** + **11$_B$**), 4.28 – 4.15 (m, 1H, **11$_A$** + **11$_B$**), 4.00 (dd, J = 9.9, 3.0 Hz, 1H, **11$_A$**), 3.90 (dd, J = 9.9, 2.8 Hz, 1H,

11ᴮ), 3.81 (2 s, 3H, **11ᴀ** + **11ᴮ**), 3.79 (dd, J = 9.9, 3.1 Hz, 1H, **11ᴮ**), 3.66 (dd, J = 9.8, 3.1 Hz, 1H, **11ᴀ**), 2.15 – 2.04 (m, 2H, **11ᴀ** + **11ᴮ**), 1.90 – 1.78 (m, 1H, **11ᴀ** + **11ᴮ**), 1.69 – 1.30 (m, 7H, **11ᴀ** + **11ᴮ**); ^{13}C NMR (101 MHz, CDCl₃) δ 169.4, 169.3, 132.6, 132.5, 131.2, 131.2, 78.0, 77.7, 67.7, 67.4, 53.3 (x2), 53.1 (x2), 35.7, 35.7, 29.2, 29.1, 26.6, 26.6, 26.2 (x2), 23.6, 23.6; HRMS: calculated for $C_{14}H_{20}F_3NO_4Na$ 346.12366 [M+Na]⁺; found 346.12350.

*Note: the ^{13}C signals associated with the trifluoroacetate protecting group (C=O and CF₃) were not reported due to a lack of resolution in the spectrum of **11**. Full conditions investigated for the synthesis of **11** are reported in Table S2.*
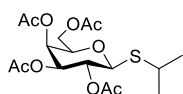
Peracetylated IPTG (14): Isopropyl β-D-1-thiogalactopyranoside (**13**, 477 mg, 2.0 mmol, 1.0 equiv) was dissolved in anhydrous pyridine (6.0 mL) in a 50 mL round-bottom flask under N₂. Acetic anhydride (4.0 mL, 42.4 mmol, 21 equiv) was added and the reaction mixture was stirred for 20 h. The reaction mixture was concentrated *in vacuo*. The crude product was redissolved in Et₂O (50 mL) and washed with HCl (1 M, 3 x 50 mL) and brine (50 mL). The organic layer was dried over MgSO₄, filtered and concentrated *in vacuo* to obtain **14** (827 mg, 2.0 mmol, 100%) as an oil: ^{1}H NMR (400 MHz, CDCl₃) δ 5.43 (dd, J = 3.4, 0.9 Hz, 1H), 5.22 (t, J = 10.0 Hz, 1H), 5.06 (dd, J = 10.0, 3.4 Hz, 1H), 4.58 (d, J = 10.0 Hz, 1H), 4.18 (dd, J = 11.3, 6.9 Hz, 1H), 4.10 (dd, J = 11.3, 6.4 Hz, 1H), 3.93 (td, J = 6.7, 1.0 Hz, 1H), 3.19 (hept, J = 6.8 Hz, 1H), 2.16 (s, 3H), 2.06 (s, 3H), 2.04 (s, 3H), 1.99 (s, 3H), 1.33 (d, J = 2.8 Hz, 3H), 1.31 (d, J = 2.9 Hz, 3H); ^{13}C NMR (101 MHz, CDCl₃) δ 170.5, 170.4, 170.2, 169.6, 84.0, 74.4, 72.1, 67.6, 67.4, 61.7, 35.8, 24.1, 23.9, 21.0, 20.8, 20.8, 20.7; HRMS: calculated for $C_{17}H_{26}O_9SNa$ 429.11897 [M+Na]⁺; found 429.11875. Spectroscopic data was in agreement with literature.[48]

Evaluation of conditions typical for photochemical isomerization with 14: Acetylated IPTG (**14**, 413 mg, 1.02 mmol, 1 equiv) was irradiated (λ = 254 nm) for 24 h in the presence of methyl benzoate (360 mg, 2.64 mmol, 2.6 equiv) in a quartz flask containing a solution of Et₂O in heptane (1:1, 100 mL). During irradiation, the reaction mixture was continuously circulated over a silica column (4 g size, containing dry silica and 2.5 g of AgNO₃ impregnated silica[25](10% w/w, containing 1.47 mmol AgNO₃, 1.5 equiv)) at a flowrate of 25 mL/min. The column was placed in the dark and shielded with aluminium foil during the irradiation. Afterwards, the column was flushed with Et₂O in heptane (1:1, 250 mL) before drying over a stream of air. Subsequently, the contents of the column were emptied into an Erlenmeyer flask containing NH₄OH (28% w/w, 25 mL) and DCM (25 mL). The biphasic mixture was stirred for 1 h before filtration of the silica gel. The organic layer was separated and the aqueous layer was extracted with DCM (25 mL). The combined organic layers were washed with H₂O (50 mL), dried over MgSO₄, filtered and concentrated *in vacuo* to obtain **14** (252 mg, 0.62 mmol, 61%) as an oil.

*Note: Based on this experiment, we concluded that **14** has significant affinity for AgNO₃ (despite not forming a (trans)-cyclooctene moiety during irradiation), which would hamper the development of a TCO-caged IPTG.*
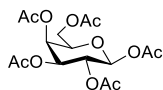
**Peracetylated β-D-galactopyranoside 16:** Synthesis was performed according to a modified procedure.[49] A suspension of sodium acetate (25.0 g, 305 mmol, 1.1 equiv) in acetic anhydride (350 mL, 3.71 mol, 13.4 equiv) was

stirred in a three-neck, round-bottom flask and heated towards reflux in an oil bath set at 160°C. When the suspension was fully refluxing, the flask was removed from the oil bath and D-galactose (50.0 g, 278 mmol, 1.0 equiv) was slowly added in portions to the mixture. The reaction mixture turned into a clear, yellow solution and was stirred for a further 5-10 min before pouring it into ice water (2 L). The aqueous mixture was stirred for 1 h at room temperature. DCM (600 mL) was added and the organic layer was washed with H_2O (1.5 L), $NaHCO_3$ (satd., 1.5 L), brine (1 L), dried over $MgSO_4$, filtered and concentrated *in vacuo*. The crude product was obtained as a light yellow solid and purified by recrystallization in EtOH to obtain **16** (56.4 g, 144 mmol, 52%) as white crystals: R_f = 0.4 (30% EtOAc in pentane); ^{1}H NMR (400 MHz, $CDCl_3$) δ 1H NMR (400 MHz, CDCl3) δ 5.71 (d, J = 8.3 Hz, 1H), 5.43 (dd, J = 3.4, 1.1 Hz, 1H), 5.34 (dd, J = 10.4, 8.3 Hz, 1H), 5.09 (dd, J = 10.4, 3.4 Hz, 1H), 4.21 – 4.03 (m, 3H), 2.17 (s, 3H), 2.13 (s, 3H), 2.05 (2 s, 6H), 2.00 (s, 3H); ^{13}C NMR (101 MHz, $CDCl_3$) δ 170.4, 170.2, 170.0, 169.5, 169.1, 92.2, 71.8, 70.9, 67.9, 66.9, 61.1, 20.9, 20.7, 20.7, 20.6; HRMS: calculated for $C_{16}H_{22}O_{11}Na$ 413.10543 [M+Na]+, found 413.10521. Spectroscopic data was in agreement with literature.[49]
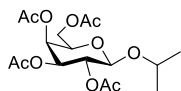
Compound 17: Peracetylated galactopyranoside **16** (50.0 g, 128 mmol, 1.0 equiv) was co-evaporated with anhydrous toluene (200 mL) in a 2 L round-bottom flask before dissolving the starting material in DCM (513 mL) under N_2. The solution was cooled to 0°C (ice bath) before adding acetic anhydride (24.2 mL, 256 mmol, 2.0 equiv) and HBr (33% w/w in AcOH, 133 mL, 769 mmol, 6.0 equiv). The reaction mixture was stirred overnight and allowed to warm to room temperature. TLC confirmed complete conversion of **16** into the corresponding anomeric bromide: R_f = 0.7 (30% EtOAc in pentane). The crude reaction mixture was concentrated *in vacuo*, placed under N_2 and redissolved in anhydrous isopropanol (640 mL) in the presence of flame-dried molecular sieves (4 Å, 75 g). The solution was cooled to 0°C (ice bath) before adding I_2 (48.7 g, 192 mmol, 1.5 equiv). The reaction mixture was stirred for 24 h at 4°C (cold room).* $Na_2S_2O_3$ (satd., 500 mL) was slowly added to quench the reaction whilst stirring. The reaction mixture was filtered, diluted with H_2O (500 mL) and subsequently extracted with EtOAc (3 x 500 mL). The combined organic layers were dried over $MgSO_4$, filtered and concentrated *in vacuo*. The crude product was purified by silica gel chromatography (15% EtOAc in pentane → 20% EtOAc in pentane). The beta-glycosylated product **17** (37.5 g, 96.1 mmol, 75% over 2 steps) was obtained as an oil: R_f = 0.5 (30% EtOAc in pentane); ^{1}H NMR (400 MHz, $CDCl_3$) δ 5.38 (dd, J = 3.5, 1.2 Hz, 1H), 5.18 (dd, J = 10.5, 7.9 Hz, 1H), 5.02 (dd, J = 10.5, 3.5 Hz, 1H), 4.51 (d, J = 7.9 Hz, 1H), 4.19 (dd, J = 11.2, 6.6 Hz, 1H), 4.12 (dd, J = 11.2, 6.9 Hz, 1H), 3.98 – 3.84 (m, 2H), 2.15 (s, 3H), 2.05 (2 s, 6H), 1.99 (s, 3H), 1.25 (d, J = 6.2 Hz, 3H), 1.15 (d, J = 6.2 Hz, 3H); ^{13}C NMR (101 MHz, $CDCl_3$) δ 170.6, 170.5, 170.4, 169.5, 100.4, 73.4, 71.1, 70.6, 69.2, 67.2, 61.5, 23.4, 22.2, 20.9, 20.8, 20.8, 20.8; HRMS: calculated for $C_{17}H_{26}O_{10}Na$ 413.14182 [M+Na]+; found 413.14146.

Note: This reaction can also be stirred overnight and allowed to warm to room temperature, obtaining a similar yield over 2 steps at 50 mmol reaction scale.
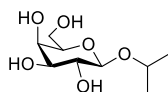
Isopropyl β-D-1-galactopyranoside (IPG; 15): Beta-galactopyranoside **17** (37.5 g, 96.1 mmol, 1 equiv) was dissolved in a mixture of anhydrous DCM (480 mL) and anhydrous MeOH (480 mL) in a 2 L round-bottom flask under

N_2. Sodium methoxide (1.04 g, 19.2 mmol, 0.2 equiv) was added and the reaction mixture was stirred overnight at room temperature. The reaction mixture was neutralized by adding Amberlyst® (H^+ form, washed 3 x with MeOH prior to usage) in small portions, gently swirling the flask and monitoring the pH until neutral. The neutralized solution was filtered and concentrated *in vacuo* to obtain IPG (**15**, 19.5 g, 87.7 mmol, 91%) as a solid: R_f = 0.4 (20% MeOH in DCM); [^1H] NMR (400 MHz, MeOD) δ 4.33 – 4.24 (m, 1H), 4.04 (hept, *J* = 6.2 Hz, 1H), 3.84 (br s, 1H), 3.73 (d, *J* = 6.2 Hz, 2H), 3.53 – 3.42 (m, 3H), 1.22 (d, *J* = 6.2 Hz, 3H), 1.19 (d, *J* = 6.1 Hz, 3H); [^13C] NMR (101 MHz, MeOD) δ 103.1, 76.4, 75.0, 72.5, 72.4, 70.2, 62.4, 23.8, 22.0; HRMS: calculated for $C_9H_{18}O_6Na$ 245.09956 $[M+Na]^+$; found 245.09950. **15** was redissolved in H_2O and lyophilized in small quantities for recombinant gene expression experiments.
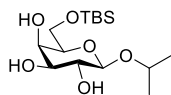
6-TBS-IPG (27): IPG (**15**, 1.117 g, 5.03 mmol, 1.0 equiv) was co-evaporated with anhydrous toluene (3 x 10 mL) in a 250 mL round-bottom flask before dissolving in anhydrous pyridine (20 mL) under N_2. The solution was cooled to 0°C before adding TBDMS-Cl (50% w/w in toluene, 2.09 mL, 6.03 mmol, 1.2 equiv). The reaction mixture was stirred and allowed to warm to room temperature. Additional TBDMS-Cl (50% w/w in toluene, 0.525 mL, 1.5 mmol, 0.3 equiv) was added after 4 and 24 h to achieve full conversion. After a total reaction time 48 h, the reaction was quenched by adding H_2O (~100 mL) and subsequently extracted with DCM (3 x 75 mL). The combined organic layers were washed with $CuSO_4$ (1 M, 50 mL), H_2O (50 mL) and brine (50 mL), dried over $MgSO_4$, filtered and concentrated *in vacuo*. The crude product was purified by silica gel chromatography (50% EtOAc in pentane → 60% EtOAc in pentane) to obtain the 6-O-silylated galactopyranoside **27** (1.55 g, 4.61 mmol, 92%) as an oil: R_f = 0.1 (50% EtOAc in pentane); [^1H] NMR (400 MHz, CDCl$_3$) δ 4.28 (d, *J* = 7.5 Hz, 1H), 4.06 – 3.94 (m, 2H), 3.89 (dd, *J* = 10.4, 6.1 Hz, 1H), 3.82 (dd, *J* = 10.4, 5.5 Hz, 1H), 3.64 (dd, *J* = 9.6, 7.5 Hz, 1H), 3.57 (dd, *J* = 9.6, 3.3 Hz, 1H), 3.47 (t, *J* = 5.8 Hz, 1H), 3.29 (br s, 3OH), 1.25 (d, *J* = 6.2 Hz, 3H), 1.20 (d, *J* = 6.2 Hz, 3H), 0.89 (s, 9H), 0.08 (2 s, 6H); [^13C] NMR (101 MHz, CDCl$_3$) δ 101.6, 74.8, 73.9, 72.0, 71.9, 69.0, 62.6, 26.0 (x3), 23.6, 22.0, 18.4, -5.3, -5.3; HRMS: calculated for $C_{15}H_{32}O_6SiNa$ 359.18604 $[M+Na]^+$; found 359.18589.
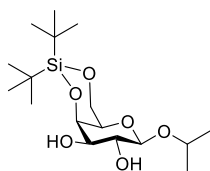
4,6-DTBS-IPG (28): IPG (**15**, 1.123 g, 5.05 mmol, 1.0 equiv) was co-evaporated with anhydrous toluene (3 x 10 mL) in a round-bottom flask before dissolving in anhydrous pyridine (20 mL) under N_2. The solution was cooled to 0°C before adding di-*tert*-butylsilanediyl bis(trifluoromethanesulfonate) (2.0 mL, 6.14 mmol, 1.2 equiv) at a rate of 0.5 mL/h (syringe pump). The reaction mixture was stirred overnight and allowed to warm to room temperature. The reaction was quenched by adding H_2O (2 mL) and subsequently diluted with EtOAc (150 mL). The mixture was washed with HCl (1 M, 3 x 75 mL), $NaHCO_3$ (satd., 100 mL) and brine (100 mL). The organic layer was dried over $MgSO_4$, filtered and concentrated *in vacuo*. The crude product was purified by silica gel chromatography (40% EtOAc in pentane, isocratic) to obtain the 4,6-O-silylated galactopyranoside **28** (1.31 g, 3.61 mmol, 72%) as an oil: R_f = 0.3 (50% EtOAc in pentane); [^1H] NMR (400 MHz, CDCl$_3$) δ 4.39 – 4.34 (m, 1H), 4.31 (d, *J* = 7.6 Hz, 1H), 4.28 (dd, *J* = 12.3, 2.2 Hz, 1H), 4.22 (dd, *J* = 12.3, 1.7 Hz, 1H), 4.00 (hept, *J* = 6.2 Hz, 1H), 3.64 (dd, *J* = 9.4, 7.6 Hz, 1H), 3.52 (dd, *J* = 9.4, 3.4 Hz, 1H), 3.41 (br s, 1H), 2.68 (br s, 1OH), 2.47 (br s, 1OH), 1.24 (d, *J* = 6.2 Hz, 3H), 1.19 (d, *J* = 6.2 Hz, 3H), 1.05 (2 s, 18H); [^13C] NMR (101 MHz,

CDCl$_3$) δ 101.2, 73.9, 72.8, 72.3, 71.3, 71.2, 67.2, 27.6 (x3), 27.5 (x3), 23.8, 23.5, 22.0, 20.9; HRMS: calculated for C$_{17}$H$_{34}$O$_6$SiNa 385.20169 [M+Na]$^+$; found 385.20122.
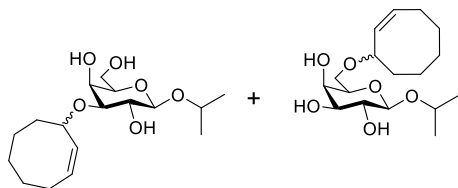

3-CCO-IPG (19) and 6-CCO-IPG (20): IPG (**15**, 248 mg, 1.12 mmol, 1.0 equiv) and dibutyltin oxide (333 mg, 1.34 mmol, 1.2 equiv) were combined in a 10 mL round-b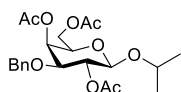ottom flask and dissolved in anhydrous toluene (5 mL) under N$_2$. The reaction mixture was stirred at 105°C (oil bath) under N$_2$ overnight. The reaction mixture was subsequently concentrated *in vacuo*, co-evaporated with anhydrous toluene (3 x) and placed under N$_2$. Cyclooctene bromide **18** (528 mg, 2.79 mmol, 2.5 equiv) was dissolved in anhydrous toluene (1 mL) in a separate 10 mL pear-shaped flask under N$_2$. The solution containing **18** and cesium fluoride (424 mg, 2.79 mmol, 2.5 equiv) were added to the reaction mixture. The combined reaction mixture was stirred overnight at 105°C (oil bath) under N$_2$. The reaction mixture was diluted with EtOAc, sonicated (5 min), transferred to a 50 mL round-bottom flask, impregnated with Celite and concentrated *in vacuo*. The impregnated crude product was purified by silica gel chromatography (10% acetone in pentane → 20% acetone in pentane → 30% acetone in pentane) to obtain the regioisomers **19** (**3-CCO-IPG**; 81 mg, 0.245 mmol, 22%) and **20** (**6-CCO-IPG**; 68 mg, 0.206 mmol, 18%) separately as diastereomeric mixtures: **3-CCO-IPG (19$_A$ + 19$_B$, 0.4 : 0.6)**: R$_f$ = 0.3 (30% acetone in pentane), 0.5 (EtOAc); ^{1}H NMR (400 MHz, CDCl$_3$) δ 5.82 – 5.65 (m, 1H, **19$_A$ + 19$_B$**), 5.62 – 5.46 (m, 1H, **19$_A$ + 19$_B$**), 4.66 – 4.58 (m, 1H, **19$_A$**), 4.57 – 4.47 (m, 1H, **19$_B$**), 4.31 (d, *J* = 7.8 Hz, 1H, **19$_B$**), 4.30 (d, *J* = 7.9 Hz, 1H, **19$_A$**), 4.08 – 3.89 (m, 3H, **19$_A$ + 19$_B$**), 3.88 – 3.75 (m, 1H, **19$_A$ + 19$_B$**), 3.73 – 3.59 (m, 1H, **19$_A$ + 19$_B$**), 3.55 – 3.48 (m, 1H, **19$_A$ + 19$_B$**), 3.46 (dd, *J* = 9.5, 3.4 Hz, 1H, **19$_B$**), 3.40 (dd, *J* = 9.4, 3.4 Hz, 1H, **19$_A$**), 2.95 – 2.52 (m, 3OH, **19$_A$ + 19$_B$**), 2.15 – 2.06 (m, 2H, **19$_A$ + 19$_B$**), 2.05 – 1.96 (m, 1H, **19$_A$**), 1.96 – 1.83 (m, 1H, **19$_B$**), 1.71 – 1.29 (m, 7H, **19$_A$ + 19$_B$**), 1.27 (d, *J* = 6.2 Hz, 3H, **19$_A$ + 19$_B$**), 1.20 (d, *J* = 6.1 Hz, 3H, **19$_A$ + 19$_B$**); ^{13}C NMR (101 MHz, CDCl$_3$) δ 133.4, 133.0, 131.3, 130.5, 101.5, 101.5, 79.7, 78.1, 78.1, 74.4, 74.4, 74.4, 71.7 (x2), 71.2, 70.0, 68.5, 65.9, 62.2, 62.2, 36.4, 35.9, 29.3, 29.1, 26.7, 26.7, 26.3, 26.2, 23.7, 23.7, 23.6 (x2), 21.9, 21.9; HRMS: calculated for C$_{17}$H$_{30}$O$_6$Na 353.19346 [M+Na]$^+$; found 353.19316; **6-CCO-IPG (20$_A$ + 20$_B$, 1 : 1)**: R$_f$ = 0.15 (30% acetone in pentane), 0.3 (EtOAc); ^{1}H NMR (400 MHz, CDCl$_3$) δ 5.68 (dddd, *J* = 10.5, 8.9, 7.3, 1.3 Hz, 1H, **20$_A$ + 20$_B$**), 5.53 – 5.43 (m, 1H, **20$_A$ + 20$_B$**), 4.35 – 4.26 (m, 1H, **20$_A$ + 20$_B$**), 4.28 (d, *J* = 7.7, 1H, **20$_A$**), 4.27 (d, *J* = 7.7, 1H, **20$_B$**), 4.23 (br s, 1OH, **20$_A$ + 20$_B$**), 4.06 – 3.97 (m, 1H, **20$_A$ + 20$_B$**), 3.95 (dd, *J* = 10.7, 3.3 Hz, 1H, **20$_A$ + 20$_B$**), 3.90 – 3.81 (m, 1OH, **20$_A$ + 20$_B$**), 3.78 (dd, *J* = 9.0, 4.0 Hz, 1H, **20$_A$**), 3.72 – 3.52 (m, 3H, **20$_A$ + 20$_B$**; 1OH, **20$_A$ + 20$_B$**; 1H, **20$_B$**), 2.21 – 2.02 (m, 2H, **20$_A$ + 20$_B$**), 1.97 – 1.86 (m, 1H, **20$_A$ + 20$_B$**), 1.70 – 1.30 (m, 7H, **20$_A$ + 20$_B$**), 1.29 – 1.23 (m, 3H), 1.20 (d, *J* = 6.1 Hz, 3H, **20$_A$**), 1.19 (d, *J* = 6.1 Hz, 3H, **20$_B$**); ^{13}C NMR (101 MHz, CDCl$_3$) δ 133.7, 133.7, 130.3, 130.3, 101.7, 101.7, 77.7, 77.6, 73.9 (x3), 73.6, 72.0 (x2), 71.6, 71.5, 69.4, 69.3, 68.2, 67.9, 35.9, 35.8, 29.2 (x2), 26.6 (x2), 26.3 (x2), 23.7, 23.7, 23.6, 23.6, 22.1 (x2); HRMS: calculated for C$_{17}$H$_{30}$O$_6$Na 353.19346 [M+Na]$^+$; found 353.19312. **19** and **20** were redissolved in dioxane and lyophilized in small quantities for recombinant gene expression experiments.

*Note: Full conditions investigated for the synthesis of **19** and **20** are reported in Table S3.*
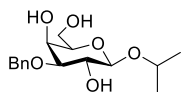
3-OBn-IPG (29): This procedure was based on the reported procedure by Geng *et al.*[50] for the regioselective benzylation of IPTG. IPG (**15**, 19.5 g, 87.7 mmol, 1.0 equiv) was co-evaporated with anhydrous toluene (3 x 100 mL) in a 1 L round-bottom flask before adding dibutyltin oxide (32.7 g, 131 mmol, 1.5 equiv) and suspending the reactants in anhydrous toluene (440 mL) under N_2. The reaction mixture was stirred overnight at 105°C (oil bath) under N_2. The reaction mixture was concentrated *in vacuo*, co-evaporated with anhydrous toluene (3 x 100 mL), placed under N_2 and redissolved in anhydrous toluene (440 mL). Tetrabutylammonium bromide (5.65 g, 17.5 mmol, 0.2 equiv) and benzyl bromide (15.6 mL, 131 mmol, 1.5 equiv) were added and the reaction mixture was stirred for 23 h at 70°C (oil bath) under N_2. The reaction mixture was allowed to cool to room temperature, concentrated *in vacuo*, redissolved in DCM (500 mL) and washed with a mixture of H_2O (500 mL) and brine (1 L). The aqueous phase was extracted with DCM (5 x 500 mL). The combined organic layers were dried over $MgSO_4$, filtered and concentrated *in vacuo*. The crude product was purified by silica gel chromatography (DCM → 2% MeOH in DCM) to obtain **29** (27.6 g) as a crude product (including a tetrabutylammonium derived impurity; marked in the NMR spectra) which was used in the next step without further purification: R_f = 0.5 (EtOAc); ^1H NMR (400 MHz, $CDCl_3$) δ 7.42 – 7.28 (m, 5H), 4.75 (s, 2H), 4.30 (d, *J* = 7.8 Hz, 1H), 4.07 – 3.97 (m, 2H), 3.93 (ddd, *J* = 11.2, 6.6, 4.3 Hz, 1H), 3.85 – 3.79 (m, 1H), 3.76 (ddd, *J* = 9.7, 7.8, 2.1 Hz, 1H), 3.51 – 3.46 (m, 1H), 3.44 (dd, *J* = 9.5, 3.4 Hz, 1H), 2.78 (dd, *J* = 2.3, 1.0 Hz, 1OH), 2.49 (d, *J* = 2.2 Hz, 1OH), 2.46 (dd, *J* = 8.3, 4.4 Hz, 1OH), 1.26 (d, *J* = 6.2 Hz, 3H), 1.20 (d, *J* = 6.2 Hz, 3H); ^{13}C NMR (101 MHz, $CDCl_3$) δ 137.8, 128.7 (x2), 128.2, 128.0 (x2), 101.5, 80.2, 74.5, 72.2, 71.9, 71.2, 67.0, 62.3, 23.6, 22.0; HRMS: calculated for $C_{16}H_{24}O_6Na$ 335.14651 [M+Na]+; found 335.14610.

3-OBn-2,4,6-OAc-IPG (21): Crude 3-OBn-IPG (**29**, 23.6 g, max. 87.7 mmol, 1.0 equiv) was dissolved in anhydrous pyridine (530 mL, 6.55 mol, 74.5 equiv) and acetic anhydride (350 mL, 3.71 mol, 42.2 equiv) in a 2 L round-bottom flask under N_2. The reaction mixture was stirred overnight at room temperature under N_2, concentrated *in vacuo*, redissolved in Et_2O (1 L) and washed with HCl (1 M, 3 x 500 mL). The combined aqueous layers were extracted with Et_2O (500 mL). The combined organic layers were washed with $NaHCO_3$ (satd., 500 mL) and brine (500 mL), dried over $MgSO_4$, filtered and concentrated *in vacuo* to obtain 3-OBn-2,4,6-OAc-IPG **21** (35.0 g, 79.8 mmol, 91% over 2 steps) as a solid: R_f = 0.2 (30% Et_2O in pentane); ^1H NMR (400 MHz, $CDCl_3$) δ 7.37 – 7.24 (m, 5H), 5.50 (dd, *J* = 3.4, 0.9 Hz, 1H), 5.08 (dd, *J* = 10.0, 8.1 Hz, 1H), 4.70 (d, *J* = 12.4 Hz, 1H), 4.40 (d, *J* = 12.1 Hz, 1H), 4.40 (d, *J* = 8.1 Hz, 1H), 4.16 (dd, *J* = 6.7, 0.9 Hz, 2H), 3.88 (hept, *J* = 6.2 Hz, 1H), 3.78 (td, *J* = 6.6, 1.1 Hz, 1H), 3.53 (dd, *J* = 10.0, 3.5 Hz, 1H), 2.15 (s, 3H), 2.07 (s, 3H), 2.02 (s, 3H), 1.22 (d, *J* = 6.2 Hz, 3H), 1.11 (d, *J* = 6.1 Hz, 3H); ^{13}C NMR (101 MHz, $CDCl_3$) δ 170.7, 170.7, 169.5, 137.7, 128.5 (x2), 127.9 (x3), 100.4, 76.8, 73.1, 71.3, 70.9, 70.9, 66.0, 62.2, 23.4, 22.2, 21.0, 21.0, 20.9; HRMS: calculated for $C_{22}H_{30}O_9Na$ 461.17820 [M+Na]+; found 461.17787.

*Note: precipitation of **21** may occur in the residue when filtering off the dried organic layers. If so, dilution with extra Et_2O or EtOAc ensures no product is lost.*
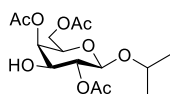
2,4,6-OAc-IPG (**22**): 3-OBn-2,4,6-OAc-IPG (**21**, 35.0 g, 79.8 mmol, 1.0 equiv) was co-evaporated with toluene (200 mL) in a 1 L round-bottom flask and subsequently dissolved in EtOAc (800 mL) under N_2. N_2 was purged through the stirring solution for 15 min (flow) before adding Pd(OH)$_2$/C (20% w/w loading, 5.61 g, 7.99 mmol, 0.1 equiv) and purging N_2 through the stirred suspension for 45 min (flow). The reaction mixture was purged with H_2 (balloon) whilst stirring and was subsequently left to stir under H_2 (balloon) for 72 h. The reaction mixture was purged with N_2 (flow), filtered over a pad of Celite and concentrated *in vacuo* to obtain 2,4,6-OAc-IPG (**22**, 23.9 g, 68.6 mmol, 86%) as an off-white sold: R_f = 0.3 (50% EtOAc in pentane); ^{1}H NMR (400 MHz, CDCl$_3$) δ 5.32 (dd, *J* = 3.6, 0.9 Hz, 1H), 4.94 (dd, *J* = 10.1, 7.9 Hz, 1H), 4.47 (d, *J* = 8.0 Hz, 1H), 4.15 (d, *J* = 6.6 Hz, 2H), 3.92 (hept, *J* = 6.2 Hz, 1H), 3.86 – 3.79 (m, 1H), 3.83 (td, *J* = 6.6, 0.9 Hz, 1H), 2.82 (d, *J* = 6.5 Hz, 1OH), 2.17 (s, 3H), 2.11 (s, 3H), 2.06 (s, 3H), 1.24 (d, *J* = 6.2 Hz, 3H), 1.16 (d, *J* = 6.1 Hz, 3H); ^{13}C NMR (101 MHz, CDCl$_3$) δ 171.3, 171.1, 170.7, 100.0, 73.2, 73.1, 71.6, 71.0, 69.8, 62.1, 23.4, 22.2, 21.1, 21.0, 20.8; HRMS: calculated for C$_{15}$H$_{24}$O$_9$Na 371.13125 [M+Na]$^+$; found 371.13101.
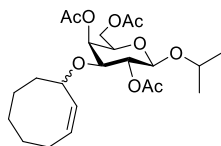
2,4,6-OAc-3-CCO-IPG (23): 2,4,6-OAc-IPG (**22**, 7.60 g, 21.8 mmol, 1.0 equiv) and cyclooctene imidate **3** (23.3 g, 86 mmol, 3.95 equiv) were co-evaporated with anhydrous toluene (3 x 150 mL) in a 1 L round-bottom flask and dissolved in anhydrous DCM (200 mL) under N_2. The reaction mixture was cooled to -40°C (ethanol bath) before adding triflic acid (0.194 mL, 2.18 mmol, 0.1 equiv). The reaction mixture was stirred for 4 h and allowed to warm to -30°C and subsequently quenched by adding Et$_3$N (0.608 mL, 4.36 mmol, 0.2 equiv). The neutralized reaction mixture was diluted with Et$_2$O (1 L), washed with NaOH (1 M, 3 x 1 L) and brine (1 L), dried over MgSO$_4$, filtered and concentrated *in vacuo*. The crude product was purified by silica gel chromatography (10% Et$_2$O in pentane → 30% Et$_2$O in pentane) to obtain the diastereomeric mixture **23** (**23$_A$** + **23$_B$**, ~ 0.6 : 0.4, 3.40 g, 7.45 mmol, 34%) as a crystalline solid: R_f = 0.35 (30% Et$_2$O in pentane); ^{1}H NMR (400 MHz, CDCl$_3$) δ 5.80 – 5.72 (m, 1H, **23$_B$**), 5.71 – 5.62 (m, 1H, **23$_A$**), 5.49 (dd, *J* = 10.7, 7.1 Hz, 1H, **23$_A$**), 5.38 (dd, *J* = 3.5, 0.9 Hz, 1H, **23$_B$**), 5.35 (dd, *J* = 3.6, 1.0 Hz, 1H, **23$_A$**), 5.31 (ddd, *J* = 10.7, 7.3, 1.3 Hz, 1H, **23$_B$**), 5.06 (dd, *J* = 10.1, 8.1 Hz, 1H, **23$_A$**), 5.00 (dd, *J* = 10.1, 8.1 Hz, 1H, **23$_B$**), 4.44 – 4.37 (m, 1H, **23$_B$**), 4.42 (d, *J* = 8.1 Hz, 1H, **23$_A$**), 4.41 (d, *J* = 8.1 Hz, 1H, **23$_B$**), 4.36 – 4.28 (m, 1H, **23$_A$**), 4.19 – 4.09 (m, 2H, **23$_A$** + **23$_B$**), 3.95 – 3.84 (m, 1H, **23$_A$** + **23$_B$**), 3.82 – 3.77 (m, 1H, **23$_A$** + **23$_B$**), 3.58 – 3.47 (m, 1H, **23$_A$** + **23$_B$**), 2.15 – 2.05 (m, 2H, **23$_A$** + **23$_B$**), 2.14 (s, 3H, **23$_B$**), 2.12 (s, 3H, **23$_A$**), 2.10 (s, 3H, **23$_A$**), 2.09 (s, 3H, **23$_B$**), 2.07 (s, 3H, **23$_B$**), 2.06 (s, 3H, **23$_A$**), 1.83 – 1.74 (m, 1H, **23$_A$**), 1.70 – 1.27 (m, 7H, **23$_A$** + **23$_B$**; 1H, **23$_B$**), 1.23 (d, *J* = 6.3 Hz, 3H, **23$_A$** + **23$_B$**), 1.14 (d, *J* = 6.2 Hz, 3H, **23$_A$**), 1.13 (d, *J* = 6.0 Hz, 3H, **23$_B$**); ^{13}C NMR (101 MHz, CDCl$_3$) δ 170.8 (x2), 170.6, 170.5, 169.4, 169.4, 133.4, 133.0, 131.7, 130.1, 100.6, 100.5, 78.6, 76.5, 75.0, 74.5, 73.0, 73.0, 71.8, 71.2, 70.9, 70.7, 68.7, 66.1, 62.4, 62.4, 36.0, 35.7, 29.3, 29.3, 26.9, 26.7, 26.4, 26.3, 23.7, 23.7, 23.4, 23.4, 22.2 (x2), 21.1 (x2), 21.0, 21.0, 20.9 (x2); HRMS: calculated for C$_{23}$H$_{36}$O$_9$Na 479.22515 [M+Na]$^+$; found 479.22483.
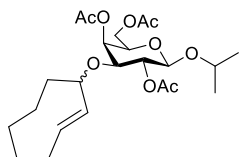
2,4,6-OAc-3-TCO-IPG (24): 2,4,6-OAc-3-CCO-IPG (**23**, 228 mg, 0.50 mmol, 1 equiv) was irradiated (λ = 254 nm) for 24 h in the presence of methyl benzoate (385 mg, 2.83 mmol, 5.7 equiv) in a quartz flask containing a solution of 5% isopropanol in Et_2O (150 mL). During irradiation, the reaction mixture was continuously circulated over a silica column (4 g size) containing 2.5 g of TAg silica[41] (0.6 mmol/g, containing 1.5 mmol Ag (I), 3.0 equiv) at a flowrate of 20 mL/min. The column was placed in the dark and shielded with aluminium foil during the irradiation. Afterwards, the column was flushed with 5% isopropanol in Et_2O (300 mL) before disconnecting the stationary phase from the HPLC system and drying over a stream of N_2. The column was eluted with NH_3 (7 N in MeOH) and fractions containing the product were combined and concentrated *in vacuo* to obtain the crude, partially deacetylated product **24** as an oil which was used for the next step without further purification: R_f = 0.4 (30% Et_2O in pentane).*

Note: **24 was partially deacetylated during treatment with NH_3. An analytical sample used for the NMR assignment shown below was obtained from a separate experiment (Entry 4, Table S6) in which the crude product was purified by silica gel chromatography (10% Et_2O in pentane $\rightarrow$ 30% Et_2O in pentane). This leads to loss of partially deacetylated product. Full conditions investigated for the photochemical conversion of **23** to **24** are listed in Table S6.*

Diastereomeric mixture **24** (**24$_A$** + **24$_B$**, ~ 0.6 : 0.4): ^{1}H NMR (400 MHz, CDCl$_3$) δ 5.88 (ddd, *J* = 15.7, 11.2, 3.5 Hz, 1H, **24$_A$** + **24$_B$**), 5.45 (d, *J* = 3.0 Hz, 1H, **24$_B$**), 5.42 (d, *J* = 2.9 Hz, 1H, **24$_A$**), 5.40 – 5.32 (m, 1H, **24$_A$** + **24$_B$**), 5.14 – 5.08 (m, 1H, **24$_A$** + **24$_B$**), 4.44 (d, *J* = 8.1 Hz, 1H, **24$_B$**), 4.42 (d, *J* = 8.1 Hz, 1H, **24$_A$**), 4.42 (br s, 1H, **24$_B$**), 4.27 (br s, 1H, **24$_A$**), 4.20 – 4.09 (m, 2H, **24$_A$** + **24$_B$**), 3.90 (hept, *J* = 6.2 Hz, 1H, **24$_A$** + **24$_B$**), 3.83 – 3.74 (m, 1H, **24$_A$** + **24$_B$**), 3.68 (dd, *J* = 10.2, 3.2 Hz, 1H, **24$_B$**), 3.55 (dd, *J* = 9.9, 3.6 Hz, 1H, **24$_A$**), 2.52 – 2.38 (m, 1H, **24$_A$** + **24$_B$**), 2.14 (s, 3H, **24$_B$**), 2.13 (s, 3H, **24$_B$**), 2.11 (s, 3H, **24$_A$**), 2.06 (2 x s, 6 H, **24$_A$**; 3 H, **24$_B$**), 2.02 – 1.73 (m, 4H, **24$_A$** + **24$_B$**), 1.61 – 1.33 (m, 3H, **24$_A$** + **24$_B$**), 1.24 (d, *J* = 6.2 Hz, 3H, **24$_A$** + **24$_B$**), 1.14 (d, *J* = 6.2 Hz, 3H, **24$_A$** + **24$_B$**), 1.00 – 0.87 (m, 1H, **24$_A$** + **24$_B$**), 0.77 – 0.63 (m, 1H, **24$_A$** + **24$_B$**); ^{13}C NMR (101 MHz, CDCl$_3$) δ 170.7, 170.6, 170.5, 170.4, 169.3, 169.2, 133.2, 132.6, 132.1, 131.6, 100.6, 100.4, 78.1, 75.6, 75.3, 74.5, 73.1, 73.0, 71.4, 71.0, 70.8, 70.7, 67.5, 65.8, 62.3, 62.1, 41.8, 40.1, 36.2, 36.0, 36.0, 35.8, 29.4, 29.3, 23.8, 23.4, 23.4, 23.3, 22.2, 22.2, 21.0, 21.0, 20.9, 20.9, 20.8 (x2).
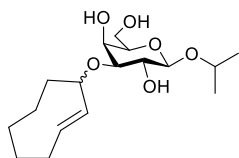
3-TCO-IPG (25): The crude product (**24**) obtained from the photoisomerization reaction was suspended in NaOMe (0.5 M in MeOH, 5.0 mL, 2.5 mmol, 5.0 equiv) in a 50 mL round-bottom flask under N_2. The reaction mixture was stirred overnight at room temperature, concentrated *in vacuo*, resuspended in H_2O (30 mL) and extracted with DCM (5 x 30 mL). The combined organic layers were dried over MgSO$_4$, filtered and concentrated *in vacuo* to obtain the diastereomeric mixture 3-TCO-IPG **25** (**25$_A$** : **25$_B$**, ~ 2 : 1, 57 mg, 0.17 mmol, 35% over 2 steps) as a solid: R_f = 0.4 (5% MeOH in DCM); ^{1}H NMR (400 MHz, CDCl$_3$) δ 6.18 (ddd, *J* = 16.0, 11.3, 3.8 Hz, 1H, **25$_B$**), 5.97 (ddd, *J* = 15.9, 11.2, 3.7 Hz, 1H, **25$_A$**), 5.51 (dd, *J* = 16.5, 1.9 Hz, 1H, **25$_A$**), 5.40 (dd, *J* = 16.5, 1.3 Hz, 1H, **25$_B$**), 4.58 (br s, 1H, **25$_A$**), 4.48 (br s, 1H, **25$_B$**), 4.32 (d, *J* = 8.0 Hz, 1H, **25$_B$**), 4.30 (d, *J* = 7.9 Hz, 1H, **25$_A$**), 4.08 – 4.00 (m, 2H, **25$_A$** + **25$_B$**), 3.99 – 3.91 (m, 1H,

25$_A$ + 25$_B$), 3.86 – 3.76 (m, 1H, **25$_A$ + 25$_B$**), 3.75 – 3.66 (m, 1H, **25$_A$ + 25$_B$**), 3.56 (dd, J = 9.5, 3.5 Hz, 1H, **25$_B$**), 3.54 – 3.47 (m, 1H, **25$_A$ + 25$_B$**), 3.43 (dd, J = 9.5, 3.4 Hz, 1H, **25$_A$**), 2.79 (br s, 1OH, **25$_A$**), 2.72 (br s, 1OH, **25$_B$**), 2.60 – 2.43 (m, 1H + 2OH, **25$_A$ + 25$_B$**), 2.13 (dd, J = 14.8, 5.8 Hz, 1H, **25$_A$**), 2.07 – 1.91 (m, 2H, **25$_A$ + 25$_B$**; 1H, **25$_B$**), 1.91 – 1.78 (m, 1H, **25$_A$ + 25$_B$**), 1.74 – 1.39 (m, 3H, **25$_A$ + 25$_B$**), 1.27 (d, J = 6.3 Hz, 3H, **25$_A$ + 25$_B$**), 1.20 (d, J = 6.2 Hz, 3H, **25$_A$ + 25$_B$**), 1.17 – 1.05 (m, 1H, **25$_A$ + 25$_B$**), 0.82 – 0.69 (m, 1H, **25$_A$ + 25$_B$**); ¹³C NMR (101 MHz, CDCl$_3$) δ 134.2, 133.2, 132.8, 131.2, 101.6, 101.5, 79.4, 79.3, 77.9, 76.0, 74.5, 74.4, 71.9, 71.8, 71.6, 70.5, 68.4, 66.0, 62.4 (x2), 42.1, 41.5, 36.1, 36.0, 35.9, 35.8, 29.4 (x2), 23.9, 23.8, 23.6 (x2), 22.0, 21.9; HRMS: calculated for C$_{17}$H$_{30}$O$_6$Na 353.19346 [M+Na]$^+$; found 353.19313. **25** was redissolved in dioxane and lyophilized in small quantities for recombinant gene expression experiments.

*Note: deacetylation in the presence of catalytic quantities of NaOMe and/or shorter reaction times did not result in complete conversion. This instead led to a mixture of products, in which the fully deprotected product (**25**) was difficult to isolate.*

6.7 Experimental procedures – molecular biology

General methods: Samples taken (corrected for OD_{600} according to the formula: $(1 / OD_{600})$ * 200 µL) from *E.coli* cultures were pelleted and stored at -20°C for indicated timepoints in each individual experiment described below. Samples were dissolved in a mixture of H_2O and 2x sample loading buffer (supplemented with 4% SDS, 20% glycerol, 10% 2-mercaptoethanol, 0.004% bromophenol blue, 1U/µL Benzonase in 0.125 M Tris HCl, pH 6.8; see individual experiments for deviations and amounts). Subsequently, dissolved samples were incubated for 5 min at 95°C for denaturation. 15 µL of each sample was loaded onto a 15% SDS-PAGE gel (0.75 or 1.5 mm) along with 4 µL PageRuler™ Plus Protein Marker (Thermo Scientific) unless stated otherwise and run for ~70 min at 180 V. Coomassie staining (Coomassie Brilliant Blue G-250) and in-gel fluorescence, using wavelength filters for Alexa 488 (eGFP) and Alexa 555 (dsRed2), were measured using a Chemidoc Imager (Bio-Rad). Data was subsequently processed and quantified (relative quantification using a t = 0 h band as the reference; results in Tables S7 – S14) using ImageLab software (Bio-Rad).

Lac* operon dependent overexpression protocol for ovalbumin:** The gene for ovalbumin (hereafter referred to as OVA, accession number V00383) was cloned into the pMCSG7 vector as described elsewhere[51] and transformed into the methionine auxotroph expression strain, namely *E.coli* B834(DE3) (met-aux, Genotype: F- ompT hsdSB (rB- mB-) gal dcm met(DE3), Novagen #ref 69041). The construct contained an N-terminal M<u>HHHHHH</u>SSGVDLGTENLYFG***SNA sequence for Ni-NTA purification (underlined) and a TEV-cleavage (italic bold) site. The protein was expressed from the overnight culture of a single colony. Briefly, 10 mL of this overnight culture (Ampicillin 50 µg/mL, 1% Glucose v/v, 18 h, 37°C, and 150 rpm) was used for the inoculation per 100 mL LB medium (Ampicillin 50 µg/mL, 37°C, 150 rpm). The cells were grown to an optical density at 600 nm, OD_{600}, of 0.6-1.0, washed twice (sedimented 3428 rcf, 15 min, 4°C) to remove excess glucose and resuspended with LB medium (Ampicillin 50 µg/mL) prior to the addition of the corresponding inducer (IPTG **13**, IPG **15** and its TCO caged and CCO caged derivatives).

***Lac* operon dependent overexpression protocol for dsRed and GFP:** To obtain pET16b_GFP and pET16b_DsRed2_S4T constructs, DNA fragments encoding the fluorophores were amplified by PCR. Using this PCR reaction, DsRed2 was mutated to DsRed2_S4T, to enhance the fluorescent signal.[52] GFP was derived from ATCC construct 25922.[53] The resulting fragments were ligated into the pET16b vector using the NcoI and BamHI restriction sites. All sequences were verified by Sanger sequencing (Macrogen).

primer ID	sequence 5' → 3'
T7_GFP_fwd	GGCGGCCGTCTCCCATGAGTAAAGGAGAAGAAC
T7_GFP_rev	GGCGGCGGATCCTTATTTGTATAGTTCATCC
T7_DsRed2_S4T_fwd	GGCGGCCGTCTCCCATGGCCTCCACCGAGAACG
T7_DsRed2_rev	GGCGGCCGTCTCGGATCCTTTATCTAGATCCGGTGG

fwd: forward, rev: reverse

Both constructs were transformed into B834(DE3) expression strain and the protein was expressed from the overnight culture of a single colony. 5-10 mL of this overnight culture (Ampicillin 50 µg/mL, 1% Glucose v/v, 18 h, 37°C, and 150 rpm) was used for the inoculation per 50-100 mL LB medium (Ampicillin 50 µg/mL, 37°C, 150 rpm). The cells were grown to an optical density at 600 nm, OD_{600}, of 0.6-1.0, washed twice (sedimented 3428 rcf, 15 min, 4°C) to remove excess glucose and resuspended with LB medium (Ampicillin 50 µg/mL) prior to the addition of the corresponding inducer (IPTG **13**, IPG **15** and its TCO caged and CCO caged derivatives).

Experiment 1: Induction of expression with IPTG or IPG – Figure S2: Ovalbumin was expressed as described above. For the induction, IPTG (**13**) or IPG (**15**) were used at 1 mM final concentration (stock dissolved in water 0.1 M). Samples were taken before (t = 0 h) and after (t = 1, 2, 3, 4 h and overnight) the addition of the inducer, centrifuged and pellets were dissolved in 20 µL of H_2O and 10 µL of 2x sample loading buffer. 15 µL of sample was loaded to SDS gel and analyzed as described above.

Experiment 2: Impact of DMSO on expression – Figure S3: For the induction, IPG (**15**) was used at 1 mM final concentration with varying DMSO concentrations (0.1, 1, 5 and 10% v/v). Samples were taken before (t = 0 h) and after (t = 3 h and overnight) the addition of the inducer, centrifuged and pellets were dissolved in 30 µL of H_2O and 30 µL of 2x sample loading buffer. 15 µL of sample was loaded to SDS gel and analyzed as described above.

Experiment 3A: Inhibition of OVA expression with 3-CCO-IPG – Figure S4: To check the degree of inhibition, 3-CCO-IPG (**19**) was used at distinct concentrations varying from 1, 0.5, 0.25, 0.125 mM final concentration (stock dissolved in DMSO 0.1 M). Positive (1% v/v glucose, 1% v/v DMSO) and negative controls (1% v/v DMSO) were included. Samples were taken before (t = 0 h) and after (t = 4 h and overnight) the addition of the inducer, centrifuged and pellets were dissolved in 30 µL of H_2O and 30 µL of 2x sample loading buffer. 15 µL of sample was loaded to SDS gel and analyzed as described above.

Experiment 3B: Impact of caged 3-TCO-IPG on OVA expression – Figure S4: To determine the impact of caged 3-TCO-IPG (**25**) on OVA expression levels, standard expression protocol was used. 3-TCO-IPG (**25**) was then added at distinct concentrations varying from 1, 0.5, 0.25, 0.125 mM final concentration (stock dissolved in DMSO 0.1 M). Positive (1% v/v glucose, 1% v/v DMSO) and negative controls (1% v/v DMSO) were included. Samples were taken before (t = 0 h) and after (t = 4 h and overnight) the addition of the inducer, centrifuged and pellets were dissolved in 30 µL of H_2O and 30 µL of 2x sample loading buffer. 15 µL of sample was loaded to SDS gel and analyzed as described above.

Experiment 4: Impact of tetrazine 26 on expression – Figure S5: For the induction, IPG (**15**) was used at 1 mM final concentration with 3,6-dimethyl-tetrazine (**26**) to mimic uncaging conditions (2.5 mM final concentration in DMSO). Samples were taken before (t = 0 h) and after (t = 1, 2, 3, 4 h and overnight) the addition of the inducer, centrifuged and pellets were dissolved in 30 µL of H_2O and 30 µL of 2x sample loading buffer. 15 µL of sample was loaded to SDS gel and analyzed as described above.

Experiment 5: Temporal control of ovalbumin expression via decaging of 3-TCO-IPG (25) – Figure 2C-D: For the expression, general ovalbumin expression protocol outlined in this section was utilized. Four different samples of each 10 mL were induced as follows: To all samples 3-TCO-IPG (**25**) was added in 1 mM final concentration (in DMSO). First sample was directly reacted with 3,6-dimethyl-tetrazine (DMT, **26**; 2.5 mM final concentration in DMSO), second sample after 1 h of expression and third sample after 2 h. The fourth sample served as a control not containing any DMT. Samples were taken before (t = 0 h) and after (t = 1 h, 2 h, 3 h, 5 h and overnight) adding **25** and launching the experiment, centrifuged and pellets were dissolved in 30 μL of H_2O and 30 μL of 2x sample loading buffer. 10 μL of sample was loaded to SDS gel and analyzed as described above.

Experiment 6: Comparison of inhibitory levels of 3-CCO-IPG and 6-CCO-IPG – Figure 2-B: 3-CCO-IPG (**19**) and 6-CCO-IPG (**20**) were compared with respect to their degree of inhibition on ovalbumin expression. Both caged IPGs were used at a final concentration of 1 mM (stock dissolved in DMSO 0.1 M). IPG (**15**, 1 mM) and DMSO (1% v/v) were used as positive and negative control conditions, respectively. Samples were taken before (t = 0 h) and after (t = 2, 4 h and overnight) the addition of the conditions, centrifuged and pellets were dissolved in 30 μL of H_2O and 30 μL of 2x sample loading buffer. 15 μL of sample was loaded to SDS gel and analyzed as described above.

Experiment 7: Replicate expression experiments for OVA (Figure 3A): An overnight culture of B834(DE3) containing pMSCG7_Ova was diluted 1:100 in LB medium supplemented with 50 μg/mL ampicillin and 1% glucose. Cells were grown at 37°C, 180 rpm to an OD_{600} of ~0.6-1.0 and sedimented (3428 rcf, 10 min, 4°C) before being resuspended in LB medium containing 50 μg/mL ampicillin. Cultures of 3 mL were induced with either compound **25** (1 mM), followed by the addition of **26** (2.5 mM) at t = 1 h, compound **25** (1 mM), compound **15** (1 mM) or DMSO (vehicle control; 1% *v/v*), an uninduced sample was taken along as a true negative control. Samples were taken ((0.2 / OD_{600}) x 1000 μL) before (t = 0 h) and after (t = 1 h, 2 h, 3 h, 5 h and overnight) starting the experiment, centrifuged and pellets were dissolved in 50 μL of 1*Laemmli buffer supplemented with Benzonase (0.2 U/μL). Subsequently, dissolved samples were incubated for 5 min at 90°C for denaturation and briefly centrifuged. 10 μL of each sample was resolved over a 10% SDS-PAGE (0.75 mm) along with 10 μL PageRuler™ Plus Protein Marker (Thermo Scientific) for 70 min at 180 V. Coomassie staining (Coomassie Brilliant Blue G-250) was used for protein analysis and resulted in the graph (representing N = 3) shown in Figure 2E, using t = 0 h as the reference.

Experiment 8: Replicate expression experiments for eGFP (Figure 3B): An overnight culture of B834(DE3) containing pET16b_eGFP was diluted 1:100 in LB medium supplemented with 50 μg/mL ampicillin and 1% glucose. Cells were grown at 37°C, 180 rpm to an OD_{600} of ~0.6-1.0 and sedimented (3428 rcf, 10 min, 4°C) before being resuspended in LB medium containing 50 μg/mL ampicillin. Cultures of 3 mL were induced with either compound **25** (1 mM), followed by the addition of **26** (2.5 mM) at t = 1 h, compound **25** (1 mM), compound **15** (1 mM) or DMSO (vehicle control; 1% *v/v*), an uninduced sample was taken along as a true negative control. Samples were taken ((0.4 / OD_{600}) x 1000 μL) before (t = 0 h) and after (t = 1 h, 2 h, 3 h, 5 h and overnight)

starting the experiment, centrifuged and pellets were dissolved in 100 μL of 1*Laemmli buffer (without β-mercaptoethanol) supplemented with Benzonase (0.4 U/μL). Subsequently, dissolved samples were incubated for 5 min at 37°C and briefly centrifuged. 10 μL of each sample was resolved over a 10% SDS-PAGE (0.75 mm) along with 10 μL PageRuler™ Plus Protein Marker (Thermo Scientific) for 70 min at 180 V. Coomassie staining (Coomassie Brilliant Blue G-250) was used for protein analysis) after scanning Cy2, Cy3 and Cy5 multichannel settings (532/528, 605/50 and 695/55 filters, respectively; ChemiDoc™ MP System, Bio-Rad). This resulted in the graph (representing N = 4) shown in Figure 2F, using t = 0 h as the reference.

Experiment 9: Induction of dsRED2 expression with temporal chemical control – Figure S6: dsRed2 was cloned and expressed as described above. For the induction, optimal conditions from Experiment 5 were used (addition of **25** at t = 0 h and at 1.0 mM final concentration in DMSO; addition of DMT (**26**) after 1 h and at 2.5 mM final concentration in DMSO). Samples were taken before (t = 0 h) and after (t = 1 h, 2 h, 3 h, 5 h and overnight) the addition of **25**, centrifuged and pellets were dissolved in 30 μL of H_2O and 30 μL of 2x sample loading buffer. 15 μL of sample was loaded to SDS gel (10%) and analyzed as described above. In-gel fluorescence was measured at the wavelength filter for Alexa 555 (dsRed) prior to Coomassie staining.

6.8 References

[1]   J. Li, P. R. Chen, *Nat. Chem. Biol.* **2016**, *12*, 129–137.

[2]   J. Tu, M. Xu, R. M. Franzini, *ChemBioChem* **2019**, *20*, 1615–1627.

[3]   K. Neumann, A. Gambardella, M. Bradley, *ChemBioChem* **2019**, *20*, 872–876.

[4]   N. K. Devaraj, *ACS Cent. Sci.* **2018**, *4*, 952–959.

[5]   R. M. Versteegen, R. Rossin, W. ten Hoeve, H. M. Janssen, M. S. Robillard, *Angew. Chem. Int. Ed.* **2013**, *52*, 14112–14116.

[6]   M. L. Blackman, M. Royzen, J. M. Fox, *J. Am. Chem. Soc.* **2008**, *130*, 13518–13519.

[7]   J. C. T. Carlson, H. Mikula, R. Weissleder, *J. Am. Chem. Soc.* **2018**, *140*, 3603–3612.

[8]   R. M. Versteegen, W. ten Hoeve, R. Rossin, M. A. R. de Geus, H. M. Janssen, M. S. Robillard, *Angew. Chem. Int. Ed.* **2018**, *57*, 10494–10499.

[9]   B. L. Oliveira, Z. Guo, G. J. L. Bernardes, *Chem. Soc. Rev.* **2017**, *46*, 4895–4950.

[10]   J. Li, S. Jia, P. R. Chen, *Nat. Chem. Biol.* **2014**, *10*, 1003–1005.

[11]   G. Zhang, J. Li, R. Xie, X. Fan, Y. Liu, S. Zheng, Y. Ge, P. R. Chen, *ACS Cent. Sci.* **2016**, *2*, 325–331.

[12]   J. Zhao, Y. Liu, F. Lin, W. Wang, S. Yang, Y. Ge, P. R. Chen, *ACS Cent. Sci.* **2019**, *5*, 145–152.

[13]   R. Rossin, R. M. Versteegen, J. Wu, A. Khasanov, H. J. Wessels, E. J. Steenbergen, W. ten Hoeve, H. M. Janssen, A. H. A. M. van Onzen, P. J. Hudson, M. S. Robillard, *Nat. Commun.* **2018**, *9*, 1484.

[14]   R. Rossin, S. M. J. van Duijnhoven, W. ten Hoeve, H. M. Janssen, F. J. M. Hoeben, R. M. Versteegen, M. S. Robillard, *Bioconjug. Chem.* **2016**, *27*, 1697–1706.

[15]   S. Du, D. Wang, J.-S. Lee, B. Peng, J. Ge, S. Q. Yao, *Chem. Commun.* **2017**, *53*, 8443–8446.

[16]   I. Khan, L. M. Seebald, N. M. Robertson, M. V. Yigit, M. Royzen, *Chem. Sci.* **2017**, *8*, 5705–5712.

[17]   Q. Yao, F. Lin, X. Fan, Y. Wang, Y. Liu, Z. Liu, X. Jiang, P. R. Chen, Y. Gao, *Nat. Commun.* **2018**, *9*, 5032.

[18]   J. M. Mejia Oneto, I. Khan, L. Seebald, M. Royzen, *ACS Cent. Sci.* **2016**, *2*, 476–482.

[19]   M. Czuban, S. Srinivasan, N. A. Yee, E. Agustin, A. Koliszak, E. Miller, I. Khan, I. Quinones, H. Noory, C. Motola, R. Volkmer, M. Di Luca, A. Trampuz, M. Royzen, J. M. Mejia Oneto, *ACS Cent. Sci.* **2018**, *4*, 1624–1632.

[20] S. Davies, L. Qiao, B. L. Oliveira, C. D. Navo, G. Jiménez-Osés, G. J. L. Bernardes, *ChemBioChem* **2019**, *20*, 1541–1546.

[21] S. Davies, B. L. Oliveira, G. J. L. Bernardes, *Org. Biomol. Chem.* **2019**, *17*, 5725–5730.

[22] E. Jiménez-Moreno, Z. Guo, B. L. Oliveira, I. S. Albuquerque, A. Kitowski, A. Guerreiro, O. Boutureira, T. Rodrigues, G. Jiménez-Osés, G. J. L. Bernardes, *Angew. Chem. Int. Ed.* **2017**, *56*, 243–247.

[23] K. Neumann, S. Jain, A. Gambardella, S. E. Walker, E. Valero, A. Lilienkampf, M. Bradley, *ChemBioChem* **2017**, *18*, 91–95.

[24] H. Wu, S. C. Alexander, S. Jin, N. K. Devaraj, *J. Am. Chem. Soc.* **2016**, *138*, 11429–11432.

[25] M. Royzen, G. P. A. Yap, J. M. Fox, *J. Am. Chem. Soc.* **2008**, *130*, 3760–3761.

[26] S. Fletcher, *Org. Chem. Front.* **2015**, *2*, 739–752.

[27] F. Guibe, Y. S. M'leux, *Tetrahedron Lett.* **1981**, *22*, 3591–3594.

[28] J. Muzart, *Tetrahedron* **2005**, *61*, 5955–6008.

[29] A. R. Haight, E. J. Stoner, M. J. Peterson, V. K. Grover, *J. Org. Chem.* **2003**, *68*, 8092–8096.

[30] F. Cramer, N. Hennrich, *Chem. Ber.* **1961**, *94*, 976–989.

[31] H.-P. Wessel, T. Iversen, D. R. Bundle, *J. Chem. Soc. Perkin Trans. 1* **1985**, 2247-2250.

[32] F. Jacob, J. Monod, *J. Mol. Biol.* **1961**, *3*, 318–356.

[33] M. Lewis, *C. R. Biol.* **2005**, *328*, 521–548.

[34] C. E. Bell, M. Lewis, *Nat. Struct. Biol.* **2000**, *7*, 209–214.

[35] M. Lewis, *J. Mol. Biol.* **2013**, *425*, 2309–2316.

[36] D. D. Young, A. Deiters, *Angew. Chem. Int. Ed.* **2007**, *46*, 4290–4292.

[37] S. L. Collins, J. Saha, L. C. Bouchez, E. M. Hammond, S. J. Conway, *ACS Chem. Biol.* **2018**, *13*, 3354–3360.

[38] K. P. R. Kartha, M. Aloui, R. A. Field, *Tetrahedron Lett.* **1996**, *37*, 8807–8810.

[39] S. Kobayashi, K. Fukuda, M. Kataoka, M. Tanaka, *Macromolecules* **2016**, *49*, 2493–2501.

[40] M. Heuckendorff, H. H. Jensen, *Carbohydr. Res.* **2017**, *439*, 50–56.

[41] A. Darko, S. J. Boyd, J. M. Fox, *Synthesis* **2018**, *50*, 4875–4882.

[42]   L. Liu, Y. Liu, G. Zhang, Y. Ge, X. Fan, F. Lin, J. Wang, H. Zheng, X. Xie, X. Zeng, P. R. Chen, *Biochemistry* **2018**, *57*, 446–450.

[43]   A. M. F. van der Gracht, M. A. R. de Geus, M. G. M. Camps, T. J. Ruckwardt, A. J. C. Sarris, J. Bremmers, E. Maurits, J. B. Pawlak, M. M. Posthoorn, K. M. Bonger, D. V. Filippov, H. S. Overkleeft, M. S. Robillard, F. Ossendorp, S. I. van Kasteren, *ACS Chem. Biol.* **2018**, *13*, 1569–1576.

[44]   S. Kobayashi, L. M. Pitet, M. A. Hillmyer, *J. Am. Chem. Soc.* **2011**, *133*, 5794–5797.

[45]   N. Becker, E. M. Carreira, *Org. Lett.* **2007**, *9*, 3857–3858.

[46]   T. Maji, J. A. Tunge, *Org. Lett.* **2015**, *17*, 4766–4769.

[47]   H.-K. Kim, K.-J. J. Park, *Tetrahedron Lett.* **2012**, *53*, 4090–4092.

[48]   Y. Du, M. Zhang, F. Yang, G. Gu, *J. Chem. Soc. Perkin Trans. 1* **2001**, 3122–3127.

[49]   G. A. van der Marel, J. D. C. Codée, P. Kovác, *Carbohydrate Chemistry: Proven Synthetic Methods, Volume 2*, **2014**.

[50]   X. Geng, L. Wang, G. Gu, Z. Guo, *Carbohydr. Res.* **2016**, *427*, 13–20.

[51]   N. Del Cid, L. Shen, J. BelleIsle, M. Raghavan, *PLoS One* **2012**, *7*, e41727.

[52]   M. Sörensen, C. Lippuner, T. Kaiser, A. Mißlitz, T. Aebischer, D. Bumann, *FEBS Lett.* **2003**, *552*, 110–114.

[53]   D. M. van Elsland, E. Bos, W. de Boer, H. S. Overkleeft, A. J. Koster, S. I. van Kasteren, *Chem. Sci.* **2016**, *7*, 752–758.

Summary and future prospects

The inverse electron demand Diels-Alder (IEDDA) pyridazine elimination[1] emerged in 2013 as a new bioorthogonal reaction and constitutes a prime example of what is now known as dissociative bioorthogonal chemistry.[2–4] The research described in this Thesis aims to develop synthetic strategies which enable the IEDDA pyridazine elimination to be applied as a versatile toolbox in chemical biology studies. More specifically, it entails modification of antigenic (MHC-I) peptides and (CD1d) glycolipids with a *trans*-cyclooctene (TCO) moiety to allow chemical control over the recognition of these biomolecules by immune cells. Synthetic advances which encompass the entire scope of the IEDDA pyridazine elimination are additionally described.

Chapter 1 introduces the IEDDA pyridazine elimination within the context of dissociative bioorthogonal chemistry. Mechanistic aspects of the reaction are discussed, as well as various applications where this technique has been utilized. An overview of other novel bioorthogonal bond cleavage reactions is presented.
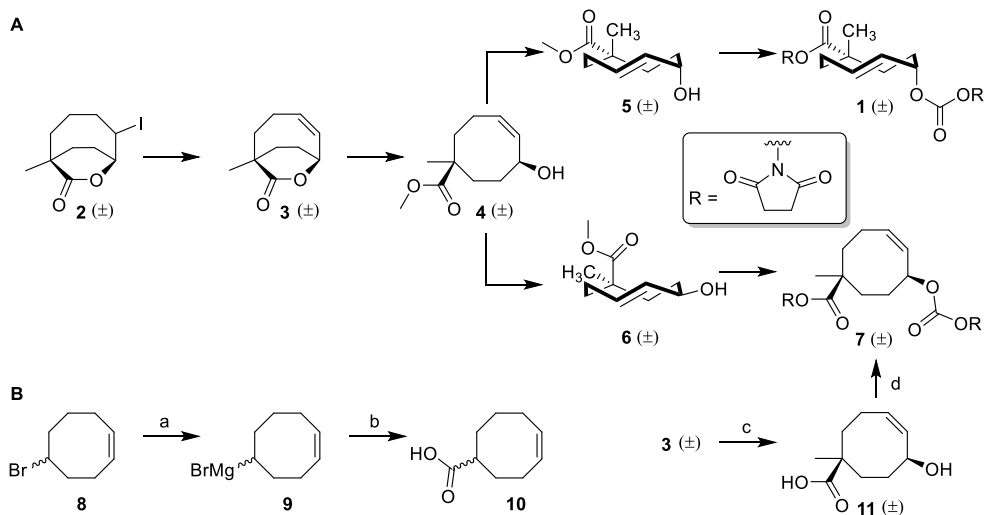
Scheme 1 A) Key intermediates in the synthesis of TCO reagent **1** and CCO reagent **7** from 1,5-cyclooctadiene as presented in Chapter 2. B) Reagents/conditions (Thurecht and co-workers)[7]: (a) Mg, THF, I$_2$, reflux; (b) CO$_2$, 65% over 2 steps; (c) KOH, MeOH; (d) N,N'-disuccinimidyl carbonate, DIPEA, MeCN, rt, 28% over 2 steps.

Chapter 2 describes a streamlined synthesis of bifunctional TCO reagent (**1**) which has been extensively applied for click to release chemistry (Scheme 1).[5,6] A key modification of existing literature procedures features the crystallization of iodolactone **2** after initial functionalization of 1,5-cyclooctadiene. Transesterification of bicyclic lactone **3** was replaced by a one pot, two step saponification-methylation procedure to obtain methyl ester **4**. Photoisomerization afforded a mixture of **5** and **6**, which could be separated after selective saponification of **5**. Bis-NHS functionalization to obtain **1** was accelerated using nucleophilic catalysis. The unprecedented *cis*-cyclooctene (CCO) reagent (**7**) was obtained by functionalization and *trans*-to-*cis* isomerization of **6**. Additionally, reagent **1** was equipped with an EDANS fluorophore and a DABCYL quencher to obtain a fluorogenic TCO-reporter-quencher probe for kinetic analysis of the IEDDA pyridazine elimination.[6]

Another route to obtain **1** was published by Thurecht and co-workers.[7] Instead of employing cyanide substitution, they converted cyclooctene bromide **8** into the corresponding Grignard reagent (**9**), which was treated with CO$_2$ to obtain cyclooctene carboxylic acid **10** in 65% yield over two steps. This alternative route to intermediate **10** is projected to improve the synthetic accessibility of iodolactone **2**. Additionally, the two step synthesis of CCO reagent **7** is reported from bicyclic lactone **3** in 28% yield.[7] While this finding confirms the intramolecular cyclization observed for the attempted functionalization of carboxylic acid **11**, it also shows that small quantities of CCO reagent **7** can be obtained directly.
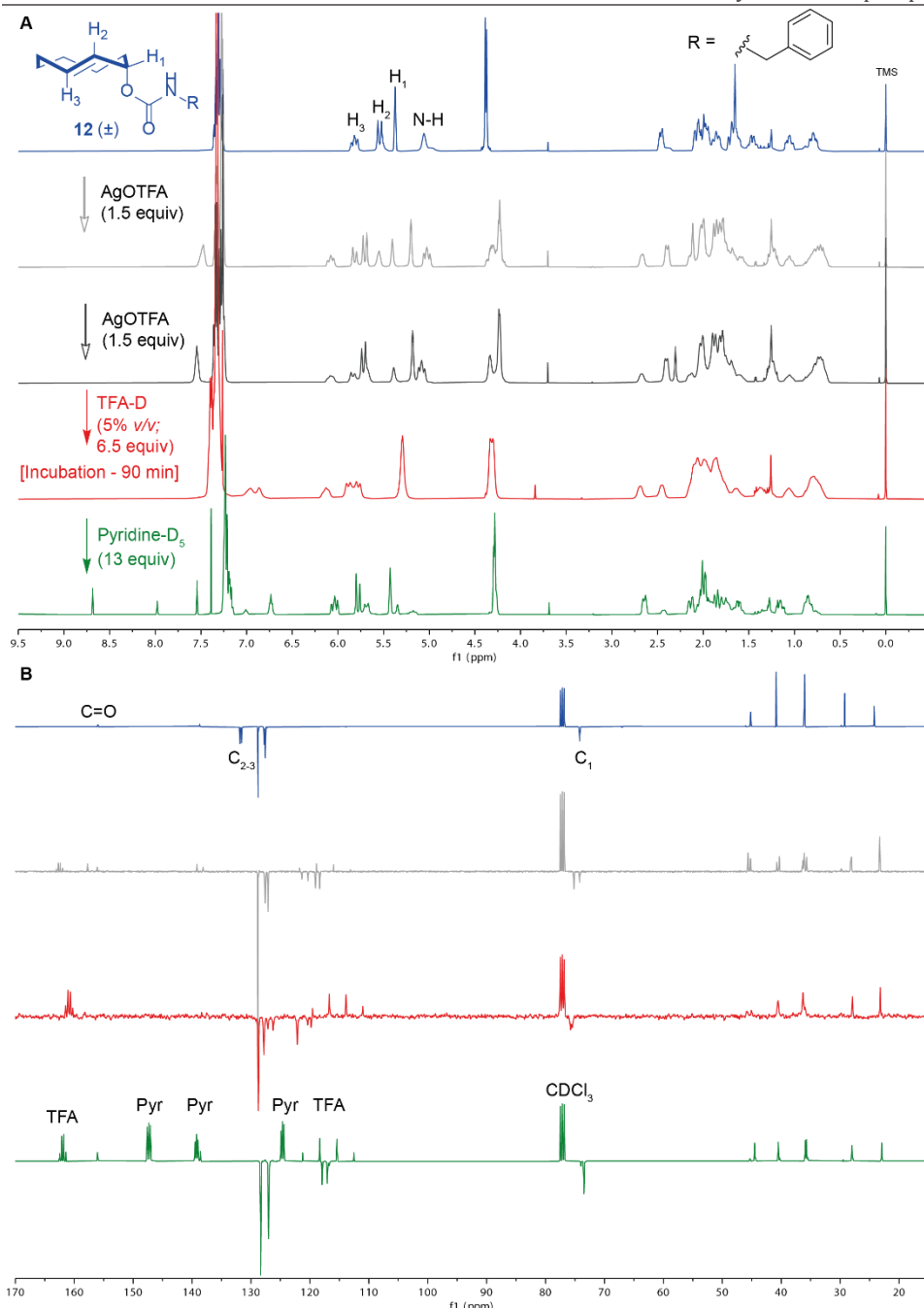
Figure 1 Stacked ^{1}H (A; δ 9.5/-0.5 ppm) and ^{13}C-APT (B; 170/15 ppm) NMR spectra of model TCO carbamate **12** before and upon treatment with AgOTFA (1.5 equiv; then another 1.5 equiv), followed by exposure to TFA-D (5% *v/v* in CDCl$_3$; 6.5 equiv). After 90 minutes, the mixture was quenched by adding pyridine-D$_5$ (13 equiv). Experiments in Chapter 3 (without AgOTFA addition) exposed **12** to 5/10/20% *v/v* TFA-D, resulting in an estimated stability of 94/75/<10%.
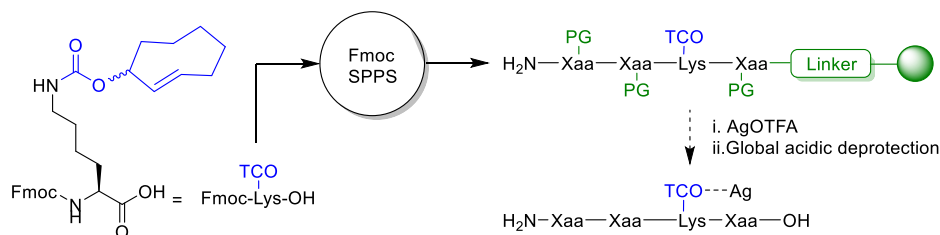
Figure 2 Proposed updated synthetic strategy for an Fmoc SPPS-based strategy for TCO-modified peptide synthesis. PG = protecting group; Xaa = unspecified amino acid.

Chapter 3 describes the attempted development of an Fmoc SPPS-based strategy for TCO-modified peptide synthesis. A model axial allylic substituted TCO carbamate (Figure 1, **12**) was studied in the presence of TFA-D using ^{1}H and ^{13}C NMR. The observed stability under dilute TFA concentrations (< 10% *v/v*) was attributed to preferential protonation on C_3 and anchimeric assistance of the carbamate moiety towards C_2 of the cationic species. An Fmoc-Lys(TCO)-OH building block was synthesized and incorporated in the SIINFEKL peptide sequence on solid support. Global deprotection of this peptide led to substantial TCO isomerization and carbamate hydrolysis, even under dilute TFA concentrations (for instance 5% *v/v*) which appeared to be tolerated in the NMR stability experiments.

Another approach to minimize isomerization of the *trans*-double bond would be to apply conditions which stabilize this moiety in the presence of acids such as TFA. It has been established that complexation of $AgNO_3$ with TCO readily occurs over binding with CCO.[8,9] This energetically favored metal complexation has previously been exploited for extractive separations,[10] but also for the isolation of TCO during photochemical synthesis[11] and to prolong the shelf-life of conformationally unstable TCOs after synthesis.[12,13] It was hypothesized that the formation of a silver-TCO complex could act as a temporary protecting group during global acidic deprotection of the peptide sequence from the solid support. Model allylic TCO **12** was treated with AgOTFA (3.0 equivalents) to obtain a diastereomeric mixture of axial TCO carbamate-Ag complexes on ^{1}H and ^{13}C NMR (Figure 1 A/B). Subsequent addition of TFA-D (5% *v/v* in CDCl$_3$; 6.5 equivalents) led to the appearance of a species which was distinct from the cationic species observed for the experiments described in Chapter 3. Furthermore, after the mixture was quenched by adding pyridine-D$_5$ (13 equivalents), the resulting allylic TCO appeared to be present as the TCO-Ag complex. The results of this initial NMR experiment may provide a basis for further investigations to improve the strategy proposed in Chapter 3 with the addition of AgOTFA during global acidic deprotection of peptides (Figure 2).
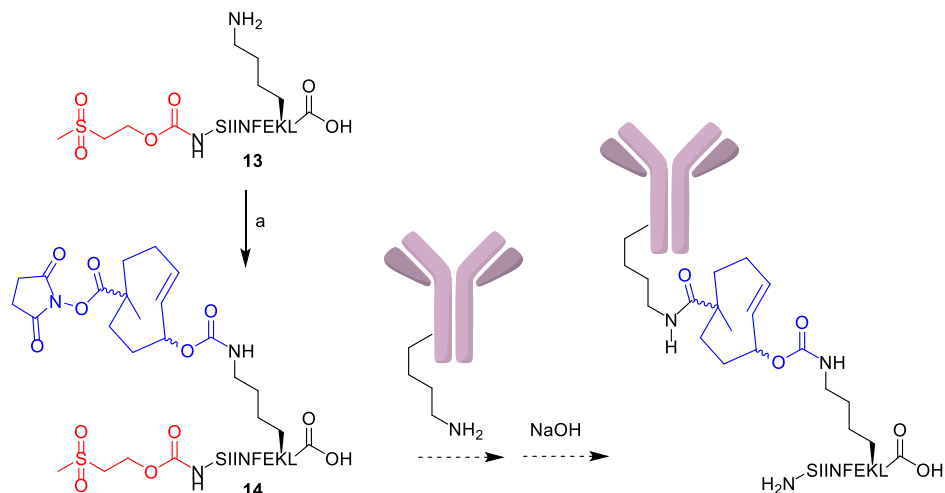
Figure 3 Proposed strategy for conjugation of caged epitopes with antibodies for improved tissue specificity of T-cell activation. Reagents/conditions: (a) NHS-bTCO (Chapter 2; **1**), DIPEA, DMF, rt, 12%.

Chapter 4 reports a new method for chemical control over T-cell activation *in vitro* and *in vivo*. MHC-I epitopes were designed with allylic substituted TCO modification on lysine residues on the premise that this modification would obstruct recognition of such epitopes by T-cells, whilst the IEDDA pyridazine elimination could selectively restore this recognition event. In contrast to the attempted synthetic method described in Chapter 3, the MHC-I peptide sequence was synthesized using Fmoc SPPS before installing the TCO moiety. N-terminal protection with the base-labile MSc-group before acidic cleavage of the peptide sequence enabled regioselective TCO modification of the ε-amino group of lysine. MSc deprotection under basic conditions was followed by HPLC purification to obtain the desired caged epitopes. Lysine-caged epitopes of OVA$_{257-264}$ (OT-I, SIINFEKL) and D^{b}M$_{187-195}$ (NAITNAKII) displayed binding to MHC-I whilst T-cell recognition was absent. IEDDA pyridazine elimination effectively restored T-cell activation *in vitro* and *in vivo*. In addition, the 'click to release' approach was applied to study antigen cross presentation with an N-terminally extended epitope, OVA$_{247-264}$ (DEVSGLEQLESIINFEKL).

Future developments are aimed to improve the spatiotemporal control by which the antigen recognition is switched on. This is especially important for *in vivo* experiments where high tissue specificity is desired. One way to achieve this is to attach a targeting moiety to the caged MHC-I antigen. In this regard, the bifunctional TCO scaffold initially employed to add an additional polar functionality can be repurposed to enable, for instance, the conjugation of an antibody to the caged antigen (Figure 3). To this end, MSc-SIINFEKL (Chapter 4; **13**) was reacted with bifunctional NHS-TCO (Chapter 2; **1**),

followed by HPLC purification of the resulting NHS-ester (**14**) as a reagent for lysine conjugation. Conversely, the conjugation of an antibody to a tetrazine represents an alternative strategy for tissue specific decaging, as previously shown by Du *et al.*[14]

In vitro deprotection experiments in Chapter 4 revealed 3,6-dipyrimidinyl-tetrazine does not induce detectable elimination upon IEDDA ligation. An *in vitro* 'blocking and decaging' approach, where IEDDA ligation events with a non-elimination tetrazine are followed by a kinetic window before uncaging with a regular tetrazine, would be especially valuable to delineate antigen cross presentation. In order for such a strategy to succeed, however, the 'blocking' tetrazine employed must perform IEDDA ligation on the cell surface without also affecting caged antigens which are still being processed inside the antigen presenting cell (APC). It was reasoned that (sufficiently large) polymer-modified tetrazines[15] could prevent passive cellular diffusion and would therefore enable the envisioned kinetic antigen cross presentation experiments. The addition of an exocyclic *para*-amino group on 2-pyridine and/or 2-pyrimidine substituents of electron poor tetrazines was assessed as a suitable conjugation handle for this purpose.

Cyclization of 5-amino-2-pyridine carbonitrile (**15**) and 2-pyridine carbonitrile in the presence of hydrazine hydrate afforded a crude dihydrotetrazine mixture. Subsequent oxidation in the presence of (diacetoxyiodo)benzene (BAIB)[16] afforded a mixture of **16**[17] and **17** which were separated using silica gel chromatography (Scheme 2). Acylation of **16** in the presence of glutaric anhydride required extended reaction times and a large excess of reagent to obtain **18**. Boc-protected nitrile **19** was reacted with 2-pyrimidine carbonitrile in the presence of hydrazine hydrate to obtain dihydrotetrazine **20**, which was readily isolated using silica gel chromatography. Subsequent oxidation with BAIB afforded tetrazine **21**. Deprotection of the Boc group in a mixture of HCl and dioxane afforded a complex mixture of products.

It is projected that installation of the amide bond before initiating formation of the (dihydro)tetrazine, as described by Maggi *et al.*,[18] would enhance isolation of the desired product and circumvent the poor nucleophilicity of the *para*-amino group. Conjugation of **15** and glutaric anhydride afforded **22**[18] in 80% yield. Cyclization of **22** with 2-pyridimidine carbonitrile and subsequent oxidation with BAIB would result in tetrazine **23**. In a similar manner, conjugation of 5-amino-2-cyanopyrimidine (**24**) with glutaric anhydride would afford **25**, which could be used to obtain tetrazine **26**. Tetrazines **18, 23** and **26** would be amenable for conjugation with amino functionalized dextran polymers.[5]
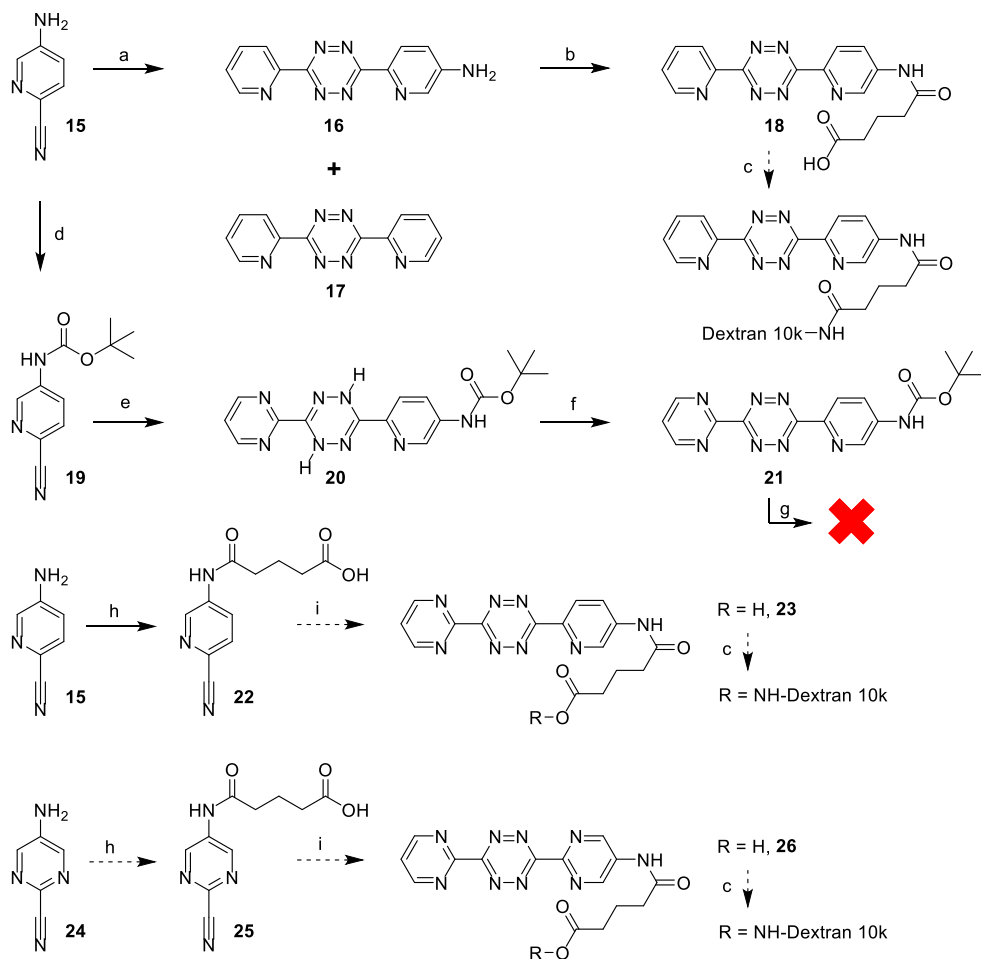
Scheme 2 Attempted and projected syntheses of electron poor tetrazines for polymer conjugation. Reagents/conditions: (a) *i.* 2-pyridine carbonitrile, hydrazine hydrate, 90°C, 59%. *ii.* BAIB, DCM, rt, 10% (**16**); (b) glutaric anhydride, THF, 70°C, 64%; (c) amino dextran 10kDa, N-methyl morpholine, PyBOB, DMSO, rt; (d) Boc₂O, Et₃N, DMAP, THF, 60°C, 46%; (e) pyrimidine-2-carbonitrile, hydrazine hydrate, dioxane, 90°C, 43%; (f) BAIB, DCM, rt, 72%; (g) HCl, dioxane, rt; (h) glutaric anhydride, dioxane, 80°C, 80% (**22**); (i) *i.* pyrimidine-2-carbonitrile, hydrazine hydrate, 90°C. *ii.* BAIB, DCM, rt.

Chapter 5 describes the design and synthesis of TCO caged derivatives of α-galactosylceramide (αGalCer; Scheme 3A, **27**) and α-galactosylphytosphingosine (αGalPhs; Scheme 3A, **28**). The self-adjuvanting strategy by Painter, Hermans and co-workers,[19] where an inactive pro-αGalcer rearranges into αGalcer upon esterase or protease activity, formed the basis for the design of this approach to obtain chemically induced activation of invariant natural killer T-cells (iNKT cells). It was reasoned that the amine functionality of αGalPhs could be protected as a TCO carbamate and that subsequent acylation with hexacosanoic acid would result in a TCO caged pro-αGalcer. Key steps in the synthesis included an α-selective glycosylation under NIS/TMSOTf activation, using a 2,3-TBS-4,6-DTBS protected thiogalactoside donor and a 2-azido-3,4-cyclic carbonate protected phytosphingosine acceptor, followed by hydrogenation, TCO carbamate formation and saponification. Direct desilylation afforded the TCO protected αGalPhs (**28**), whereas esterification and subsequent deprotection gave the TCO protected pro-αGalcer (**27**).

Pending the immunological evaluation of compounds **27** and **28** in presence and absence of a tetrazine activator, it would be of interest to attach an MHC-I peptide antigen onto the caged glycolipid, thereby obtaining a covalent glycolipid-peptide vaccine which can be activated using 'click to release' chemistry. This would be synthetically feasible by combining the established synthetic route of Chapter 5 with the bifunctional TCO presented in Chapter 2 (**1**) and 2-(aminooxy)acetyl-FFRKSIINFEKL[19] to obtain αGalPhs-TCO-FFRKSIINFEKL (Scheme 3B, **29**). Functionalization of α-galactosylated azido phytosphingosine **30** would have to be slightly adjusted towards this synthetic strategy. Saponification of **30** to obtain diol **31** would be followed by Staudinger reduction of the azide to obtain **32**. This would then allow the introduction of the bifunctional TCO moiety to obtain **33** without inducing hydrolysis of the sterically hindered NHS-ester under alkaline conditions. Desilylation may then afford intermediate **34**, which can subsequently undergo selective conjugation of the NHS-ester with the hydroxylamine functionality to obtain **29**. Additionally, it would be of interest to extend this proposed synthetic scheme with the regioselective acylation of **33** in the presence of hexacosonoic acid to obtain **35**. Organoborinate catalysis[20–22] may offer enhanced conversion and regioselectivity for this step without compromising the NHS-ester. Desilylation would then afford **36**, which can undergo selective hydroxylamine conjugation to obtain αGalCer-TCO-FFRKSIINFEKL (**37**).
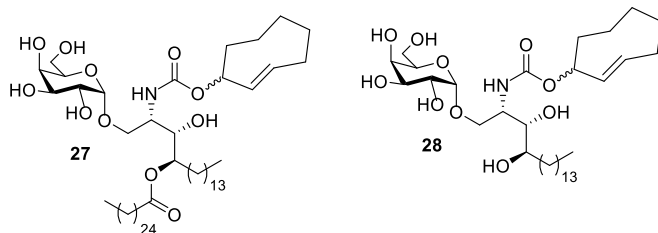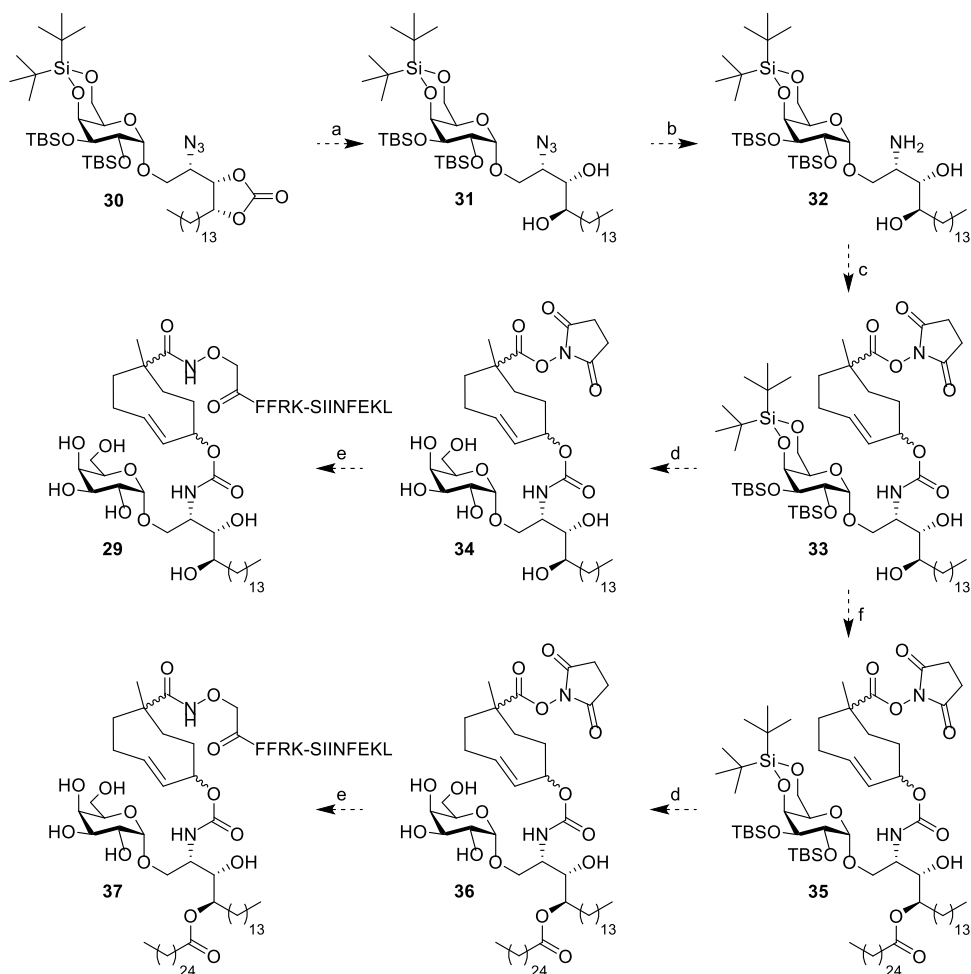
Scheme 3 A) TCO caged αGalcer (**27**) and αGalPhs (**28**) probes described in Chapter 5. B) Proposed synthesis of a TCO caged αGalPhs-MHC-I peptide conjugate (**29**) and αGalCer-MHC-I peptide conjugate (**37**). Reagents/conditions: (a) LiOH, THF, H$_2$O, 0° to rt; (b) *i.* trimethylphosphine, THF, rt. *ii.* NaOH, H$_2$O, rt; (c) **1**, DIPEA, DMF, rt; (d) Et$_3$N · 3HF, THF, rt; (e) 2-(aminooxy)acetyl-FFRKSIINFEKL, MeOH, THF, H$_2$O, rt; (f) *i.* hexacosanoic acid, EDC · HCl, DIPEA, THF. *ii.* **33**, 2-aminoethyl diphenylborinate.
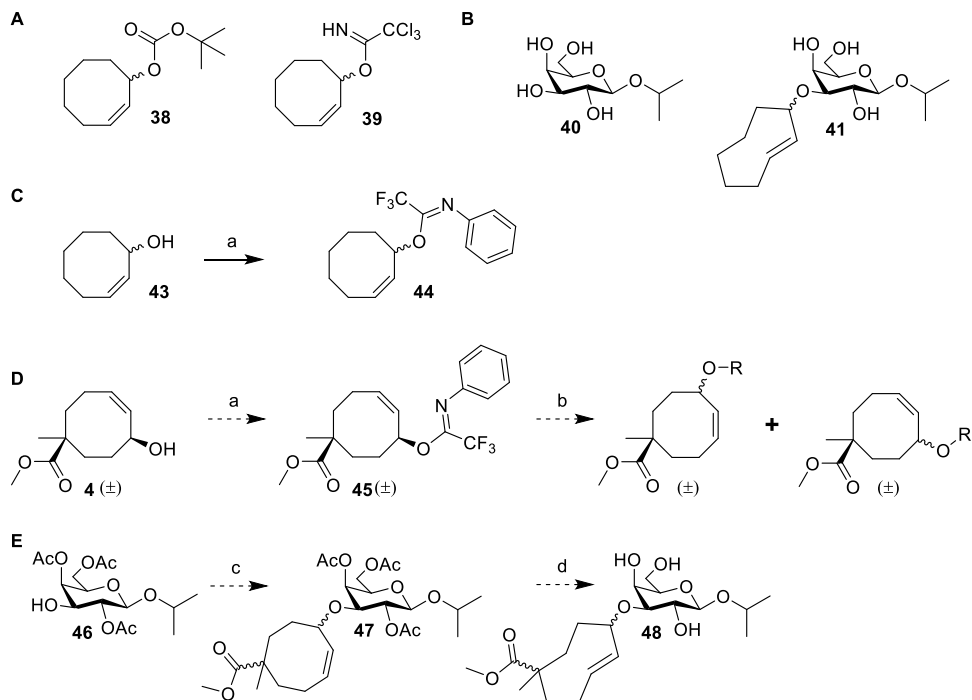
Scheme 4 A) Cyclooctene reagents **38** and **39** employed in Chapter 6 for the synthesis of allylic TCO-ethers. B) *lac* operon inducer **40** and caged *lac* operon inducer **41** described in Chapter 6. C) Synthesis of trifluoroimidate **44** from **43**. D) Proposed synthesis of bifunctional trifluoroimidate **45** from **4** and subsequent investigation of stereo- and regioselectivity upon activation in the presence of a Lewis acid. E) Proposed synthesis of caged *lac* operon inducer **48** from **46**. Reagents/conditions: (a) NaH, (Z)-2,2,2,-trifluoro-*N*-phenylacetimidoyl chloride, THF, 0°C to rt, 83% (**44**); (b) TfOH, R-OH, DCM, -40°C to rt; (c) **45**, TfOH, DCM, -40°C to rt; (d) *i.* methyl benzoate, hv (254 nm), Et$_2$O/isopropanol, rt. ii. NaOMe, MeOH, rt.

Chapter 6 reports synthetic methodology towards allylic TCO-ethers by employing two novel reagents (Scheme 4A, **38** and **39**). Cyclooctene *tert*-butyl carbonate **38** was designed to afford CCO-ethers upon reaction with phenols under palladium catalysis whereas Lewis acid triggered activation of cyclooctene trichloroimidate **39** afforded CCO-ethers from aliphatic alcohols. Subsequently, photochemical isomerization of the CCO-ether affords the corresponding TCO-ether. The activity of a novel *lac* operon inducer (IPG, Scheme 4B, **40**) was manipulated by attaching a TCO-ether moiety to the 3-OH position, thereby obtaining 3-TCO-IPG (**41**). Recombinant expression experiments in *E. coli* revealed **41** did not affect expression levels in the absence of 3,6-dimethyl-tetrazine (**42**), whereas deprotection of **41** in the presence of **42** was able to switch on recombinant protein expression.
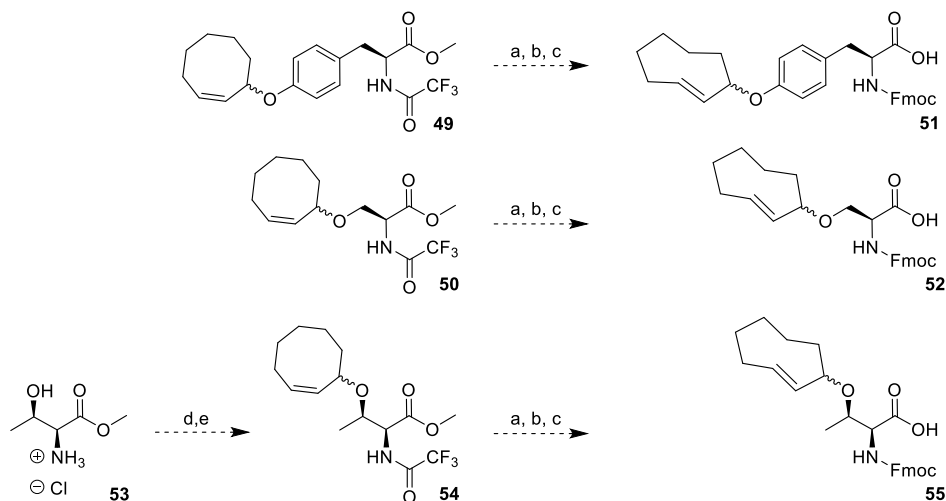
Scheme 5 Proposed synthesis of TCO-ether protected amino acids for Fmoc SPPS. Reagents/conditions: (a) methyl benzoate, hv (254 nm), Et$_2$O/isopropanol, rt; (b) KOH, MeOH, H$_2$O, rt; (c) Fmoc-OSu, Na$_2$CO$_3$, dioxane, H$_2$O, rt; (d) ethyl trifluoroacetate, Et$_3$N, MeOH, 0°C to rt; (e) **39**, TfOH, DCM, -40°C to rt.

It would be of interest to further improve the Lewis acid promoted formation of CCO-ethers from aliphatic alcohols. One way to achieve this is to slow down competing elimination and rearrangement pathways by employing a more stabilized cyclooctene electrophile. To this end, cyclooctenol **43** (Chapter 3 and 6) was reacted with (Z)-2,2,2,-trifluoro-*N*-phenylacetimidoyl chloride in the presence of NaH to obtain cyclooctene trifluoroimidate **44** in 83% yield (Scheme 4C). The conversion of substituted cyclooctenes into CCO ethers would certainly demand a higher efficiency for the corresponding CCO imidates and additionally offers the possibility to examine the stereo- and regioselectivity of these transformations (Scheme 4D). For instance, the conversion of cyclooctene methyl ester **4** into cyclooctene imidate **45** would allow activation with TfOH and a model nucleophile to examine the subsequent stereo- and regiochemical outcomes. Additionally, **45** could be employed to alkylate **46** to obtain **47**, which could be subjected to photochemical isomerization and deacetylation obtain **48** (Scheme 4E). It would be of interest to evaluate whether **48** is able to act as an allosteric *lac* operon antagonist prior to IEDDA pyridazine elimination to form the agonist **40**.

Provided the updated Fmoc SPPS-based strategy for TCO-modified peptide synthesis (Figure 2) works as intended, the CCO-ethers of L-tyrosine and L-serine (Scheme 5, **49** and **50**) described in Chapter 6 could be subjected to photochemical isomerization, alkaline deprotection[23] and Fmoc functionalization to obtain Fmoc-protected TCO-ether amino acids **51** and **52**. It would also be of interest to subject L-threonine methyl
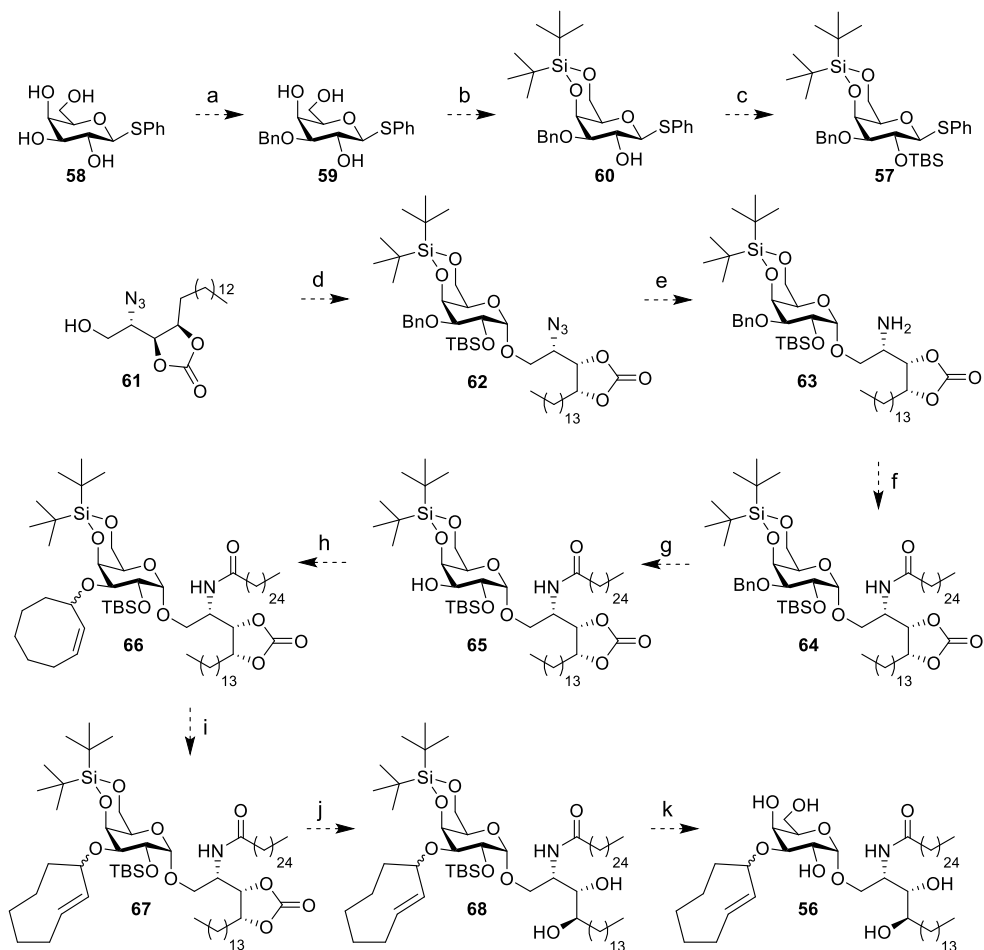
Scheme 6 Proposed synthesis of TCO-ether protected αGalcer (**56**). Reagents/conditions: (a) i. Bu₂SnO, toluene, 105°C; ii. benzyl bromide, TBABr, toluene, 70°C; (b) DTBS(OTf)₂, pyridine, DMF, -40°C; (c) TBS-OTf, DMAP, pyridine, 0°C to rt; (d) **57**, NIS, TMS-OTf, DCM, -40°C; (e) PtO₂, H₂ (g), THF, rt; (f) hexacosonoic acid, EDC · HCl, DIPEA, DMAP, DCM; (g) Pd(OH)₂/C, H₂ (g), EtOAc, rt; (h) **39** or **44**, TfOH, DCM, -40°C to rt; (i) methyl benzoate, h𝑣 (254 nm), Et₂O/isopropanol, rt; (j) LiOH, THF, H₂O, rt; (k) Et₃N · 3HF, THF, rt.

ester **53** to N-trifluoroacetyl protection[24] and subsequent CCO-etherification to obtain **54**, which can also be transformed into the corresponding Fmoc-protected TCO-ether amino acid (**55**). It is conceivable that competing β-elimination necessitates a modified protecting group strategy for compounds **52** and **55**.

The synthesis of a TCO-ether protected αGalcer derivative (**56**) would provide a means to directly interfere with recognition of the exposed galactose moiety in the CD1d-TCR interface (Scheme 6). Orthogonally protected thioglycoside donor (**57**) could be

accessed from thioglycoside **58** by regioselective introduction of a benzyl group using stannylene-acetal chemistry to obtain **59**,[25,26] followed by installation of the 4,6-DTBS protecting group to give **60**. Silylation in the presence of TBSOTf would then provide **57**. NIS/TMSOTf-mediated glycosylation between **57** and **61** (Chapter 5) would afford intermediate **62**, which can be selectively hydrogenated in the presence of PtO_2 to obtain **63**. Installation of the amide bond to obtain **64** would be followed by hydrogenation in the presence of Pearlman's catalyst to obtain **65**. Installation of the CCO-ether moiety in the presence of cyclooctene imidates **39** or **44** and TfOH would give **66**, which is amenable for photoisomerization towards TCO-ether **67**. Saponification of the cyclic carbonate moiety would afford **68** and subsequent desilylation would result in TCO-ether protected αGalcer **56**.

7.2 Experimental procedures

General methods: Commercially available reagents and solvents were used as received. Moisture and oxygen sensitive reactions were performed under N_2 atmosphere (balloon). DCM, toluene, THF, dioxane and Et_2O were stored over (flame-dried) 4 Å molecular sieves (8-12 mesh). Methanol was stored over (flame-dried) 3 Å molecular sieves. DIPEA and Et_3N were stored over KOH pellets. TLC analysis was performed using aluminum sheets, pre-coated with silica gel (Merck, TLC Silica gel 60 F_{254}). Compounds were visualized by UV absorption (λ = 254 nm), by spraying with either a solution of $KMnO_4$ (20 g/L) and K_2CO_3 (10 g/L) in H_2O, a solution of $(NH_4)_6Mo_7O_{24} \cdot 4H_2O$ (25 g/L) and $(NH_4)_4Ce(SO_4)_4 \cdot 2H_2O$ (10 g/L) in 10% H_2SO_4, 20% H_2SO_4 in EtOH, or phosphomolybdic acid in EtOH (150 g/L), where appropriate, followed by charring at ca. 150°C. Column chromatography was performed on Screening Devices b.v. Silica Gel (particle size 40-63 μm, pore diameter 60 Å). Celite Hyflo Supercel (Merck) was used to impregnate the reaction mixture prior to silica gel chromatography when indicated. ^1H, ^{13}C APT, ^1H COSY, HSQC and HMBC spectra were recorded with a Bruker AV-400 (400/100 MHz) spectrometer. Chemical shifts are reported as δ values (ppm) and were referenced to tetramethylsilane (δ = 0.00 ppm) or the residual solvent peak as internal standard. J couplings are reported in Hz.

LC-MS analysis was performed on a Finnigan Surveyor HPLC system (detection at 200-600 nm) with an analytical C_{18} column (Gemini, 50 x 4.6 mm, 3 μm particle size, Phenomenex) coupled to a Finnigan LCQ Advantage MAX ion-trap mass spectrometer (ESI+). The applied buffers were H_2O, MeCN and 1.0% TFA in H_2O (0.1% TFA end concentration). HPLC purification was performed on a Gilson HPLC system (detection at 214 nm) coupled to a semi-preparative C_{18} column (Gemini, 250 x 10 mm, 5 μm particle size, Phenomenex). The applied buffers were H_2O, MeCN and 100 mM NH_4OAc in H_2O (10 mM NH_4OAc end concentration). High resolution mass spectra were recorded by direct injection (2 μL of a 1 μM solution in H_2O/MeCN 1:1 and 0.1% formic acid) on a mass spectrometer (Q Exactive HF Hybrid Quadrupole-Orbitrap) equipped with an electrospray ion source in positive mode (source voltage 3.5 kV, sheath gas flow 10, capillary temperature 275°C) with resolution R = 240,000 at m/z 400 (mass range m/z = 160-2,000) and an external lock mass. The high resolution mass spectrometer was calibrated prior to measurements with a calibration mixture (Thermo Finnigan).

Preparation of neutralized silica gel: Unmodified silica gel (500 gram) was slowly dispersed into a 3 L round-bottom flask containing a stirring volume of H_2O (1.7 L). NH_4OH (28% w/w, 100 mL) was added and the alkaline suspension was stirred for 30 min. The suspension was filtered, washed with H_2O and the silica gel was dried on aluminium foil overnight at rt. The silica was transferred into a glass container and remaining traces of H_2O were removed by drying in an oven at 150°C overnight.
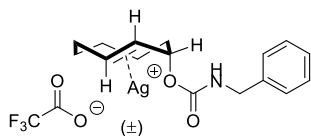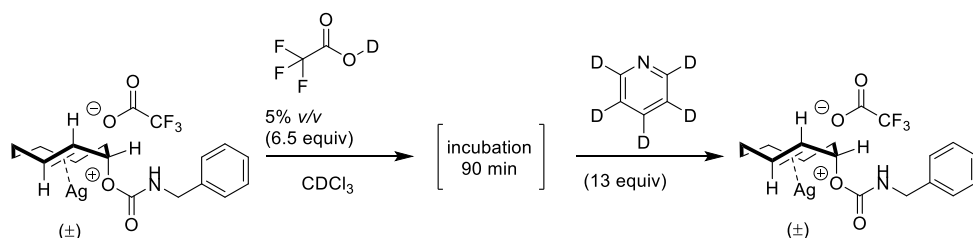
Silver trifluoroacetate complex of axial TCO carbamate 12 (69): An NMR tube was charged with silver trifluoroacetate (19.9 mg, 90 µmol, 1.5 equiv). Axial TCO-carbamate **12** (Chapter 3; 15.5 mg, 60 µmol, 1.0 equiv) was dissolved in CDCl$_3$ (600 µL) and the solution was added to the NMR tube. After vortexing, a diastereomeric mixture of axial TCO carbamate-Ag complexes **69** (**69$_A$** : **69$_B$**, 0.55 : 0.40) was observed: ^{1}H NMR (400 MHz, CDCl$_3$) δ 7.43 (t, J = 5.6 Hz, 1NH, **69$_A$**), 7.37 – 7.21 (m, 5H, **69$_A$** + **69$_B$**), 6.17 – 5.99 (m, 1H, **69$_B$**), 5.81 (d, J = 15.9 Hz, 1H, **69$_B$**), 5.70 (d, J = 15.8 Hz, 1H, **69$_A$**), 5.53 (t, J = 5.8 Hz, 1NH, **69$_B$**), 5.40 (s, 1H, **69$_B$**), 5.21 (s, 1H, **69$_A$**), 5.12 – 4.93 (m, 1H, **69$_A$**), 4.42 – 4.12 (m, 2H, **69$_A$** + **69$_B$**), 2.66 (d, J = 8.6 Hz, 1H, **69$_B$**), 2.40 (d, J = 11.6 Hz, 1H, **69$_A$**), 2.19 – 1.50 (m, 6H, **69$_A$** + **X$_B$**; 1H, **69$_B$**), 1.32 – 1.16 (m, 1H, **69$_A$**), 1.12 – 0.98 (m, 1H, **69$_B$**), 0.92 – 0.61 (m, 1H, **69$_A$** + **69$_B$**; 1H, **69$_A$**); ^{13}C NMR (101 MHz, CDCl$_3$) δ 162.5 (q, J = 35.2 Hz; TFA), 157.7, 156.1, 139.2, 138.1, 128.8 (x4), 127.7, 127.6, 127.5, 127.1 (x3), 121.4, 120.3, 119.1, 118.3, 117.4 (q, J = 290.8 Hz; TFA), 75.2, 74.2, 45.6, 45.2, 40.7, 40.3, 36.4, 36.1, 36.1, 35.7, 28.2, 28.1, 23.3 (x2).

Note: After 72 h the diastereomeric mixture of axial TCO carbamate-Ag complexes was analyzed once again with NMR to obtain identical ^{1}H and ^{13}C spectra.


Stability NMR experiment with silver trifluoroacetate complex of axial TCO carbamate 12 (69) - 5% *v/v* TFA-D in DCM - incubation 90 min - quenching with pyridine D$_5$: Axial TCO-carbamate **12** (Chapter 3; 15.5 mg, 60 µmol, 1.0 equiv) was dissolved in CDCl$_3$ (570 µL) in an NMR tube. After measuring a reference spectrum (^{1}H NMR), silver trifluoroacetate (19.9 mg, 90 µmol, 1.5 equiv) was added. After vortexing for 1 min and measuring a reference spectrum (^{1}H NMR), additional silver trifluoroacetate (19.88 mg, 90 µmol, 1.5 equiv) was added. After vortexing for 1 min and measuring a reference spectrum (^{1}H NMR), TFA-D (30 µL, 0.39 mmol, 6.5 equiv) was added to obtain a 0.1 M solution of **69** in 5% TFA-D (*v/v* in CDCl$_3$). The mixture was vortexed for 1 min, and subsequently characterized with NMR (^{1}H, ^{13}C, COSY, HSQC). After 90 min, the mixture was neutralized by adding pyridine-D$_5$ (63 µL, 0.78 mmol, 13 equiv), vortexed for 1 min and characterized with NMR (^{1}H, ^{13}C, COSY, HSQC).
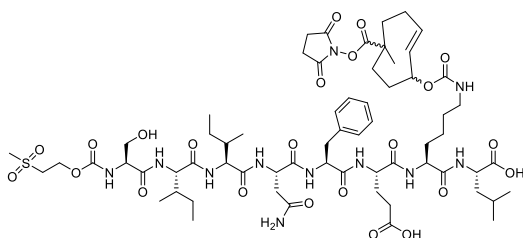

MSc-SIINFEK(NHS-bTCO)L (14): MSc-SIINFEKL (Chapter 4; **13**, 116.8 mg, 105 µmol, 1.0 equiv) and NHS-bTCO (**1**, 52.9 mg, 125 µmol, 1.2 equiv) were combined in a 50 mL tube and dissolved in anhydrous DMF (10 mL) under N$_2$. Anhydrous DIPEA (73 µL, 418 µmol, 4.0 equiv) was added and

the reaction mixture was shaken for 19 h at room temperature. The tube was shielded with aluminum foil during the reaction. The crude reaction mixture was purified by HPLC (MeCN in H_2O with 10 mM NH_4OAc) to obtain **14** (17.59 mg, 12.0 μmol, 12%) as a solid after lyophilization: LC-MS (linear gradient 10 → 90% MeCN, 0.1% TFA, 12.5 min): R_t (min): 6.39 (ESI-MS (m/z): 1420.27 (M+H$^+$)); HRMS: calculated for $C_{64}H_{99}N_{11}O_{23}S$ 710.83125 [M+2H]$^{2+}$; found 710.83120.


mixture
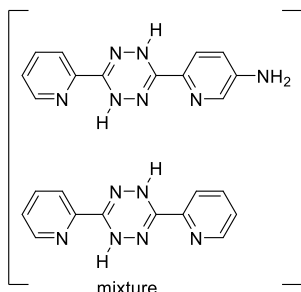
Dihydrotetrazines 70 and 71: Synthesis was performed according to a modified procedure.[16] 2-Pyridine carbonitrile (2.78 mL, 28.8 mmol, 1.0 equiv), 5-amino-2-pyridine carbonitrile (**15**, 3.43 g, 28.8 mmol, 1.0 equiv) and hydrazine monohydrate (5.59 mL, 115 mmol, 4.0 equiv) were combined in a microwave tube. The tube was briefly purged with N_2 before capping the tube and stirring the reaction mixture at 90°C (oil bath) for 16 h. Subsequently, the reaction mixture was cooled to 0°C (ice bath). A precipitate formed, which was collected by filtration and rinsed with cold H_2O. The filtrate was cooled to 0°C (ice bath) and additional precipitate was collected by filtration. The residue was co-evaporated with toluene (3x) to obtain the crude mixture of dihydrotetrazines **70** and **71** (4.31 g, ≥ 17.02 mmol, 59%) as an orange solid which was used for the next step without further purification.
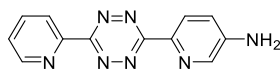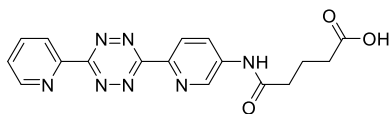

Tetrazine 16: Synthesis was performed according to a modified procedure.[16] The crude mixture of dihydrotetrazines **70** and **71** described in the previous step (1.00 g, 3.95 mmol, 1.0 equiv) was suspended in anhydrous DCM (50 mL) before adding (Diacetoxyiodo)benzene (BAIB, 2.60 g, 8.07 mmol, 2.0 equiv). The reaction mixture was stirred for 3 h at room temperature. The crude reaction mixture was applied directly onto a silica gel column (neutralized silica gel) and purified using column chromatography (DCM → 1% MeOH in DCM → 1.5 % MeOH in DCM) to obtain **16** (104 mg, 0.41 mmol, 10%) as a red solid: R_f = 0.2 (5% MeOH in DCM); ^1H NMR (400 MHz, DMSO) δ 8.90 (ddd, J = 4.7, 1.7, 0.9 Hz, 1H), 8.53 (dt, J = 7.9, 1.0 Hz, 1H), 8.36 (d, J = 8.6 Hz, 1H), 8.23 (d, J = 2.7 Hz, 1H), 8.12 (td, J = 7.8, 1.8 Hz, 1H), 7.69 (ddd, J = 7.6, 4.7, 1.1 Hz, 1H), 7.13 (dd, J = 8.7, 2.8 Hz, 1H), 6.39 (s, 2NH); ^{13}C NMR (101 MHz, DMSO) δ 162.9, 162.6, 150.5, 148.0, 137.7, 137.2, 136.0, 126.2, 125.7, 123.7, 119.0. Spectroscopic data was in agreement with literature.[17,27,28]
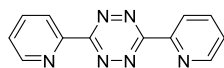
Tetrazine 17: This compound was encountered as a crude byproduct during column chromatography purifications of compound **16**. Purification using silica gel chromatography (DCM → 1% MeOH in DCM) afforded **17** as a pink solid: R_f = 0.3 (5% MeOH in DCM); ^1H NMR (400 MHz, DMSO) δ 8.99 – 8.91 (m, 2H), 8.62 (d, J = 7.9 Hz, 2H), 8.17 (td, J = 7.8, 1.7 Hz, 2H), 7.74 (ddd, J = 7.6, 4.7, 1.0 Hz, 2H); ^{13}C NMR (101 MHz, DMSO) δ 163.3 (x2), 150.7 (x2), 150.1 (x2), 137.9 (x2), 126.7 (x2), 124.4 (x2); ^1H NMR (400 MHz, CDCl$_3$) δ 9.05 – 8.96 (m, 2H), 8.81 – 8.73 (m, 2H), 8.03 (td, J = 7.8, 1.7 Hz, 2H), 7.60 (ddd, J = 7.6, 4.8, 1.0 Hz, 2H); ^{13}C NMR (101 MHz, CDCl$_3$) δ 164.0 (x2), 151.2 (x2), 150.2 (x2), 137.7 (x2), 126.8 (x2), 124.7 (x2). Spectroscopic data was in agreement with literature.[1]

Tetrazine 18: Synthesis was performed according to a modified procedure.[27] Tetrazine **16** (30 mg, 0.119 mmol, 1.0 equiv) and glutaric anhydride (68 mg, 0.597 mmol, 5.0 equiv) were combined in a 25 mL round-bottom flask and suspended in anhydrous dioxane (7 mL) under N_2. The flask was sealed and the reaction mixture was stirred for 48 h at 60°C (oil bath). Additional glutaric anhydride (68 mg, 0.60 mmol, 5.0 equiv) was added and the reaction mixture was stirred for 48 h at 70°C (oil bath). The crude reaction mixture was concentrated *in vacuo* and purified by successive sonication, centrifugation and decanting steps in anhydrous DCM (3 x 14 mL) and distilled EtOAc (14 mL), respectively, to obtain **18** (28 mg, 77 µmol, 64%) as a pink solid: LC-MS (linear gradient $0 \rightarrow 50\%$ MeCN, 0.1% TFA, 12.5 min): R_t (min): 6.67 (ESI-MS (m/z): 366.07 (M+H$^+$)); ^{1}H NMR (400 MHz, DMSO) δ 12.14 (br s, 1OH), 10.58 (s, 1NH), 9.04 (d, *J* = 2.2 Hz, 1H), 8.93 (d, *J* = 4.3 Hz, 1H), 8.60 (dd, *J* = 11.5, 8.3 Hz, 2H), 8.43 (dd, *J* = 8.7, 2.4 Hz, 1H), 8.15 (td, *J* = 7.8, 1.5 Hz, 1H), 7.72 (dd, *J* = 7.8, 4.7 Hz, 1H), 2.47 (t, *J* = 7.3 Hz, 2H), 2.32 (t, *J* = 7.3 Hz, 2H), 1.86 (p, *J* = 7.3 Hz, 2H); ^{13}C NMR (101 MHz, DMSO) δ 172.0, 163.1, 162.8, 150.6, 150.2, 143.8, 141.3, 138.5, 137.8, 126.6, 126.2, 124.9, 124.2, 35.4, 32.9, 20.2. Spectroscopic data was in agreement with literature.[27]
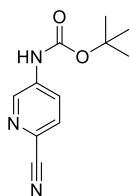

Carbonitrile 19: 5-Amino-2-pyridine carbonitrile (**15**, 1.19 g, 10.0 mmol, 1.0 equiv) was dissolved in anhydrous THF (12 mL) under N_2. The solution was cooled to 0°C (ice bath) before adding Et$_3$N (6.97 mL, 50.0 mmol, 5.0 equiv), DMAP (61 mg, 0.5 mmol, 5 mol%) and Boc$_2$O (2.32 mL, 10.0 mmol, 1.0 equiv). The reaction mixture was gradually heated to 60°C (oil bath) and stirred for 20 h. The reaction mixture was diluted with H_2O (10 mL) and extracted with EtOAc (10 mL). The organic layer was dried over MgSO$_4$, filtered and concentrated *in vacuo*. The crude product was purified by silica gel chromatography (5% EtOAc in pentane $\rightarrow$ 20% EtOAc in pentane) to obtain **19** (1.00 g, 4.56 mmol, 46%) as a white solid: R_f = 0.5 (10% EtOAc in pentane); ^{1}H NMR (400 MHz, DMSO) δ 10.15 (s, 1NH), 8.73 (d, *J* = 2.4 Hz, 1H), 8.11 – 8.02 (m, 1H), 7.92 (dd, *J* = 8.6, 3.0 Hz, 1H), 1.49 (s, 9H); ^{13}C NMR (101 MHz, DMSO) δ 152.4, 141.0, 139.7, 129.6, 124.8, 124.3, 117.8, 80.7, 27.9 (x3).
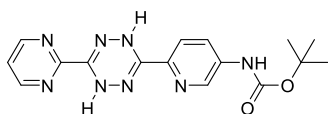
Dihydrotetrazine 20: Carbonitrile **19** (110 mg, 0.5 mmol, 1.0 equiv), pyrimidine-2-carbonitrile (53 mg, 0.5 mmol, 1.0 equiv), dioxane (98 µL) and hydrazine monohydrate (98 µL, 2.0 mmol, 4.0 equiv) were combined in a microwave tube. The tube was briefly purged with N_2 before capping the tube and stirring the reaction mixture at 90°C (oil bath) for 19 h. An orange precipitate had formed, which was suspended in cold H_2O, filtered, washed with cold H_2O and dried *in vacuo*. The crude product was dissolved in THF, impregnated with Celite and concentrated *in vacuo*. The impregnated crude product was purified by silica gel chromatography (DCM $\rightarrow$ 3% MeOH in DCM) to obtain **20** (76 mg, 0.21 mmol, 43%) as an orange solid: R_f = 0.5 (3% MeOH in DCM); ^{1}H NMR (400 MHz, DMSO) δ 9.89 (s, 1NH), 9.03 (s, 1H), 8.92 (d, *J* = 4.9 Hz, 2H), 8.87 (s, 1H), 8.67 (d, *J* = 1.9 Hz, 1H), 8.03 (dd, *J* = 8.8, 2.5 Hz, 1H), 7.89 (d, *J* = 8.6 Hz, 1H), 7.61 (t, *J* = 4.9 Hz, 1H), 1.49 (s, 9H).
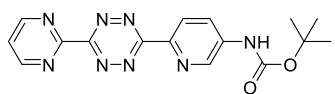
Tetrazine 21: Dihydrotetrazine **20** (76 mg, 0.21 mmol, 1.0 equiv) was suspended in anhydrous DCM (1.0 mL) before adding (Diacetoxyiodo)benzene (BAIB, 104 mg, 0.32 mmol, 1.5 equiv). The reaction mixture was stirred for 2 h at room temperature and was subsequently concentrated *in vacuo.* The crude product was purified by silica gel chromatography (DCM → 3% MeOH in DCM) to obtain **21** (54 mg, 0.153 mmol, 72%) as a red solid: R_f = 0.3 (2% MeOH in DCM); ^{1}H NMR (400 MHz, DMSO) δ 10.14 (s, 1NH), 9.20 (d, *J* = 4.8 Hz, 2H), 8.99 – 8.89 (m, 1H), 8.62 (d, *J* = 8.7 Hz, 1H), 8.26 (d, *J* = 8.5 Hz, 1H), 7.83 (t, *J* = 4.7 Hz, 1H), 1.53 (s, 9H); ^{13}C NMR (101 MHz, DMSO) δ 162.9, 162.8, 159.2, 158.6 (x2), 152.7, 142.8, 140.7, 139.3, 125.4, 125.0, 123.1, 80.6, 28.1 (x3).
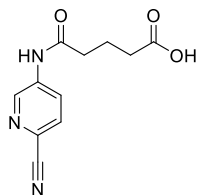
Carbonitrile 22: Synthesis was performed according to a modified procedure.[18] 5-Amino-2-pyridine carbonitrile (**15**, 596 mg, 5.00 mmol, 1.0 equiv) and glutaric anhydride (2.85 g, 25.0 mmol, 5.0 equiv) were combined in a 100 mL round-bottom flask and suspended in anhydrous dioxane (20 mL) under N_2. The flask was sealed and the reaction mixture was stirred for 72 h at 80°C (oil bath). The reaction mixture was allowed to cool down to room temperature and was subsequently concentrated *in vacuo*. The crude product was refluxed in anhydrous MeOH to precipitate the product, followed by filtration. The residue was collected and the filtrate was allowed to crystallize overnight to collect additional residue. Carbonitrile **22** (937 mg, 4.02 mmol, 80%) was obtained as a solid: ^{1}H NMR (400 MHz, DMSO) δ 10.67 (s, 1NH), 8.84 (d, *J* = 2.6 Hz, 1H), 8.26 (dd, *J* = 8.6, 2.6 Hz, 1H), 7.96 (d, *J* = 8.6 Hz, 1H), 2.44 (t, *J* = 7.4 Hz, 2H), 2.26 (t, *J* = 7.3 Hz, 2H), 1.80 (p, *J* = 7.3 Hz, 2H); ^{13}C NMR (101 MHz, DMSO) δ 174.3, 172.3, 141.8, 139.1, 129.7, 125.7, 125.6, 117.8, 35.5, 33.1, 20.2. Spectroscopic data was in agreement with literature.[18]
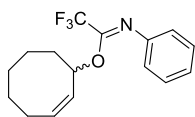
Cyclooctene reagent 44: Cyclooctenol **43** (Chapter 3 and 6; 138 mg, 1.09 mmol, 1.0 equiv) was dissolved in anhydrous THF (1.0 mL) under N_2. The solution was cooled to 0°C (ice bath) before adding sodium hydride (70 mg, 1.75 mmol, 1.6 equiv). After 15 min, (Z)-2,2,2,-trifluoro-N-phenylacetimidoyl chloride (309 mg, 1.49 mmol, 1.4 equiv) was dissolved in anhydrous THF (2.0 mL) under N_2 and was slowly added to the reaction mixture. The reaction mixture was stirred for 16 h and allowed to warm to room temperature. The reaction mixture was concentrated *in vacuo* and the crude product was purified by silica gel chromatography (pentane → 2% Et$_2$O in pentane) to obtain **44** (269 mg, 0.91 mmol, 83%) as a yellow oil: R_f = 0.8 (2% Et$_2$O in pentane); ^{1}H NMR (400 MHz, CDCl$_3$) δ 7.33 – 7.19 (m, 2H), 7.10 – 6.98 (m, 1H), 6.80 (d, *J* = 7.8 Hz, 2H), 5.78 (br s, 1H), 5.68 (q, *J* = 9.1, 8.4 Hz, 1H), 5.62 – 5.47 (m, 1H), 2.38 – 1.85 (m, 3H), 1.76 – 1.22 (m, 7H); ^{13}C NMR (101 MHz, CDCl$_3$) δ 144.8, 130.4, 130.1, 128.8 (x2), 123.8, 119.7 (x2), 116.5 (q, *J* = 285.2 Hz), 76.2, 34.5, 28.8, 26.5, 25.9, 23.3.

*Note: the ^{13}C signal associated with the imidate moeity (C=O) was not reported due to a lack of resolution in the spectrum of **44**.*

7.3 References

[1] R. M. Versteegen, R. Rossin, W. ten Hoeve, H. M. Janssen, M. S. Robillard, *Angew. Chem. Int. Ed.* **2013**, *52*, 14112–14116.

[2] J. Li, P. R. Chen, *Nat. Chem. Biol.* **2016**, *12*, 129–137.

[3] K. Neumann, A. Gambardella, M. Bradley, *ChemBioChem* **2019**, *20*, 872–876.

[4] J. Tu, M. Xu, R. M. Franzini, *ChemBioChem* **2019**, *20*, 1615–1627.

[5] R. Rossin, S. M. J. van Duijnhoven, W. ten Hoeve, H. M. Janssen, F. J. M. Hoeben, R. M. Versteegen, M. S. Robillard, *Bioconjug. Chem.* **2016**, *27*, 1697–1706.

[6] M. A. R. Geus, E. Maurits, A. J. C. Sarris, T. Hansen, M. S. Kloet, K. Kamphorst, W. Hoeve, M. S. Robillard, A. Pannwitz, S. A. Bonnet, J. D. C. Codée, D. V. Filippov, H. S. Overkleeft, S. I. Kasteren, *Chem. Eur. J.* **2020**, *26*, 9900–9904.

[7] G. R. Ediriweera, J. D. Simpson, A. V Fuchs, T. K. Venkatachalam, M. Van De Walle, C. B. Howard, S. M. Mahler, J. P. Blinco, N. L. Fletcher, Z. H. Houston, C. A. Bell, K. J. Thurecht, *Chem. Sci.* **2020**, *11*, 3268–3280.

[8] M. A. Muhs, F. T. Weiss, *J. Am. Chem. Soc.* **1962**, *84*, 4697–4705.

[9] D. L. Cedeño, R. Sniatynsky, *Organometallics* **2005**, *24*, 3882–3890.

[10] A. C. Cope, R. D. Bach, *Org. Synth.* **1969**, *49*, 39.

[11] M. Royzen, G. P. A. Yap, J. M. Fox, *J. Am. Chem. Soc.* **2008**, *130*, 3760–3761.

[12] H. E. Murrey, J. C. Judkins, C. W. Am Ende, T. E. Ballard, Y. Fang, K. Riccardi, L. Di, E. R. Guilmette, J. W. Schwartz, J. M. Fox, D. S. Johnson, *J. Am. Chem. Soc.* **2015**, *137*, 11461–11475.

[13] Y. Fang, J. C. Judkins, S. J. Boyd, C. W. am Ende, K. Rohlfing, Z. Huang, Y. Xie, D. S. Johnson, J. M. Fox, *Tetrahedron* **2019**, *75*, 4307–4317.

[14] S. Du, D. Wang, J.-S. Lee, B. Peng, J. Ge, S. Q. Yao, *Chem. Commun.* **2017**, *53*, 8443–8446.

[15] N. K. Devaraj, G. M. Thurber, E. J. Keliher, B. Marinelli, R. Weissleder, *Proc. Natl. Acad. Sci.* **2012**, *109*, 4762–4767.

[16] R. Selvaraj, J. M. Fox, *Tetrahedron Lett.* **2014**, *55*, 4795–4797.

[17] M. L. Blackman, M. Royzen, J. M. Fox, *J. Am. Chem. Soc.* **2008**, *130*, 13518–13519.

[18] A. Maggi, E. Ruivo, J. Fissers, C. Vangestel, S. Chatterjee, J. Joossens, F. Sobott, S. Staelens, S. Stroobants, P. Van Der Veken, L. Wyffels, K. Augustyns, *Org. Biomol. Chem.* **2016**, *14*, 7544–7551.

[19]   R. J. Anderson, C. Tang, N. J. Daniels, B. J. Compton, C. M. Hayman, K. a Johnston, D. a Knight, O. Gasser, H. C. Poyntz, P. M. Ferguson, D. S. Larsen, F. Ronchese, G. F. Painter, I. F. Hermans, *Nat. Chem. Biol.* **2014**, *10*, 943–949.

[20]   D. Lee, M. S. Taylor, *J. Am. Chem. Soc.* **2011**, *133*, 3724–3727.

[21]   D. Lee, C. L. Williamson, L. Chan, M. S. Taylor, *J. Am. Chem. Soc.* **2012**, *134*, 8260–8267.

[22]   M. S. Taylor, *Acc. Chem. Res.* **2015**, *48*, 295–305.

[23]   R. M. Versteegen, W. ten Hoeve, R. Rossin, M. A. R. de Geus, H. M. Janssen, M. S. Robillard, *Angew. Chem. Int. Ed.* **2018**, *57*, 10494–10499.

[24]   K. Murayama, H. Asanuma, *ChemBioChem* **2017**, *18*, 142–149.

[25]   J. G. Taylor, X. Li, M. Oberthür, W. Zhu, D. E. Kahne, *J. Am. Chem. Soc.* **2006**, *128*, 15084–15085.

[26]   H. Xu, Y. Lu, Y. Zhou, B. Ren, Y. Pei, H. Dong, Z. Pei, *Adv. Synth. Catal.* **2014**, *356*, 1735–1740.

[27]   C. F. Hansell, P. Espeel, M. M. Stamenović, I. A. Barker, A. P. Dove, F. E. Du Prez, R. K. O'Reilly, *J. Am. Chem. Soc.* **2011**, *133*, 13828–13831.

[28]   B. L. Oliveira, Z. Guo, O. Boutureira, A. Guerreiro, G. Jiménez-Osés, G. J. L. Bernardes, *Angew. Chem. Int. Ed.* **2016**, *55*, 14683–14687.

Nederlandse samenvatting

Chemische strategieën hebben de opheldering van nieuwe elementen van de biologie mogelijk gemaakt door nauwkeurige controle uit te oefenen op processen in cellen en zelfs in hele organismen. Dit is mogelijk dankzij bio-orthogonale chemie: reacties die gemakkelijk en selectief optreden onder fysiologische omstandigheden zonder te interfereren met natuurlijke biochemische processen. De 'inverse electron demand Diels-Alder' (IEDDA) pyridazine eliminatie ontstond in 2013 als een nieuwe bio-orthogonale reactie en vormt een goed voorbeeld van wat nu bekend staat als dissociatieve bio-orthogonale chemie. Het onderzoek dat in dit Proefschrift wordt beschreven, beoogt om synthetische strategiën te ontwikkelen die het mogelijk maken om de IEDDA pyridazine eliminatie als een veelzijdige 'toolbox' te benutten in de chemische biologie. Zo beschrijft het de modificatie van antigene (MHC-I) peptiden en (CD1d) glycolipiden met een *trans*-cyclo-octeen (TCO) om chemische controle over de herkenning van deze biomoleculen door immuuncellen mogelijk te maken. Synthetische vorderingen die de volledige reikwijdte van de IEDDA pyridazine eliminatie omvatten, worden aanvullend beschreven.

Hoofdstuk 1 introduceert de IEDDA pyridazine eliminatie in de context van dissociatieve bio-orthogonale chemie. Mechanistische aspecten van de reactie worden besproken, evenals verschillende toepassingen waar deze techniek voor is gebruikt. Een overzicht van andere nieuwe bio-orthogonale reacties, waarbij eveneens covalente bindingen worden verbroken, wordt gepresenteerd.

Hoofdstuk 2 beschrijft een geoptimaliseerde synthese van een bifunctioneel TCO-reagens dat veelvuldig is toegepast voor 'click to release' chemie. Een belangrijke wijziging van bestaande literatuurprocedures is de kristallisatie van een iodolacton intermediair na initiële functionalisatie van 1,5-cyclo-octadieen. Transesterificatie van het bicyclische lacton werd vervangen door een één pot, twee-staps verzeping-methylering procedure om de gewenste methyl ester te verkrijgen. Foto-isomerisatie leverde een mengsel van twee TCO isomeren op, dat kon worden gescheiden na een selectieve verzepingsreactie van de axiale isomeer. N-hydroxysuccinimide (NHS) functionalisatie van deze isomeer werd versneld met behulp van nucleofiele katalyse. De equatoriale isomeer werd na NHS functionalisatie onderworpen aan een *trans*-naar-*cis* isomerisatie om het corresponderende *cis*-cyclo-octeen reagens te verkrijgen. Het bifunctionele TCO reagens werd eveneens uitgerust met een EDANS-fluorofoor en een

DABCYL-quencher om een fluorogene 'TCO-reporter-quencher' te verkrijgen voor kinetische analyse van de IEDDA pyridazine eliminatie.

Hoofdstuk 3 beschrijft de poging tot ontwikkeling van een op 'Fmoc solid phase peptide synthesis' (Fmoc SPPS) gebaseerde strategie voor TCO-gemodificeerde peptidesynthese. Een model verbinding, een axiaal, allylisch gesubstitueerde TCO-carbamaat, werd bestudeerd in aanwezigheid van gedeutereerd trifluorazijnzuur (TFA-D) met behulp van ^{1}H en ^{13}C nucleaire magnetische resonantie (NMR). De waargenomen stabiliteit onder verdunde TFA concentraties (<10% *v/v*) werd toegeschreven aan preferentiële protonering op C3 en anchimere assistentie van de carbamaatgroep naar C2 van het verkregen kation. Een Fmoc-Lys(TCO)-OH bouwsteen werd gesynthetiseerd en geïncorporeerd in de SIINFEKL-peptidesequentie op vaste drager. Globale ontscherming van dit peptide leidde tot substantiële TCO-isomerisatie en zelfs carbamaat hydrolyse onder verdunde TFA concentraties (bijvoorbeeld 5% *v/v*) die wel leken te worden verdragen in de NMR-stabiliteitsexperimenten.

Hoofdstuk 4 beschrijft een nieuwe methode voor *in vitro* en *in vivo* chemische controle van T-cel activatie. MHC-I epitopen werden ontworpen met allyl-gesubstitueerde TCO-modificatie op lysine residuen met de aanname dat deze modificatie de herkenning van dergelijke epitopen door T-cellen zou belemmeren, terwijl de IEDDA pyridazine eliminatie deze herkenning selectief zou kunnen herstellen. In tegenstelling tot de synthetische methode die werd onderzocht in Hoofdstuk 3, werd de MHC-I peptidesequentie gesynthetiseerd met Fmoc SPPS voordat de TCO-groep werd geïnstalleerd. N-terminale bescherming met de base-labiele MSc-groep vóór zure afsplitsing van de peptidesequentie maakte regioselectieve TCO-modificatie van de ε-aminogroep van lysine mogelijk. MSc-ontscherming onder basische omstandigheden werd gevolgd door HPLC-zuivering om de gewenste beschermde epitopen te verkrijgen. Lysine-beschermde epitopen van OVA257-264 (OT-I, SIINFEKL) en DbM187-195 (NAITNAKII) vertoonden binding aan MHC-I terwijl T-cel herkenning afwezig was. IEDDA pyridazine eliminatie herstelde effectief de T-cel activatie *in vitro* en *in vivo*. Bovendien werd de 'click to release' benadering toegepast om antigeenkruispresentatie te bestuderen met een N-terminaal verlengd epitoop, OVA247-264 (DEVSGLEQLESIINFEKL).

Hoofdstuk 5 beschrijft het ontwerp en de synthese van TCO-beschermde derivaten van α-galactosylceramide (αGalCer) en α-galactosylphytosphingosine (αGalPhs). De zelfadjuverende strategie door Painter, Hermans en collega's, waar een inactieve pro-αGalCer na esterase of protease-activiteit kan omleggen tot αGalCer, vormde de basis voor het ontwerp van deze benadering om chemisch geïnduceerde activatie van 'invariant natural killer T-cellen' (iNKTs) te bewerkstelligen. Er werd geredeneerd dat de amino-functionaliteit van αGalPhs zou kunnen worden beschermd als een TCO-carbamaat en dat daaropvolgende acylering met hexacosaanzuur zou resulteren in een

TCO-beschermde pro-αGalCer. De belangrijkste stappen van de synthese waren onder meer een α-selectieve glycosylering onder NIS / TMSOTf activatie, met behulp van een 2,3-TBS-4,6-DTBS-beschermde thiogalactoside donor en een 2-azido-3,4-cyclisch carbonaat beschermde phytosphingosine, gevolgd door hydrogenering, TCO-carbamaat formatie en verzeping. Directe desilylering resulteerde in de TCO-beschermde αGalPhs, terwijl verestering en daaropvolgende ontscherming de TCO-beschermde pro-αGalCer opleverde.

Hoofdstuk 6 beschrijft synthetische methodologie voor de synthese van allylische TCO-ethers gebruikmakende van twee nieuwe reagentia. Een cyclo-octeen-*tert*-butylcarbonaat was ontworpen om CCO-ethers op te leveren na reactie met fenolen onder palladiumkatalyse terwijl Lewis-zuur activering van een cyclo-octeen-trichloroimidaat resulteerde in CCO-ethers uit alifatische alcoholen. Fotochemische isomerisatie van de CCO-ether levert de overeenkomstige TCO-ether op. De activiteit van een nieuwe '*lac* operon' inductor (IPG) werd gemanipuleerd door een TCO-ethergroep aan de 3-OH-positie te bevestigen, waardoor 3-TCO-IPG werd verkregen. Recombinante expressie experimenten in *E. coli* onthulden dat 3-TCO-IPG geen invloed had op de expressieniveaus in afwezigheid van 3,6-dimethyl-tetrazine, terwijl ontscherming van 3-TCO-IPG in aanwezigheid van 3,6-dimethyl-tetrazine in staat was om recombinante eiwitexpressie aan te zetten.

Tot slot beschrijft **Hoofdstuk 7** een gedetailleerde samenvatting van het Proefschrift, waarbij na ieder Hoofdstuk aanbevelingen worden gepresenteerd voor vervolgonderzoek.

List of publications

1) **Synthetic methodology towards allylic *trans*-cyclooctene-ethers enables modification of carbohydrates: bioorthogonal manipulation of the *lac* repressor**
   de Geus, M. A. R.; Groenewold G. J. M.; Maurits E.; Araman, C.; van Kasteren, S. I.
   Chem. Sci. **2020**, *11* (37), 10175-10179.

2) **Conditionally controlling human TLR2 activity via *trans*-cyclooctene caged ligands**
   van de Graaff, M. J.; Oosenbrug, T.; Marqvorsen, M. H. S.; Nascimento, C. R.; de Geus, M. A. R.; Manoury, B.; Ressing, M. E.; van Kasteren, S. I.
   Bioconjug. Chem. **2020**, *31* (6), 1685-1692.

3) **Fluorogenic bifunctional *trans*-cyclooctenes as efficient tools for investigating click-to-release kinetics**
   de Geus, M. A. R.[#]; Maurits, E.[#]; Sarris, A. J. C.[#]; Hansen, T.; Kloet, M. S.; Kamphorst, K.; ten Hoeve, W.; Robillard, M. S.; Pannwitz, A.; Bonnet, S. A.; Codée, J. D. C.; Filippov, D. V.; Overkleeft, H. S.; van Kasteren, S. I.
   Chem. Eur. J. **2020**, *26* (44), 9900-9904.

4) **Fast and pH-independent elimination of *trans*-cyclooctene by using aminoethyl-functionalized tetrazines**
   Sarris, A. J. C.; Hansen, T.; de Geus, M. A. R.; Maurits, E.; Doelman, W.; Overkleeft, H. S.; Codée, J. D. C.; Filippov, D. V.; van Kasteren, S. I.
   Chem. Eur. J. **2018**, *24* (68), 18075-18081.

5) **Click-to-release from *trans*-cyclooctenes: mechanistic insights and expansion of scope from established carbamate to remarkable ether cleavage**
   Versteegen, R. M.; ten Hoeve, W.; Rossin, R.; de Geus, M. A. R.; Janssen, H. M.; Robillard, M. S.
   Angew. Chem. Int. Ed. **2018**, *57* (33), 10494–10499.

6) **Chemical control over T-cell activation *in vivo* using deprotection of *trans*-cyclooctene-modified epitopes**
de Geus, M. A. R.[#]; van der Gracht, A. M. F.[#]; Camps, M. G. M.; Ruckwardt, T. J.; Sarris, A. J. C.; Bremmers, J.; Maurits, E.; Pawlak, J. B.; Posthoorn, M. M.; Bonger, K. M.; Filippov, D.V.; Overkleeft, H.S.; Robillard, M.S.; Ossendorp, F.; van Kasteren, S.I.
ACS Chem. Biol. **2018**, *13* (6), 1569–1576.

7) **Human alpha galactosidases transiently produced in *nicotiana benthamiana* leaves: new insights in substrate specificities with relevance for Fabry disease**
Kytidou, K.; Beenakker, T. J. M.; Westerhof, L. B.; Hokke, C. H.; Moolenaar, G. F.; Goosen, N.; Mirzaian, M.; Ferraz, M. J.; de Geus, M.; Kallemeijn, W. W.; Overkleeft, H. S.; Boot, R. G.; Schots A.; Bosch, D.; Aerts, J. M. F. G.
Front. Plant Sci. **2017**, *8, 1026*.

8) **Synthesis of 6-hydroxysphingosine and α-hydroxy ceramide using a cross-metathesis strategy**
Wisse, P.; de Geus, M. A. R.; Cross, G.; van den Nieuwendijk, A. M. C. H.; van Rooden, E. J.; van den Berg, R. J. B. H. N.; Aerts, J. M. F. G.; van der Marel, G. A.; Codée, J. D. C.; Overkleeft, H. S.
J. Org. Chem. **2015**, *80* (14), 7258–7265.

# denotes equal contribution.

0000-0002-1639-5890

Curriculum Vitae

Mark Alexander Ruben de Geus was born on the 25th of August 1990 in Nootdorp, the Netherlands. After completing his secondary education (VWO, cum laude) at the Stanislas College Delft in 2009, he commenced his studies at Leiden University. In 2012, he obtained his Bachelor of Science (BSc) degree in Bio-Pharmaceutical Sciences after an internship in the group of Prof. dr. A.P. IJzerman where he worked on the synthesis of adenosine A_1 receptor antagonists.

He enrolled for the Master's program Research in Chemistry – Design & Synthesis at Leiden University in September 2012 and worked on two research internships. In the Bio-organic Synthesis group, he worked on the synthesis of sphingolipids using a cross-metathesis strategy under supervision of Prof. dr. G.A. van der Marel, Prof. dr. J.D.C. Codée and Prof. dr. H.S. Overkleeft. Subsequently, he studied α-galactosidase A using aziridine-type activity-based probes in the Medical Biochemistry department under supervision of Prof. dr. J.M.F.G. Aerts. The Master of Science (MSc) degree was obtained in July 2015 (cum laude).

From Januari 2016 until October 2020, he conducted his PhD studies at Leiden University in the Bio-organic Synthesis group under supervision of Dr. S.I. van Kasteren and Prof. dr. H.S. Overkleeft. Parts of the research described in this Thesis were presented on posters at CHAINS (Veldhoven, The Netherlands, 2016-2019), Molecular Machines Nobel Prize Conference (Groningen, The Netherlands 2017), 4th Chemical Immunology Conference (Amsterdam, The Netherlands, 2018) and EuroCARB (Leiden, The Netherlands, 2019). Oral presentations about his research were presented at the KNCV International Symposium on Organic Chemistry (Wageningen, The Netherlands, 2018) and at the 18th RSC Chemical Biology and Bioorganic Group (CBBG) conference (Firbush, United Kingdom, 2019).

In Januari 2021, Mark started working as a postdoctoral fellow in the group of Prof. dr. C.P.R. Hackenberger at the Leibniz Institute for Molecular Pharmacology (FMP) in Berlin, Germany.